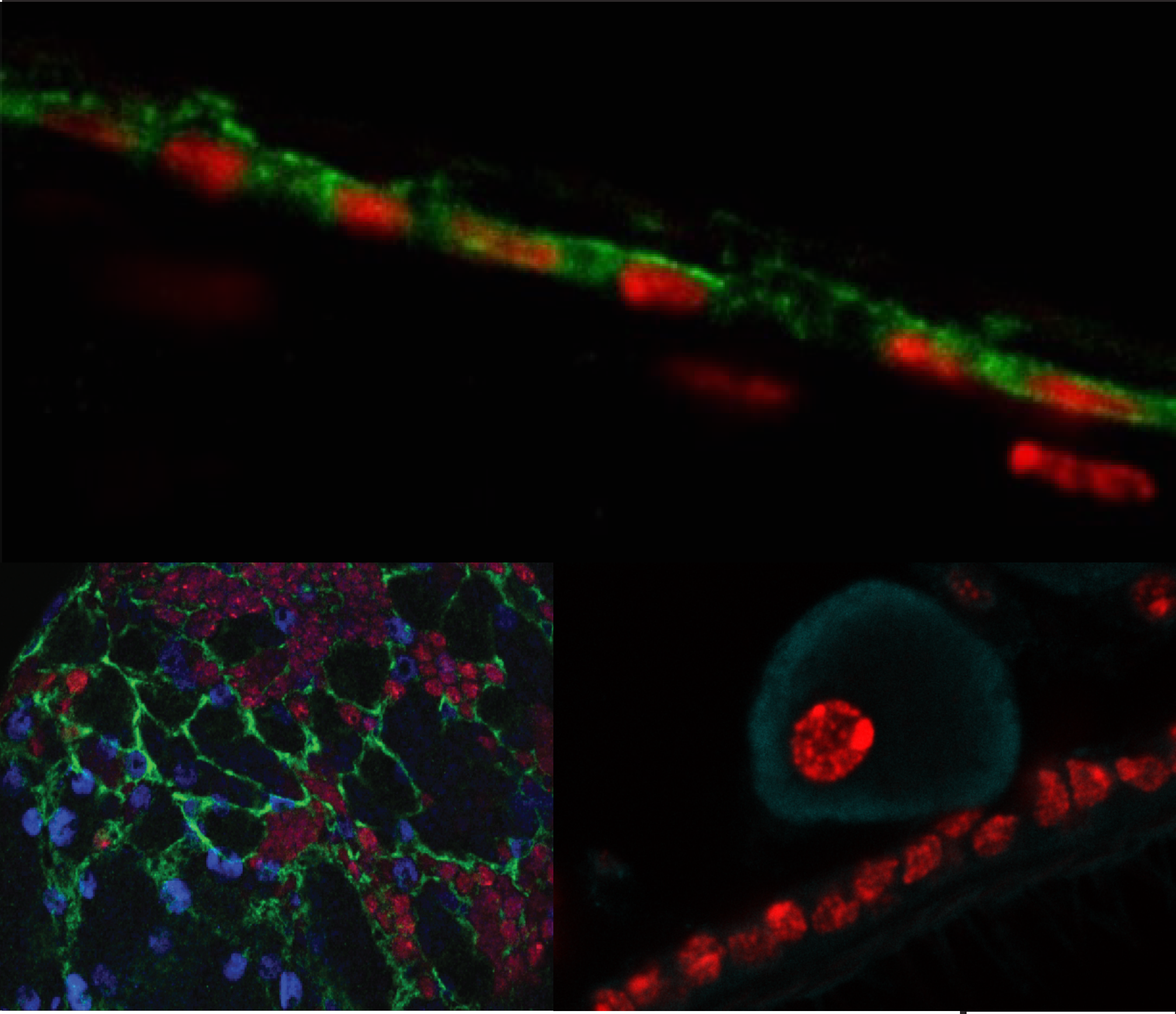

The Achilles' heel of the malaria vector *Anopheles coluzzii*

Doctoral thesis by

Mary Kefi

Heraklion, 2022

University of Crete, Biology Department

Doctoral thesis

“The Achilles’ heel of the malaria vector *Anopheles coluzzii*”.

Mary Kefi, PhD candidate

Scientific Supervisor: Prof. John Vontas

Academic Supervisor: Prof. George Chalepakis

«This research is co-financed by Greece and the European Union (European Social Fund- ESF) through the Operational Programme «Human Resources Development, Education and Lifelong Learning» in the context of the project “Strengthening Human Resources Research Potential via Doctorate Research” (MIS-5000432), implemented by the State Scholarships Foundation (IKY)»

Heraklion, Crete, 2022

Πανεπιστήμιο Κρήτης, Τμήμα Βιολογίας

Διδακτορική διατριβή

“Η αχίλλειος πτέρνα του κουνουπιού-φορέα της ελονοσίας *Anopheles coluzzi*”.

Μαρία Κέφη, Βιολόγος

Επιστημονικός Υπεύθυνος: Καθηγητής Ιωάννης Βόντας

Ακαδημαϊκός Υπεύθυνος: Καθηγητής Γεώργιος Χαλεπάκης

«Το έργο συγχρηματοδοτείται από την Ελλάδα και την Ευρωπαϊκή Ένωση (Ευρωπαϊκό Κοινωνικό Ταμείο) μέσω του Επιχειρησιακού Προγράμματος «Ανάπτυξη Ανθρώπινου Δυναμικού, Εκπαίδευση και Διά Βίου Μάθηση», στο πλαίσιο της Πράξης «Ενίσχυση του ανθρώπινου ερευνητικού δυναμικού μέσω της υλοποίησης διδακτορικής έρευνας» (MIS-5000432), που υλοποιεί το Ίδρυμα Κρατικών Υποτροφιών (ΙΚΥ)»

Ευρωπαϊκή Ένωση
Ευρωπαϊκό Κοινωνικό Ταμείο

Επιχειρησιακό Πρόγραμμα
Ανάπτυξη Ανθρώπινου Δυναμικού,
Εκπαίδευση και Διά Βίου Μάθηση
Με τη συγχρηματοδότηση της Ελλάδας και της Ευρωπαϊκής Ένωσης

ΕΣΠΑ 2014-2020
ανάπτυξη - εργασία - αλληλεγγύη

Ηράκλειο, Κρήτη, 2022

Thesis Committee

- George Chalepakis

Professor, Department of Biology, University of Crete

- John Vontas

Professor, Agricultural University of Athens

Institute of Molecular Biology & Biotechnology, Foundation for Research and Technology Hellas (FORTH-IMBB)

- Vassilis Douris

Assistant Professor, Department of Biological Applications and Technology, University of Ioannina

Biomedical Research Institute, Foundation for Research and Technology Hellas (FORTH-BRI)

- Christos Delidakis

Professor, Department of biology, University of Crete

Institute of Molecular Biology & Biotechnology, Foundation for Research and Technology Hellas (FORTH-IMBB)

- George Gouridis

Researcher B grade

Institute of Molecular Biology and Biotechnology (IMBB-FORTH), Foundation for Research and Technology Hellas (FORTH-IMBB)

- Kriton Kalantidis

Associate Professor, Department of biology, University of Crete

Institute of Molecular Biology & Biotechnology, Foundation for Research and Technology Hellas (FORTH-IMBB)

- Thomas Van Leeuwen

Professor, Department of Plants and Crops, Faculty of Bioscience Engineering, Ghent University, Ghent, Belgium

Table of contents

Acknowledgements 7
Περίληψη..9
Abstract 11
General introduction 13-35
    Malaria: a huge public health problem..13
    Africa encounters the vast malaria burden 13
    Malaria parasite life cycle (Human-Parasite-Mosquito) 13
    Mosquitoes are responsible for malaria transmission 14
    Malaria prevention heavily relies on controlling mosquito vectors through the use of insecticides 17
    Pyrethroids are the main insecticides used for malaria control..21
    Insecticide resistance threatens vector control..22
    Mosquito legs: The first barrier against insecticides..27
    Literature..32
Aim of PhD thesis 36
Chapter 1 “LEGOMICS : High-throughput approaches (-omcis) to delineate alteration in the legs of resistant mosquitoes”..37-63
    1.1 Abstract 38
    1.2 Introduction..39
    1.3 Materials and Methods 41
        1.3.1 Mosquito strains..41
        1.3.2 Leg dissection, induction and RNA isolation 41
        1.3.3 Preparation of Illumina libraries..41
        1.3.4 dsRNA design, generation, nano-injections and silencing efficiency 42
        1.3.5 Deltamethrin toxicity assays..43
    1.4 Results-Discussion 44
        1.4.1 Evaluation of resistance of the VK7 *An. coluzzii* strains 44
        1.4.2 Leg transcripts differentially expressed in resistant *An. coluzzii*..45
        1.4.3 Leg transcripts regulated by short-term deltamethrin induction 50
        1.4.4 Combined analysis of leg transcript datasets..54
        1.4.5 RNAi-mediated silencing coupled with toxicity bioassays of cuticular protein genes revealed by proteome and transcriptome analyses 55
    1.5 Conclusions..58
    1.6 Literature 59
Chapter 2 “The leg/appendage specific ABCH2 transporter mediates toxicity in the malaria vector *Anopheles coluzzii*...64- 86
    2.1 Abstract 65
    2.2 Introduction..66
    2.3 Materials and Methods 68
        2.3.1 Mosquito strains..68
        2.3.2 Antibodies..68
        2.3.3 Western blot analysis 68
        2.3.4 Tissue distribution and relative expression estimation..68
        2.3.5 Cryosectioning, immunofluorescence and confocal microscopy..68
        2.3.6 dsRNA design, generation, nano-injections and silencing efficiency 69
        2.3.7 Deltamethrin toxicity assays..69
        2.3.8 Extraction of cuticular lipids, cuticular hydrocarbon (CHCs) fractionation, identification and quantification 69

2.3.9 ABCH2-overexressing Sf9 insect cells, membrane preparations and ATPase activity estimation 70
2.3.10 C^{14} –deltamethrin penetration rate in dsABCH2 and dsGFP mosquitoes 71
2.4 Results 72
2.4.1 RNAi-mediated silencing of *ABCH2* revealed its implication in pyrethroid toxicity 72
2.4.2 ABCH2 is mainly present in An. coluzzii legs/appendages 73
2.4.3 ABCH2 is localized on the leg/appendage epidermis, underneath the cuticle, most probably with apical polarity...74
2.4.4 Deltamethrin toxicity is not attributed to CHC differences in the legs 75
2.4.5 In silico and in vitro tools provide evidence for a functional membrane-bound ABC transporter which functions most probably as a homodimer.........................76
2.4.6 Protein-ligand docking experiments indicate that deltamethrin is a putative substrate of ABCH2..78
2.4.7 C^{14} –deltamethrin experiments indicate that ABCH2-silenced mosquitoes exhibit increased insecticide penetration 79
2.5 Discussion 81
2.6 Literature 84
Chapter 3 “Characterization of the CYP4G enzymes implicated in cuticular alteration of resistant mosquitoes via cuticular hydrocarbon biosynthesis...87-110
3.1 Abstract 88
3.2 Introduction...89
3.3 Materials and Methods 91
3.3.1 Mosquito strains..91
3.3.2 Antibodies..91
3.3.3 Preparation of cryosection for immunohistochemistry, immunofluorescence and confocal microscopy 91
3.3.4 Topology experiments: predictions and whole mounts (preparation of abdominal walls for immunohistochemistry and immunofluorescence) 91
3.3.5 Fly strains...92
3.3.6 Generation of UAS responder flies 92
3.3.7 Generation of flies used for rescue experiment..93
3.3.8 Quantification of eclosion (adult survival and adult mortality) 93
3.3.9 Extraction of cuticular lipids, cuticular hydrocarbon (CHCs) fractionation, identification and quantifications 93
3.3.10 Western blot analysis 94
3.3.11 Desiccation assay...94
3.3.12 Permethrin toxicity assay 94
3.3.13 CYP4G/CPR-overexpressing Sf9 insect cells and membrane preparation.....94
3.4 Results 96
3.4.1 Both CYP4G17 and CYP4G16 are anchored on the plasma membrane of 4th instar larval oenocytes with the globular part facing cytoplasmically.....................96
3.4.2 Two differentially localized CYP4G17 forms in pupal oenocytes, of larval and adult origin 97
3.4.3 Oenocyte-specific expression of *CYP4G16* and *CYP4G17* (two copies) in *Cyp4g1* knock-down *Drosophila* can restore viability 99
3.4.4 Three very long-chain dimethyl branched CHCs are present in CYP4G16, CYP4G17 and CYP4G16/CYP4G17 flies, but not “wild-type” CYP4G1 flies............100
3.4.5 CYP4G17/CYP4G16 flies cope better with desiccation stress and permethrin toxicity than CYP4G16 flies..102

3.4.6 CYP4G17 and CYP4G16 were successfully expressed *in vitro* together with CPR in Sf9 insect cells using Baculovirus expression system 103
3.5 Discussion 105
3.6 Literature 109
Chapter 4 "Characterization of the brain specific CYP4G15 and analysis of the CYP4G-specific insertsion...111-132
4.1 Abstract 112
4.2 Introduction...113
4.3 Materials and Methods 115
4.3.1 Plasmid desing and preparation of Cyp4g1 deletions for UAS/Gal4 system.115
4.3.2 Generation of UAS responder flies 115
4.3.3 Quantification of eclosion (adult survival and adult mortality) 116
4.3.4 CRISPR/Cas9 genome editing strategy and generation of fly lines..............116
4.3.5 Reverse transcriptase (RT) PCR for validation of UAS/oenocyte-Gal4 expression of *Cyp4g1Δ* and *Cyp4g15* ectopical expression 117
4.3.6 Extraction of cuticular lipids, cuticular hydrocarbons (CHCs) fractionation, identification and quantitation 117
4.3.7 Antibodies...118
4.3.8 Western blot analysis 118
4.3.9 CYP4G15/CPR-overexpressing Sf9 insect cells and membrane preparation.118
4.3.10 CYP4G15 and CYP4G1 immunofluorescence and microscopy on dissected CNS. 118
4.4 Results 119
4.4.1 Oenocyte-specific expression of CYP4G15 in *Cyp4g1* knock-down *D.melanogaster* can partially restore viability, suggesting CYP4G15 acts partially as decarbonylase 119
4.4.2 CYP4G15 can produce a blend of 27 cuticular hydrocarbons in *D. melanogaster* oenocytes favoring the production of methyl- and dimethyl-branched species 120
4.4.3 CYP4G15 is localized in cortex glia of larval CNS while CYP4G1 is found in CNS surface glia..121
4.4.4 *In vitro* expression of CYP4G15 together with CPR using in *Sf9* insect cells using *Baculovirus* expression system 123
4.4.5 Generation of *Cyp4g1* deletions in *D. melanogaster*. 124
4.4.5.1 Generation of *D. melanogaster* bearing the 32aa-deletion results in arrest upon eclosion...124
4.4.5.1.1 Generation of 32aa-deletion using CRiSPR-Cas9 genome editing technique...124
4.4.5.1.2 Complementation of *Cyp4g1 D. melanogaster* null mutants with *Cyp4g1Δ* 32aa-deletion in oenocytes using UAS/ReGal4 system.....................................125
4.4.5.2 Complementation of *Cyp4g1 D. melanogaster* null mutants with *Cyp4g1Δ* 26aa-deletion in oenocytes using UAS/ReGal4 system, restores the lethality of null-mutant flies..126
4.5 Discussion 128
4.6 Literature 131
Supplementary Information 134-143
General discussion and future directions...144
Concluding remarks 149
Literature...150

Acknowledgements

During my PhD thesis I was supervised by great scientists who helped me shape my scientific character, collaborated with many others, always gaining more insights and perspectives and I had the great pleasure to be supported by lots of other people: my family, relatives, friends and colleagues. In these paragraph I would like to acknowledge these people and give my warmest thanks.

First of all, I would like to acknowledge my scientific supervisor Prof. Vontas. I joined his group as an undergraduate student and he was actually the first person who gave me the opportunity to work in a scientific laboratory. With guidance by himself and other group members I worked on well-structured projects and learnt plethora of techniques and later on with his support I applied in "Molecular Biology and Biomedicine" Msc. What I characteristically recall is his urge in an e-mail after finishing my bachelor thesis "Think of keep doing research, you can do it ". And I followed his advice joining again his group as a master student in a collaboration with Dr. Siden-Kiamos laboratory and finally started my PhD thesis on November 2017. As a junior PhD student I was lucky to be supported and trusted by Prof. Vontas. He gave me opportunities, ideas and room to work and "play" actually with different projects. I felt free to propose things, to discuss ideas, even to disagree sometimes. And it was always fruitful. Every time after a presentation in the lab or at a conference, after a discussion, or after getting comments on drafts and posters I felt I had a lesson, a useful feedback. This was provided straight as a piece of information/advice or accompanied by his characteristic sarcastic and ironic sense of humor! Always productive and to the point in either case. Apart from his scientific advice Prof. Vontas cared about my interaction with other people of the scientific world to build my research network, collaborations and be supervised by other great scientists of the field, experienced researchers and other students. I am deeply grateful to your support for this PhD and all my scientific achievements so far and later if any, and more importantly for the belief in me.

Secondly, Vasileia Balabanidou, a post-doctoral researcher in the laboratory is the second person with an impact on my scientific understanding. She was the first day-to-day supervisor I had and she taught me plethora of skills and techniques. I really appreciate the fact that she introduced me in projects she was working on and she made room for me to evolve and find my interests. During the years of my PhD she was always supportive and helpful in my attempt to go a step further sometimes and try more ideas! We worked great as a team and I am grateful for our useful discussions, the technical support and the precious scientific feedback and last but not least for the personal relationship we built during these years of supervision/collaboration. Vasileia your belief in me was unwavering and it enhanced my self-confidence in the lab!

Next, I would like to express my sincere gratitude to Prof. Douris. Vassilis Douris co-supervised a project during my master thesis and the first years of my PhD. He introduced me in *Drosophila* world and he advanced my methodological and conceptual thinking. Always the person who gave a solution to a scientific problem and who contributed to deep scientific understanding of all students, including myself. I appreciate all the time you invested to guide me through the knowledge and I will always remember you as the "philosopher". You greatly contributed to my scientific development form a young, immature student to a critical and confident scientist. Lastly, I thank you for your contribution in this thesis as a member of my three-member committee.

Additionally, I would like to offer special thanks to Dr. Siden-Kiamos. As a master student I joined her laboratory and she was a co-supervisor on my main master thesis project. I learnt many things by her, including molecular techniques, presentation skills, writing skills and experimental design. She was a member of my three-member committee and she gave useful feedback and advice during all these years. Next, I would like to thank Dr. Monastirioti. She supervised me on *Drosophila* brain project. Her expertise and knowledge in that field was very important. Apart from technical support and sharing of protocols she generously gave scientific insights and help me organize and prioritize my work. Our interaction was very constructive for me and I would like to express my honest gratitude for that.

The next person I would like to thank is Prof. Rene Feyereisen. I feel very lucky for meeting him. Our first communication was via e-mail when he generously sent his advice and feedback. We then started a collaboration, during which he always shares his wisdom and knowledge on the field. His ideas and enthusiasm inspired me and gave me support. I will always be grateful for his insightful comments and suggestions and for advancing my conceptual and scientific knowledge!

I would like to offer my special thanks to Dr. Gouridis for his participation in my seven member committee and for his implication in one of my projects. With his deep knowledge on protein modeling and biophysics he gave useful feedback in one of my projects, specific scientific advice and directions and his contribution provided support to my work. Moreover, I would like to offer my special thanks to Prof. Chalepakis. He was part of my three- member committee during my master thesis and academic supervisor and member of my PhD committee too. All these years of interaction were very fruitful for me. He gave insightful comments and directions to my work, enhanced my scientific presentation skills and he was always polite and supportive! Next, I would like to express my sincere gratitude to Prof. Delidakis for being part of my committee. During these years of work in fly room at IMBB Prof. Delidakis generously shares his scientific knowledge with all the students, including myself. I would like to thank him for the useful discussions and insightful comments and for being always so approachable and willing to help! I am deeply grateful to Prof. Kalantidis and Prof. van Leeuwen who accepted to be members of my committee. They gave useful feedback and helped with the improvement of this thesis and they shared brilliant comments and suggestions during and after my PhD Defense.

Additionally, I cannot skip to acknowledge other people who contributed to the projects presented in this PhD. Dr. Ioannidis and Jason Charamis performed the RNAseq analysis and we worked great as a team. Panos thank you for the useful discussions, scientific explanations and directions you gave to this project. Jason, thank you for your scientific enthusiasm, your inspiration, your willingness to help and learn and for our great collaboration in LEGOmic project. Finally for all the other times I came to you with a question and you combined your knowledge and bioinformatics tools to help me answer it! Also, I would like to deeply thank Konstantinos Parasyris. Konstantinos started as a rotator student and continued as a master student working in the last chapter of this PhD under my supervision. Through our interaction I advanced my supervising skills and received valuable help and insights from a younger, motivated student. Konstantinos was willing and productive and we made much and quick progress as a team during the time he elaborated his master thesis! Thank you for your contribution and our collaboration! Chara Sarafoglou another master student in the laboratory contributed in this work performing protein modeling! Our interaction was great and productive and thanks to Chara's talent and detailed work we managed to make extra points in the projects she was involved and I am grateful for that! I would also like to thank all the fly room members and especially Yannis Livadaras for the injections in *D. melanogaster* embryos! Next, Dimitra Tsakireli, provided great support with the *in vitro* work of CYP4Gs and she provided great help as a lab manager! Finally, I would like to acknowledge all other IMBB and Biology Department members who shared protocols, materials and useful comments!!

I would like to extend my sincere thanks to all the lab mates, who shared this journey with me! Their support was unwavering! We went through happy moments and difficulties, we were a team and helped each other. I am deeply grateful for meeting you all!! Special thanks to lab-member-friends: George Samantsidis, Kelly Papapostolou, Dimitra Tsakireli, Sofia Balaska, Amalia Anthousi and Ioanna Kavelaki. I honestly feel you are the family I found here in Heraklion. We were together in the lab, in lab-breaks and also shared our personal time out of work! You shared my happy moments and filled them with your beautiful smiles and also you were supportive and consolatory when problems and difficulties arose.

Next, I would like to thank my friends! Chrysanthi, Katerina, Evangelia, Gioula, my cousins Argiro, Orestis, Maria and Yannis who are always by my side! I appreciate your presence in my life! Every moment with you is well-spend! Additionally, I would like to thank friends from Crete: all the people who were partners in my hobbies: volleyball, beach-volleyball, cross-fit training and dance! I am really grateful for interacting with you coaches, co-athletes and friends! You contributed in my balanced and happy every-day life! Special thanks to Giannis and Anna-Maria for our valuable friendship!

Last but not least, I would like to express my sincere gratitude to my family: My parents Antonis and Aleka who live in my home-town Chios and my sister Cleopatra who lives in Athens. Although we are physically separated, I feel they are always there to help and support me. My parents supported me during all these years I moved in Crete to study biology. They know it is the path I selected and are willing to do anything to help me make my dreams come true. My sister, my other half, is always by my side protecting and supporting me! These people are proud of me without really understanding my research achievements and seeing them flaunting my work is one more reason for eternally thanking and deeply loving them!

Περίληψη

Η ελονοσία είναι μία από τις πιο απειλητικές για τη ζωή λοιμώδεις ασθένιες και αποτελεί παγκοσμίως ένα σημαντικό ζήτημα δημόσιας υγείας, με την Αφρική να αντιμετωπίζει το μεγαλύτερο πρόβλημα. Έως τώρα την πιο αποτελεσματική μέθοδος καταπολέμησης της ασθένειας αποτελεί η χρήση χημικών εντομοκτόνων που στοχεύουν στα κουνούπια-φορείς. Απουσία όμως νέων σκευασμάτων, η κατανόηση της ανθεκτικότητας που έχει προκύψει έναντι στα υπάρχοντα εντομοκτόνα είναι υψίστης σημασίας. Ο έλεγχος ενήλικων κουνουπιών φορέων εφαρμόζεται σε ψεκασμένες επιφάνειες κατοικιών και με κουνουπιέρες εμβαπτισμένες με εντομοκτόνο. Βάσει αυτού του τρόπου καταπολέμησης τα πόδια των κουνουπιών αποτελούν τον πρώτο ιστό με τον οποίο έρχεται σε επαφή το χημικό ώστε να περάσει στον οργανισμό και να βρει το στόχο του. Είναι γεγονός ότι σε πληθυσμούς κουνουπιών από την Αφρική, που είναι ανθεκτικοί στα εντομοκτόνα, η εισχώρηση του γίνεται με βραδύτερο ρυθμό λόγω των παχύτερων εξωσκελετών που έχουν σχηματίσει. Ο εξωσκελετός, αποτελεί ένα μη κυτταρικό στρώμα, που εκείνεται πάνω από την επιδερμίδα και είναι πλούσιο σε δομικές πρωτεινες, χιτίνη και λιπίδια, κυρίως επιδερμικούς υδρογονάνθρακες (Cuticular Hydrocarbons, CHCs). Κατά τη διάρκεια της διδακτορικής διατριβής μου με τίτλο "Η αχίλλειος πτέρνα του κύριου φορέα της ελονοσίας *Anopheles coluzzii*" : I) ανέλυσα πόδια ανθεκτικών και ευαίσθητων στα εντομοκτόνα κουνουπιών, II) μελέτησα μία πρωτείνη-μεταφορέα της οικογένειας ABC (ATP-binding cassette) που εντοπίζεται στα πόδια των κουνουπιών, ως προς τη συμμετοχή της στην τοξικότητα που προκαλεί το εντομοκτόνο, III) μελέτησα ένζυμα που εμπλέκονται στη βιοσύνθεση των υδρογονανθράκων του εξωσκελετού του *Anopheles coluzzii* και της *Drosophila melanogaster*.

Αρχικά, εφαρμόστηκε συγκριτική ανάλυση μεταγραφώματος μεταξύ ποδιών ανθεκτικών και ευαίσθητων στα εντομοκτόνα κουνουπιών, καθώς και μεταξύ ποδιών κουνουπιών μετά από έκθεση σε εντομοκτόνα. Τα ευρήματα της ανάλυσης υποδεικνύουν ότι τα πόδια των ανθεκτικών κουνουπιών εμφανίζουν αυξημένη έκφραση ενζύμων αποτοξικοποίησης κάθως και δομικών πρωτεϊνών του εξωσκελετού. Επιπρόσθετα, από τη συγκριτική ανάλυση των ποδιών των κουνουπιών που είχαν υποστεί έκθεση στο πυρεθροειδές εντομοκτόνο δελταμεθρίνη με δείγματα ελέγχου που δεν είχαν υποστεί έκθεση, εντοπίστηκαν αρκετές πρωτεΐνες-μεταφορείς της οικογένειας ATP-Binding Cassette (ABC-μεταφορείς), υποδοχείς συζευγμένοι με G-πρωτεΐνες (G-Protein Coupled Receptors, GPCRS) καθώς και πρωτεΐνες δέσμευσης οσφρητικών ουσιών (Odorant Binding Proteins, OBPs) μεταξύ άλλων. Συγκεκριμένα, ασχολήθηκα με έναν ABC-μεταφορέα, της H υποοικογενειας (ABCH2), που εμφανίστηκε να υπερεκφράζεται στα πόδια έπειτα από έκθεση σε δελταμεθρίνη, δείχνταντας την εμπλοκή του στην τοξικοτητα που οφείλεται σε αυτή. Η RNAi σίγηση του μεταφορέα και η επακόλουθη έκθεση των κουνουπιών στο εντομοκτόνο είχε ως αποτέλεσμα την ολική σχεδόν θνησιμότητα των ανθεκτικών κουνουπιών. Εντοπίσαμε, εν συνεχεία, την πρωτεΐνη αυτή στα πόδια και τα κεφάλια (στις κεραίες, την προβοσκίδα και τα οσφρητικά αισθητήρια όργανα) και συγκεκριμένα στην επιδερμίδα τους. Εν συνεχεία, εφαρμόσαμε ανάλυση *in silico* με σκοπό τη μοντελοποίηση του μεταφορέα υποδεικνύοντας ότι πρόκειται για μόριο που φυσιολογικά δομείται ως ομοδιμερές προκειμένου να είναι λειτουργικό. Αυτή η παρατήρηση, επιβεβαιώθηκε μετά από τη λειτουργική *in vitro* εκφραση του μεταφορέα σε κύτταρα εντόμων. Έπειτα, πειράματα ελλιμενισμού (docking) για την εύρεση πιθανής αλληλεπίδρασης του μεταφορέα με τη δελταμεθρίνη έδειξαν ότι το μόριο αυτό αποτελεί

πιθανό προσδέτη, ενώ σίγηση του μεταφορέα στα κουνούπια είχε ως αποτέλεσμα την αυξημένη διείσδυση δελταμεθρίνης. Τα ευρήματα αυτά συνηγορούν σε πιθανό ρόλο του μεταφορέα ως αντλία εξόδου της δελταμεθρίνης από τον οργανισμό.

Λόγω της αυξημένης παρουσίας των υδρογονανθράκων του εξωσκελετού, στα πόδια των ανθεκτικών κουνουπιών, μελέτησα επίσης πρωτεΐνες-ένζυμα που εμπλέκονται στη βιοσύνθεσή τους. Αυτή λαμβάνει χώρα στα οινοκύτταρα, με τις μονοξυγενάσες του κυτοχρώματος της υποοικογένειας 4G (CYP4G) να καταλύουν την τελευταία αντίδραση αποκαρβονυλίωσης προς παραγωγή υδρογονανθράκων. Μελετώντας τις δύο CYP4Gs (AcCYP4G16 και AcCYP4G17) του *An. coluzzii*, έδειξα ότι εντοπίζονται σε διαφορετικές κυτταρικές περιοχές κατά την ανάπτυξη, ότι διαθέτουν και οι δύο δυνατότητα αποκαρβονυλίωσης και παραθέτω τα διαφορετικά προφίλ υδρογονανθράκων που η κάθεμια παράγει μετά από εκτοπική έκφραση τους στα οινοκύτταρα της *D. melanogaster*, με ταυτόχονη σίγηση του ενδογενούς γονιδίου (Dm*Cyp4g1*). Σύμφωνα με τα δεδομένα οι δύο CYP4Gs του *An. coluzzii* εμφανίζουν ελαφρώς διαφορετικές ικανότητες κατάλυσης υποστρωμάτων, μιας και οι *D. melanogaster* που εκφράζουν το *CYP4G17* διαγονίδιο παράγουν περισσότερους διμέθυλ-υδρογονάνθρακες, πολύ μακριάς αλυσίδας. Το χαρακτηριστικό αυτό μελετήθηκε και ως προς την ικανότητα των μυγών να ανταπεξέρχονται σε συνθήκες αποξήρανσης και τοξικότητας, με αυτές που παράγουν τους εν λόγω υδρογονάνθρακες να εμφανίζουν πλεονεκτήμα. Μιας και τα CYP4G ενζυμα δεν εντοπίζονται μόνο στα οινοκύτταρα αλλά και σε άλλους ιστούς, με το χαρακτηριστικό παράδειγμα της *D. melanogaster* CYP4G15 που εντοπίζεται στο νευρικό σύστημα, ασχολήθηκα επίσης με το χαρακτηρισμό αυτού του ενζύμου. Υποδεικνύεται ότι και αυτή η πρωτεΐνη δρα ως αποκαρβονυλάση και παρατίθεται το προφίλ υδρογονανθράκων που παράγει όταν εκφραστεί εκτοπικά στα οινοκύτταρα της *Drosophila*. Για τα τρία αυτά ένζυμα (AcCYP4G16, AcCYP4G17, DmCYP4G15) επιτεύχθηκε η λειτουργική *in vitro* έκφρασή τους σε κύτταρα εντόμων, κάτι που αποτελεί χρήσιμο εργαλείο για τη μελέτη και ανίχνευση της καταλυτικής τους ικανότητας σε διάφορα υποστρώματα. Τέλος, μιας και όλα τα ένζυμα της υποοικογένειας CYP4G, διαθέτουν μία επιπλέον, χαρακτηριστική πρωτεϊνική περιοχή, με αξιοσημείωτη παρουσία όξινων αμινοξέων, χρησιμοποίησα εργαλεία γενετικής τροποποίησης για την εκτίμηση της συνεισφοράς της στην, συνειφασμένη με τα οινοκύτταρα, απαραίτητη για τη ζωή λειτουργία των ενζύμων αυτών. Συγκεκριμένα, εφαρμόζωντας δύα διαφορετικές απαλειφές της περιοχής ενδιαφέροντος προέκυψαν δύο διαφορετικοί φαινότυποι: από τη μικρότερη απαλειφή προέκυψαν άτομα με ικανότητα επιβίωσης, ενώ από τη μακρύτερη όχι. Αυτά τα δεδομένα καταδεικνύουν ότι η συγκεκριμένη περιοχή επιτελεί σημαντικό ρόλο στη λειτουργία του ενζύμου, πιθανά μέσω αλληλεπιδράσεων με άλλες πρωτεΐνες ή λιπιδικά υποστρώματα.

Στο σύνολό της αυτή η διδακτορική διατριβή συνηγορεί στην κατανόηση των ποδιών των ανθεκτικών στα εντομοκτόνα κουνουπιών, αφενός παρέχοντας μία συγκριτική ανάλυση δεδομένων μεταγραφώματος και αφετέρου εμβαθύνοντας στους μηχανισμούς που διέπουν τους ανθεκτικούς φαινοτύπους, μέσω της μελέτης μια πρωτεΐνης-μεταφορέα των ποδιών και συγκεκριμένων βιοσυνθετικών ενζύμων των επιδερμικών υδρογονανθράκων, που βρίσκονται σε μεγάλα ποσοστά στα πόδια. Η γνώση αυτή συνεισφέρει στον εντοπισμό της αχιλλείου πτέρνας των κουνουπιών-φορέων της ελονοσίας, ώστε να αντιμετωπιστεί η ανθεκτικότητα , βελτιώνοντας τον έλεγχο των φορέων.

Abastract

Malaria is one of the most life-threatening infectious diseases representing a global health concern, with Africa carrying the vast burden. The most effective tools against malaria are insecticides; yet their scale up has resulted in severe insecticide resistance. In the lack of new compounds understanding insecticide resistance molecular mechanisms is fundamental. Based on vector control implementation, legs comprise the first tissue the insecticide bypasses to enter the body. Interestingly, African resistant populations have slower insecticide penetration due to their thicker cuticles. Cuticle, the insect exoskeleton, is a non-cellular layer above the epidermis rich in cuticular proteins (CPs), chitin and lipids, mainly cuticular hydrocarbons (CHCs). During my PhD entitled "The Achilles heel of the malaria vector *Anopheles coluzzii'* : I) I analyzed the legs of insecticide resistant *An. Coluzzii* compared to susceptible controls, II) studied role of an ATP-Binding Cassette (ABC-transporter) leg transporter in insecticide toxicity and III) provided insights into enzymes implicated in CHC biosynthesis in *An. coluzzii* and *D. melanogaster*.

Comparative transcriptome analyses of legs from resistant and susceptible mosquitoes and transcriptome analysis of induced legs with deltamethrin (widely-used insecticide) were performed. The findings highlighted that legs of resistant mosquitoes have cuticles, with enhanced expression of cuticular proteins CPs and elevated detoxification processes. Additionally, transcriptomic data of deltamethrin-induced mosquitoes, underlined the divergent response upon insecticide induction with plethora of up-regulated genes including ABC transporters, G-protein coupled receptors (GPCRs) and odorant binding proteins (OBPs) among others. Interestingly, an ATP-binding cassette transporter (ABCH2), up-regulated upon induction was shown to be involved in deltamethrin toxicity. RNAi-silencing followed by deltamethrin toxicity assays almost completely restored susceptibility of the resistant mosquitoes. We found ABCH2 mainly in legs and head appendages and specifically on apical epidermis. Additionally, we provided evidence on the dimeric nature of this half-transporter, based on *in silico* modelling and *in vitro* data both indicating that it most probably acts as a homodimer. Further, protein-ligand docking analysis, demonstrate that deltamethrin could be a potential substrate, while silencing this gene in mosquitoes followed by deltamethrin exposure, results in increased penetration of insecticides. These lines of evidence suggest that this transporter is implicated in deltamethrin toxicity, perhaps via pumping out deltamethrin.

As CHCs are enhanced in resistant mosquito legs, I studied proteins implicated in their biosynthesis. This takes place in oenocytes, where cytochrome P450 enzymes of 4G family (CYP4Gs) catalyze the last decarbonylation step. We provided the distinct developmental localization patterns of the two *An. coluzzii* CYP4Gs (AcCYP4G16 and AcCYP4G17), revealed they act as decarbonylases and provided their CHC blends by ectopically expressing them in *D. melanogaster,* while simultaneously silencing the endogenous oenocyte gene (Dm*Cyp4g1*). The data revealed that *An. coluzzii* CYP4Gs, both exhibit slightly different substrate specificities, with flies expressing *CYP4G17* transgene producing more dimethyl-branched hydrocarbon species. This feature was studied in respect to desiccation and toxicity and the aforementioned flies were shown to cope better with these stresses. Since, CYP4Gs are not only found in oenocytes, with the most characteristic example *D. melanogaster* CYP4G (DmCYP4G15), previously reported in larval heads/brains, we were interested in characterization of this enzyme too. We revealed its decarbonylase activity and the distinct

CHCs it produces when ectopically expressed in oenocytes. CYP4Gs of interest (AcCYP4G16, AcCYP4G17, DmCYP4G15) were also functionally expressed in insect cells using *Baculovirus* system. This is a valuable tool for *in vitro* substrate screenings. Finally, as all CYP4Gs share a specific, acidic-rich insertion, with unknown contribution to CYP4G function, I generated tools using reverse genetics in *D. melanogaster* to study its contribution in essentiality. The two deletions we generated, resulted in different phenotypes; the short one resulted in survival, while the longer one in mortality. These results perhaps dictate an essential region on this loop, which probably mediates useful interactions with proteins or with the lipid substrates.

Overall, the thesis supports the understanding of the legs of resistant mosquitoes providing an informative, comparative dataset (RNA sequencing data) and going deeper into the mechanisms underlying the resistance phenotype by studying a leg transporter and biosynthetic enzymes of the cuticular hydrocarbons which are the major components of *An. coluzzii* leg epicuticles. This knowledge may contribute to identifying the Achilles' heel of the major malaria vector, to tackle insecticide resistance and improve vector control.

General Introduction

Malaria: a huge public health problem

Malaria is considered one of the most life-threatening infectious diseases [1]. Its name from the medieval Italian phrase “mala aria” which literally translates to “bad air”, derives from the initial association of the disease with the miasmas evaporated by swampy and marshy areas, by ancient populations [2]. From the second half of the nineteenth century, when malaria received its first attention from scientific perspective [2] and until today the disease represents a major global health problem with tropical and sub-tropical regions carrying the vast burden [3]. According to the last annual malaria report of the World Health Organization (WHO), malaria cases are estimated to be 241 million during 2020 globally, while malaria deaths annually are almost half a million [4]. Characteristically, residents of poorest countries encounter deaths from malaria, especially children under 5 years of age in Sub-Saharan Africa [5].

Africa encounters the vast malaria burden

According to the World Health Organization (WHO) and the last malaria report, during 2020 241 million malaria cases occurred, a number increased compared to the previous year (227 million cases in 2019) [4]. Remarkably 95% of these concerns WHO African region, with the increase also being attributed to this region [4]. Malaria deaths during 2020 were 627.000, an increased number by 12% compared to 2019 due to service disruptions caused by the COVID-19 pandemic, with 602,000 of them happening in WHO African Region [4]. It is remarkable that 77% of the deaths concern children aged under 5 years [4]. In 2000 the number of malaria cases was 268 per 1000 population at risk, while two decades later this number was decreased to 232. The malaria mortality rate halved from 2000 to 2015 and continued to decrease but slower. However, in the last two years (2020) an increase is observed. 29 countries globally carry that burden with six African countries (Nigeria, Democratic Republic of the Congo, Uganda, Mozambique, Angola and Burkina Faso) encountering more than half of these deaths [4].

Malaria parasite life cycle (Human-Parasite-Mosquito)

Malaria infection is caused by pathogens of *Plasmodium* genus. Six *Plasmodium* species threaten humans [3]: *P. falciparum*, *P. vivax*, *P. malariae*, *P. knowlesi*, *P. ovale wallikeri*, *P. ovale curtisi.* The first two species have as exclusive mammalian host the humans [1]. Typical symptoms are fever, headache and chills, with *P. falciparum* and *P. knowlesi* also causing severe disease manifestations such as anemia, seizures, acidosis and respiratory distress or affect multiple organs in adults and result in death [6].

Between vertebrate and invertebrate host the life cycle of *Plasmodim* is differentiated, with asexual blood cycle (schizogony) taking place to the former and sexual cycle (sporogony) to the latter with the parasite taking many forms [7, 8].

- ***Plasmodim* life cycle into vertebrate host (human host):** Parasites are transmitted to humans when female mosquitoes of *Anopheles* genus take a blood meal and inject the parasites together with their anticoagulating saliva. The parasites (sporozoites) enter the blood stream and within 30-60 minutes they infect hepatocytes, where they mature into schizonts. Schizonts contain thousands of merozoites which are the invasive forms entering into erythrocytes after liver cell rupture. Concomitant to the erythrocyte ring-forms are the trophozoites which are further differentiated into schizonts containing daughter merozoites, able to invade new red blood cells. 4-8 hours after red blood cell invasion the symptoms of the disease are developed. The asexual reproductive stage is the symptomatic. As merozoites' replication lasts 36-72 hours (invasion-haemolysis), fever occurs every 36-72 hours. Male and female gametocytes, which are the sexual forms of the parasites are formed within erythrocytes, which they next concentrate in skin capillaries [3, 7, 9].

- ***Plasmodium* life cycle into invertebrate host (mosquito vector):** The sexual parasite stages produced in the erythrocytes of the vertebrate host are ingested by mosquitoes during a blood meal. Sexual fertilization takes place into the mosquito midgut. Three rounds of mitosis of male gametocytes result into eight microgametes. These are motile forms with flagella that fuse to female macrogamete resulting into zygotes. This process takes place only in the invertebrate host. Ookinetes are motile, elongated zygotes and they traverse the midgut epithelium to exit from the lumen and be eventually transformed into oocysts. Oocysts reside underneath the extracellular matrix and undergo replication cycles until their maturation (~10 days), where sporozoites are formed and are released into the hemolymph. Circulating sporozoites invade salivary glands via protein-interactions, where they are stored until the mosquito takes a blood meal and injects them into the vertebrate host [3, 7, 9-11].

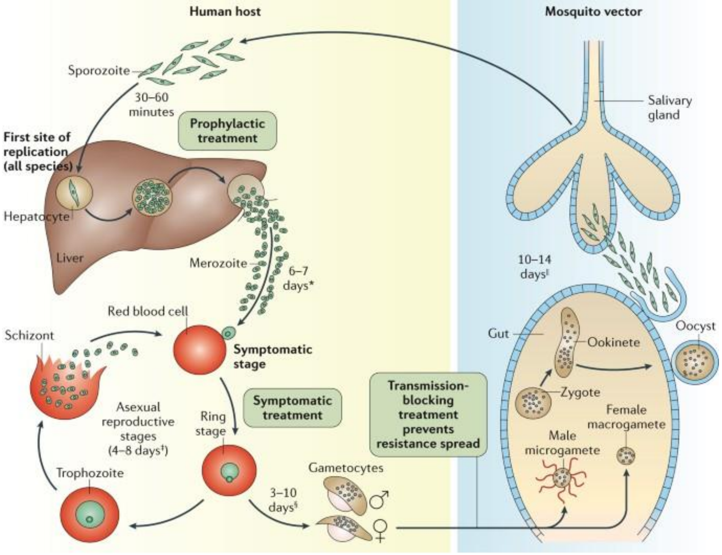
Human host
Mosquito vector
Sporozoite
30–60 minutes
Prophylactic treatment
First site of replication (all species)
Hepatocyte
Liver
Merozoite
6–7 days*
Red blood cell
Schizont
Symptomatic stage
Asexual reproductive stages (4–8 days†)
Ring stage
Symptomatic treatment
Transmission-blocking treatment prevents resistance spread
Trophozoite
Gametocytes
3–10 days§
♂
♀
Salivary gland
10–14 days‖
Gut
Ookinete
Oocyst
Zygote
Female macrogamete
Male microgamete

Nature Reviews | Disease Primers

Figure 1. *Plasmodium* life cycle into human host (left) and mosquito vector (right), from [3].

Mosquitoes are responsible for malaria transmission

Mosquitoes are responsible for epidemics and outbreaks [12], as the majority of them have zoophilic and/or anthropophilic behavior and hence they transmit pathogens, worms and arboviruses to reptiles and mammals including humans [13], passing along to subsequent bites the virulent microorganisms ingested from their blood meals [6]. Mortality and morbidity owing to mosquito-borne diseases are very high [6]. Some of the most common mosquito-borne diseases are malaria, dengue fever, zika, chikungunya, filariasis, yellow fever, west Nile virus and encephalitis [6]. Mosquitoes are a large insect group from the Culicidae family. They are classified into two subfamilies: Anophelinae and Culicinae, both including 41 genera which are further divided into 3.567 valid species [12]. The *Anophelinae* subfamily is divided into three genera: *Anopheles* (Cosmopolitan), *Bironella* (Australian) and *Chagasia* (Neotropical) [14].

Anopheles mosquitoes transmit both malaria and filariasis and is the genus that has affected more human lives than any other insect [15]. Due to its great epidemiological importance it is also the most studied genus among mosquitoes [15]. The majority of the Anophelinae species belong to genus *Anopheles* [14]. More specifically, *Anopheles* genus includes 465 formally-named species, of the 537 known, divided into seven subgenera (*Anopheles*, *Cellia*, *Kereszia*, *Nyssorhynchus*, *Lophopodomyia*, *Baimaia* and *Stethomyia*). Species that transmit *Plasmodium* parasites are included in the first four subgenera [15]. The malaria vector species are more than 70 [16] and are further grouped in complexes of sibling species [15]. Apart from the recognized species there are also more than 50 unnamed members of species complexes [16].

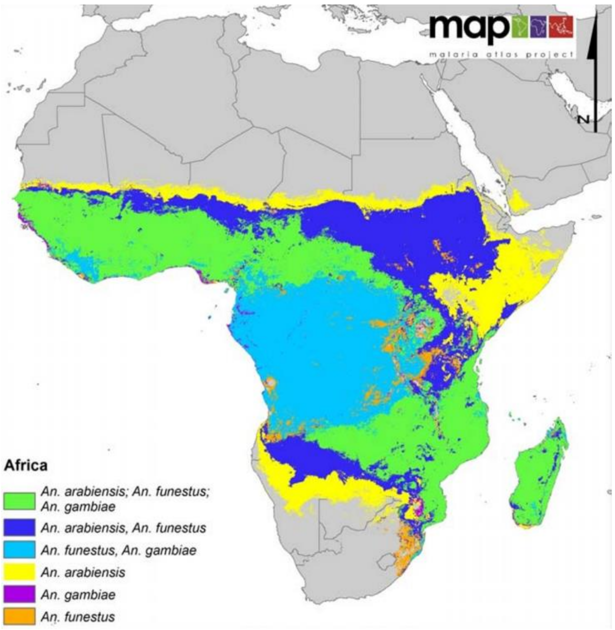
map
malaria atlas project
N
Africa
🟩 An. arabiensis; An. funestus; An. gambiae
🟦 An. arabiensis, An. funestus
🟦 An. funestus, An. gambiae
🟨 An. arabiensis
🟪 An. gambiae
🟧 An. funestus

Figure 2. The distribution of the most dominant *Anopheles* malaria vectors across Africa, from [17].

The *Anopheles gambiae* complex, contained six cryptic species when initially described, distributed across sub-Saharan Africa. These are *An. gambiae sensu stricto*, *An. arabiensis*, *An. bwambae*, *An. melas*, *An. merus* and *An. quadriannulatus* [18] and are morphologically indistinguishable, and discriminated by other *An. gambiae sensu lato (An. gambiae* in the wider sense) populations via subsequent hybrid sterility among crosses [18]. Later, additional *Anopheles* species were described: *An. comorensis*, *An. amharicus* and *An. coluzzii* [18, 19]. The latter was described as separate species on the basis of an X-linked molecular marker [18, 19]. *An. gambiae* were known to naturally exist as two sympatric and distinct populations named "M" and "S" forms [19]. The *An. gambiae* "M form" was named *An. coluzzii*, while the "S form" retained the name *An. gambiae Giles* [19]. *An. gambiae sensu stricto*, *An. coluzzii* and *An. arabiensis* are major malaria vectors, exhibiting the broadest geographical distribution of all nine species [18]. The first whole-genome mosquito sequence was that of *An. coluzzii*, although described then as *An. gambiae* [20]. The original strain used was an *An. gambiae*/*An. coluzzii* hybrid, including the *An. coluzzii* X-linked molecular marker, hence it is technically the *An. coluzzii* sequence [18]. Although they exhibit reproductive isolation in certain degrees due to assortative mating and reduced fitness of the hybrids, often isolation periods are interrupted by hybridization events with abrupt presence of F1 progeny [19].

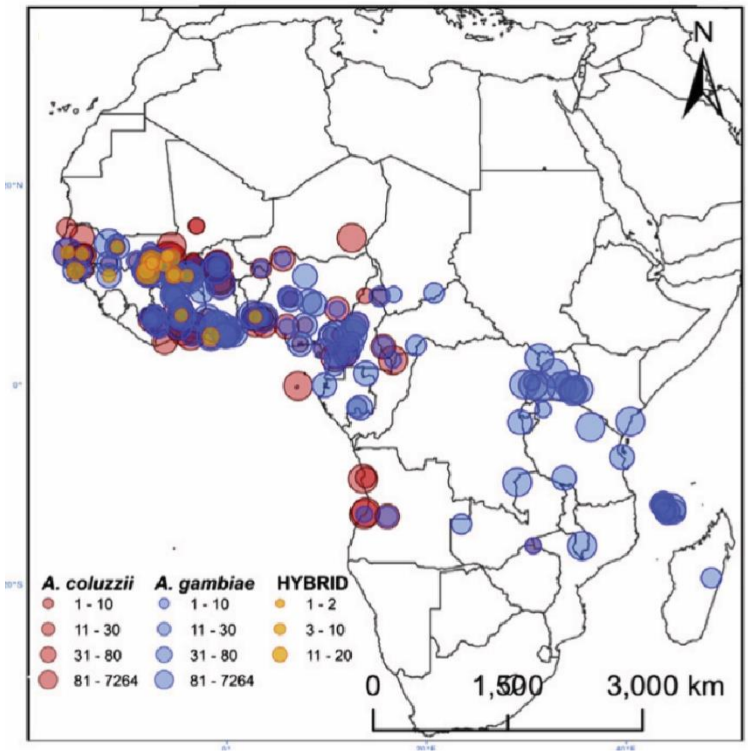

Figure 3. The geographical distribution and relative abundance of *An. gambiae s.s., An. coluzzii* and their hybrid in Africa, adapted from [19].

Like all insects, mosquitoes possess three pairs of legs and like all Diptera a single pair of wings and their body is divided into three main parts: head, thorax and abdomen [21]. The head includes the eyes, the elongated proboscis used for feeding, two sensory palps and the antennae useful for detecting odors, hence this part is essential for feeding and acquiring sensory information [21]. The three leg pairs, the single wing pair and the halters are attached on the thorax, so this body part is required for locomotion. The abdomen is a segmented body part containing the organs which are useful for food digestion and egg productions [21]. In particular morphological differences of *Anopheles* mosquitoes which discriminate them from other mosquitoes are their sensory palps which are as long as their proboscis, the discrete blocks of black and white scales on their wings, as well as their resting position, which is characteristic both for males and females; they do not rest parallel to the surface rather than their abdomens stick up in the air [21]. Concerning their life stages Anophelinae go through the aquatic and the aerial phases, like all mosquitoes. The former includes the eggs, the larva and the pupa stages and last 5-14 days depending on the species and the environmental conditions and the latter refers to the adults [21]. Both adult males and females feed on sugar sources for energy but adult females require a substantial blood meal for their egg development [21]. In particular, *An. coluzzii* feeds at night and are either endophagic (i.e. they feed indoors) or exophagic (i.e. they feed outdoors)[21]. After their blood meal females rest for 2 to 3 days, when the blood is digested and the eggs are developed [21]. Fertilized eggs begin embryonic development which lasts 2-3 days [22]. In *An. coluzzii* and all mosquito species in general there are four larval stages (instars), when larval organs are functional and adult organs start to develop slowly. Fourth-instar larvae are transformed to pupae and pupae into adults (metamorphosis)[22]. During this process some larval organs persist or grow, while some others are histolysed [22].

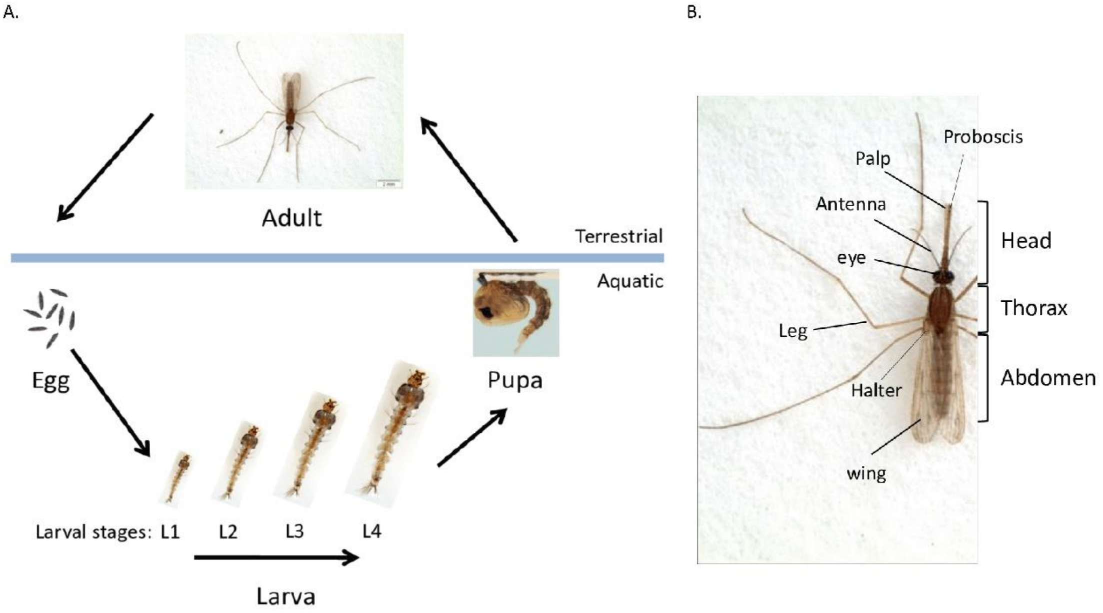

Figure 4. A. Stages of *Anopheles* mosquito life cycle, B. Anatomy of *Anopheles* adult mosquito, adapted from [23].

Malaria prevention heavily relies on controlling mosquito vectors through the use of insecticides

The World Health Organization (WHO) has recommended malaria prevention tools and strategies to reduce the global malaria threat [4]. These include:

- Preventive chemotherapies: These therapies rely on the use of medicine alone or in combination and include prevention in infants and pregnant women, mass drug administration and seasonal malaria chemoprevention [4]. They mainly complement other strategies. There are several approved antimalarial drugs, belonging to different classes, and are administrated as first-line treatment [24] to prevent progression to severe disease and recrudescence [8]. These are cinchona alkaloids (quinine and quinidine) and artemisinin derivatives [8]. Artemisinin led to a shift in antimalarial therapy from quinolone-based compounds [25]. Artemisinin-based combination therapy (ACT), is based on a artemisinin derivative which rapidly clears blood parasites combined with a long acting antimalarial which kills the remaining ones [8]. It is recommended by WHO for *Pl. falciparum* infections [25]. Apart from that artemisinin derivatives generated a new direction in antimalarial drug development, with antiparasitic drugs with similar structure currently being under development [25]. However, drug resistance occurred due their extensive usage [4].

- Vaccines: Although early attempts to generate a malaria vaccine were done (1930s) there was not an effective licensed vaccine against malaria during all these decades of malaria threat[4, 5]. Malaria vaccine research faced many challenges[5]. First trials using inactivated or killed parasites resulted to immunization failure [5]. Additionally, these limitations include the more complicated parasite life cycle comparing to viruses and bacteria, meaning distinct immunogenicity among different stages, the low infrastructure in malaria endemic countries which discourages vaccine manufacturers and the stringent and costly regulations regarding licensing which require funding support by non-government organizations and public-private partnerships [26]. Vaccine development efforts using model malaria systems, such as rodents-parasites were more promising exhibiting some efficacy and currently optimization efforts for improved efficacy are performed. Synthetic antigen peptide technology around 1980s was more challenging than initially thought due to specificity issues during the parasite life-cycle and parasite antigenic diversity [5]. While candidate antigenic vaccines have been developed in the laboratory the long phase 1 testing process to reach phase 2 field trials in target populations and the high financial support requirements for this arduous process hindered malaria vaccine development [5]. The first malaria vaccine, targeting *P. falciparum* sporozoites (pre-erythrocytic vaccine), was RTS.S/AS01 (brand name Mosquirix). It was approved for children immunization in phase III trial (2009-2014), albeit exhibiting transient protection to children and infants in sub-Saharan Africa pilot program [27, 28]. Its low efficacy is owed to multiple factors. The efficacy has been shown to culminate in older children but it wanes with time and it is even lower in genetically diverse parasites [26]. Currently a next-generation RTS,S vaccine (R21) has been developed with the intent to overcome some of the aforementioned limitations [26]. After many decades there is a recommended malaria vaccine (since October 2021) targeting *P. falciparum* malaria transmission and recommended only in young children in regions with moderate or high risk [4].
- Diagnostic testing: Early diagnosis of the disease through microscopy or rapid diagnostic tests (RDT) reduces the risk of malaria transmission and prevents deaths via early treatment. These are immunochromatographic flow devices, which offer qualitative diagnosis based on the detection of *Plasmodium* antigens on patients' blood [29].
- Vector control: It is the component with the greater impact on malaria control, as it is highly effective both in preventing infection and in reducing transmission [4]. Core interventions for malaria vector control are Long-Lasting Insecticide Mosquito Nets (LLINs), also mentioned as Insecticide-treated net (ITNs), and Indoor Residual Spraying (IRS)[4]. These two, target the indoor biting-resting behavior: LLINs both create a physical barrier between the host and the vector and kill, deter and irritate the latter due to the fact that they are insecticide-impregnated and IRS involves application of long-lasting insecticide on the interior surfaces of houses to target indoor resting vectors post feeding [30, 31]. Insecticides, applied in IRS and ITNs, in combination with artemisinin-based treatment were the cornerstone for malaria control which was especially successful during the first 15 years of the millennium [32]. Continuous international financing for malaria prevention enabled the scale-up of these control interventions and resulted in 40% reduction in clinical incidences between 2000 and 2015 and total aversion of approximately 663 million clinical cases in these 15 years in Africa. Remarkably, 68% of the cases averted is attributed to ITNs increasing

coverage , which was the most important intervention [32]. Noteworthy, 1.7 billion malaria cases and 10.6 million deaths have been averted during the last two decades [4]. These numbers correspond to reduction in Africa by 82% and 95% respectively [4]. Noteworthy, during the period of malaria aversion almost 2 billion of ITNs were distributed in sub-Saharan Africa [4], hence the success is mainly attributed to insecticide-based vector control measurements.

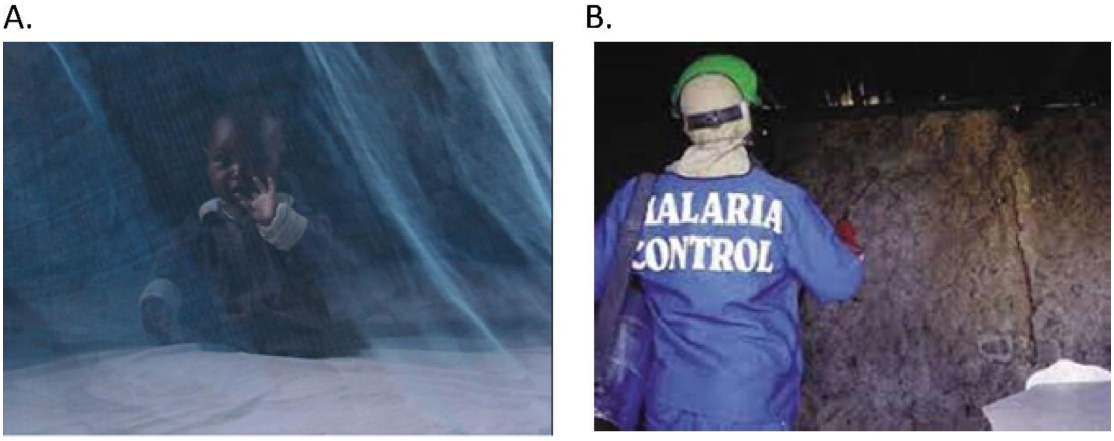

Figure 5. A. Insecticide-treated bed-nets, B. Indoor residual spraying, from National Geographic and World Health Organization.

These core interventions which take into consideration the biology and behavioral characteristics of the vectors are of major importance[33]. Repeated blood-feeding of *An. coluzzii* adult females and their extreme anthropophilic behavior have led malaria control campaigns around human habitations [22].Many of the most dangerous malaria vectors, including *An. coluzzii* blood feed at night and indoors and rest on surfaces after feeding to digest their meal [33, 34]. Targeting larval stages is also a solution for controlling vectors[35]. This involves habitat modification or manipulation, larvicide application and introduction of natural predators for larval killing [35]. Large in number, dispersed and constantly changing breeding sites have made larval source management challenging or even impossible to implement[36].

Insecticides are of chemical (synthesized) or biological origin (plant extracts or microbial products)[37] and are used for insect control and killing both for pest control in agriculture and forestry and for targeting vectors, such as mosquitoes and other insects [37]. Due to their divergent structures and consequent interactions with different targets (enzymes, receptors) they differ on how they exert toxicity [37]. A common insecticide classification is based on their mode of actions [37]. Similar structures usually advocate similar mode of actions and physicochemical properties, however different compounds exhibit divergent biological and environmental characteristics [38]. These are selectivity for pests, degradation products, persistence and unique physicochemical properties , such as aqueous solubility and volatility with varying rates of degradation and dissipation processes [38]. According to Insecticide Resistance Action Committee (IRAC) mode of action classification insecticides are categorized to five main groups: a) Nerve and muscle targets, b) growth and development targets, c) respiration targets, d) midgut targets and e) unknown or non-specific targets [39] (Figure 1.6).

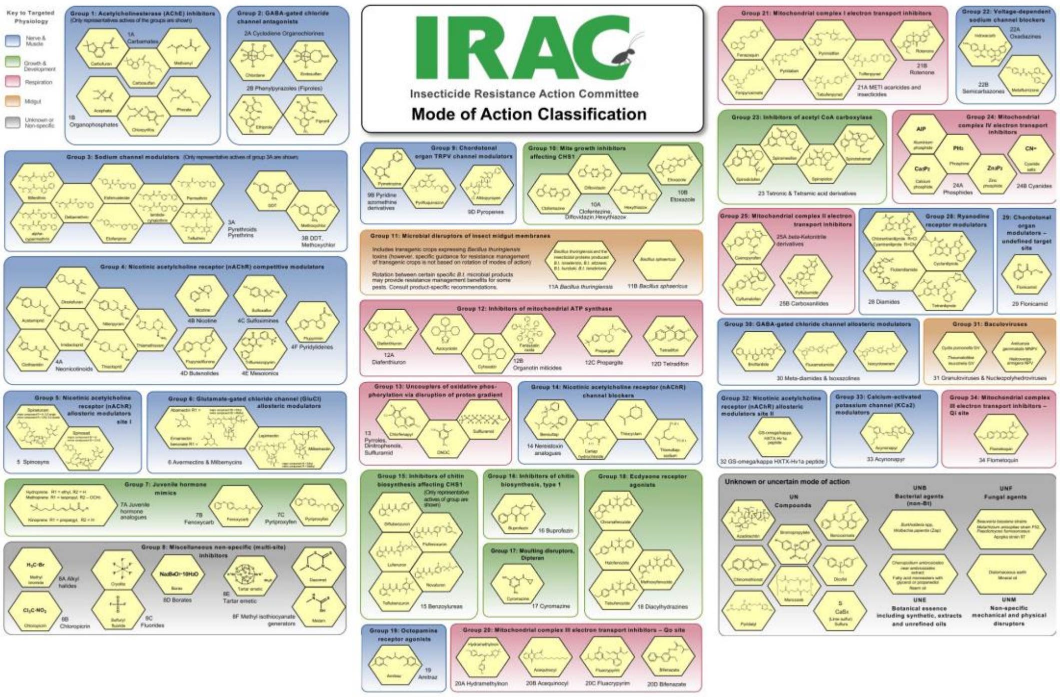

Figure 1.6. The IRAC mode of action (MoA) insecticide classification. Blue: Nerve and muscle insecticide groups, Green: Growth and development insecticide groups, Pink: Respiration insecticide groups, Orange: Midgut insecticide groups, Grey: Unknown and non-specific insecticide groups, from [39].

Among all insecticides nerve-muscle targets include more groups than any other category (10 groups) ,account for 85% of the value among all other classes and are fast-acting [39]. One group of this category includes acetylcholinesterase (AChE) inhibitors, where organophosphates (OPs) and Carbamates (CMs) belong. Both OPs and CMs are esters, the former of phosphoric or phosphonic and the latter of carbamic acids, targeting acetylcholinesterase (AChE) enzyme [37]. OPs cover 50% of the worldwide insecticide use [37]. GABA-activated chloride channel blockers consist another group including cyclodiene organochlorines and phenylpyrazoles (fiproles). These chemical molecules antagonize GABA post-synaptic receptor binding, causing neuronal stimulation, hyperexcitation and convulsions [37]. The third IRAC group consists of Sodium channel modulators where pyrethroids, pyrethrins and the chlorinated hydrocarbons dichlorodiphenylethanes (DTT and methoxychlor) belong [39], which decrease action potentials in the peripheral neurons and brains by affecting Na+ influx and K+ efflux hence leading to paralysis [37]. Voltage-dependent sodium channel blockers, are a separate group including indoxacarb and metaflumizone [39]. Another group of nerve-muscle targets is composed of nicotinic acetylcholine receptor (nAChR) competitive modulators, and its members are neonicotinoids, nicotine, sulfoxaflor and butenolids. Neonicotinoids are a relatively new insecticide class, including imidacloprid, acetamiprid, thiacloprid, dinotefuran, netenpyram, thiamethoxam and clothianidin [37]. The risk for non-target organisms is relatively low while their insect specificity is high [37]. They account for 20% of the global insecticide market [37]. Neonicotinoids act on central nervous system (CNS) postsynaptic nicotinic acetylcholine receptors (nAChRs) eventually blocking nerve propagation [37]. Their selectivity towards insects lies on the distinct binding properties they exhibit to insects and mammals, with high affinity against insect receptors and low affinity against the vertebrate receptors of various subtypes [37]. Nicotinic acetylcholine receptor allosteric modulators are a separate group including spinosyns (spinosad, spinetoram) and they allosterically activate nAChRs causing neural hyperexcitation [39]. Other allosteric modulators target glutamate-gated chloride channel which cause paralysis by activating this channel. In this group avermectins and milbemycins belong [39]. Nicotinic acetylcholine receptor (nAChR) channel blockers including nereistoxin analogues, modulators of chordotonal organs (flonicamid, pymetrozine), octopamine receptor agonists (amitraz) and ryanodine receptor modulators (diamides) also belong to the nerve and muscle insecticide class[39].

Pyrethroids are the main insecticides used for malaria vector control

Pyrethrins are extracts of *Chrysanthemum cinerariaefolium* while the "pyrethroid" term is used to describe their synthetic derivatives [37]. This class has been used extensively in agricultural, public and residential setting applications [37]. Pyrethrin insecticidal properties had been observed in ancient Asian populations, while the first pyrethroids were developed in 1960s. Their second generation was improved in terms of mammalian toxicity and included deltamethrin, permethrin and cypermethrin [37]. Permethrin is a chlorinated derivative of chrysanthemic acid, while deltamethrin has a unique bromine substituent [40]. They primarily act on the α subunit of the voltage-gated sodium channel and cause its permanent opening, resulting into a permanent sodium ion influx [40]. They also affect chloride and calcium channels of sensory nerve endings, leading to cell hyperexcitation. Additionally pyrethroids are lipid soluble and the degree of their penetration depends on the permeability of the barrier [40]. Most pyrethroids exhibit neurotoxic effects primarily due to interaction at voltage-gated sodium channels with 100 time higher sensitivity in insect isoforms compared to mammals, providing an explanation about their low mammal and bird toxicity [37]. Apart from low mammalian toxicity pyrethroids possess some other important characteristics which make them successful insecticides, accounting for more than 25% of the global market and these are their low environmental persistence, their high insecticidal potency and their broad-spectrum activity [37]. They consist of a central ester bond an alcohol moiety and an acid moiety with two chiral carbons (cis and trans)[41]. Based on cis or trans stereoisomeric forms they are classified into two classes: Type I and type II pyrethroids [37, 41]. In insect control mixtures of cis and trans stereoisomers are used [40].

For years, deltamethrin and/or permethrin pyrethroid insecticides use was recommended in anti-malarial programs [40]. More specifically, indoor residual spraying (IRS) programs were conducted only with pyrethroids until recently, when organophosphates and carbamates were also approved, while for bednets only pyrethroid insecticides are approved so far [42, 43]. The reason why pyrethroids are preferred as opposed to other insecticide classes in such applications is that their usage in recommended concentrations is very little or not at all hazardous to people treating the nets or those using them [44]. Frequent exposures to low pyrethroid concentrations are linked with low risk of toxicity [44]. Due to the emergence of insecticide resistance (discussed in detail below), since 2017 WHO approved piperonyl butoxide (PBO)-pyrethroid bed-nets, as PBO acts synergistically with the insecticide [45]. This next generation of LLINs, is currently under evaluation with the first results showing greater entomological and epidemiological efficacy compared to standard nets [45].

Insecticide resistance threatens vector control

The extensive use of insecticides has led to severe insecticide resistance. During 2010-2020 88 countries reported data concerning insecticide resistance for *Anopheles* mosquitoes to WHO [4]. Of these 85 are malaria endemic, while 78 confirmed resistance to at least one malaria vector species [4]. Globally, pyrethroid resistance was detected in at least one malaria vector in 87% of the countries [4].

Insecticide resistance according to the Insecticide Resistance Action Committee (IRAC) is defined as a heritable change in the sensitivity of a pest population that is reflected in the repeated failure of a product to achieve the expected level of control when used according to the label recommendation for that pest species [46]. Due to its genetic basis, resistance results from selection of one or more genetic characteristics (heritable) upon selection pressure (insecticide exposure) of a population. Individuals which survive the insecticide exposure owing to this characteristic reproduce and upon constant application of the same insecticide the genetic modification(s) providing this advantage will become more prevalent and will eventually be fixed in the population which will be resistant against this compound [46](Figure 7). It should be noted that there are two mechanisms by which the organisms can reduce their sensitivity to xenobiotics [47]. The first is the adaptation which takes place at population level and involves alterations in its genetic constitution, so as more individuals surpass the toxic effects of the chemical/xenobiotic (resistance) and the second is the process happening at the individual level via acclimatory process involving genetic or epigenetic alterations not transmitted to next generations and this is termed tolerance [47]. Another term, “induction”, refers to the response after sub-lethal or low dose exposure to an insecticide or a xenobiotic and is also not passed on to offspring [47]. The adaptation mechanism acts at the population level and in order to occur the resistant alleles must be present in the population [47]. The selection process will be slower if the genetic characteristic is rare or at low prevalence in the population [46] while the volume and frequency of insecticide application in combination to the insect characteristics determine the amount of resistance [48]. The life cycle of the insect, reproduction rate, number of progeny, migration rates and intrinsic characteristics of the resistant genes (such as dominance or associated fitness cost) in combination with operational characteristics (frequency, dosage) are factors that influence development of insecticide resistance [46, 49]. Mosquitoes are insect species with a short life cycle and abundant progeny, characteristics which favor rapid insecticide resistance occurrence [48]. The first insecticide introduced for vector control was DTT in 1946 [48] with the first cases of DTT resistance reported one year later in *Aedes* species, while six years later *An. sacharovi* DTT resistance was reported in Greece [50]. More than a hundred concomitant resistant cases among mosquito species have been reported so far, with more than 50% of them belonging to *Anopheles* genus[48].

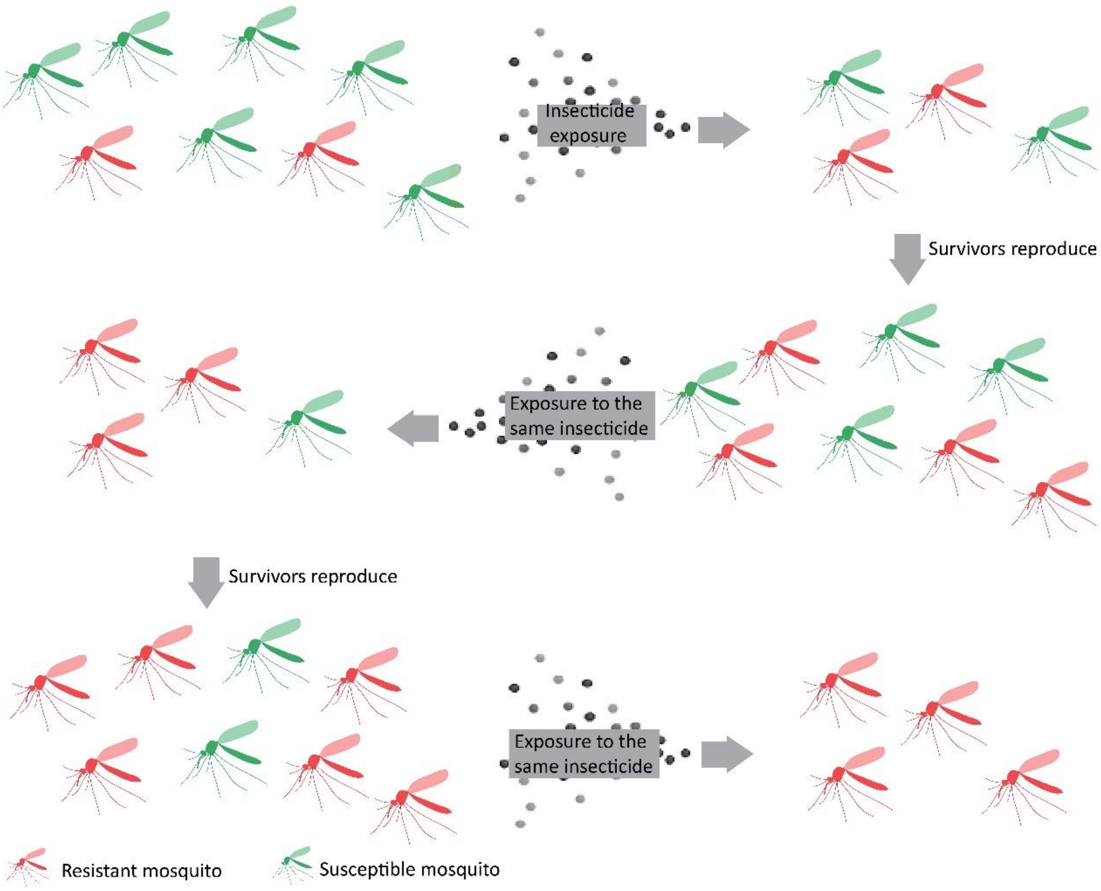
Insecticide exposure
Survivors reproduce
Exposure to the same insecticide
Survivors reproduce
Exposure to the same insecticide
Resistant mosquito
Susceptible mosquito

Figure 7. Schematic illustration of resistance development in a mosquito population after a series of exposures to the same insecticide, modified from [46].

Resistance in malaria vectors has been detected to pyrethroids, organochlorines, organophoshates and carbamates (Figure 8) [43]. Especially for pyrethroids the heavy reliance on this specific insecticide class exclusively in bed-nets and to a large extend in IRS [43], resulted in dramatic levels of insecticide resistance in countries encountering the vast malaria burden. Resistance against pyrethroids was initially identified in 1970s in African *Anopheles* mosquitoes [51, 52] due to their agricultural usage, and currently, due to their extensive usage in malaria control it is highly increased both in geographical distribution and in intensity [42]. Characteristically, it is hard to detect a pyrethroid susceptible *An. gambiae s.l.* population [42] (Figure 8). Heavy reliance on pyrethroids for mosquito control in combination with the fact that the general pesticide market has used the same chemicals for wide scale applications for many decades has led to severe insecticide resistance in existing compounds, hence representing huge public health concerns [53].

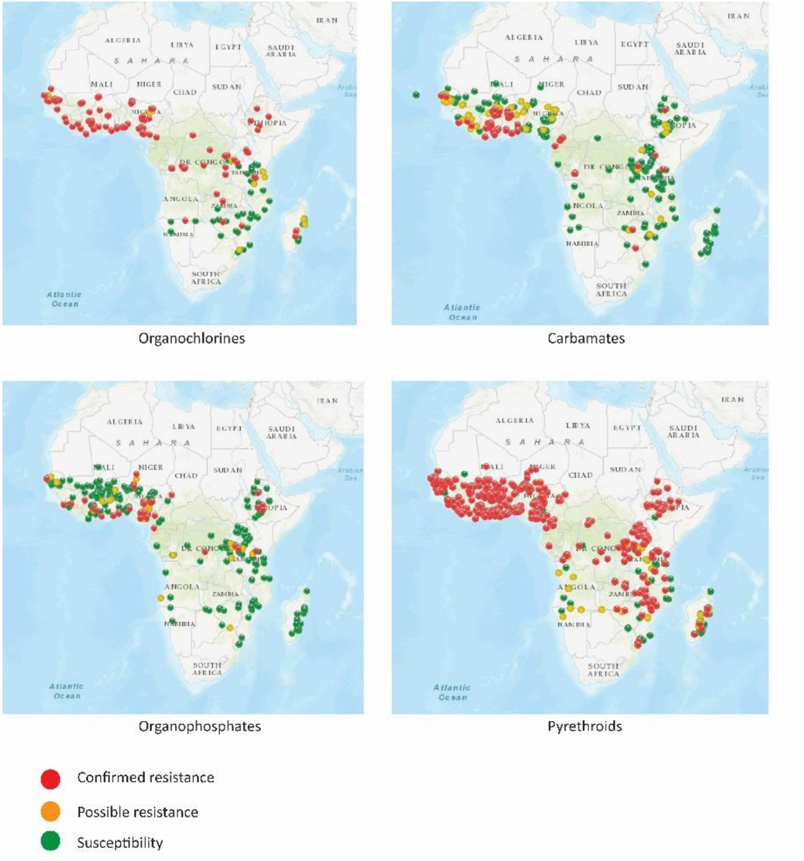

Figure 8. Insecticide resistance maps in *An. gambiae s.l.* in different insecticide classes (organochlorines, carbamates, orgranophosphates and pyrethroirs) in Africa (from: IR Mapper V.2.0).

The insects can resist to insecticides via various different mechanisms or combinations of them. The strategies they use vary from molecular and biochemical to behavioral level and currently, there are four distinct groups of insecticide resistance mechanisms including metabolic or detoxification resistance, target-site resistance, penetration or cuticular resistance and behavioral avoidance or adaptation [46, 47, 53, 54] (Figure 9).

- **Metabolic resistance:** This is the most common resistance mechanism occurring in insects [46] and is a dynamic process involving regulation of insect detoxification to face up to the insecticide threat [55]. Detoxification of insecticides is enhanced in resistant insects compared to susceptible ones and this is attributed to alterations such as overexpression of metabolic enzymes or conformation changes due to point mutations[54]. Overexpression is very common in resistant mosquitoes and occurs due to gene amplification such as duplications, or due to changes in cis regulatory elements (such as gene promoters) or trans-acting regulatory elements [46]. In all cases the result is the enzyme amount increase in resistant insects leading to enhanced metabolism. Enhanced insecticide detoxification in resistant insects results in significant metabolism and subsequent reduced amounts of insecticide molecules reaching their targets [55]. Xenobiotic elimination involves the processes of metabolism and transport and includes the biotransformation steps of phase I and II and the transport phases 0 and III [47][56]. Phases I and II convert lipophilc compounds to more hydrophilic metabolites with phase I enzymes mainly involving P450-dependent oxidation reactions and phase II involving coupling (conjugation) of phase I intermediates with endogenous molecules, resulting in easily eliminating hydrophilic metabolites [47].Transport of phase 0 refers to the prevention of toxic chemicals from entering the cell by transporters , while phase III involves the efflux of modified products of the toxic compound resulting by the action of phase I and/or II biotransformation enzymes [47]. Enzymatic families mediating phase I and II have been associated with metabolic resistance mechanism: cytochrome P450 monooxygenases (P450s or CYPs), Carboxyl esterases (CCEs), glutathione S-transferases (GSTs), while additional families implicated in insecticide resistance via enhanced metabolism are uridine diphosphate (UDP) glucosyl transferases (UGTs), ATP-binding cassette transporters (ABC transporters), solute carrier transporters (SLC transporters)[47] and chemosensory proteins (CSPs)[57]. Different families can act simultaneously or sequentially as well [55]. Particularly for mosquitoes, metabolic resistance has been identified for all major classes of insecticides used for vector control to date [46]. Pyrethroid metabolism is primarily attributed to cytochrome P450s, which are heme-thiolated enzymes catalyzing a plethora of different reactions, but are best known for their monooxygenase activity, acting in phase I detoxification process and introducing polar groups on xenobiotics or endogenous compounds [55]. In *An. coluzzii*, there are 111 such enzymes with a small amount of them being capable of performing insecticide detoxification [53, 58]. Characteristic P450s repeatedly found to be overexpressed in pyrethroid resistant *An. coluzzii* populations are CYP6M2, CP6P3 and CYP6Z2, with proven insecticide binding activities [53]. These enzymes hydrolyze ester bonds or bind and sequestrate the insecticide molecules preventing or slowing down interaction with their targets [46, 55]. Carboxyl esterases have been associated mainly to resistance against organophosphates and carbamates, however they are also implicated in pyrethroid resistance in *An. coluzzii* [59]. Carboxyl esterases (CCEs) represent more than 40 mosquito genes [58]. GST enzymes consist a large multifunctional enzyme family [54] and are known to conjugate reduced glutathione to chemical substrates [55]. They confer insecticide resistance either by taking place in phase I or in phase II detoxification process [47]. In the former case GST conjugation reactions take place [47]. These involve conjugation of reduced glutathione to chemical substrates causing their increased water solubility and subsequent excretion, or the dehydrochlorination by hydrogen removal of its substrates [54, 55]. In phase II GSTs perform detoxification of secondary products derived by action of other enzymes such as P450s [54]. Additionally, some GSTs bind or detoxify lipid peroxidases and reactive oxygen species that are produced due to oxidative stress hence conferring resistance [54]. In mosquitoes around 30 GSTs have been found [58] and the overexpression of many of them has been implicated to insecticide resistance [55]. Specifically GSTs of epsilon subfamily in mosquitoes are associated to DTT and pyrethroid resistance [55]. UGTs catalyze the transfer of glucuronic acid from uridine diphospate (UDP)-glucuronic acid (UDPGA) on the acceptor molecule [47]. Finally, ABC and SLC transporters prevent toxic chemicals from entering the cells acting as first line defense (phase 0 detoxification) or facilitate transport of the modified products by phase I and II detoxification (phase III detoxification) [47]. Finally, chemosensory proteins (CSPs) are soluble ligand-binding proteins known to detect and release chemical signals, capturing and transporting hydrophobic compounds [60, 61]. Recently, a CSP was shown to bind and sequestrate pyrethroid insecticides, with evident overexpression in resistant and insecticide induced mosquitoes [57].

- **Target-site resistance**: Target-site resistance is one of the most common and probably the best understood insecticide resistance mechanism [46]. As insecticides are highly specific for their insect targets, in this mechanism the site for the insecticide action is genetically modified, limiting the interaction with the chemical [54]. This reduction in target specificity results from non-silent point mutations, leading to less effective insecticide binding [46]. Such examples are point mutations on acetylcholinesterase gene, the target of OPs and CMs, the GABA receptor leading to dieldrin resistance and in the voltage-gated sodium channel leading to DTT and pyrethroid resistance [46]. Several mutations have been associated with pyrethroid resistance in many mosquito species [53]. In *An. coluzzii* in particular, the most common mutations have been identified in the domain II of VGSC and are the substitution of leucine with phenylalanine at position 1014 (L1014F), or with serine at the same position (L1014S)[46, 53].

- **Cuticular resistance:** In this resistance mechanism group, also known as penetration resistance, alterations concerning reduced penetration due to the insect cuticle are included [46]. These changes in resistant insects involve the enhanced thickening of the cuticle, the altered cuticular composition or the combination of these two [62]. The modified/thicker cuticles result in slower absorption of insecticide into the bodies, providing simultaneously more time for detoxification process and thus this mechanism is usually involved in cross-resistance against many distinct insecticides [54, 63]. Noteworthy this mechanism is not specific against a compound, acting against a broad range of insecticides [46]. Regarding insects which uptake the insecticide via feeding/ingestion this mechanism is of minor importance, however for mosquito control, as mentioned, insecticides are applied through impregnated surfaces and bed-nets and uptake is primarily through the appendages, hence reduced penetration rates of lipophilic insecticide molecules is much more crucial[46, 53]. Cuticular alterations have been associated to resistance observed in many mosquito species including *An. funestus* [64], *An. stephensi* [65] and *An. gambiae*[66]. This resistance mechanism has recently received more attention and has been attributed to alterations of many different cuticular components [62].

- **Behavioral resistance:** Behavioral resistance refers to the changes in the behavior of the insects, resulting in insecticide avoidance [46]. This avoidance is temporal, spatial and trophic eventually leading to reduced insecticide contact [54]. Behaviors such as rapid escape response from insecticide-treated houses after contact (irritancy) or by non-contact repellency have been described [46, 53]. Additionally, shift in biting preference from indoor to outdoor (spatial) and from night to early morning (temporal) are evident in *Anopheles* mosquitoes or avoidance of blood-feeding on hosts in areas where insecticides are employed (trophic)[46, 54]**.**

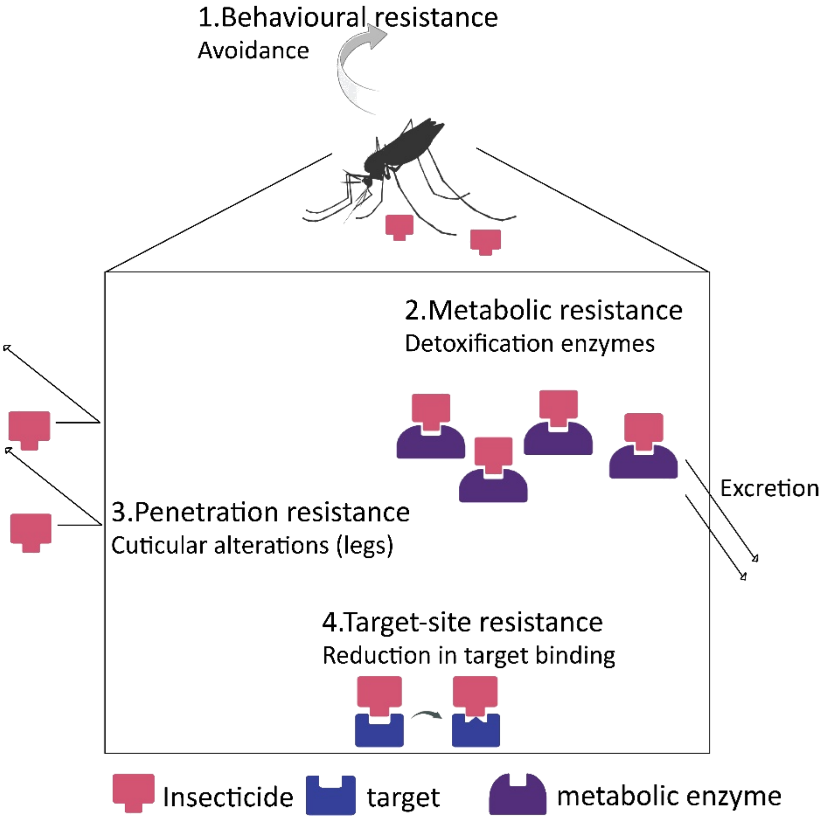
1.Behavioural resistance
Avoidance
2.Metabolic resistance
Detoxification enzymes
Excretion
3.Penetration resistance
Cuticular alterations (legs)
4.Target-site resistance
Reduction in target binding
Insecticide
target
metabolic enzyme

Figure 9. Graphical illustration of the four groups of insecticide resistance mechanisms i.e. behavioral resistance (1), metabolic resistance (2), penetration resistance (3) and target site resistance (4), modified from [54].

Mosquito legs: the first barrier against insecticides

Small arthropods such as mosquitoes walk or jump on surfaces using their legs, which are long and slender, but provide superior weight-bearing ability [67]. Mosquitoes possess six legs (three pairs), each one attached to one thorax segment (fore legs on prothorax, middle legs on mesothorax and hind legs on metathorax) [67, 68]. Each leg is divided into five segments: the coxa which is the basal segment, followed by the trochanter, the femur, the tibia and finally the most proximal tarsus[68] (Figure 10). The tarsus is further divided into five subunits, the tarsomeres [68]. The apical tarsomeres terminate in a claw [68]. They are also covered by hairs endowing them protection from wetness [67], possess grid-like scales which provide super-hydrophobic properties and are also characterized by high flexibility enabling them to conform to water and other surfaces [67].

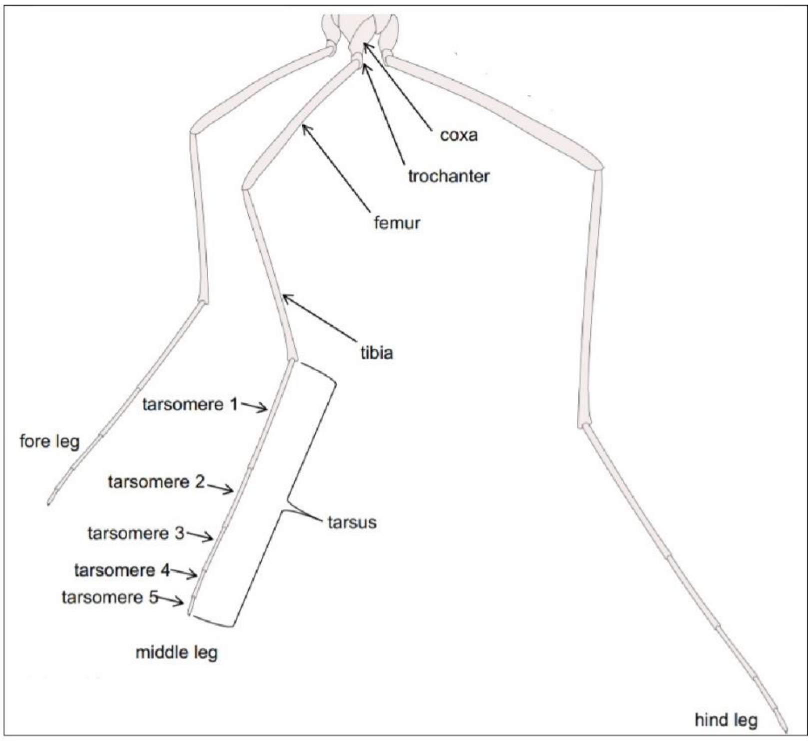
coxa
trochanter
femur
tibia
tarsomere 1
fore leg
tarsomere 2
tarsus
tarsomere 3
tarsomere 4
tarsomere 5
middle leg
hind leg

Figure 10. Mosquito legs (fore leg, middle leg, hind leg) and leg segments (coxa, trochanter, tibia, tarsus and tarsomeres), adapted from [67].

Apart from serving key physiological functions mosquito legs are also epidemiologically important. Based on how malaria vector control is implemented, mosquito appendages constitute the first root for the insecticide to enter the body and reach its targets [46, 53]. This has been also visualized by an exposure assay performed with fluorescent dust particles on electrostatic netting. The fluorescent particles which lighted up orange under ultraviolet (UV) light were present in leg tarsi and proboscis (Figure 11A), while three minutes later the whole legs, antennae, proboscis and some parts of the thorax and abdomen were coated with fluorescent particles [69] (Figure 11B).

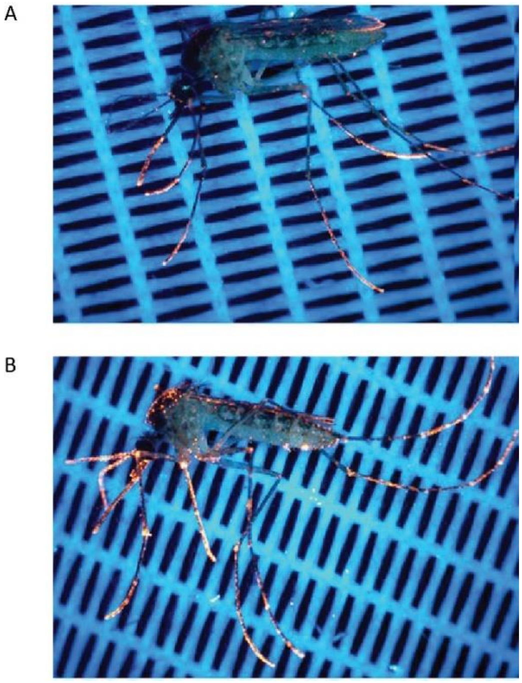

Figure 11. A. Mosquito contaminated with fluorescent dust particles lighting up orange under UV light after 5 second of contact with the netting. B. Mosquito after 3 minutes of contact with the netting, adapted from [69].

This is also evident in terms of insecticide resistance by studies associating thicker leg cuticles to the resistance observed. An *An. funestus* resistant strain was shown to have thicker leg cuticle (tarsi)[70], while according to a recent study, mosquito leg femurs were thicker in a multi-resistant *An. coluzzii* population [66]. This enhanced thickness created a barrier to the insecticide leading to 50% reduction in penetration of radiolabeled deltamethrin in resistant mosquitoes compared to susceptible controls [66]. Analysis of legs revealed that the thickness was attributed to the leg exoskeleton: the cuticle [66] and hence it is a cuticular or permeability resistance mechanism.

Insect cuticle or exoskeleton is the apical extracellular matrix which constrains body shape, facilitates muscle attachment and locomotion, is the basis of specialized organs, [71], enables selective exchanges with the environment [72] and protects from environmental stressors such as physical injury, chemicals (insecticides) desiccation and pathogens [73]. The cuticle is synthesized by epidermal cells during every molting cycle [74] and is composed of chitin, proteins and lipids structured in two morphologically and functionally distinct layers: the procuticle which is subdivided into endo- and exocuticle and the epicuticle which is subdivided into inner- and outer-epicuticle (envelope) [72] (Figure 12). The procuticle is the thicker layer composed of chitin fibers and proteins [62, 72, 74, 75]. Chitin is a polysaccharide made of N-acetyl glucosamine units [76] and together with cuticular proteins contributes to the basic structure of insect cuticle [62, 72, 74, 75]. This is determined by the combination, quantitative distribution and physical properties of cuticular proteins to result in hard or soft, rigid or pliant, flexible or less flexible cuticular structures in different insects, developmental stages or sub-regions of the exoskeleton [74]. Cuticular proteins are clustered in twelve different families based on specific amino acid motifs [77]. In *An. coluzzii*, so far 298 cuticular proteins have been identified comprising almost 2% of its total protein coding genes [78]. The epicuticle contains lipoproteins and lipids, the vast majority of which are cuticular hydrocarbons (CHCs)[66]. In particular, in *An. coluzzii* CHCs constitute approximately 80% of the total epicuticular lipid content [66]. Outermost of the epicuticle there are waxy and cement patches that further provide protection against dehydration and are probably synthesized by specialized epidermal cells, the dermal glands [76]. Underlying the cuticle there is a single cell layer, the epidermal cells, also referred as cuticular epithelium [79]. These cells are separated by the circulating hemolymph by a basal lamina or basement membrane [79]. Epidermal cell lateral sides and especially towards their apical side (cuticular) are characterized by the presence of septate desmosomes and junctional contacts playing important roles in preventing inward and outward movement of materials between the cells [79]. Epidermal cells also have projections and microvilli on their apical side from where they secrete cuticular components [79].

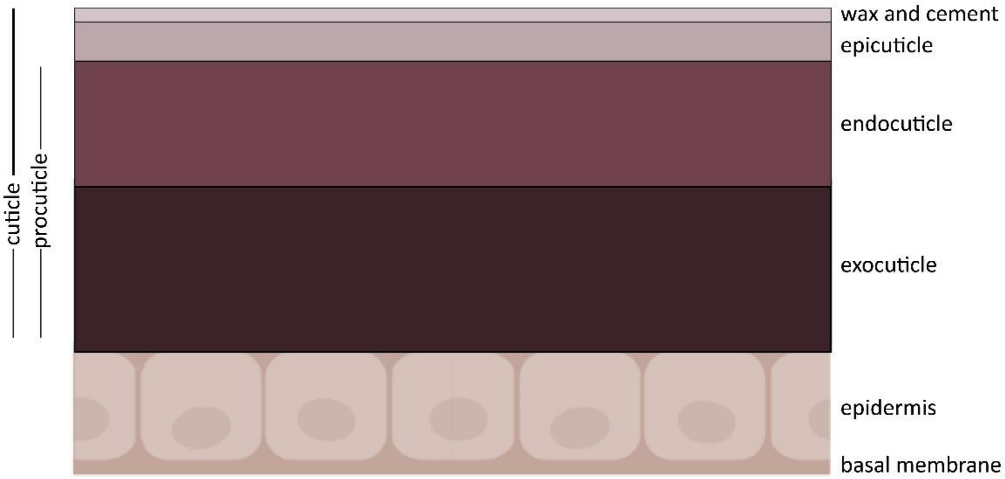
cuticle
procuticle
wax and cement
epicuticle
endocuticle
exocuticle
epidermis
basal membrane

Figure 12. Graphical illustration of main cuticular structures laying above the epidermis.

The cuticle and specifically the leg cuticle, comprising the first barrier for insecticides has been shown to exhibit thickening and/or remodeling in all of its parts (Figure 13) [62]. Additionally, in legs of resistant *An. coluzzii* enhanced chitin levels and a remarkable amount of cuticular proteins were found, revealing enhanced procuticles [80].

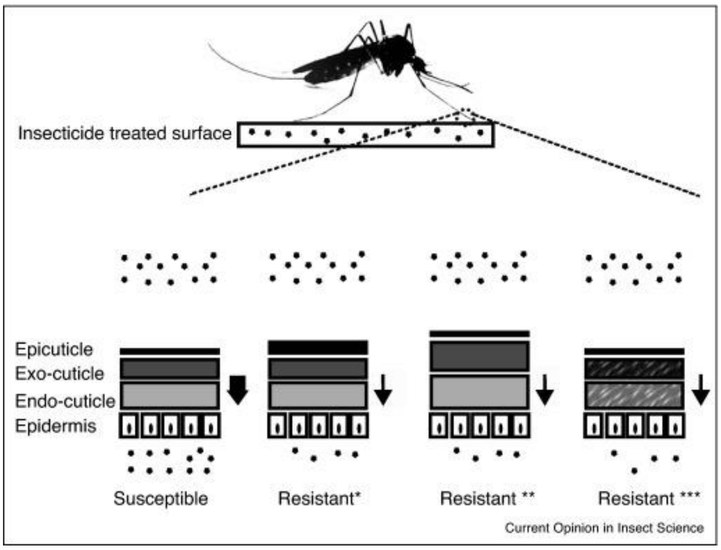
Insecticide treated surface
Epicuticle
Exo-cuticle
Endo-cuticle
Epidermis
Susceptible
Resistant*
Resistant **
Resistant ***
Current Opinion in Insect Science

Figure 13. Penetration resistance mechanisms. All cuticular modifications that have been proposed to underlie reduced insecticide uptake are depicted. *Resistant: thickening of the epicuticle, **Resistant: thickening of the procuticle, ***Resistant: altered cuticle composition, from [62].

Furthermore, *An. coluzzii* leg epicuticles, whose dominant fraction are CHCs, apart from being thicker [66], they are also differentiated regarding their cuticular hydrocarbon contents, compared to susceptible counterparts, exhibiting both quantitative and qualitative differences [80]. These have been associated with overexpression of CHC biosynthetic genes: the cytochrome P450s of the 4G subfamily (CYP4Gs) CYP4G16 and CYP4G17 [66]. These are localized in the oenocytes, which are large, ectodermally-derived, cells of the integument where the CHC biosynthetic pathway takes place [81]. The biosynthetic pathway involves a plethora of enzymes such as fatty acid synthases (FAS), elongases, desaturases, fatty acid reductases (FARs), and cytochrome P450s of the 4G subfamily (CYP4Gs) that catalyze the conversion of the initial acetyl-coA precursors to the final CHCs products through intermediate fatty-acid derivatives [81, 82] (Figure 14) .

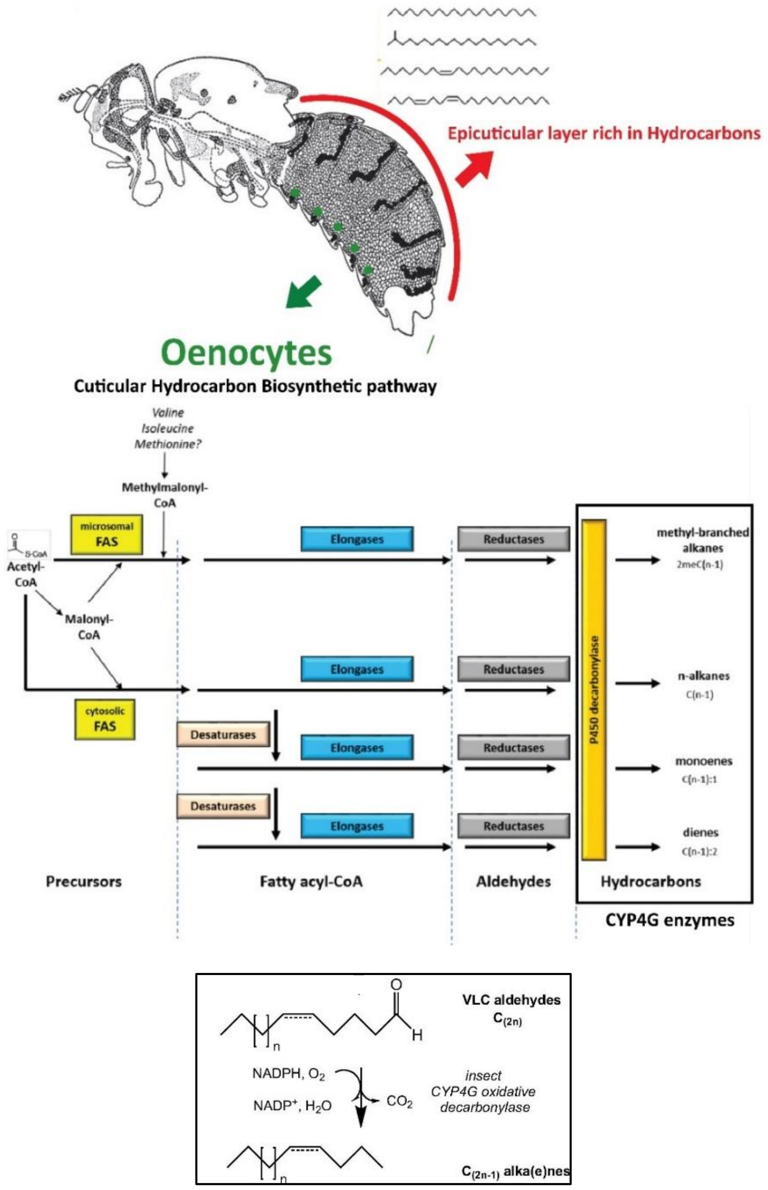
Epicuticular layer rich in Hydrocarbons
Oenocytes
Cuticular Hydrocarbon Biosynthetic pathway
Valine
Isoleucine
Methionine?
Methylmalonyl-CoA
microsomal FAS
S-CoA
Acetyl-CoA
Malonyl-CoA
cytosolic FAS
Elongases
Desaturases
Reductases
P450 decarbonylase
methyl-branched alkanes
2meC(n-1)
n-alkanes
C(n-1)
monoenes
C(n-1):1
dienes
C(n-1):2
Precursors
Fatty acyl-CoA
Aldehydes
Hydrocarbons
CYP4G enzymes
O
H
n
VLC aldehydes
C(2n)
NADPH, O2
NADP+, H2O
CO2
insect
CYP4G oxidative
decarbonylase
C(2n-1) alka(e)nes

Figure 14. Graphical illustration of cuticular hydrocarbons localized on the epicuticle of insects and oenocytes localized on insect integument, where the CHCs biosynthetic pathway takes place. The oxidative decarbonylation reaction of very long chain (VLC) aldehydes to hydrocarbons (alkanes/alkenes), performed by CYP4G enzymes is also depicted at the bottom, adapted from [73, 81, 83].

Literature

1. Phillips, M.A., et al., *Malaria.* Nat Rev Dis Primers, 2017. **3**: p. 17050.
2. Capanna, E., *Grassi versus Ross: who solved the riddle of malaria?* Int Microbiol, 2006. **9**(1): p. 69-74.
3. Cowman, A.F., et al., *Malaria: Biology and Disease.* Cell, 2016. **167**(3): p. 610-624.
4. WHO, *World malaria report 2021.* World Health Organization, 2021.
5. Laurens, M.B., *The Promise of a Malaria Vaccine—Are We Closer?* Annual Review of Microbiology, 2018. **72**(1): p. 273-292.
6. Lee, H., S. Halverson, and N. Ezinwa, *Mosquito-Borne Diseases.* Prim Care, 2018. **45**(3): p. 393-407.
7. Whitten, M.M.A., S.H. Shiao, and E.A. Levashina, *Mosquito midguts and malaria: cell biology, compartmentalization and immunology.* Parasite Immunology, 2006. **28**(4): p. 121-130.
8. Basu, S. and P.K. Sahi, *Malaria: An Update.* Indian J Pediatr, 2017. **84**(7): p. 521-528.
9. Ghosh, A.K. and M. Jacobs-Lorena, *Plasmodium sporozoite invasion of the mosquito salivary gland.* Curr Opin Microbiol, 2009. **12**(4): p. 394-400.
10. de Koning-Ward, T.F., P.R. Gilson, and B.S. Crabb, *Advances in molecular genetic systems in malaria.* Nat Rev Microbiol, 2015. **13**(6): p. 373-87.
11. Singh, M., et al., *Plasmodium's journey through the Anopheles mosquito: A comprehensive review.* Biochimie, 2021. **181**: p. 176-190.
12. da Silva, A.F., et al., *Culicidae evolutionary history focusing on the Culicinae subfamily based on mitochondrial phylogenomics.* Scientific Reports, 2020. **10**(1): p. 18823.
13. Molaei, G., et al., *Host-feeding patterns of potential mosquito vectors in Connecticut, U.S.A.: molecular analysis of bloodmeals from 23 species of Aedes, Anopheles, Culex, Coquillettidia, Psorophora, and Uranotaenia.* J Med Entomol, 2008. **45**(6): p. 1143-51.
14. Harbach, R., *The Culicidae (Diptera): a review of taxonomy, classification and phylogeny*.* Zootaxa, 2007. **1668**: p. 591-638.
15. Harbach, R.E. *The Phylogeny and Classification of Anopheles*. 2013.
16. Sinka, M.E., et al., *A global map of dominant malaria vectors.* Parasit Vectors, 2012. **5**: p. 69.
17. Sinka, M.E., et al., *A global map of dominant malaria vectors.* Parasites & Vectors, 2012. **5**(1): p. 69.
18. Dorn, P.L., et al., *15 - Genetics of Major Insect Vectors*, in *Genetics and Evolution of Infectious Diseases (Second Edition)*, M. Tibayrenc, Editor. 2017, Elsevier: London. p. 341-382.
19. Coetzee, M., et al., *Anopheles coluzzii and Anopheles amharicus, new members of the Anopheles gambiae complex.* Zootaxa, 2013. **3619**: p. 246-74.
20. Holt, R.A., et al., *The genome sequence of the malaria mosquito Anopheles gambiae.* Science, 2002. **298**(5591): p. 129-49.
21. Burgess, I.F., *The Biology of Mosquitoes, volume 2: Sensory Reception and Behaviour. A. N. Clements. Wallingford: CAB1 Publishing, 1999. xvi+740 pp. Price £95.00/US $175.00. ISBN 0-85199-313-3.* Transactions of The Royal Society of Tropical Medicine and Hygiene, 2000. **94**(1): p. 82-82.
22. Koutsos, A.C., et al., *Life cycle transcriptome of the malaria mosquito &lt;em&gt;Anopheles gambiae&lt;/em&gt; and comparison with the fruitfly &lt;em&gt;Drosophila melanogaster&lt;/em&gt;.* Proceedings of the National Academy of Sciences, 2007. **104**(27): p. 11304.
23. Williams, J. and J. Pinto, *Training Manual on Malaria Entomology*. 2012.
24. Patel, O.P.S., R.M. Beteck, and L.J. Legoabe, *Antimalarial application of quinones: A recent update.* Eur J Med Chem, 2021. **210**: p. 113084.

25. Su, X.-Z. and L.H. Miller, *The discovery of artemisinin and the Nobel Prize in Physiology or Medicine.* Science China Life Sciences, 2015. **58**(11): p. 1175-1179.
26. Arora, N., C.A. L, and A.K. Pannu, *Towards Eradication of Malaria: Is the WHO's RTS,S/AS01 Vaccination Effective Enough?* Risk Manag Healthc Policy, 2021. **14**: p. 1033-1039.
27. Benelli, G. and J.C. Beier, *Current vector control challenges in the fight against malaria.* Acta Tropica, 2017. **174**: p. 91-96.
28. Gosling, R. and L. von Seidlein, *The Future of the RTS,S/AS01 Malaria Vaccine: An Alternative Development Plan.* PLOS Medicine, 2016. **13**(4): p. e1001994.
29. Cunningham, J., et al., *A review of the WHO malaria rapid diagnostic test product testing programme (2008–2018): performance, procurement and policy.* Malaria Journal, 2019. **18**(1): p. 387.
30. Shah, M.P., et al., *The effectiveness of older insecticide-treated bed nets (ITNs) to prevent malaria infection in an area of moderate pyrethroid resistance: results from a cohort study in Malawi.* Malaria Journal, 2020. **19**(1): p. 24.
31. Pryce, J., N. Medley, and L. Choi, *Indoor residual spraying for preventing malaria in communities using insecticide-treated nets.* Cochrane Database Syst Rev, 2022. **1**(1): p. Cd012688.
32. Bhatt, S., et al., *The effect of malaria control on Plasmodium falciparum in Africa between 2000 and 2015.* Nature, 2015. **526**(7572): p. 207-211.
33. Bartilol, B., et al., *Bionomics and ecology of Anopheles merus along the East and Southern Africa coast.* Parasites & Vectors, 2021. **14**(1): p. 84.
34. Baeshen, R., *Swarming Behavior in Anopheles gambiae (sensu lato): Current Knowledge and Future Outlook.* J Med Entomol, 2022. **59**(1): p. 56-66.
35. Fillinger, U. and S.W. Lindsay, *Larval source management for malaria control in Africa: myths and reality.* Malaria Journal, 2011. **10**(1): p. 353.
36. World Health, O., *Malaria vector control : decision making criteria and procedures for judicious use of insecticides*. 2003, World Health Organization: Geneva.
37. Gupta, R.C. and D. Milatovic, *Chapter 23 - Insecticides*, in *Biomarkers in Toxicology*, R.C. Gupta, Editor. 2014, Academic Press: Boston. p. 389-407.
38. Karlik, J.F., *INSECTS AND OTHER ANIMALS | Insecticides*, in *Encyclopedia of Rose Science*, A.V. Roberts, Editor. 2003, Elsevier: Oxford. p. 460-466.
39. Sparks, T.C. and R. Nauen, *IRAC: Mode of action classification and insecticide resistance management.* Pesticide Biochemistry and Physiology, 2015. **121**: p. 122-128.
40. Hołyńska-Iwan, I. and K. Szewczyk-Golec, *Pyrethroids: How They Affect Human and Animal Health?* Medicina, 2020. **56**(11).
41. Mohammadi, H., et al., *Pyrethroid exposure and neurotoxicity: a mechanistic approach.* Arh Hig Rada Toksikol, 2019. **70**(2): p. 74-89.
42. Ranson, H., *Current and Future Prospects for Preventing Malaria Transmission via the Use of Insecticides.* Cold Spring Harb Perspect Med, 2017. **7**(11).
43. Cook, J., et al., *Implications of insecticide resistance for malaria vector control with long-lasting insecticidal nets: trends in pyrethroid resistance during a WHO-coordinated multi-country prospective study.* Parasites & Vectors, 2018. **11**(1): p. 550.
44. Zaim, M., A. Aitio, and N. Nakashima, *Safety of pyrethroid-treated mosquito nets.* Med Vet Entomol, 2000. **14**(1): p. 1-5.
45. Gleave, K., et al., *Piperonyl butoxide (PBO) combined with pyrethroids in insecticide-treated nets to prevent malaria in Africa.* Cochrane Database Syst Rev, 2021. **5**(5): p. Cd012776.

46. Corbel, V. and R. N'Guessan, *Distribution, Mechanisms, Impact and Management of Insecticide Resistance in Malaria Vectors: A Pragmatic Review.* Anopheles mosquitoes - New insights into malaria vectors, 2013.
47. Kennedy, C. and K. Tierney, *Xenobiotic Protection/Resistance Mechanisms in Organisms*. 2013. p. 689-721.
48. Hemingway, J. and H. Ranson, *Insecticide resistance in insect vectors of human disease.* Annu Rev Entomol, 2000. **45**: p. 371-91.
49. Denholm, I. and M.W. Rowland, *Tactics for managing pesticide resistance in arthropods: theory and practice.* Annu Rev Entomol, 1992. **37**: p. 91-112.
50. Livadas, G.A. and G. Georgopoulos, *Development of resistance to DDT by Anopheles sacharovi in Greece.* Bull World Health Organ, 1953. **8**(4): p. 497-511.
51. Brown, A.W., *Insecticide resistance in mosquitoes: a pragmatic review.* J Am Mosq Control Assoc, 1986. **2**(2): p. 123-40.
52. Metcalf, R.L., *Insect resistance to insecticides.* Pesticide Science, 1989. **26**(4): p. 333-358.
53. Ranson, H., et al., *Pyrethroid resistance in African anopheline mosquitoes: what are the implications for malaria control?* Trends Parasitol, 2011. **27**(2): p. 91-8.
54. Gan, S.J., et al., *Dengue fever and insecticide resistance in Aedes mosquitoes in Southeast Asia: a review.* Parasites & Vectors, 2021. **14**(1): p. 315.
55. Nkya, T.E., et al., *Impact of environment on mosquito response to pyrethroid insecticides: Facts, evidences and prospects.* Insect Biochemistry and Molecular Biology, 2013. **43**(4): p. 407-416.
56. Döring, B. and E. Petzinger, *Phase 0 and phase III transport in various organs: Combined concept of phases in xenobiotic transport and metabolism.* Drug Metabolism Reviews, 2014. **46**(3): p. 261-282.
57. Ingham, V.A., et al., *A sensory appendage protein protects malaria vectors from pyrethroids.* Nature, 2020. **577**(7790): p. 376-380.
58. Ranson, H., et al., *Evolution of supergene families associated with insecticide resistance.* Science, 2002. **298**(5591): p. 179-81.
59. Vontas, J., et al., *Gene expression in insecticide resistant and susceptible Anopheles gambiae strains constitutively or after insecticide exposure.* Insect Mol Biol, 2005. **14**(5): p. 509-21.
60. Pelosi, P., et al., *Soluble proteins of chemical communication: an overview across arthropods.* Frontiers in Physiology, 2014. **5**(320).
61. Iovinella, I., et al., *Ligand-binding study of Anopheles gambiae chemosensory proteins.* Chem Senses, 2013. **38**(5): p. 409-19.
62. Balabanidou, V., L. Grigoraki, and J. Vontas, *Insect cuticle: a critical determinant of insecticide resistance.* Curr Opin Insect Sci, 2018. **27**: p. 68-74.
63. Bass, C. and C.M. Jones, *Mosquitoes boost body armor to resist insecticide attack.* Proc Natl Acad Sci U S A, 2016. **113**(33): p. 9145-7.
64. Wood, O., et al., *Cuticle thickening associated with pyrethroid resistance in the major malaria vector Anopheles funestus.* Parasit Vectors, 2010. **3**: p. 67.
65. Vontas, J., et al., *Transcriptional analysis of insecticide resistance in Anopheles stephensi using cross-species microarray hybridization.* Insect Mol Biol, 2007. **16**(3): p. 315-24.
66. Balabanidou, V., et al., *Cytochrome P450 associated with insecticide resistance catalyzes cuticular hydrocarbon production in &lt;em&gt;Anopheles gambiae&lt;/em&gt;.* Proceedings of the National Academy of Sciences, 2016. **113**(33): p. 9268.
67. Kong, X., et al., *Load-bearing ability of the mosquito tarsus on water surfaces arising from its flexibility.* AIP Advances, 2015. **5**: p. 037101.

68. Burkett-Cadena, N.D., *Mosquitoes of the southeastern United States.* 2013.
69. Andriessen, R., et al., *Electrostatic coating enhances bioavailability of insecticides and breaks pyrethroid resistance in mosquitoes.* Proceedings of the National Academy of Sciences, 2015. **112**(39): p. 12081.
70. Wood, O.R., et al., *Cuticle thickening associated with pyrethroid resistance in the major malaria vector Anopheles funestus.* Parasites & Vectors, 2010. **3**(1): p. 67.
71. Ferveur, J.-F., et al., *Desiccation resistance: effect of cuticular hydrocarbons and water content in Drosophila melanogaster adults.* PeerJ, 2018. **6**: p. e4318-e4318.
72. Moussian, B., *Recent advances in understanding mechanisms of insect cuticle differentiation.* Insect Biochem Mol Biol, 2010. **40**(5): p. 363-75.
73. Qiu, Y., et al., *An insect-specific P450 oxidative decarbonylase for cuticular hydrocarbon biosynthesis.* Proc Natl Acad Sci U S A, 2012. **109**(37): p. 14858-63.
74. Charles, J.P., *The regulation of expression of insect cuticle protein genes.* Insect Biochem Mol Biol, 2010. **40**(3): p. 205-13.
75. Blomquist, G.J. and A.-G. Bagnères, *Insect Hydrocarbons: Biology, Biochemistry and Chemical Ecology.* Cambridge Univ., 2010.
76. Doucet, D. and A. Retnakaran, *Targeting Cuticular Components for Pest Management*. 2016. p. 369-407.
77. Willis, J.H., *Structural cuticular proteins from arthropods: annotation, nomenclature, and sequence characteristics in the genomics era.* Insect Biochem Mol Biol, 2010. **40**(3): p. 189-204.
78. Zhou, Y., et al., *Proteomics reveals localization of cuticular proteins in Anopheles gambiae.* Insect biochemistry and molecular biology, 2019. **104**: p. 91-105.
79. Nation, J.L., *Integument: Structure and Function*, in *Encyclopedia of Entomology*. 2005, Springer Netherlands: Dordrecht. p. 1200-1203.
80. Balabanidou, V., et al., *Mosquitoes cloak their legs to resist insecticides.* Proc Biol Sci, 2019. **286**(1907): p. 20191091.
81. Makki, R., E. Cinnamon, and A.P. Gould, *The development and functions of oenocytes.* Annu Rev Entomol, 2014. **59**: p. 405-25.
82. Chung, H. and S.B. Carroll, *Wax, sex and the origin of species: Dual roles of insect cuticular hydrocarbons in adaptation and mating.* BioEssays : news and reviews in molecular, cellular and developmental biology, 2015. **37**(7): p. 822-830.
83. Chung, H. and S.B. Carroll, *Wax, sex and the origin of species: Dual roles of insect cuticular hydrocarbons in adaptation and mating.* BioEssays, 2015. **37**(7): p. 822-830.

Aim of the PhD thesis

The research conducted during this PhD thesis is focused on the legs of the major malaria vector *An. coluzzii* and aimed to address two main questions: A) What are the alterations of the legs of insecticide resistant mosquitoes, B) Characterization of enzymes implicated in leg alterations. These two major components of the thesis are expanded in detail in four chapters.

Chapter 1 entitled "LEGOmics: High-throughput approaches (-omics) to delineate alterations in the legs of resistant mosquitoes", aims to shed light to the differences of the legs derived both from constitutively resistant mosquitoes and from insecticide induced ones and finally to evaluate the implication of key-candidates in insecticide resistance phenotype.

Chapter 2 entitled "The leg/appendage specific ABCH2 transporter mediates insecticide toxicity in the malaria vector *Anopheles coluzzii*", is focused on an ATP-binding cassette (ABC) transporter derived from the leg dataset presented in Chapter 1, with the intention to study its implication in deltamethrin toxicity.

Chapter 3 entitled "Characterization of enzymes implicated in cuticular alterations in legs of insecticide resistant mosquitoes", aims to study the contributions of cytochrome P450 monoxygenases of 4G subfamily (CYP4Gs), which participate in cuticular hydrocarbon biosynthesis and have been associated to the altered leg epicuticles of resistant *An. coluzzii*.

Chapter 4 entitled "Characterization of the brain specific CYP4G15 in *Drosophila melanogaster* and analysis of the CYP4G-specific insertion" aims to provide further knowledge in CYP4G enzymes by addressing two different topics: The characterization of *D. melanogaster* CYP4G15, which is absent from oenocytes and present in central nervous system, and studying contribution of the characteristic, acidic-rich, CYP4G-specific insertion in CYP4G essentiality.

Chapter 1

LEGOmics: High-throughput approaches (-omics) to delineate alterations in the legs of resistant mosquitoes.

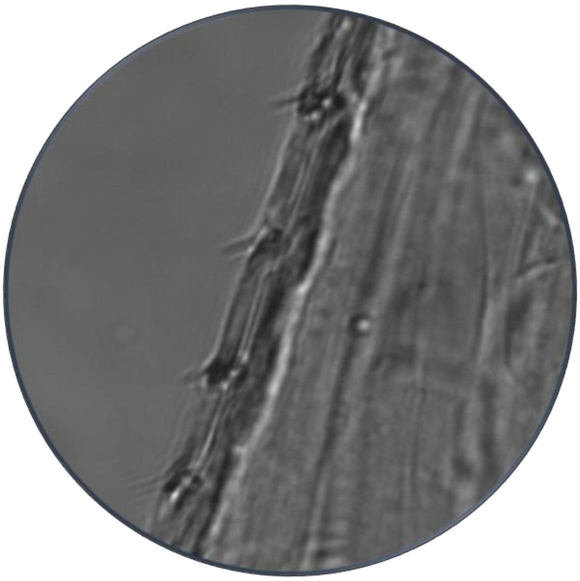

Publications

Kefi,M.,Charamis,J.,Balabanidou,V.,Ioannidis,P.,Ranon,H.,Ingham,VA.,Vontas,J.(2021) Transcriptomic analysis of resistance and short-term induction response to pyrethroids, in *Anopheles coluzzii* legs. *BMC Genomics 22, 891* https://doi.org/10.1186/s12864-021-08205-w

Balabanidou,V., **Kefi,M.**, Aivaliotis,M.,Koidou,V., Girotti,JR., Mijailovsky,SJ., Juarez,MP., Papadogiorgaki,E., Chalepakis,G., Kampouraki,A., Nikolaou, C., Ranson,H., & Vontas,J. (2019). Mosquitoes cloak their legs to resist insecticides. Proc. R. Soc. B. doi: http://dx.doi.org/10.1098/rspb.2019.1091

1.1 Abstract

Insecticide-treated bed nets and indoor residual spraying comprise the major control measures against *Anopheles gambiae sl*, the dominant vector in sub-Saharan Africa. The primary site of contact with insecticide is through the mosquitoes' legs, hence consisting the first barrier it has to bypass to reach its target. Proteomic changes and leg cuticle modifications have been associated with insecticide resistance, jeopardizing the sustainability of malaria control interventions. Here, we performed a multiple transcriptomic analysis focusing on *An. coluzzi* legs and validated interesting candidates using RNAi-mediated silencing coupled with toxicity bioassays.

Firstly, we compared transcript expression in the legs of a highly resistant strain (VK7-HR) to both a strain with very similar genetic background which has reverted to susceptibility, after several generations without insecticide pressure (VK7-LR) and a lab susceptible population. 232 differentially expressed genes (73 up-regulated and 159 down-regulated) were identified in the resistant strain when compared to the two counterparts, indicating an over-expression of phase I detoxification enzymes and cuticular proteins, with decrease in hormone-related metabolic processes.

Next, we analyzed the short-term effect of pyrethroid exposure on *An. coluzzi* legs, comparing 1 hour-deltamethrin-exposed (VK7-IN) to unexposed (VK7-HR) leg transcriptomes, highlighting 348 up-regulated genes encoding for GPCRs, ABC transporters, odorant-binding proteins and members of the divergent salivary gland protein family.

Finally, we performed RNAi-mediated silencing in cuticular proteins found overrepresented in leg transcriptome and proteome of resistant and susceptible mosquitoes with concomitant deltamethrin toxicity bioassays and revealed that silencing individual cuticular genes is not sufficient to restore part of susceptibility.

We provide a detailed *An. coluzzi* leg-specific transcriptome, with important reference information of what the first defense line is in pyrethroid resistant and short-term deltamethrin-exposed mosquitoes. Our results demonstrate for the first time that detoxification is likely occurring in legs, while the enrichment of sensory proteins, ABCG transporters and cuticular genes is also evident. Constitutive resistance is primarily attributed to detoxification and cuticular genes with simultaneously decreased hormone-related processes, while short-term insecticide-induced tolerance is linked with overexpression of transporters, GPCRs and GPCR-related genes, sensory/binding and salivary gland proteins.

1.2 Introduction

With malaria continuing to claim more than 400,000 lives each year, causing a severe global health problem [1] the use of insecticide-treated bed nets (ITNs) still remains the primary measurement for its prevention [2] . However, their reliance on pyrethroid insecticide class [3], results in dramatic development of pyrethroid resistance in malaria vectors posing a major threat for malaria control, especially in countries encountering the highest malaria burden [4, 5].

Reduced penetration or cuticular resistance has been linked to pyrethroid resistance and has been correlated to thickening and/or altered composition of the cuticle in various insects [6]. This putative resistance mechanism is now being more widely reported in African malaria vectors [5], with several studies associating insecticide resistance with abundance of cuticular proteins [6-9].

Increasing resistance to pyrethroids in *Anopheles* populations across Africa has increased the impetus to develop new ingredients active against these resistant populations. Reduced penetration could potentially confer cross resistance to new insecticide classes but there are critical gaps in our understanding of the uptake and subsequent clearance of the insecticide by mosquitoes both through constitutive and induced mechanisms; filling these gaps is important to develop resistance mitigation strategies and inform the design and formulation of new insecticides. The primary site of contact in the case of both ITNs and sprayed surfaces are the legs, and hence, the insecticides must first penetrate the leg cuticle in order to reach their target [6, 10]. Dipteran legs are complex, poorly characterized structures compared to other tissues. Recent evidence generated from *Drosophila* single-cell transcriptomic atlas describes the existence of distinct cell types in legs including epidermal cells, muscles, neural cells (peripheral glia, sensory, gustatory and mechanosenosry neurons) and hemocytes along with cells of unannotated types [11].

Resistance can occur as the end result of several distinct mechanisms. Most of the studies are focusing on constitutive resistance, a term which refers to the mechanisms that are continuously present in resistant mosquitoes (constitutive resistance). Recent studies underline the importance of the legs in constitutive pyrethroid resistance both due to the thicker cuticle being enriched in chitin content and structural cuticular components [4, 7] and through sequestration mechanisms in resistant *Anopheles* legs mediated by the chemosensory protein *SAP2* [12]. It is not known if metabolic resistance is also taking place in mosquito legs; detoxification enzymes have previously been identified in the *An. coluzzii* leg proteome [7], and the tick leg transcriptome contained a small number of P450s and GSTs, specifically in Haller's organ, which were postulated as odorant degrading enzymes [13].

Resistance can often be observed because rapid metabolism of insecticide can happen so as its toxic effects can be decreased once the chemical can induce certain enzyme systems [14]. In this context, we refer to induction as the mechanisms which are activated in response to a stimulus (in our case, deltamethrin) and are associated to increased tolerance. Although the majority of studies in resistant mosquitoes look at constitutive expression of transcripts of interest, a recent transcriptional time-course of sub-lethal pyrethroid exposure in whole *An. coluzzii* resistant mosquitoes demonstrated that over two thirds of transcripts change upon insecticide exposure [15]. These changes were seen in *a priori* insecticide resistance candidates, such as detoxification genes, but the study also identified a decrease of oxidative phosphorylation and elevated DNA-repair [15]. Induction of metabolic resistance-related enzymes has also been observed post DDT exposure in *Drosophila* which induced the expression of *Cyp6g1* and *Cyp12d1* [16] and in permethrin-challenged house flies resulting in co-upregulation of three P450 genes in a time and dose-dependent manner [17]. Furthermore, transcription factors and pathways have been associated with transcriptional regulation of genes involved in response to xenobiotics such as cytochrome P450s or other detoxification enzymes. Such pathways include *D. melanogaster* Nrf2 (NE-E2-related factor 2)[18, 19], *An. gambiae* Maf-S[5] and *C. pipiens* NYD-OP7, which belongs to the GPCR family that has been associated with deltamethrin resistance probably through NYD-OP7/PLC-mediated signaling of key P450s [20]. Additionally, oxidative stress elicited by insecticides has also been studied in various insects with a focus on hormonal-regulated triggering responses, involving neuropeptides such as insect adipokinetic hormones (AKH), which further implicated GPCR signaling [21]. Moreover, ATP-Binding-Cassette (ABC) transporters, thought to participate in detoxification process in Phase 0 and Phase III [22, 23], have been found up-regulated post pyrethroid exposure in multiple studies [15, 24-27]. In addition to metabolic enzymes and changes to key signaling pathways, sensory proteins have been found to be induced in *Anopheles* resistant populations post pyrethroid exposure [12, 15]. These carrier proteins, found in the lymph of chemosensilla, are divided in insects in two different classes: Odorant-binding proteins (OBPs) and Chemosensory proteins (CSPs) [28] and are soluble ligand-binding proteins, known to detect and release chemical signals [29, 30].

Here, we perform two distinct transcriptomic experiments identifying: (i) transcripts involved in constitutive resistance in the legs of a pyrethroid resistant population and (ii) leg transcripts up- and down- regulated after pyrethroid exposure. We demonstrate that legs from pyrethroid resistant mosquitoes have higher expression of phase I detoxification and cuticular genes with simultaneous decreased expression of genes involved in hormone related processes. Short-term insecticide-induced tolerance in the legs is associated with increased expression of transporters, GPCRs and GPCR-related genes, sensory/binding proteins and members of the divergent salivary gland protein family.

1.3 Materials and Methods

1.3.1 Mosquito strains

The mosquito strains used in the study belong to the *An. gambiae* species complex and were maintained in the laboratory under the same conditions for several generations before analysis. The standard insectary conditions for all strains were 27°C and 70-80% humidity under a 12-h: 12-h photoperiod with a 1-hour dawn : dusk cycle. The susceptible *An. coluzzii* N'Gousso strain (NG) collected from Cameroon is susceptible to almost all pyrethroid insecticides (some dieldrin resistance has been recorded) whilst the *An. coluzzii* strains from Burkina Faso (VK7) are highly resistant to pyrethroids and DDT [31, 32]. Two colonies from VK7 were maintained in the laboratory: i) VK7-LR (lowly resistant) that almost completely lost resistance to deltamethrin, after several generations in the laboratory without pyrethroid selection, and ii) VK7-HR (highly resistant), a re-colonized population, highly resistant to deltamethrin (0% mortality after 1h exposure with deltamethrin diagnostic dose) which was maintained under deltamethrin selection pressure.

1.3.2 Leg dissection, induction and RNA isolation

Whole legs from 3-5 day old, non-blood fed female mosquitoes were dissected including all leg segments (coxa, trochanter, femur, tibia, and tarsus), using micro-dissection forceps (Figure 1.2). Four biological replicates each including legs from 20-30 female mosquitoes were prepared from each strain/condition. All collections were carried out between 1-3 hours after beginning of dawn period. For deltamethrin-induced sample preparation almost 100 mosquitoes from VK7-HR strain were exposed in 0.05% deltamethrin using WHO tubes and the survivors were let to recover for 1 hour (VK7-IN), after which all individuals were still alive. Legs were immediately dissected and put into RNA extraction buffer and proceeded to RNA extraction the same day (no storage of dissected tissues took place). RNA extraction was carried out using the Arcturus PicoPure RNA Isolation Kit (Thermo Fischer Scientific), coupled with RNase-Free DNase Set (QIAGEN), following the manufacturer's instructions. Nanodrop spectrometer readings confirmed that submitted RNA quantity fell within ranges expected by the sequencing centre.

1.3.3 Preparation of Illumina libraries

RNA-seq analysis took place in the Polo Genomics-Genetics-Biology (Polo GGB) facility using a NextSeq 550 Sequencer. The libraries were prepared in accordance with the Illumina TruSeq Stranded mRNA Sample Preparation Guide (Part # 1000000040498 v00, Rev. E, Date October 2017) for Illumina Paired-End Indexed Sequencing. According to the Illumina mRNA libraries preparation protocol, poly-A mRNA in the tRNA samples were first purified using Illumina poly-T oligo-attached magnetic beads and two rounds of purification. During the second elution of the poly-A-RNA, the mRNA was also fragmented and primed with random hexamers for cDNA synthesis. Cleaved mRNAs were reverse transcribed into first strand cDNA using reverse transcriptase and random primers. The RNA template was then removed, and a replacement strand synthesized to generate double-stranded cDNA. Following the standard protocol, after the first and second strand cDNA synthesis, a single “A” nucleotide is added to the 3’ ends of the blunt fragments, and Illumina indexing adapters were ligated. Finally, cDNA fragments that have adapter molecules on both ends underwent 15 cycles of PCR to amplify the amount of prepared material. The resulting libraries were validated using the Fragment Analyzer to check size distribution. Concentration of library samples was defined on the basis of the Qubit® 3.0 Fluorometer quantification and average library size. Indexed DNA libraries were normalized to 4 nM and then pooled in equal volumes. The pool was loaded at a concentration of 1.1 pM onto an Illumina NextSeq 550 Flowcell High Output, with 1%of Phix control. The samples were then sequenced using the Illumina chemistry V2.5, 2x75bp paired end run.

Dr Panagiotis Ioannidis and Jason Charamis performed the transcriptomi analysis, assessed the data quality and generated the heatmaps as described in detail in [33]

1.3.4 dsRNA design, generation, nano-injections and silencing efficiency

Primers for dsRNA against cuticular proteins genes were designed using PrimerBlast and they amplify products of about 500-600 bp (Table S1.1). T7 promoter sequence (5’ TAATACGACTCACTATAGGG 3’) was added at the 5’ end of both forward and reverse oligos. VK7 cDNA was used as template for PCR amplification using Phusion High-Fidelity DNA Polymerase (New England Biolabs), following manufacturer’s instructions. Specific amplification was verified on a 1.5% agarose gel and the rest reaction was purified using Macherey-Nagel^{TM} Nucleospin^{TM} Gel and PCR Clean-up Kit. The purified product was used as template for dsRNA synthesis using HiScribe^{TM} T7 High Yield RNA Synthesis Kit (New England Biolabs) with subsequent purification with MEGAclear^{TM} Transcription Clean-Up Kit (Ambion). The purified dsRNAs were diluted in a 3 μg/μl concentration and 69 nl of this were injected into CO_2-anaesthetized female 0-day mosquitoes. The injections were performed intrathoracically using Nanoinject II Auto-Nanoliter Injector (Drummond Scientific Company). As control a 500bp dsRNA prepared from Green fluorescent protein (GFP) non-endogenous gene was used following the same preparation. Injected mosquitoes were placed in cups and were kept in insectary conditions with 10% impregnated sugar cottons for 72 hours. After that their legs were dissected and RNA was extracted, cDNA was synthesized, and RT-qPCR was conducted. cDNA synthesis was carried out using EnzyQuest Reverse Transcriptase and oligodTs according to the guidelines and the reaction products were used for RT-qPCR. RT-qPCR was performed in a BIO-RAD cycler in the following conditions: 3 min at 95°C, 40 cycles of 15 seconds at 95°C and 30 seconds at 60°C and the analysis included three biological and two technical replicates within each biological replicate. Relative expression was normalized with *An. coluzzii Ribosomal Protein S7* (*S7*) housekeeping gene. Primers for qPCR were designed out of the region-targeted by dsRNA resulting in 150-200 bp product (Table S1.2) and according to standard curve construction their efficiency was 96%. Silencing efficiency for each dsRNA was estimated after comparison of relative expression of each gene of interest in dsRNA-injected against relative expression levels in ds*GFP*-injected female mosquitoes. Graphs were produced and statistically analyzed using GraphPad Prism software version 8 using Student’s t-test.

1.3.5 Deltamethrin toxicity assays

For deltamethrin toxicity assays 0-Day injected females with ds*GFP* and ds*RNA* against genes of interest were kept into cups supplied with sugar-water for 72 hours in insectary conditions. After this timeframe they were exposed to deltamethrin using insecticide impregnated papers in WHO tubes. Deltamethrin concentration was 0.05% for VK7-HR strain. The exposure lasted for 1 hour and after this knocked-down mosquitoes were recorded. This was followed by 24 hour recovery in control tubes in insectary conditions. A mosquito was classified as dead or knocked down if it was immobile or unable to stand or take off respectively. The whole procedure (injections followed by bioassays) was repeated three times (~15 mosquitoes per condition/per biological replicate). In each round, ds*GFP* and ds*RNA* of genes of interest were injected concomitantly, to ensure comparable injection, insectary and bioassay conditions. Graphs were produced and statistically analyzed using GraphPad Prism software version 8 using Student’s t-test.

1.4 Results-Discussion

1.4.1 Evaluation of resistance of the VK7 *An. coluzzii* strains

VK7-LR originates from the VK7-HR population but was maintained without insecticide selection, resulting in a gradual loss of resistance. VK7-HR is highly resistant as 1 hour exposure to 0.05% deltamethrin diagnostic dose does not result to mortality at all (Figure 1.1). Concerning VK7-LR after testing different deltamethrin doses in 1 hour exposures we estimated the LC_{50} dose at 0.0016% (Figure 1.1). We also maintained in the laboratory a fully susceptible strain which has a completely different genetic background compared to the two VK7 populations. Before RNA extraction whole legs were carefully dissected, just on their attachment point to the thorax to ensure all leg segments were included (Figure 1.2A). For the comparison of constitutive resistance evaluation we selected both susceptible strains (NG and VK7-LR) against the VK7-HR (Figure 1.2B), while for the deltamethrin induction experiment we selected to expose the VK7-HR strain in 0.05% deltamethrin for one hour and compare it to the unexposed state (Figure 1.2C).

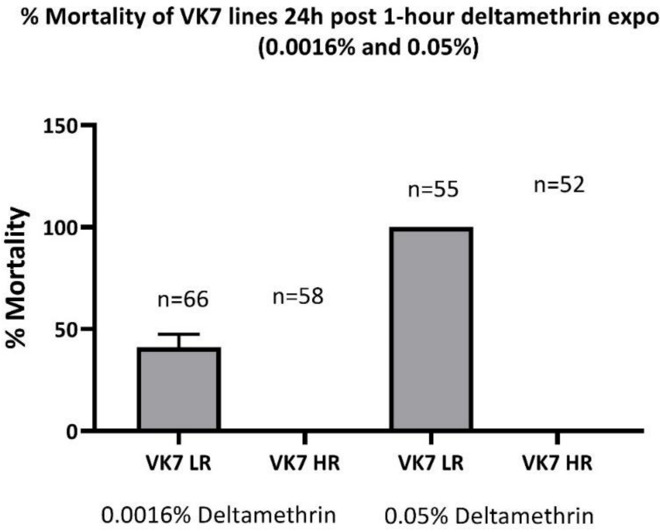

Figure 1.1 % Mortality of VK7 (lowly resistant, LR) and VK7 (highly resistant, HR) after 24 hours of 1 hour deltamethrin exposure. Two doses were used, the diagnostic (0.05% deltamethrin), where all VK7-LR were dead and all VK7-HR tested were alive and one lower dose (0.0016%), where almost half VK7-LR survived (LC_{50}) and no mortality was recorded for VK7-HR**.**

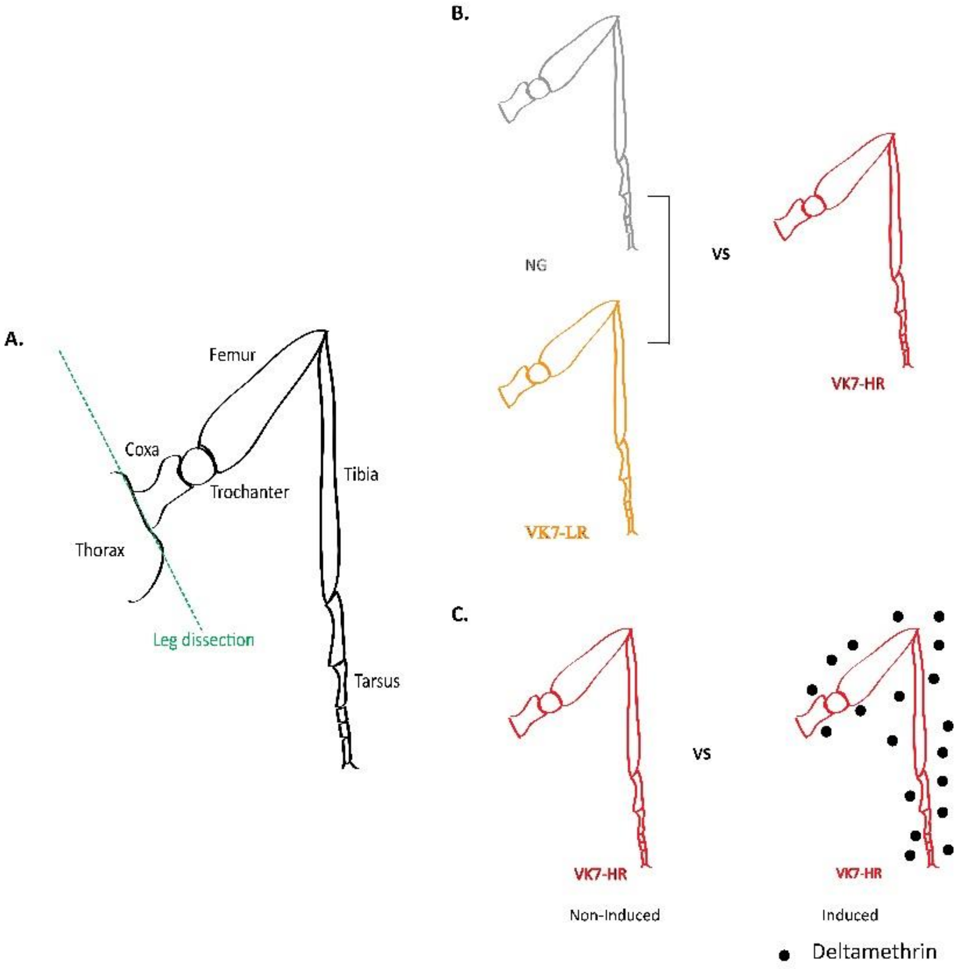
B.
NG
VS
VK7-HR
VK7-LR
A.
Femur
Coxa
Trochanter
Tibia
Thorax
Leg dissection
Tarsus
C.
VS
VK7-HR
Non-Induced
VK7-HR
Induced
● Deltamethrin

Figure 1.2. Graphical depiction of leg dissections. A. Dissections just on their attachment point to the thorax, in order to isolate whole legs including all their segments (coxa, trochanter, femur, tibia, tarsus) B. Graphical depiction of the comparisons made to assess constitutive resistance, C. Graphical depiction of the comparison made to assess differences after deltamethrin exposure.

1.4.2 Leg transcripts differentially expressed in resistant *An. coluzzii*

In the comparisons to assess constitutive resistance (Figure 1.2B) we identified 542 differentially expressed genes in VK7-HR against NG (109 up-regulated, 433 down-regulated) and 415 differentially expressed genes in VK7-HR against VK7-LR (108 up-regulated, 307 down-regulated). Of these, 73 genes were up-regulated and 159 genes were down-regulated in both comparisons and likely represent the genes contributing to the resistance phenotype (Figure 1.3).

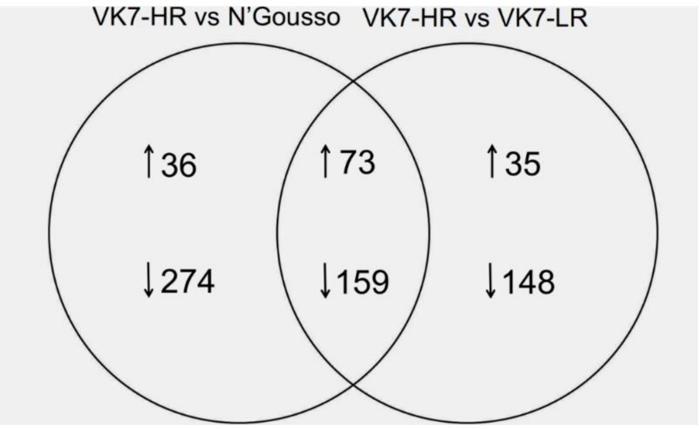

Figure 1.3. Number of differentially expressed genes. ($\log_2|FC| > 2$, $FDR < 0.01$) between VK7-HR (resistant) and the two susceptible strains, VK7-LR and N'Gousso. Upward arrows indicate over-expressed genes, whereas downward arrows represent under-expressed genes in VK7-HR compared to each of the susceptible strains.

Up-regulated transcripts in resistant *An. coluzzii*

Among the up-regulated genes there are two functional classes with previous links to insecticide resistance: detoxification enzymes and cuticular proteins (Figure 1.4A).

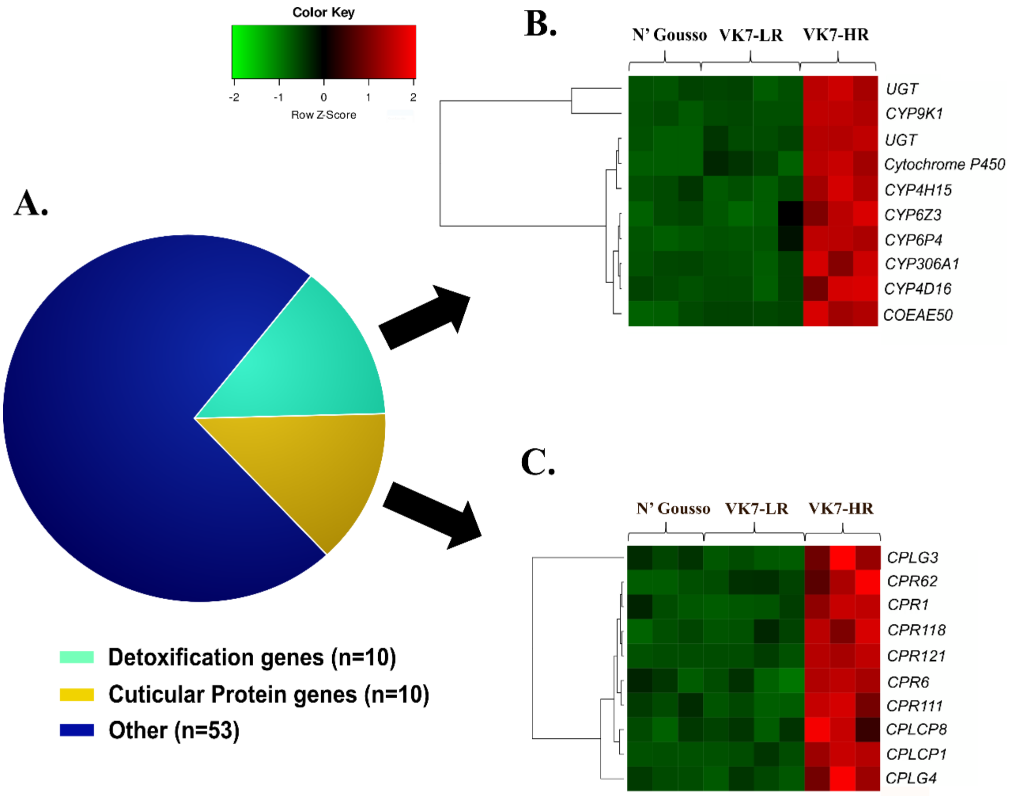

Figure 1.4. Up-regulated genes in resistant *An. coluzzii*. A. Functional classification of the 73 commonly up-regulated genes in the two comparisons related to constitutive resistance, VK7-HR vs VK7-LR and VK7-HR vs N'Gousso. Normalized expression levels (z-scores) for B. detoxification enzymes and C.

cuticular proteins, Gene functions were obtained from the official *An. gambiae* gene annotation. Gene prefixes are as follows: CYP - cytochrome P450s; UGT – UDP glucurunosyl-transferases; COEAE - carboxylesterase; CPLC/CPR - cuticular proteins.

Detoxification enzymes

Among the 73 up-regulated genes, there are 10 detoxification enzymes (13.70%) including seven cytochrome P450s (CYP), two UDP-Glycosyltransferases (UGTs) and one carboxylesterase (CCE) (Figure 1.4B), with none of these being identified in the leg-specific transcriptome. Enrichment analysis identified the over-represented GO terms include iron ion binding (GO:0005506), oxidation-reduction process (GO:0055114), monooxygenase activity (GO:0004497), heme binding (GO:0020037), tetrapyrrole binding (GO:0046906) and oxidoreductase activity and insecticide detoxification activity (GO:0016491) (Figure S1.1A), all of which are related to CYPs. Most of these GO terms (Figure S1.1A) have been recently associated with high levels of pyrethroid resistance in *An. funestus* [8], whilst *CYP9K1* and *CYP6P4* have been previously implicated in pyrethroid resistance in *Anopheles* mosquitoes [34-36]. Furthermore, *CYP6Z3* was previously associated with DDT, bendiocarb and pyrethroid resistance in *An. gambiae*, *An. funestus* and *An. arabiensis* populations [37-41]. The remaining detoxification genes in the above list are functionally uncharacterized with regard to insecticide resistance.

An enrichment in the transcription of detoxification gene transcripts has been observed in the midgut and Malpighian tubules of *An. gambiae* [5]; however, this study included limited numbers of tissues and resistance associated cytochrome P450s show a varied profile of tissue enrichment (including the head) (reviewed in [42]). Notably, midgut specific transgenic overexpression of the known pyrethroid metabolizers CYP6M2 or CYP6P3 did not induce the pyrethroid resistance phenotypes in susceptible *An. gambiae* [43] seen when these genes were ubiquitously expressed indicating that other tissues are also critical for detoxification.

Detoxification enzymes have been previously identified in the leg-specific proteome [7]. However, none of these detoxification enzymes were up-regulated in the VK7 leg transcriptome of this study. In the recent transcriptomic dataset of *D. melanogaster* single-cell transcriptomic atlas, transcripts of several detoxification enzymes including cytochrome P450s, glutathione-S-transferases and UDP-glucoronotransferases have been identified in cell types constituting the legs [11] , but their precise role remains elusive.

The constitutive up-regulation of detoxification genes here supports the hypothesis that the legs are involved in immediate detoxification of insecticides and act as the first line of defence where at least partial detoxification of insecticides could occur. Consequently, this would lead to at least some deactivation of the toxic effects of the insecticide before it enters the insect body and exerts its toxic effects, or even protect the peripheral nerves that are present in Diptera legs [11], from pyrethroid toxicity.

Cuticular proteins (CPs)

Cuticular thickening has been associated with insecticide resistance in *Anopheles* and *Culex*, as multiple CPs have been found up-regulated in resistant populations [8, 44-48] and attenuation of expression of *CPLCG5* leads to increased pyrethroid resistance in *Culex* [48]. The current dataset further supports the hypothesis that cuticle remodeling plays a crucial role in insecticide resistance; 10 of the up-regulated genes (13.7%) in VK7-HR encode for cuticular proteins (Figure 1.4C). These include members of the CPR family (CPR1, CPR6, CPR62, CPR111, CPR18 and CPR121), as well as the CPLCP (CPLCP1, CPLCP8) and the CPLCG (CPCLG3, CPLCG4) families (Figure 1.4C).

A recent proteomic analysis of resistant versus susceptible mosquito legs revealed that cuticular proteins and specifically the CPR family were the most up-regulated proteins in resistant legs of the same resistant strain (VK7-HR) with the one used in this study [7], although only CPR62 and CPR121 are found up regulated in both the VK7-HR leg proteome and transcriptome comprised in this study [7]. CPLCG3 and CPLCG4 have been previously found localized in the leg endocuticle potentially contributing to cuticle thickening and penetration rate of the insecticide [44]. *CPCLP1* (AGAP013465; 19.5-86.5 fold) was among the most up-regulated genes against both susceptible strains, while the ortholog of *CPLCP3* (AGAP008817; 8-fold) in *D. melanogaster*, *Vajk-4*, participates in cuticle barrier formation [49]. *CPR111* was recently found to be overexpressed in multiple pyrethroid-resistant *An. funestus* strains [8].

Down-regulated genes in resistant *An. coluzzii*

Amongst the down-regulated genes (Figure 1.5, Figure S1.1B) the most noteworthy are odorant binding proteins and the ones related to hormone metabolism and salivary gland proteins (Figure 1.5A).

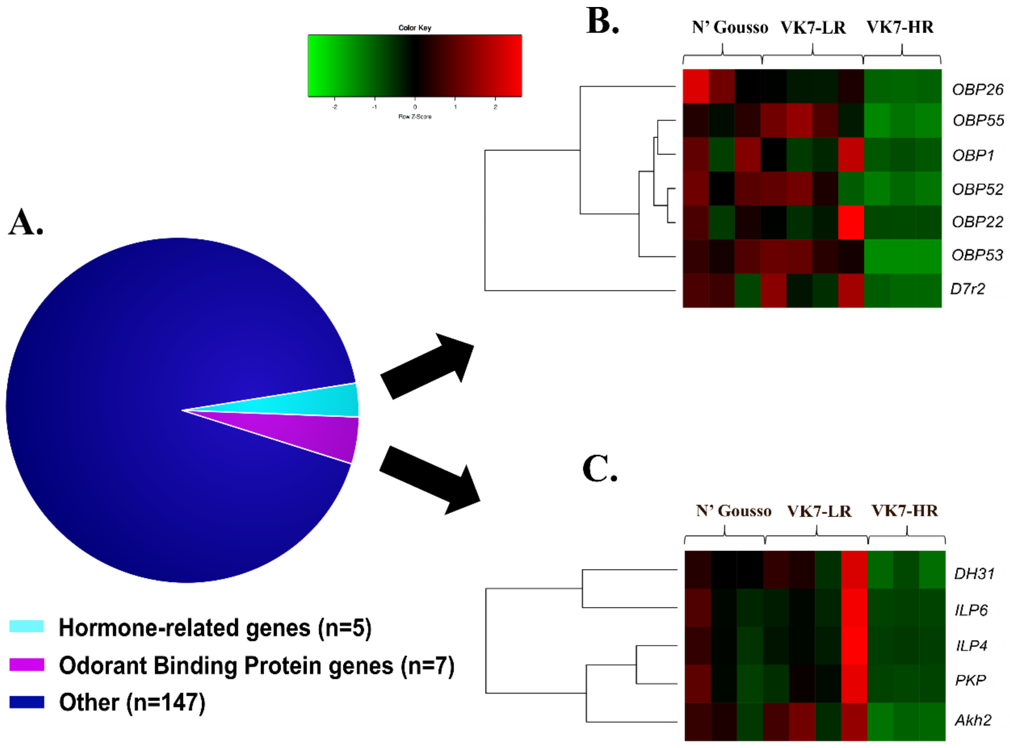

Figure 1.5. Down-regulated genes in resistant *An. coluzzii* A. Functional classification of the 159 commonly down-regulated genes in the two comparisons related to constitutive resistance, VK7-HR vs VK7-LR and VK7-HR vs NG. Normalized expression levels (z-scores) for B. odorant binding proteins and C. hormone activity-related genes. Gene functions were obtained from the official *An. gambiae* gene annotation. Genes prefixes are as follows: DH31 - diuretic hormone 31; ILP - Insulin-like peptide; PKP - pyrokinin; Akh2 - adipokinetic hormone 2.

Odorant binding proteins (OBPs)

Several genes coding for OBPs (OBP1, OBP52, OBP26, OBP55, OBP53) (Figure 1.5B) were under-expressed in the resistant strain (Figure S1.1B). Recent evidence derived from comparative proteomics supports the down-regulation of several OBPs in resistant legs. Models of *An.* *gambiae* OBPs suggest they can form hydrophobic channels enabling the transport of ligands, such as lipophilic insecticides [28, 50], and hence it is possible that down-regulation of OBPs could confer resistance due to decreased insecticide transport via these OBP-channels.

Hormone-related genes

Several hormone-related metabolic processes are under-represented in the VK7-HR resistant population (Figure 1.5C, Figure S1.1B). The corresponding GO terms include sterol metabolic process (GgO:0016125), steroid metabolic process (GO:0008202) and hormone activity (GO:0005179). More specifically, two sterol-o-transferases (AGAP012216, AGAP012217), two C-4 methylsterol oxidases (AGAP000946, AGAP002769), two insulin-like peptides (AGAP010601, AGAP010604), adipokinetic hormone 2 (Adk2, AGAP002430) and Diuretic hormone 31 (DH31, AGAP001382) were down-regulated in the constitutive resistant state. Apart from the main hormonal centers found in the brain and prothoracic glands, the insect endocrine system also includes secretory cells in neural ganglia and the epidermis [21] . Thus, transcription of such insect hormones in the legs could be attributed to these cells. It is likely that the reduction of expression in these pathways reflects an attempt to decrease heavy metabolic cost imposed by stress to support other critical physiological functions taking place in the first line of xenobiotic metabolism. This is also in accordance with leg proteomics where metabolism-related proteins were the most down-regulated in the resistant legs compared to susceptible [7]. Intriguingly, among the down-regulated genes are four CYPs that belong to the CYP4 family (CYP4AA1, CYP49A1, CYP4J5 and CYP4J10). In insects, CYPs of this family are involved in metabolism of endogenous compounds such as pheromones and ecdysosteroids and other developmental hormone metabolism processes [51, 52]. Hence, their downregulation is in agreement with the decrease in processes related to hormone metabolism.

Salivary gland proteins (SGPs)

Among the constitutively down-regulated genes there were 13 genes coding for SGPs. SGPs form a group of functionally and phylogenetically diverse protein families whose common feature is their expression in mosquito saliva [53]. This group includes proteins with enzymatic activities, implicated in blood feeding, anti-inflammatory, antihemostatic, vasodilatation and immunomodulatory responses [53, 54]. Identification of such transcripts in legs is surprising and their putative role there is unknown. Among the 13 down-regulated SGP genes only D7r2 (AGAP008282) was previously identified in the VK7 leg proteome [15].

1.4.3 Leg transcripts regulated by short-term deltamethrin induction

To study genes whose expression is induced in the legs after exposure to pyrethroids, we exposed the VK7-HR strain to deltamethrin for one hour, followed by one hour recovery. Subsequently, the leg transcriptome of this induced strain (VK7-IN) was compared to that of the unexposed VK7-HR strain (Figure 1.2C). Using the same strict statistical parameters ($\log_2|FC| > 2$, $FDR < 0.001$), we identified 404 differentially expressed genes in VK7-IN compared to VK7-HR (348 up-regulated, 56 down-regulated). The functional enrichment analysis of the up-regulated genes identified GO terms related to G protein-coupled receptor (GPCR) activity and drug catabolism (Figure 1.6 and S1.2). Interestingly, several genes coding for GPCRs, cytochrome P450s, ABC transporters and odorant binding proteins (OBPs), as well as proteins belonging to the divergent salivary gland protein family (SGPs), were up-regulated after deltamethrin exposure (Figure 1.6A). On the contrary, the functional enrichment analysis of the down-regulated genes did not identify any overrepresented GO terms.

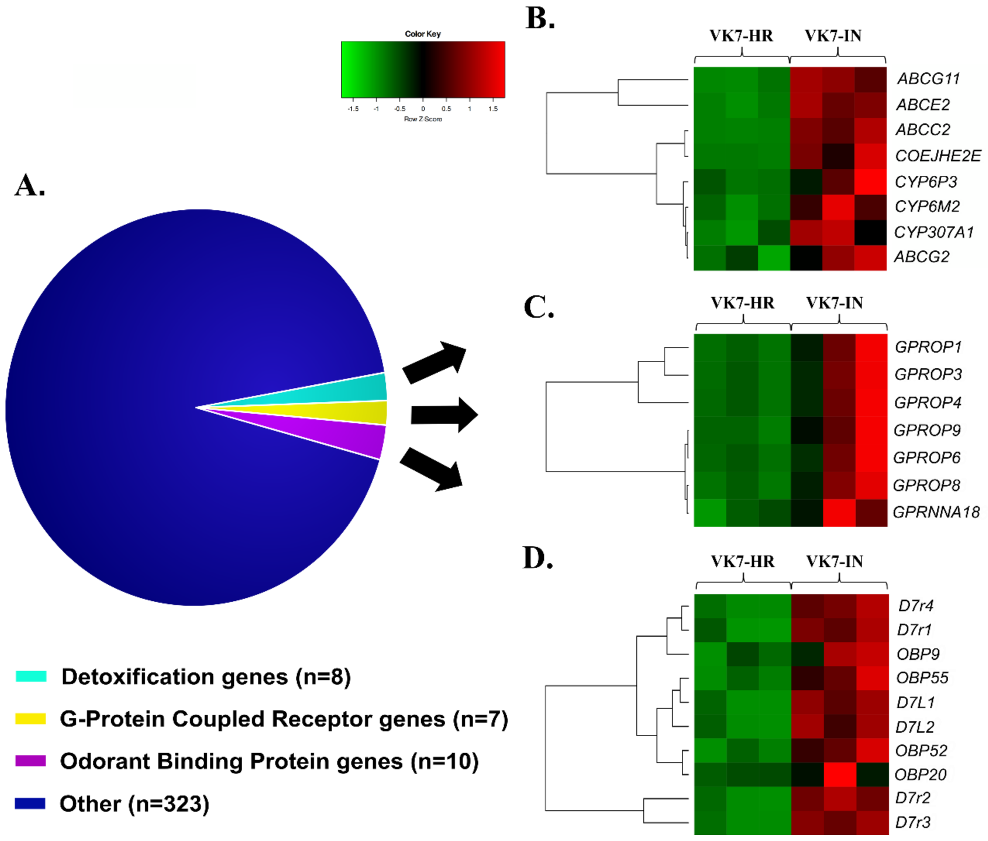

Figure 1.6. Up-regulated genes *An. coluzzii* after one hour deltamethrin exposure. A. Functional classification of the 348 up-regulated genes after 1-hour of exposure to deltamethrin. B. Normalized expression levels (z-scores) of detoxification enzymes, (C) G protein-coupled receptors, and (D) odorant

binding proteins. Gene prefixes are as follows: GPCR – G protein-coupled receptor; ABC – ATP binding cassette; CYP – cytochrome P450s; D7 - D7 salivary gland proteins; OBP – odorant binding protein.

Up-regulated leg transcripts upon deltamethrin induction

Detoxification enzymes

Among the 348 up-regulated genes post-deltamethrin exposure there were eight detoxification genes (2.30%): three CYPs (CYP6P3, CYP6M2 and CYP307A1), four ABC transporters and one carboxylesterase (Figure 1.6B). Interestingly, two of the three CYPs are known insecticide metabolizers (CYP6P3 and CYPM2) and were also induced in whole *An. coluzzii* mosquitoes after deltamethrin exposure, but also in different time points [15, 55]. Both CYP6P3 and CYP6M2 are capable of metabolizing all type I and type II pyrethroids used in vector control [56-58], in addition to bendiocarb, malathion, pirimiphos-methyl, Fenitrothion, DDT and pyriproxyfen [36] . None of the 8 detoxification enzymes overexpressed after deltamethrin exposure, including 3 p450s (CYP6M2, CYP6P3, CYP307A1) and one carboxylesterase (COEJHE2E) are leg-specific. CYP6M2 and CYP6P3 are up-regulated after 1 hour deltamethrin induction in whole *An. coluzzii* [15].

The fact that ABC transporter genes were up-regulated only upon deltamethrin exposure (Figure 1.6B), is consistent with the hypothesis that detoxification of phase 0 and/or III may take place upon induction [23]. The identified genes belong to the ABCC (n=1), ABCE (n=1) and ABCG (n=2) subfamilies (Figure 1.6B). Interestingly, ABCG11 which is identified among the leg-specific genes, is also up-regulated upon deltamethrin exposure. ABCCs have been implicated in the translocation of a range of substrates including drugs, exogenous compounds and their glutathione conjugates. ABCGs facilitate lipid, sterol and drug transport, while ABCEs comprise a highly conserved family known to participate in translational control and mRNA transport [22]. Of note, eight of the *An. gambiae* ABCGs are enriched in legs, most probably transporting lipids to the cuticle [59]. Among the over-expressed ABC transporter genes in VK7-IN legs, *ABCC2* was recently found to be over-expressed in *An. stephensi* after 6- and 12-hr deltamethrin exposure [60], while post permethrin exposure, ABCG4 of *An. stephensi* was over-expressed [27]. 1-hour induction has also been studied in respect to ABC transporter expression in whole *An. stephensi* with ABCB and ABCG members being induced [61]. Additionally, a subset of *An. gambiae sl* ABC transporters (ABCC, ABCB, ABCG) were induced upon early and/or late permethrin exposure timepoints [15, 62] in whole *An. gambiae sl* also evident in *An. stephensi* [25].

GPCR-mediated signaling

The transcriptomic analysis identified seven up-regulated GPCR genes, six of which code for opsins (Figure 1.6C). In particular, four of the six LW-sensitive and the SW-sensitive and UV-sensitive opsin genes were up-regulated after deltamethrin exposure, thus supporting the opsin-related functional enrichment.

The genome of *An. coluzzii* contains 11 opsin genes, six of which belong to the Long Wavelength (LW)-sensitive family, one in each of the Short Wavelength (SW)-sensitive, Ultraviolet (UV)-sensitive and Rh7-like opsin families, and two are characterized as non-visual pteropsins [63]. In particular, four of the six LW-sensitive, and the SW-sensitive and UV-sensitive opsin genes were up-regulated after deltamethrin exposure. Opsins are sensory GPCRs with a well-characterized role in sensing light and regulating downstream signaling pathways in insects [64]. Additionally, recent studies in *Drosophila* provide evidence suggesting several light-independent roles, thus establishing opsins as polymodal sensors with a wide array of cellular and physiological functions [64]. A recent study demonstrated that an opsin, NYD-OP7 [65], leads to deltamethrin resistance in *C. pipiens pallens* by regulating the expression of several cytochrome P450 genes through a phospholipase C (PLC)-mediated signaling pathway [20]. Knockdown of the *NYD-OP7* gene repressed the expression and the enzymatic activity of PLC, thus leading to reduced expression of downstream cytochrome P450 genes and increased susceptibility to deltamethrin [20]. Interestingly, among the six up-regulated opsin genes in VK7-HR legs after deltamethrin exposure (Figure 1.5C), there are three genes (*GPROP1*, *GPROP3* and *GPROP4*) that belong to the expanded LW-sensitive opsin family [63] . Two of these genes, *GRPOP1* and *GRPOP3*, were also found to be over-expressed in a previous study that characterized the transcriptomic profile of the *An. coluzzi* VK multi-resistant populations [66].

Two arrestin genes, *ARRESTIN-1* (AGAP006263) and *ARR2* (AGAP010134), were over-expressed after deltamethrin exposure. Arrestins are small proteins that interact with GPCRs and regulate their activity [67]. Expression of *ARRESTIN-1* has been previously reported in the olfactory organs (antennae, palps, proboscis) of *An. gambiae* and *D. melanogaster*, thus demonstrating that arrestin expression is not limited to photoreceptors [68]. Further, as olfaction is also present in the appendages, it is plausible that arrestins could also mediate such functions there. Both arrestins and GPCRs were found to be expressed in tick legs, with suggested roles in chemoreception [13].

Here we hypothesize that GPCR-mediated pathways could orchestrate the initial response to the stress imposed by deltamethrin. Such responses could be related to enhanced metabolic detoxification, as it has been demonstrated in *Culex quinquefasciatus* [69-71] and *Spodoptera frugiperda* Sf9 cells where GPCR-regulated pathways resulted in P450-mediated resistance after permethrin exposure [69].

Apart from this hypothesis, the presence of some neuropeptides in our dataset could imply some other GPCR-stimulated responses. More specifically adipokinetic hormone 2 (*AKH2*) and Diuretic hormone 31 (*DH31*) are also induced upon short-term deltamethrin exposure. Concerning the former, the AKH proteins are neuropeptides that upon stress have been shown to trigger energy catabolic reaction in insects to gain energy and also to stimulate stress responses such as enhanced locomotion, immune responses [21, 72] and energy mobilization by stimulation of lipolysis of triacylglycerols [73, 74]. Interestingly, the upregulation of AKH transcripts is profound in several studies upon insecticide stress [72, 75]. Finally, Diuretic hormone 31 (DH31), has been shown to interact with a class II G-protein-coupled receptor [76, 77] with implication in thermosensation, thermoregulation and sleep modulation [78].

Odorant binding proteins (OBPs) and salivary gland proteins (SGPs)

Ten genes coding for odorant binding proteins (OBPs) were up-regulated after exposure to deltamethrin (Figure 1.6D). Of these, only *OBP55* was identified in the leg-specific dataset too. Generally, OBPs have an important role in insect chemoreception by capturing hydrophobic chemicals from the environment and transporting them to the chemosensory receptors [79, 80]. Insect chemosensory sensilla are also present in the legs, in addition to other [81, 82]. The leg sensing role in insects is crucial for recognizing non-volatile chemical signals [83, 84] and it is mediated by many different protein families, including OBPs and chemosensory proteins (CSPs) [82].

Interestingly, pheromone/odorant binding proteins were found over-transcribed under insecticide selection pressure in *An. gambiae* [47]. In addition, a transcriptomic meta-analysis underlines the persistent presence of OBPs in insecticide resistance comparing to susceptible datasets [85], while recent data from the fruit fly also highlight increased transcription of several members of this protein family post treatment with sub-lethal concentrations of insecticides [86].

The crucial role of such chemosensory, ligand-binding proteins in insecticide resistance in *An. coluzzii*, was recently demonstrated with SAP2, a member of the lipocalin subfamily of CSPs [15, 29]. More specifically, it was demonstrated that SAP2 binds deltamethrin with high affinity, and overexpression of SAP2 in susceptible mosquitoes led to increased deltamethrin resistance [12]. In addition, *SAP2* expression was induced upon exposure to deltamethrin, whilst attenuating expression led to higher mortality to all pyrethroids [12].

Moreover, six D7 salivary gland proteins that belong to the insect odorant binding protein superfamily [87], were up-regulated in VK7-HR legs after deltamethrin exposure: four of these belong to the short-form D7 SGPs (*D7r1-4*), while the remaining two code for the long-form D7 SGPs (*D7L1-2*) [53].

There are several studies that implicate members of the D7 family with constitutive insecticide resistance [7, 88, 89], but to our knowledge this is the first dataset that shows their up-regulation upon pyrethroid exposure. The inability to detect these transcripts could be due to the "diluting" effect of whole body sequencing; legs are a relatively small tissue and so relatively contribute a small amount of RNA to the total extraction.

Whole genome microarrays of bendiocarb-resistant *An. gambiae* species from Uganda demonstrated significant over-expression of the *D7r2* and *D7r4* genes while prediction models reveal that binding of *D7r4* and bendiocarb simulates *D7r4* binding with its known ligand, serotonin [88], implying a role of D7 SGPs in direct insecticide binding. However, it should be mentioned that *D7r2* showed a sustained down-regulation 4 and 8 hours after deltamethrin exposure [15].

Apart from D7 SGPs, in total, 33 genes coding for SGPs were over-expressed in VK7-HR legs after deltamethrin exposure nine of which were among the 20 most up-regulated genes. Identification of SGP transcripts in *An. coluzzii* legs is an interesting finding as it shows that expression of this group of proteins is not salivary gland specific. Moreover, we also show that their expression is enhanced upon short-term deltamethrin induction. However, their putative role in legs and their contribution upon insecticide induction is unknown and requires further study.

Down-regulated leg transcripts upon deltamethrin induction

Only 56 genes were under-expressed upon short term deltamethrin exposure, which accounts only for 13.8% of the total differentially expressed genes. The functional enrichment analysis did not identify any over-represented GO terms in this subset. The most down-regulated genes after deltamethrin exposure were *elongation of very long chain fatty acids protein 4* (AGAP010695), three genes encoding for cuticular proteins (*CPR73* and *CPLCG2*, *CPLCP8*), two CYPs (*CYP325C2*, *CYP325H1*) and one ABC transporter (*ABCG18*). Among these, *CPR73* is also a leg-specific gene, while *CPLCP8* was up-regulated in legs of resistant mosquitoes. Other studies also show down-regulation of detoxification family members in different time points post-pyrethroid exposure [15].

1.4.4 Combined analysis of leg transcript datasets

Overall, this leg-specific transcriptomic dataset indicates that induction and constitutive resistant profile are divergent (Figure 1.7). Indicative is the fact that only three common up-regulated genes were found between the two states (constitutive and induced). Two of these encode for alpha-crystallins, previously implicated in pyrethroid resistance and long-term deltamethrin induction [85] . On the other hand, 68 genes were down-regulated in the legs of resistant mosquitoes, while they were also up-regulated upon short-term deltamethrin induction. This opposite trend between constitutive resistance and deltamethrin-induced tolerance is also reflected by the fact that 68.5% of the differentially expressed genes between resistant and susceptible strains are down-regulated, while this percentage is only 13.8% for the legs of deltamethrin exposed mosquitoes. In the former state, this is potentially indicative of an energy-saving mode compared to the more energy-costly profile of the latter stressful situation.

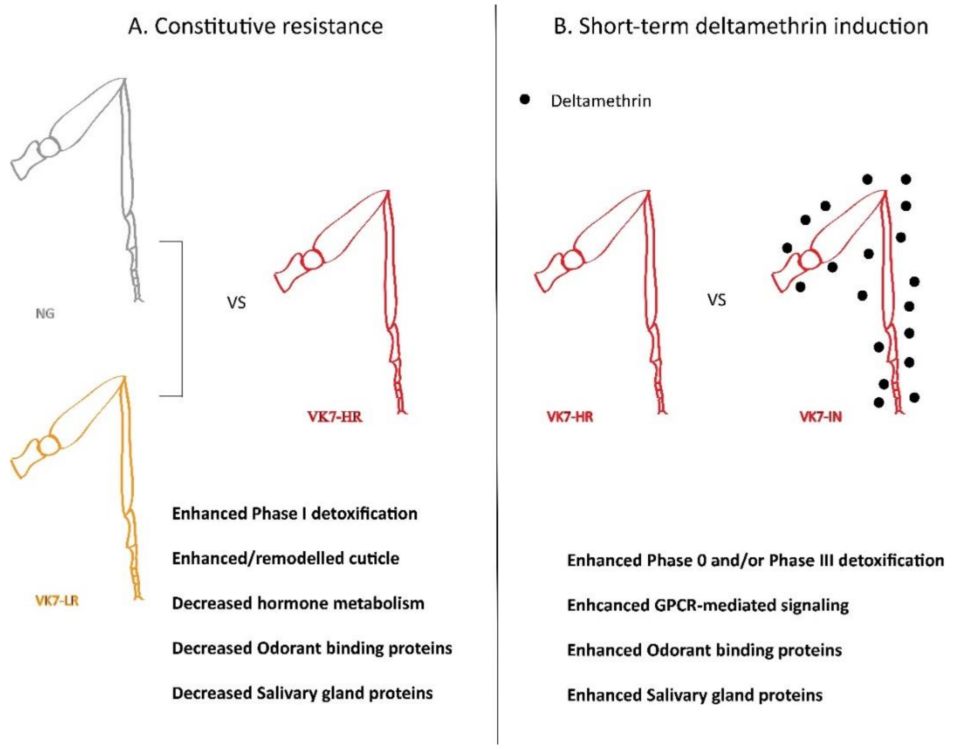
A. Constitutive resistance
NG
VS
VK7-HR
VK7-LR
Enhanced Phase I detoxification
Enhanced/remodelled cuticle
Decreased hormone metabolism
Decreased Odorant binding proteins
Decreased Salivary gland proteins
B. Short-term deltamethrin induction
● Deltamethrin
VK7-HR
VS
VK7-IN
Enhanced Phase 0 and/or Phase III detoxification
Enhcanced GPCR-mediated signaling
Enhanced Odorant binding proteins
Enhanced Salivary gland proteins

Figure 1.7. Graphical depiction of the two main comparisons made and the main findings of each one. A. Constitutive resistance in legs of multi-resistant VK7-HR mosquitoes versus two susceptible counterparts (NG and VK7-LR) revealed enhanced phase I detoxification and cuticular genes, decreased hormone-mediated metabolic processes and decreased expression of genes encoding odorant-binding and salivary gland proteins, B. Short-term deltamethrin induction in VK7-HR resulted in up-regulation of detoxification, with overrepresentation of transporters (Phase 0 and III), enhanced GPCR signaling, odorant-binding proteins and salivary gland proteins.

1.4.5 RNAi-mediated silencing coupled with toxicity bioassays of cuticular protein genes revealed by proteome and transcriptome analyses.

As several cuticular proteins were up-regulated both in this transcriptome dataset but were also remarkably enriched in a previous comparative proteome analysis conducted between legs from resistant and susceptible mosquitoes [7], some of them were chosen for validation via silencing-toxicity experiments. These were carried out using dsRNA nano-injections in newly-emerged adults, evaluation of the silencing efficiency of each construct three days after injections and toxicity bioassays using deltamethrin to estimate survival. The selected cuticular proteins were: CPR125, CPR59, CPLCG5, CPR126. All constructs resulted in more than 50% reduction of transcripts relative abundance of the respected gene when compared to control RNAs extracted from mosquitoes injected with dsGFP (Figure 1.8A). Apart from them, a dsRNA against multiple CPRs (dsCPRmult) was constructed (Figure 1.8B) and as targeting many genes no silencing efficiency was addressed for that. We next performed toxicity bioassays comparing the survival of injecting mosquitoes with dsRNAs against the genes of interest versus dsGFP controls. What we observed is that silencing each of the individual cuticular protein genes selected resulted in no difference in survival of these highly resistant mosquitoes in this developmental stage (Figure 1.9). The only case where a significant 20% reduction in survival was observed was when dsRNA targeting multiple CPRs was used (Figure 1.9).

The comparative datasets advocate their upregulation and/or remodeling in legs of resistant mosquitoes; however the silencing-toxicity experiments show that each one of them is not sufficient for restoring part of susceptibility. Cuticular proteins are structural proteins of the procuticle and there are almost 300 of them in *An. coluzzii*. Apparently, there is redundancy among all these genes and especially in adult developmental stage, where molt has successfully been carried out and dsRNA only partially reduce the transcript levels, it is hard to observe differences in susceptibility. However, when multiple CPRs were targeted (almost 7 CPRs at the same time) a significant decrease of about 20% in survival of resistant mosquitoes was observed. This is a remarkable decrease given that other resistant mechanisms are also present in these multi-resistant mosquitoes apart from cuticular resistance, advocating that indeed enhanced cuticular protein presence is crucial for resistance.

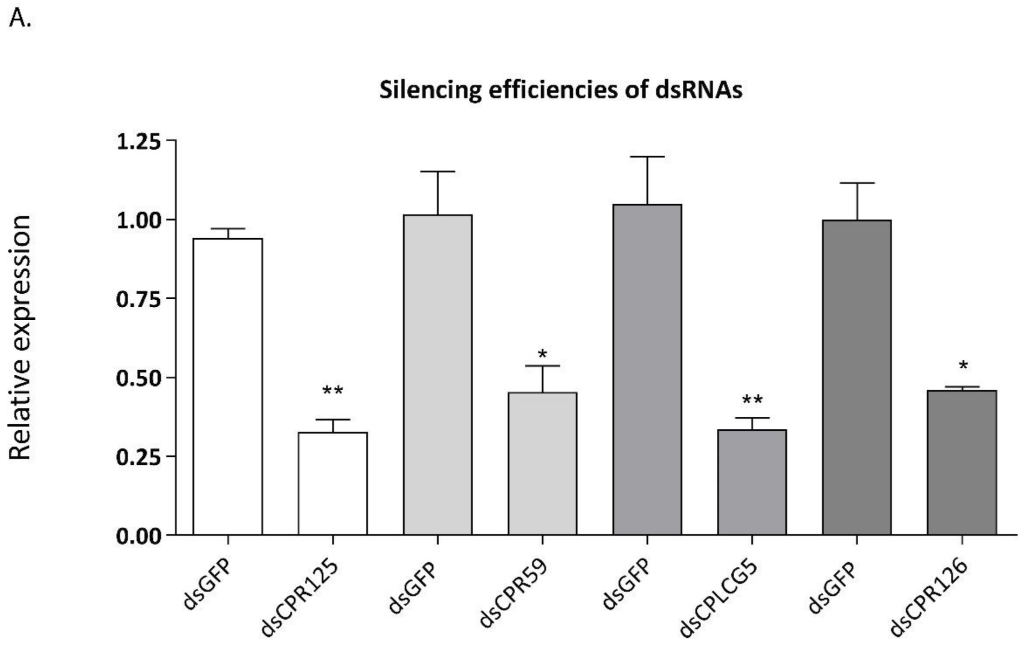

B.

CPRs targeted by dsCPRmult

Gene	ds***CPRmult*** **Identity**
AGAP003377-RA (CPR115)	100%
AGAP003379-RA (CPR117)	
AGAP003382-RA (CPR120)	
AGAP003383-RA (CPR121)	
AGAP003380-RA (CPR118)	95 %
AGAP003380-RA (CPR119)	
AGAP003385-RA (CPR123)	

Figure 1.8. Silencing of cuticular protein genes. A. Silencing efficiencies of different dsRNAs, expressed as relative expression of each gene targeted with dsRNA (reduced expression levels) compared with each dsGFP control (normal expression levels), B. Cuticular proteins targeted by the dsRNA acting against multiple genes and the identity of the dsRNA against each of the targets.

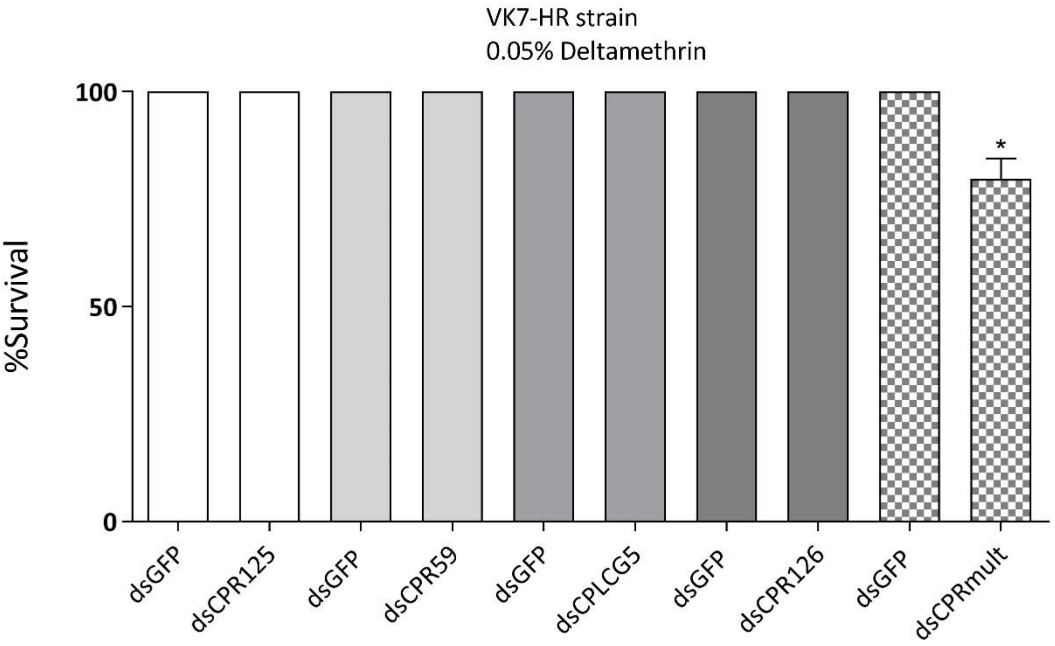

Figure 1.9. % Survival after deltamethrin exposure of dsRNA silenced mosquitoes. Mosquitoes injected with the dsRNAs against cuticular protein genes selected, were subjected to deltamethrin exposure. Mosquito survival 24 hours after 1 hour exposure to 0.05% deltamethrin insecticide for the genes of interest compared to dsGFP-injected controls.

1.5. Conclusions

Overall, this study provides detailed analysis on the transcriptional profile of mosquito legs, describing the differential expression in legs of pyrethroid resistant mosquitoes and upon exposure to pyrethroid insecticides. Taken together, these data describe what is likely to be the first line of defense against vector control tools and suggests that metabolic detoxification is likely occurring in these tissues. Analyzing the transcriptome of only the legs, effectively removes the noise of the remaining body and avoids “diluting” the transcripts specifically expressed in this relatively small tissue. Our data suggest that constitutive resistance can be attributed at a degree at least to the transcription of detoxification genes and cuticular genes, with a simultaneous decrease in hormone-related metabolism. Specifically for cuticular proteins the silencing-toxicity experiments performed indicated that targeting individually cuticular protein genes is not sufficient to restore susceptibility. Targeting multiple of them however, results in a significant decrease (~20%). Concerning short-term insecticide-induced tolerance, it seems to be linked with increased transcription of transporters, GPCRs and GPCR-related genes, sensory/binding proteins and salivary gland proteins. Additionally, according to our findings GPCR-mediated signaling has a leading role in the response observed in the legs after deltamethrin exposure, most likely via triggering the initial responses upon this stressing situation. Surprisingly, salivary gland protein genes are highly expressed in the legs: down-regulated in the legs of resistant mosquitoes albeit induced upon short-term deltamethrin exposure. Given previous links with resistance, these proteins require further study.

1.6. Literature

1. WHO, *World malaria report 2021.* World Health Organization, 2021.
2. Bhatt, S., et al., *The effect of malaria control on Plasmodium falciparum in Africa between 2000 and 2015.* Nature, 2015. **526**(7572): p. 207-211.
3. Cook, J., et al., *Implications of insecticide resistance for malaria vector control with long-lasting insecticidal nets: trends in pyrethroid resistance during a WHO-coordinated multi-country prospective study.* Parasites & Vectors, 2018. **11**(1): p. 550.
4. Balabanidou, V., et al., *Cytochrome P450 associated with insecticide resistance catalyzes cuticular hydrocarbon production in Anopheles gambiae.* Proc Natl Acad Sci U S A, 2016. **113**(33): p. 9268-73.
5. Ingham, V.A., et al., *The transcription factor Maf-S regulates metabolic resistance to insecticides in the malaria vector Anopheles gambiae.* BMC Genomics, 2017. **18**(1): p. 669.
6. Balabanidou, V., L. Grigoraki, and J. Vontas, *Insect cuticle: a critical determinant of insecticide resistance.* Current Opinion in Insect Science, 2018. **27**: p. 68-74.
7. Balabanidou, V., et al., *Mosquitoes cloak their legs to resist insecticides.* Proc Biol Sci, 2019. **286**(1907): p. 20191091.
8. Weedall, G.D., et al., *A cytochrome P450 allele confers pyrethroid resistance on a major African malaria vector, reducing insecticide-treated bednet efficacy.* Sci Transl Med, 2019. **11**(484).
9. Simma, E.A., et al., *Genome-wide gene expression profiling reveals that cuticle alterations and P450 detoxification are associated with deltamethrin and DDT resistance in Anopheles arabiensis populations from Ethiopia.* Pest Manag Sci, 2019. **75**(7): p. 1808-1818.
10. Andriessen, R., et al., *Electrostatic coating enhances bioavailability of insecticides and breaks pyrethroid resistance in mosquitoes.* Proc Natl Acad Sci U S A, 2015. **112**(39): p. 12081-6.
11. Li, H., et al., *Fly Cell Atlas: a single-cell transcriptomic atlas of the adult fruit fly.* bioRxiv, 2021: p. 2021.07.04.451050.
12. Ingham, V.A., et al., *A sensory appendage protein protects malaria vectors from pyrethroids.* Nature, 2020. **577**(7790): p. 376-380.
13. Carr, A.L., et al., *Tick Haller's Organ, a New Paradigm for Arthropod Olfaction: How Ticks Differ from Insects.* International journal of molecular sciences, 2017. **18**(7): p. 1563.
14. Terriere, L.C. and S.J. Yu, *Induction of detoxifying enzymes in insects.* Journal of Agricultural and Food Chemistry, 1974. **22**(3): p. 366-373.
15. Ingham, V.A., F. Brown, and H. Ranson, *Transcriptomic analysis reveals pronounced changes in gene expression due to sub-lethal pyrethroid exposure and ageing in insecticide resistance Anopheles coluzzii.* BMC Genomics, 2021. **22**(1): p. 337.
16. Festucci-Buselli, R.A., et al., *Expression of Cyp6g1 and Cyp12d1 in DDT resistant and susceptible strains of Drosophila melanogaster.* Insect Mol Biol, 2005. **14**(1): p. 69-77.
17. Zhu, F., et al., *Co-up-regulation of three P450 genes in response to permethrin exposure in permethrin resistant house flies, Musca domestica.* BMC Physiol, 2008. **8**: p. 18.
18. Misra, J.R., et al., *Transcriptional regulation of xenobiotic detoxification in Drosophila.* Genes Dev, 2011. **25**(17): p. 1796-806.

19. Shen, G. and A.N. Kong, *Nrf2 plays an important role in coordinated regulation of Phase II drug metabolism enzymes and Phase III drug transporters.* Biopharm Drug Dispos, 2009. **30**(7): p. 345-55.
20. Zhou, D., et al., *NYD-OP7/PLC regulatory signaling pathway regulates deltamethrin resistance in Culex pipiens pallens (Diptera: Culicidae).* Parasites & Vectors, 2018. **11**(1): p. 419.
21. Kodrík, D., et al., *Hormonal Regulation of Response to Oxidative Stress in Insects-An Update.* Int J Mol Sci, 2015. **16**(10): p. 25788-816.
22. Dermauw, W. and T. Van Leeuwen, *The ABC gene family in arthropods: comparative genomics and role in insecticide transport and resistance.* Insect Biochem Mol Biol, 2014. **45**: p. 89-110.
23. Kennedy, C. and K. Tierney, *Xenobiotic Protection xenobiotic protection /Resistance Mechanisms in Organisms*. 2012. p. 12293-12314.
24. Mastrantonio, V., et al., *Insecticide Exposure Triggers a Modulated Expression of ABC Transporter Genes in Larvae of Anopheles gambiae s.s.* Insects, 2019. **10**(3).
25. De Marco, L., et al., *The choreography of the chemical defensome response to insecticide stress: insights into the Anopheles stephensi transcriptome using RNA-Seq.* Scientific reports, 2017. **7**: p. 41312-41312.
26. Epis, S., et al., *Temporal dynamics of the ABC transporter response to insecticide treatment: insights from the malaria vector Anopheles stephensi.* Scientific reports, 2014. **4**: p. 7435-7435.
27. Epis, S., et al., *ABC transporters are involved in defense against permethrin insecticide in the malaria vector Anopheles stephensi.* Parasit Vectors, 2014. **7**: p. 349.
28. Pelosi, P., et al., *Soluble proteins in insect chemical communication.* Cell Mol Life Sci, 2006. **63**(14): p. 1658-76.
29. Pelosi, P., et al., *Soluble proteins of chemical communication: an overview across arthropods.* Frontiers in Physiology, 2014. **5**(320).
30. Iovinella, I., et al., *Ligand-binding study of Anopheles gambiae chemosensory proteins.* Chem Senses, 2013. **38**(5): p. 409-19.
31. Namountougou, M., et al., *Multiple Insecticide Resistance in Anopheles gambiae s.l. Populations from Burkina Faso, West Africa.* PLOS ONE, 2012. **7**(11): p. e48412.
32. Williams, J., et al., *Characterisation of Anopheles strains used for laboratory screening of new vector control products.* Parasites & Vectors, 2019. **12**(1): p. 522.
33. Kefi, M., et al., *Transcriptomic analysis of resistance and short-term induction response to pyrethroids, in Anopheles coluzzii legs.* BMC Genomics, 2021. **22**(1): p. 891.
34. Vontas, J., et al., *Rapid selection of a pyrethroid metabolic enzyme CYP9K1 by operational malaria control activities.* Proc Natl Acad Sci U S A, 2018. **115**(18): p. 4619-4624.
35. Ibrahim, S.S., et al., *The cytochrome P450 CYP6P4 is responsible for the high pyrethroid resistance in knockdown resistance-free Anopheles arabiensis.* Insect biochemistry and molecular biology, 2016. **68**: p. 23-32.
36. Yunta, C., et al., *Cross-resistance profiles of malaria mosquito P450s associated with pyrethroid resistance against WHO insecticides.* Pestic Biochem Physiol, 2019. **161**: p. 61-67.
37. Antonio-Nkondjio, C., et al., *Investigation of mechanisms of bendiocarb resistance in Anopheles gambiae populations from the city of Yaoundé, Cameroon.* Malaria Journal, 2016. **15**(1): p. 424.

38. Müller, P., M.J. Donnelly, and H. Ranson, *Transcription profiling of a recently colonised pyrethroid resistant Anopheles gambiae strain from Ghana.* BMC Genomics, 2007. **8**: p. 36.

39. Müller, P., et al., *Field-caught permethrin-resistant Anopheles gambiae overexpress CYP6P3, a P450 that metabolises pyrethroids.* PLoS Genet, 2008. **4**(11): p. e1000286.

40. Nardini, L., et al., *DDT and pyrethroid resistance in Anopheles arabiensis from South Africa.* Parasites & Vectors, 2013. **6**(1): p. 229.

41. Witzig, C., et al., *Genetic mapping identifies a major locus spanning P450 clusters associated with pyrethroid resistance in kdr-free Anopheles arabiensis from Chad.* Heredity (Edinb), 2013. **110**(4): p. 389-97.

42. Vontas, J., E. Katsavou, and K. Mavridis, *Cytochrome P450-based metabolic insecticide resistance in Anopheles and Aedes mosquito vectors: Muddying the waters.* Pestic Biochem Physiol, 2020. **170**: p. 104666.

43. Adolfi, A., et al., *Functional genetic validation of key genes conferring insecticide resistance in the major African malaria vector, Anopheles gambiae.* Proc Natl Acad Sci U S A, 2019. **116**(51): p. 25764-25772.

44. Vannini, L., T.W. Reed, and J.H. Willis, *Temporal and spatial expression of cuticular proteins of Anopheles gambiae implicated in insecticide resistance or differentiation of M/S incipient species.* Parasit Vectors, 2014. **7**: p. 24.

45. Vontas, J., et al., *Transcriptional analysis of insecticide resistance in Anopheles stephensi using cross-species microarray hybridization.* Insect Mol Biol, 2007. **16**(3): p. 315-24.

46. Koganemaru, R., D.M. Miller, and Z.N. Adelman, *Robust cuticular penetration resistance in the common bed bug (Cimex lectularius L.) correlates with increased steady-state transcript levels of CPR-type cuticle protein genes.* Pesticide Biochemistry and Physiology, 2013. **106**(3): p. 190-197.

47. Nkya, T.E., et al., *Insecticide resistance mechanisms associated with different environments in the malaria vector Anopheles gambiae: a case study in Tanzania.* Malaria Journal, 2014. **13**(1): p. 28.

48. Huang, Y., et al., *Culex pipiens pallens cuticular protein CPLCG5 participates in pyrethroid resistance by forming a rigid matrix.* Parasites & Vectors, 2018. **11**(1): p. 6.

49. Cinege, G., et al., *Genes encoding cuticular proteins are components of the Nimrod gene cluster in Drosophila.* Insect Biochem Mol Biol, 2017. **87**: p. 45-54.

50. Wogulis, M., et al., *The crystal structure of an odorant binding protein from Anopheles gambiae: evidence for a common ligand release mechanism.* Biochem Biophys Res Commun, 2006. **339**(1): p. 157-64.

51. Davies, L., et al., *Expression and down-regulation of cytochrome P450 genes of the CYP4 family by ecdysteroid agonists in Spodoptera littoralis and Drosophila melanogaster.* Insect Biochem Mol Biol, 2006. **36**(10): p. 801-7.

52. Zhang, H., et al., *Identification of cytochrome P450 monooxygenase genes and their expression in response to high temperature in the alligatorweed flea beetle Agasicles hygrophila (Coleoptera: Chrysomelidae).* Scientific Reports, 2018. **8**(1): p. 17847.

53. Arcà, B., et al., *Anopheline salivary protein genes and gene families: an evolutionary overview after the whole genome sequence of sixteen Anopheles species.* BMC Genomics, 2017. **18**(1): p. 153.

54. Calvo, E., et al., *Function and evolution of a mosquito salivary protein family.* J Biol Chem, 2006. **281**(4): p. 1935-42.

55. Bonizzoni, M., et al., *RNA-seq analyses of changes in the Anopheles gambiae transcriptome associated with resistance to pyrethroids in Kenya: identification of*

candidate-resistance genes and candidate-resistance SNPs. Parasit Vectors, 2015. **8**: p. 474.

56. Mitchell, S.N., et al., *Identification and validation of a gene causing cross-resistance between insecticide classes in Anopheles gambiae from Ghana.* Proceedings of the National Academy of Sciences of the United States of America, 2012. **109**(16): p. 6147-6152.
57. Edi, C.V., et al., *CYP6 P450 enzymes and ACE-1 duplication produce extreme and multiple insecticide resistance in the malaria mosquito Anopheles gambiae.* PLoS Genet, 2014. **10**(3): p. e1004236.
58. Stevenson, B.J., et al., *Cytochrome P450 6M2 from the malaria vector Anopheles gambiae metabolizes pyrethroids: Sequential metabolism of deltamethrin revealed.* Insect Biochem Mol Biol, 2011. **41**(7): p. 492-502.
59. Pignatelli, P., et al., *The Anopheles gambiae ATP-binding cassette transporter family: phylogenetic analysis and tissue localization provide clues on function and role in insecticide resistance.* Insect Mol Biol, 2018. **27**(1): p. 110-122.
60. Yunta, C., et al., *Cross-resistance profiles of malaria mosquito P450s associated with pyrethroid resistance against WHO insecticides.* Pesticide Biochemistry and Physiology, 2019. **161**: p. 61-67.
61. Mastrantonio, V., et al., *Gene expression modulation of ABC transporter genes in response to permethrin in adults of the mosquito malaria vector Anopheles stephensi.* Acta Trop, 2017. **171**: p. 37-43.
62. Mastrantonio, V., et al., *Insecticide Exposure Triggers a Modulated Expression of ABC Transporter Genes in Larvae of Anopheles gambiae s.s.* Insects, 2019. **10**(3): p. 66.
63. Giraldo-Calderón, G.I., M.J. Zanis, and C.A. Hill, *Retention of duplicated long-wavelength opsins in mosquito lineages by positive selection and differential expression.* BMC Evolutionary Biology, 2017. **17**(1): p. 84.
64. Leung, N.Y. and C. Montell, *Unconventional Roles of Opsins.* Annual review of cell and developmental biology, 2017. **33**: p. 241-264.
65. Hu, X., et al., *Cloning and characterization of NYD-OP7, a novel deltamethrin resistance associated gene from Culex pipiens pallens.* Pesticide Biochemistry and Physiology, 2007. **88**(1): p. 82-91.
66. Kwiatkowska, R.M., et al., *Dissecting the mechanisms responsible for the multiple insecticide resistance phenotype in Anopheles gambiae s.s., M form, from Vallée du Kou, Burkina Faso.* Gene, 2013. **519**(1): p. 98-106.
67. Merrill, C.E., R.J. Pitts, and L.J. Zwiebel, *Molecular characterization of arrestin family members in the malaria vector mosquito, Anopheles gambiae.* Insect Mol Biol, 2003. **12**(6): p. 641-50.
68. Merrill, C.E., et al., *Visual arrestins in olfactory pathways of &lt;em&gt;Drosophila&lt;/em&gt; and the malaria vector mosquito &lt;em&gt;Anopheles&lt;/em&gt; &lt;em&gt;gambiae&lt;/em&gt.* Proceedings of the National Academy of Sciences, 2002. **99**(3): p. 1633.
69. Cunningham, J., et al., *A review of the WHO malaria rapid diagnostic test product testing programme (2008–2018): performance, procurement and policy.* Malaria Journal, 2019. **18**(1): p. 387.
70. Li, T., et al., *A G-protein-coupled receptor regulation pathway in cytochrome P450-mediated permethrin-resistance in mosquitoes, Culex quinquefasciatus.* Scientific Reports, 2015. **5**(1): p. 17772.
71. Li, T., et al., *Role of G-protein-coupled receptor-related genes in insecticide resistance of the mosquito, Culex quinquefasciatus.* Sci Rep, 2014. **4**: p. 6474.

72. Kodrík, D., I. Bártů, and R. Socha, *Adipokinetic hormone (Pyrap-AKH) enhances the effect of a pyrethroid insecticide against the firebug Pyrrhocoris apterus.* Pest Manag Sci, 2010. **66**(4): p. 425-31.
73. Grönke, S., et al., *Dual lipolytic control of body fat storage and mobilization in Drosophila.* PLoS Biol, 2007. **5**(6): p. e137.
74. Caers, J., et al., *More than two decades of research on insect neuropeptide GPCRs: An overview.* Frontiers in endocrinology, 2012. **3**: p. 151.
75. Plavšin, I., et al., *Hormonal enhancement of insecticide efficacy in Tribolium castaneum: oxidative stress and metabolic aspects.* Comp Biochem Physiol C Toxicol Pharmacol, 2015. **170**: p. 19-27.
76. Shafer, O.T., et al., *Widespread receptivity to neuropeptide PDF throughout the neuronal circadian clock network of Drosophila revealed by real-time cyclic AMP imaging.* Neuron, 2008. **58**(2): p. 223-37.
77. Mertens, I., et al., *PDF Receptor Signaling in Drosophila Contributes to Both Circadian and Geotactic Behaviors.* Neuron, 2005. **48**: p. 213-9.
78. Kunst, M., et al., *Calcitonin gene-related peptide neurons mediate sleep-specific circadian output in Drosophila.* Curr Biol, 2014. **24**(22): p. 2652-64.
79. Gu, S.H., et al., *Functional characterizations of chemosensory proteins of the alfalfa plant bug Adelphocoris lineolatus indicate their involvement in host recognition.* PLoS One, 2012. **7**(8): p. e42871.
80. Bautista, M.A., et al., *Evidence for trade-offs in detoxification and chemosensation gene signatures in Plutella xylostella.* Pest Manag Sci, 2015. **71**(3): p. 423-32.
81. Rihani, K., J.-F. Ferveur, and L. Briand, *The 40-Year Mystery of Insect Odorant-Binding Proteins.* Biomolecules, 2021. **11**(4): p. 509.
82. Li, Z., et al., *Identification of Leg Chemosensory Genes and Sensilla in the Apolygus lucorum.* Front Physiol, 2020. **11**: p. 276.
83. Halon, E., et al., *Only a minority of broad-range detoxification genes respond to a variety of phytotoxins in generalist Bemisia tabaci species.* Sci Rep, 2015. **5**: p. 17975.
84. Zhang, Y.-F., J.J.A. van Loon, and C.-Z. Wang, *Tarsal taste neuron activity and proboscis extension reflex in response to sugars and amino acids in Helicoverpa armigera (Hübner).* The Journal of Experimental Biology, 2010. **213**(16): p. 2889-2895.
85. Ingham, V.A., S. Wagstaff, and H. Ranson, *Transcriptomic meta-signatures identified in Anopheles gambiae populations reveal previously undetected insecticide resistance mechanisms.* Nat Commun, 2018. **9**(1): p. 5282.
86. Gao, Y., et al., *Transcriptomic identification and characterization of genes commonly responding to sublethal concentrations of six different insecticides in the common fruit fly, Drosophila melanogaster.* Pesticide Biochemistry and Physiology, 2021. **175**: p. 104852.
87. Calvo, E., et al., *Multifunctionality and mechanism of ligand binding in a mosquito antiinflammatory protein.* Proceedings of the National Academy of Sciences, 2009. **106**(10): p. 3728-3733.
88. Isaacs, A.T., et al., *Genome-wide transcriptional analyses in Anopheles mosquitoes reveal an unexpected association between salivary gland gene expression and insecticide resistance.* BMC Genomics, 2018. **19**(1): p. 225.
89. Elanga-Ndille, E., et al., *Overexpression of Two Members of D7 Salivary Genes Family is Associated with Pyrethroid Resistance in the Malaria Vector Anopheles Funestus s.s. but Not in Anopheles Gambiae in Cameroon.* Genes, 2019. **10**(3): p. 211.

Chapter 2

The leg/appendage specific ABCH2 transporter mediates insecticide toxicity in the malaria vector *Anopheles coluzzii*

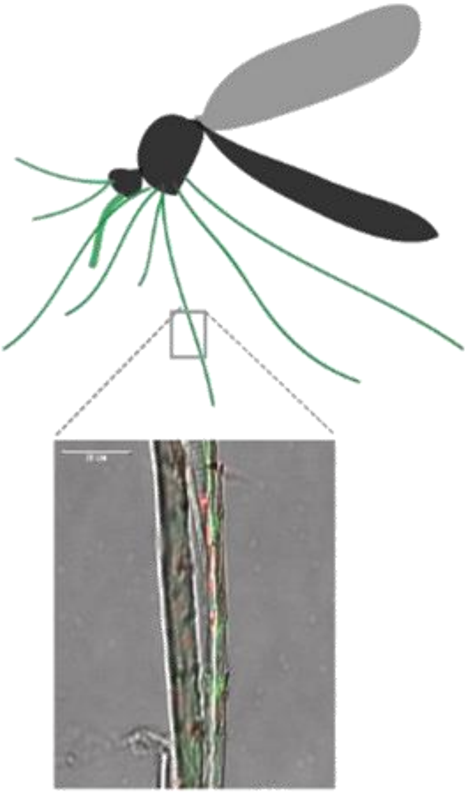

2.1 Abstract

An ATP-Binding Cassette transporter from the insect-specific H family (ABCH2) is highly expressed in *Anopheles coluzzii* legs, especially upon insecticide exposure. RNAi-mediated silencing of the ABCH2 caused a dramatic increase in mortality compared to control mosquitoes, indicating a role of this transporter in deltamethrin toxicity. RT-qPCR analysis and immunolocalization of the ABCH2 using specific antibodies showed that it is mainly present in the legs and other head appendages. More specifically, the protein is expressed in the apical part of leg epidermis, underneath the cuticle. Phylogenetic analysis indicated that this transporter is orthologous to other insect ABCH transporters previously found to be implicated in lipid transport. However, analysis of the leg cuticular hydrocarbon (CH) content was not affected by ABCH2 RNAi, indicating that the potential role of this transporter in pyrethroid toxicity is not associated with the transport of leg CHCs. We next performed protein modeling of ABCH2 based on the closest homologue structure available, the human ABCG1 which indicated ABCH2 half-transporter likely physiologically adopts a homodimeric state. This was also shown by the ATPase *in vitro* assay we set up after expressing ABCH2 in insect cells. Concomitant protein-ligand docking analysis suggests that deltamethrin could be a potential substrate of this transporter, although deltamethrin addition in the *in vitro* assay did not result in further ABCH2 stimulation. Lastly, ABCH2-silenced mosquitoes were shown to have increased C^{14} deltamethrin penetration. Our findings reveal a previously undescribed mechanism of insecticide toxicity in mosquitoes, pinpointing ABCH2 as an important player of deltamethrin toxicity and a potential target for vector control in the future.

Dr. Gouridis and Chara Sarafoglou performed the *in silico* modelling and the docking analysis presented in this chapter.

Introduction

Recent works highlight the role of mosquito legs in insecticide resistance and tolerance phenomena. Both leg procuticles and the lipid-rich epicuticles of resistant *An. gambiae/c oluzzii* mosquitoes are significantly thicker than susceptible counterparts due to enhanced structural components (proteins and chitin), as well as lipid species (Cuticular hydrocarbons, CHCs) [1]. Additionally, the leg transcriptome of susceptible, resistant and insecticide-induced *An. coluzzii* indicates that detoxification probably occurs in legs and that short-term pyrethroid induction is characterized by ABC transporter presence along with other responses (Chapter 1) [2]. ABC transporters' association post pyrethroid exposure is determined by other studies as well in whole *Anopheles* mosquitoes of divergent species [3-5]. These lines of evidence suggest that Phase 0 and/or III detoxification likely occurs upon induction [6]. The *An. coluzzii* ATP-Binding-Cassette Transporter*, ABCH2* (*ACON003680*), an ABC transporter of the H family was the only ABC transporter identified both in mosquito leg proteomic and transcriptomic datasets (Chapter 1) [1, 2]. Overexpression of this transporter by two folds in the legs of short-term deltamethrin induced mosquitoes compared to the legs of unexposed mosquitoes (Chapter 1) [2], further alludes to the role of this transporter in pyrethroid toxicity.

ATP-Binding-Cassette transporters are present in all kingdoms of life and the majority of them function as primary-active transporters that bind and hydrolyze ATP [7]. They are characterized by the presence of a highly conserved nucleotide binding domain (NBD) with characteristic motifs [8]. They also have transmembrane domains which vary significantly and based on that variation and other structural characteristics they are categorized in at least nine groups (ABCA, ABCB, ABCC, ABCD, ABCE, ABCF ABCG, ABCH, ABCI)[8]. Typical ABC pumps can be either full- or half-transporters[9]. In full-transporters, a single polypeptide arranged in TMD-NBD configuration results in two NBDs and two TMDs combined. In half-transporters, however, there are only two domains (1 NBD and 1 TMD) and need to form homo- or heterodimeric complexes to result in a functional efflux pump as for ATP hydrolysis dimerization is mandatory [9]. Bacterial ABC transporters are importers and exporters while eukaryotic ones where considered to function only as exporters, although exceptions have been recently reported on ABCA and C sub-families in algae and primitive plants [8]. Transporters of the H sub-family are present in all insects and other arthropods [10], *Dictyostelium* and zebrafish, but are absent from plants, worms, yeast, or mammalian genomes [11]. The H sub-family transporter members are exporters sharing similarities with members of the G group [8]. They are composed of one NBD and one TBD, hence they are half-transporters, which means they need to form dimers in order to be functional [12]. In *An. gambiae* there are three genes encoding for ABCH transporters (*ABCH1*, *ABCH2* and *ABCH3*) [12]. Apart from other ABC families (A,G), H transporters have been implicated to lipid transport, as knock-down experiments in *Drosophila melanogaster*, *Tribolium castaneum, Locusta migratoria, Plutella xylostella and Nezzara viridula* result in high lethality due to desiccation while downstream experiments indicate that the transporter participates in cuticle barrier construction, most probably by facilitating transport of (epi)cuticular components [13-17].

In this work, we aimed to provide insights into the functional characteristics of the ABCH2 transporter, identified in leg datasets, and elucidate its putative implication in pyrethroid toxicity. We verified the enrichment in legs and other appendages both in transcript and protein levels and generated tools such as specific antibody and RNAi to evaluate its (sub)cellular localization in these tissues and validate its implication in pyrethroid toxicity respectively. Moreover we achieved the functional *in vitro* expression and *in silico* structural modeling of this half-transporter providing evidence that it presumably acts in homodimeric state. Further, testing protein-substrate docking experiments dictate that deltamethrin is a putative substrate. However, deltamethrin was not found to affect the intrinsic ability of ABCH2 to hydrolyze ATP in Sf9 inverted membrane vesicles.

As mosquito legs/appendages comprise a highly epidemiologically relevant tissue with vector control relying on insecticide leg penetration, the association of transporter proteins with pyrethroid toxicity and the understanding of the underlying molecular mechanisms would be very useful in vector control innovations.

2.3 Materials and Methods

2.3.1 Mosquito strains

The mosquito strain used in this study belongs to the *An. coluzzii* species complex and was maintained in the laboratory under the same conditions for several generations before analysis. The standard insectary conditions for all strains were 27 °C and 70–80% humidity under a 12-h: 12-h photoperiod with a 1-h dawn : dusk cycle. The strain is derived from Burkina Faso (VK7) and the colony used for the experiment is the VK7-LR colony, which has lost part of its resistance, as described in Chapter 1 [2].

2.3.2 Antibodies

Rabbit polyclonal antibodies targeting *An. coluzzii* ABCH2 peptides were synthesized and affinity purified by Davids Biotechnologie. The sequence of the peptide is: VKEYYSDLDSALGAVRD and recognizes 466-482 residues. E-cadherin mouse antibody was kindly provided by Dr. Siden-Kiamos (IMBB/FORTH). Monoclonal mouse anti-β-tubulin used for normalization control in western blot analysis was purchased by Santa Cruz Biotechnology.

2.3.3 Western Blot Analysis

10-15 dissected tissues were homogenized into 100-150 μl RIPA Buffer (50Mm Tris pH=8, 150mM NaCl, 1% SDS, 1% NP-40, 1mM EDTA, 1mM EGTA and 1 mM PMSF). After a 10 min centrifugation step at 10.000g the supernatants were immediately supplemented with equal volume of 5X Laemmli Sample Buffer. Polypeptides were resolved by 12% acrylamide SDS-PAGE and electro-transferred on nitrocellulose membrane (GE Healthcare Whatman). The membranes were subsequently probed with anti-ABCH2 antibody at 1:250 dilution or anti-β-tubulin (Cell Signaling) at 1:500 dilution in a 1% skimmed milk/TBS-Tween buffer. Antibody binding was detected using goat anti-rabbit or anti-mouse IgG coupled to horseradish peroxidase (Cell Signaling) (dilution: 1:5000 in 1% skimmed milk in TBS-Tween). Visualization was performed using a horseradish peroxidase sensitive ECL western blotting detection kit (SuperSignal West Pico PLUS Chemiluminescent Substrate, ThermoScientific) and the result was recorded using Chemidoc Imaging System (Bio-Rad Laboratories).

2.3.4 Tissue dissection and relative expression estimation

To address *ABCH2* expression levels in different tissues, 3-4 day-old female *An. coluzzii* were dissected. Heads, thoraces, guts with the attached malpighian tubules and ovaries, abdominal walls and legs were separated into TRIzol^{TM} Reagent. 20 tissues were placed in 200 μl reagent in three replicates and then manufacturer's instructions were followed. After elution, RNA pellets were subjected to DNase I treatment (ThermoFisher Scientific, Dnase I, Rnase-free). The quantity of DNase-treated RNAs was calculated using Nanodrop spectrophotometer and equal quantities from each sample were used for cDNA synthesis. These were carried out as described in detail in paragraph 1.2.4 of Chapter 1.

2.3.5 Cryosectioning, immunofluorescence and confocal microscopy.

Legs from 3-5 day-old *An. Coluzzii* were dissected and placed for 2 hours in PCR tubes containing 4% PFA in 1x PBS buffer for fixation. After removal of fixative, legs were incubated overnight with 30% sucrose/PBS buffer at 4°C. Legs were then immobilized in 68ppendorf lids covered with Optimal Cutting Temperature O.C.T (Tissue-Tek SAKURA) and placed at -80°C. 5 μm longitudinal leg sections were obtained in cryostat (Leica CM1850UV) and were placed on superfrost microscope slides (Thermo Scientific). The slides were washed (3 x 5 min) with 0.02% Tween/PBS, followed by a 10 minute incubation with 0.03% Triton/PBS. After 1hour blocking with 1% Fetal Bovine Serum in 0.03% Triton/PBS, the slides were incubated overnight with the antibody in 1:500 dilution, at 4°C. The next day goat anti-rabbit or goat anti-mouse (Alexa Fluor 488, Molecular Probes) were used in 1:1000 dilutions. TO-PRO-3 dye (Molecular Probes) was used for nuclei staining after RNAse A (Invitrogen^{TM} Ambion^{TM}) treatment in a 1:1000 dilution for 5 min. Observation and image attainment were carried out at a Leica SP8 laser-scanning microscope, using a 40x-objective.

2.3.6 dsRNA design, generation, nano-injections and silencing efficiency

This procedure is described in detail in paragraph 2.4 of Chapter 1. Briefly, Primers for dsRNA against *ABCH2* were designed using PrimerBlast and they amplify a product of 525 bp. T7 promoter sequence (5' TAATACGACTCACTATAGGG 3') was added at the 5' end of both forward and reverse oligos (Table S2.1). VK7 cDNA and a GPF-containing plasmid were used for dsRNA construction (dsABCH2 and dsGFP). The injections were performed intrathoracically and injected mosquitoes were placed in cups and were kept in insectary conditions with 10% impregnated sugar cottons for 72 hours. After that their legs were dissected and RNA was extracted, cDNA was synthesized and RT-qPCR was conducted. Primers for qPCR were designed out of the region targeted by dsRNA resulting in a 146 bp product (Table S2.1) and according to standard curve construction their efficiency was 96%. Silencing efficiency for each dsRNA was estimated after comparison of relative expression of each gene of interest in dsRNA-injected against relative expression levels in ds*GFP*-injected female mosquitoes. Graphs were produced and statistically analyzed using GraphPad Prism software version 8 using Student's t-test. For protein estimation, polypeptide extraction from legs and western blot analysis were performed as described in paragraph 2.3.3.

2.3.7 Deltamethrin toxicity assays

Deltamethrin toxicity assays, were performed as described in detail in paragraph 2.5 of Chapter 1. Briefly, 0-Day injected females with ds*GFP* and ds*ABCH2* were exposed to deltamethrin concentration of 0,016%, as this is the estimated LC_{50} for this VK7 strain (VK7-LR) (Chapter 1, Figure 1.2) [2]. The exposure lasted for 1 hour and then knocked-down mosquitoes were recorded. This was followed by 24 hour recovery in control tubes in insectary conditions. A mosquito was classified as dead or knocked down if it was immobile or unable to stand or take off, respectively. The whole procedure (injections followed by bioassays) was repeated four times (~14-16 ds*GFP* and ~18-22 ds*ABCH2* individuals x 4 replicates). In each round, ds*GFP* and ds*ABCH2* were injected concomitantly, to ensure comparable injection, insectary and bioassay conditions. Graphs were produced and statistically analyzed using GraphPad Prism software version 8 using Student's t-test.

2.3.8 Extraction of cuticular lipids, cuticular hydrocarbons (CHCs) fractionation, identification and quantitation

3 days after dsRNA nano-injections performed in newly emerged females, 95 ds*ABCH2* and 103 ds*GFP* female mosquitoes (3 replicates/ 30-35 mosquitoes per replicate) were placed in aluminum foils until they dried. Legs of dry mosquitoes were separated from the rest of the body and their dry weight was calculated. CHC analysis was carried out in VITAS-Analytical Services (Oslo, Norway) as described in [18]. Statistics were analyzed using GraphPad Prism software, version 8 and statistical analysis carried out with Student's t-test.

2.3.9 ABCH2-Overexpressing Sf9 Insect Cells, membrane preparations and ATPase activity estimation

ABCH2 was expressed in *Spodoptera frugiperda* Sf9 insect cells using the Pfastbac1 vector, which was synthesized *de novo* (GenScript) and *ABCH2* ORF was subcloned in between BamHI and EcoRI restriction enzyme sites. The sequence was codon optimized for *S. frugiperda* using GenSmart codon optimization tool (GenScript). Recombinant baculoviruses encoding *ABCH2* cDNA were generated with BAC-TO-BAC Baculovirus Expression Systems (Invitrogen), following manufacturer's instructions. 2μg of Bacmid DNA, mixed with Escort IV Transfection Reagent (Merck) were used to transfect 5x10^5 Sf9 cells in 1ml of SF900 II SFM growth medium (ThermoFisher scientific). The complex was incubated for 45 min/RT and the lipid complexes were added dropwise to the appropriate well and were incubated at 27°C for 6 hours. After that, another 1ml of medium, supplemented with antibiotics (2x penicillin and streptomycin) and 20% FBS (ThermoFisher scientific) were added. After 24 hours DNA:lipid complexes were removed and 2ml of supplemented growth medium were added to the cells which were subsequently incubated at 27°C for 72 hours. Medium, containing the virus stock were removed and stored, while cells were also collected by pipetting in ice-cold 1 X PBS. Cell pellets (after 3000g/5min/4°C centrifugation) were resuspended in RIPA supplemented with protease inhibitors followed by a 10000g/10 min /4°C centrifugation step. The supernatant was prepared for western blot analysis with the addition of 5x Sample Buffer (SB). After validation of recombinant protein expression of expected size in Sf9 cells and determination of Viral Stock titers using baculoQUANT ALL-IN-ONE (GenWay), according to manufacturer's instructions, infection was performed. For infection 10^6 cells/ml were seeded in T75 Flasks in a final volume of 15 ml antibiotic and FBS supplemented growth medium. After 4-5 hour incubation at 27°C, viruses were added at the desired multiplicity of infection (MOI) and infected cells were incubated for additional 96 hours. Along with the ABCH2 infections, cells infected with an empty Bacmid served as negative control. Then the cells were harvested and proceeded to microsomal preparations. Following a centrifugation step at 2000g/3min/4°C, cell pellets were homogenized using glass-Teflon tissue homogenizer in a mannitol-containing buffer as described in [19]. This step favors the formation of vesicles of both orientations (right-side and inside-out vesicles) [19]. Final ultracentrifugation step at 100,000g/1hour/4°C (Beckman AirFuge CLS Ultracentrifuge) resulted in pellets which were resuspended in the same buffer. After estimation of total protein content of the membrane preparations by Bradford protein assay using BSA to generate a linear control standard curve (0.5-20μg) the membranes were further diluted in 1-2 μg/μl to be used for downstream experiments or stored at -80°C as aliquots of 20μl each. The ATPase activity of the Sf9 membranes expressing (ABCH2) or not (Empty) the transporter was estimated with a colorimetric assay by measuring inorganic Pi released from ATP hydrolysis as described in [19] [20], with some modifications. Briefly, we prepared a malachite green solution (340 mg of Malachite Green (Sigma) in 75 ml deionized water) and an ammonium molybdate solution (10.5 g ammonium molybdate in 250 ml 4N HCl). Mixing the two solutions following by filtration through paper resulted in the malachite green stock solution that was stored at 4°C. The malachite working solution (MGWS) was freshly prepared by adding 20% Triton-X-100 in malachite green stock solution in 0.1% final concentration. Phosphorus standard solutions incubated with malachite green working solution (50 ul of each with 0.8 ul MGWS) were used to generate linear control standard curve (0-20 nmoles Pi) [21]. Pi standards were incubated in MGWS for 5 minutes and after that 100ul 37% citric acid was added in each reaction. The reactions were then incubated for 40 minutes at Room Temperature and absorbance was photometrically measured using a spectrophotometer at a wave length of 630nm. For estimation of Pi release in membrane preparations reactions were set up using 0.5 ul of 0.1 M ATP, 2 ul of 10mg/ml BSA, 10 µg of membrane protein, 5 ul of a 10X buffer (500mM Tris/HCL Ph=8, 50mM $MgCl_2$, 50mM KCl and 10mM DTT) and deionized water was added up to 50ul. The reactions were incubated in a water-bath at 37°C for 15 minutes and afterwards they were mixed with 0.8ul freshly prepared MGWS. The 5 minute incubation was terminated with 100 ul of 37% citric acid which was added to avoid further ATP hydrolysis. The reactions were kept at RT for 40 minutes and then absorbance was measured at 630 nm. In every round empty and ABCH2 membranes were tested simultaneously. In every ATPase experiment two control solutions were used: a reaction containing the buffer without proteins and a two reactions containing no ATP, one for each membrane preparation. We used the first control as blank which was subjected by every absorbance value and thereafter the released phosphate was quantified based on the Pi standard curve.

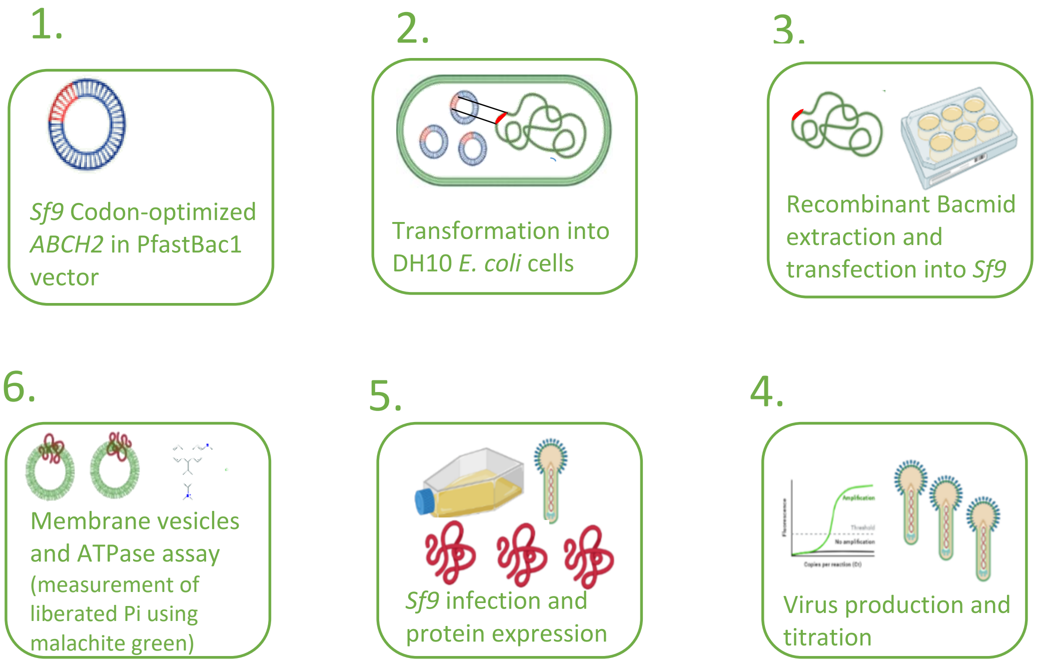
1.
Sf9 Codon-optimized *ABCH2* in PfastBac1 vector
2.
Transformation into DH10 *E. coli* cells
3.
Recombinant Bacmid extraction and transfection into *Sf9*
4.
Amplification
Threshold
No amplification
Virus production and titration
5.
Sf9 infection and protein expression
6.
Membrane vesicles and ATPase assay (measurement of liberated Pi using malachite green)

Figure 2.3.1 Graphical depiction of the steps performed for the overexpression of ABCH2 in Sf9 cells and the *in vitro* assay.

2.3.10 C^{14} penetration rate in dsABCH2 and dsGFP mosquitoes.

Penetration rate was assessed as previously described in [22]. Briefly newly-emerged dsABCH2- and dsGFP-injected mosquitoes, three days post injection, were subjected to 4 minute contact on 0.01% C^{14}-deltamethrin paper. Mosquitoes were collected in glass vials and three 1 minute-hexane washes were performed. After that they were homogenized in PBS. In all samples 10ml of liquid Scintillation Counting Mixture (Ultima Gold;6013326; PerkinElmer) were added and they were measured on a beta counter (LS1701; Beckman). Internal counts per minute correspond to the PBS-homogenized mosquitoes, while external counts per minute correspond to the average of the counts per minute of the three hexane washes. Penetration was calculated as the ratio of the internal to the total counts per minute in the two conditions. Two biological replicates were performed with 42 mosquitoes in each condition.

2.4 Results

2.4.1 RNAi-mediated silencing of *ABCH2* revealed its implication in pyrethroid toxicity

Former work of our group showed that *ABCH2* was induced upon deltamethrin exposure in mosquito legs [2].To test whether *ABCH2* exhibits any phenotype in pyrethroid toxicity, we performed RNAi-mediated silencing of this transporter in newly emerged adults coupled to bioassays. dsRNA specifically targeting *ABCH2* transcripts were designed, generated and introduced intrathoracically into newly emerged female *An. coluzzii* by nano-injections. Successful silencing efficiency was addressed both in transcript and protein level. According to RT-qPCR, dsRNA-mediated silencing reduced *ABCH2* transcript levels in whole female mosquitoes by approximately 75% (Figure 2.1A). Western blot analysis using a specific antibody indicated the recognition of a specific band at approximately 85 kDa, the expected size of the transporter and was used to show the silencing efficiency in protein level too. Indeed, ABCH2 protein levels in legs and head appendages (proboscis, antennae and maxillary palps) of female mosquitoes were significantly reduced when compared to ds*GFP* counterparts (Figure 2.1B). In order to address whether *ABCH2* silencing affects pyrethroid toxicity we next performed deltamethrin toxicity assays. Mosquito knock-down 1 hour post exposure as well as mortality 24 hours later were recorded. Notably, knock-down in ds*GFP* was 23% while in dsA*BCH2* mosquitoes reached 89.7%, showing a 66.6% significant increase. Interestingly, almost all ds*ABCH2* mosquitoes never recovered with mortality culminating in 98% after 24 hours, while in ds*GFP* controls it was almost half (55%) (Figure 2.1C, D). Overall, *ABCH2*-silenced mosquitoes exhibited a dramatic increase both in knock-down and mortality compared to the control ones, pinpointing an important role for this transporter in deltamethrin (pyrethroid) toxicity.

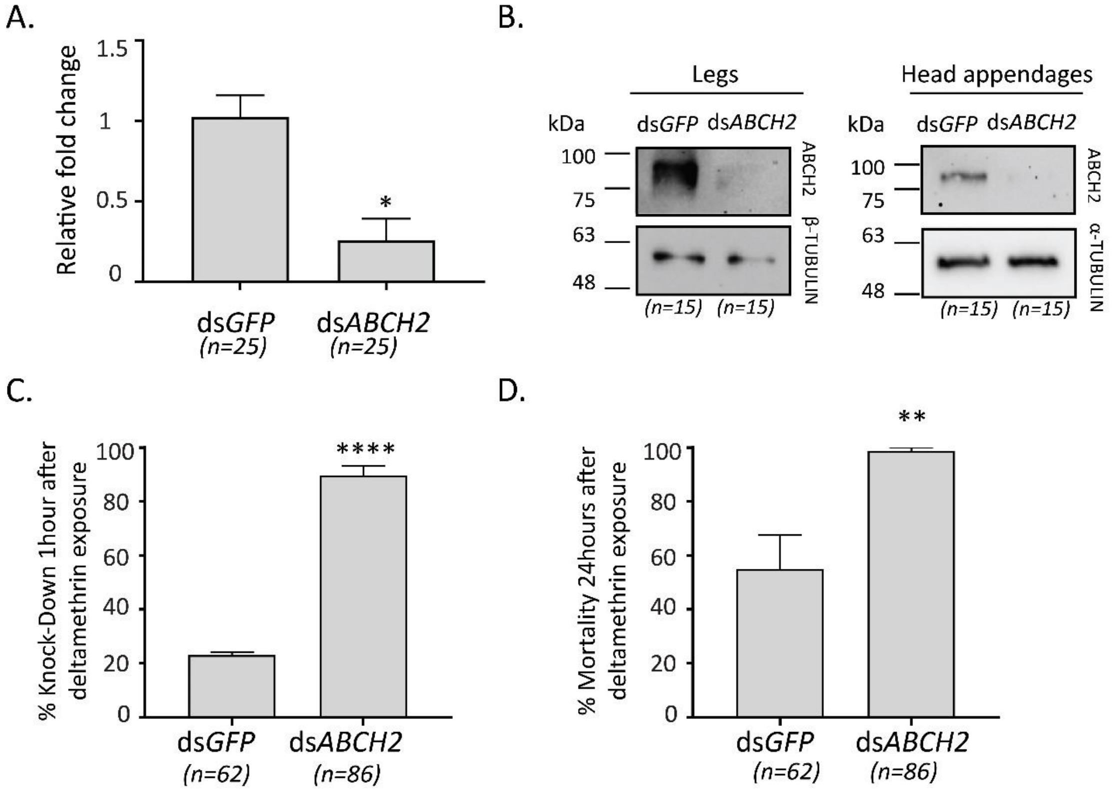

Figure 1. RNAi silencing efficiency and deltamethrin toxicity assays. A) Silencing efficiency estimation of ds*ABCH2* against ds*GFP* treated newly-emerged females with RT-qPCR. ABCH2 transcript level

reduction by 74,7% accomplished, as indicated by the mean of 3 biological replicates +SEM; *P*-value = 0,0114 (*) determined by t-test, B) Western Blot analysis of leg and head appendages protein extracts 3 days post injections, verified the reduced protein levels of ds*ABCH2* against ds*GFP* injected controls. Alpha or beta-TUBULIN were used as loading control, C) % Knock down of ds*ABCH2* and ds*GFP* female *An. coluzzii*, subjected, 72h post injection, to 1 hour deltamethrin exposure (0.016%); $\text{Mean}_{(\text{ds}GFP)}$=23% + 1.33 and $\text{Mean}_{(\text{ds}ABCH2)}$=89.6% + 3.66 for n= 4 biological replicates; *P*-value<0.0001 (****); D) % mortality 24 hours post exposure, $\text{Mean}_{(\text{ds}GFP)}$= 55% +12.58 and $\text{Mean}_{(\text{ds}ABCH2)}$= 98.75% +1.25, for n= 4 biological replicates; *P*-value= 0.0092 (**); E/ % Penetration of C^{14}-deltamethrin after 4 minutes of contact in dsGFP and dsABCH2 mosquitoes. Penetration corresponds to the ratio of the internal to the total counts per minute. Mean of two biological replicates (n=84 mosquitoes/condition).

2.4.2 ABCH2 is mainly present in *An. coluzzii* legs/appendages

As ABCH2 was previously identified in the leg proteome of *An. coluzzii*, but was not identified in the rest of the body [1] and was also identified in the leg transcriptome [2], our ensuing objective was to determine the expression levels in different tissues, both in transcript and in protein level. Transcript abundance in different dissected tissues of 3-5 day-old female *An. coluzzii* was evaluated with RT-qPCR, with expression of all tissues normalized against expression of abdominal walls. Interestingly, *ABCH2* relative expression levels in legs are greater than other dissected tissues (Figure 2.2A). The protein abundance of ABCH2 is higher in the legs with significant protein amount detected in heads too, as dictated by western blot analysis (Figure 2.2B). ABCH2 expression in the head is attributed to the head appendages (antennae, proboscis, maxillary palps) (Figure 2.2C).

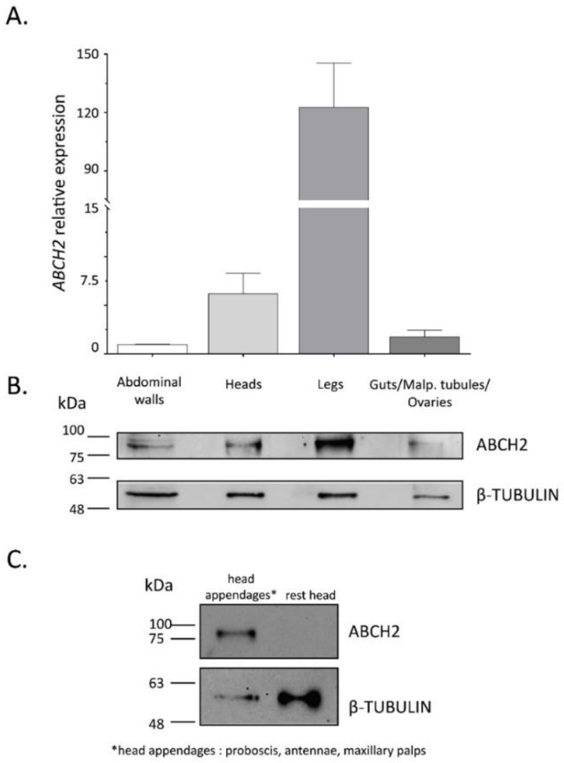

*head appendages : proboscis, antennae, maxillary palps

Figure 2.2. ABCH2 expression in different tissues. A. Relative expression levels of *ABCH2* in different dissected tissues normalized against abdominal walls of 3-5 Day old female VK7 mosquitoes. Bar graphs represent mean values; error bars standard mean error; n= 3 biological replicates and B. Western Blot using specific antibody against ABCH2, depicting ABCH2 in different dissected tissues of 3-5 day old

female VK7. Each band corresponds to the tissue of the bar above. C. Western blot analysis indicating ABCH2 presence in the head is exclusively attributed to sensory appendages. β-TUBULIN was used as a loading control.

2.4.3 ABCH2 is localized on the leg/appendage epidermis, underneath the cuticle, most probably with apical polarity.

After validating ABCH2 expression in the legs and head appendages we proceeded with the determination of its exact (sub)cellular localization in these tissues. Towards this, the specific antibody against this transporter was used in immunofluorescence experiments in leg and head appendages cryo-sections. We repeatedly obtained a specific signal (green), underneath the cuticle as the bright-field channel indicated (Figure 2.3A, C). The signal observed was line-shaped, just underneath the cuticle and right next to nuclei series stained red with TO-PRO-3 dye, with some characteristic triangle-shaped crumple spots expanded towards the cuticular structure. To gain further insight, we stained leg cryo-sections with E-cadherin antibody, known to stain epithelia [23, 24]. Indeed, green fluorescence was localized to the epithelial cells attached underneath the cuticle, presumably the epidermal cells [25, 26] (Figure 2.3C,D). Similar ABCH2 line-shaped staining was also observed in cryosections of head appendages (Figure 2.3E,F,G,H) Furthermore, bioinformatics using DeepLoc-1.0 tool [27] predicted a plasma membrane sub-cellular localization for this multi-span transmembrane protein. (Figure S2.1). These lines of evidence support that mosquito ABCH2 is localized on leg/appendage epidermal cells, most probably apically polarized towards the cuticular structure.

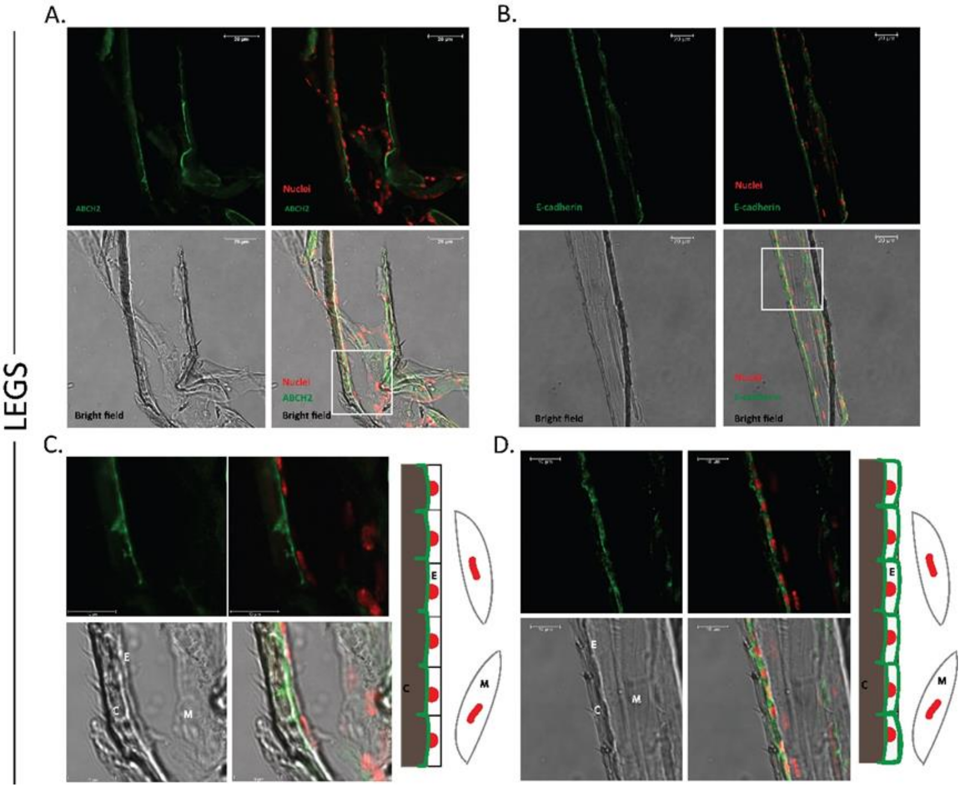

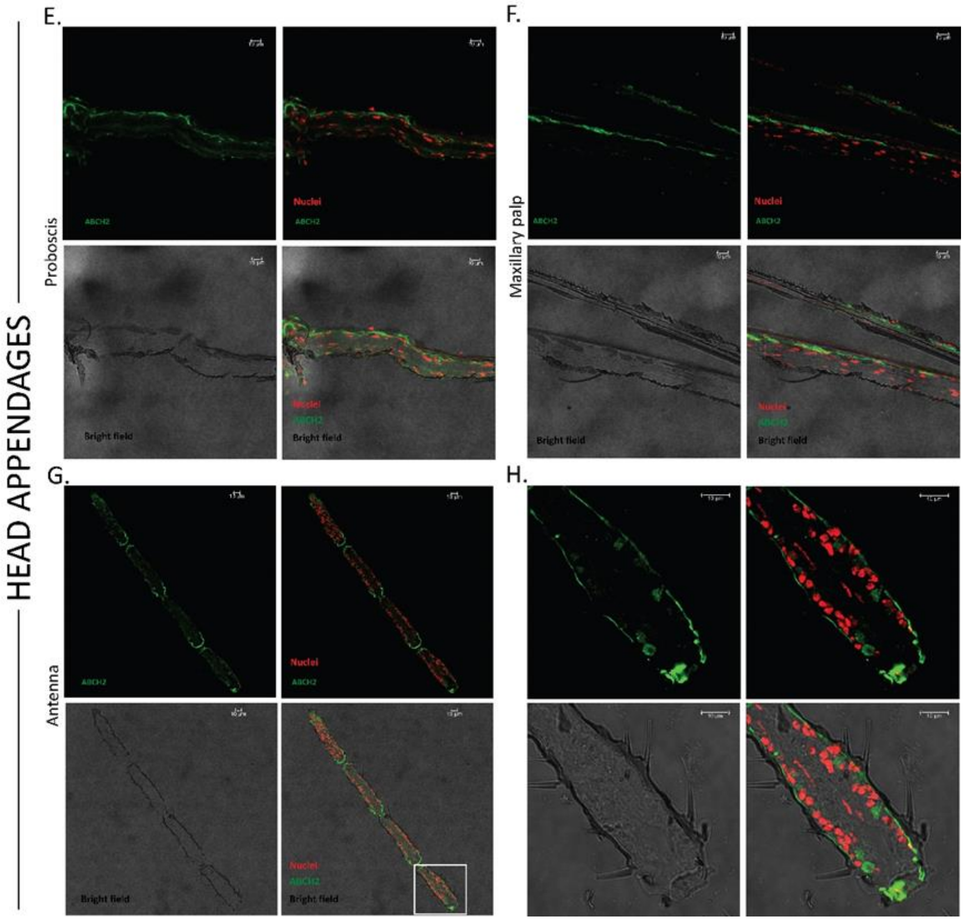

Figure 2.3. Sub-cellular localization of ABCH2 transporter. Immunohistochemical images from longitudinal leg cryosections of 3-5 day old female *An. coluzzii*. A. ABCH2 localization on epidermal cells, underneath the cuticle, polarized towards the apical side. B. Epithelial staining on leg cryosections with a marker-antibody against E-cadherin validating the presence of an epidermal layer underneath the cuticle. C, D. Zoomed images of the selected, white squares of panels A and B respectively, together with graphical depictions of the main structures observed. E,F,G. ABCH2 localization on epidermal cells of head appendages: proboscis, maxillary palp and antenna respectively. H. Zoomed image of the selected, white square of panel G. Images were obtained with confocal microscope (40x). RED: Cell nuclei are stained with TO-PRO-3; Green: antibody staining; Merged images with and without bright-field channel are also depicted; C=cuticle, E=epidermis, M= muscles; scale bars of 10-20 μm are illustrated.

2.4.4 Deltamethrin toxicity is not attributed to CHC differences in the legs.

ABC transporters of the H family are present in all insects [11]. Given that several recent works on ABCHs of other insects implicate them in lipid transport, we examined the phylogenetic relationships of *An. coluzzii ABCH2* with the characterized H transporters of other insects. *An. coluzzii* has three *ABCHs* (*ABCH1*, *ABCH2* and *ABCH3*), like *D. melanogaster* and *T. castaneum*. According to our phylogenetic analysis including *D. melanogaster*, *T. castaneum*, *L. migratoria, P. xylostells* and *N. viridula* ABCH transporters, there are one-to-one orthology relationships. Interestingly, all ABCHs with reported roles in lipid transport are clustered in the same clade with AcABCH2 (Figure S2.2). Thus, we wondered whether ABCH2 expressed in legs also participates in transport of cuticular hydrocarbons (CHCs) specifically, as the most abundant lipid species in leg *Anopheles* cuticle [22], exerting multiple functions: CHCs not only seal insects' body and prevent desiccation but are specifically deposited on insecticide resistant mosquito legs and retard the uptake of insecticide [22]. To address this, we performed CHC analysis in mosquito legs expressing (ds*GFP*) or not (ds*ABCH2*) *ABCH2* transporter. The analysis of hexane leg extracts indicated no significant difference neither in total CHC content between ds*ABCH2* and ds*GFP* mosquito legs (Figure 2.4), nor in relative abundance of individual CHC species (Figure S2.3), suggesting that the increase in deltamethrin toxicity observed in ABCH2-silenced mosquitoes is not attributed to epicuticular hydrocarbons reduction.

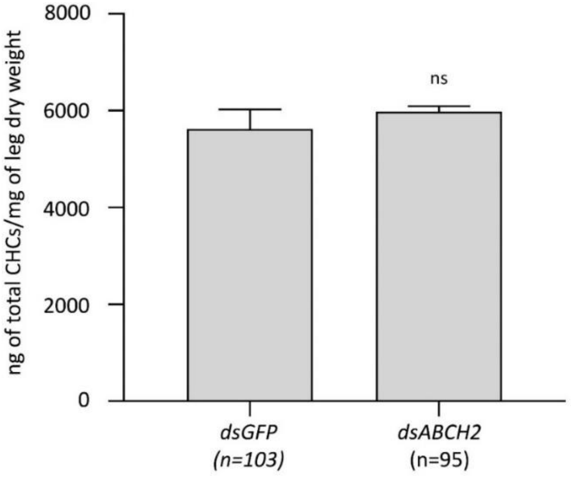

Figure 2.4. Total Cuticular Hydrocarbon content of legs derived from ds*ABCH2* and ds*GFP* injected mosquitoes. Average total CHC content from three replicates analyzed for each condition (95 ds*ABCH2* and 103 ds*GFP* female mosquitoes, 30-35 mosquitoes per replicate); Mean + SEM ; $\text{Mean}_{(\text{ds}GFP)}$=5626.33+ 401.5 and $\text{Mean}_{(\text{ds}ABCH2)}$=5981.67+ 112.5 for n= 3 biological replicates; *P*-value=0.4422 (non-significant, ns).

2.4.5 *In silico* and *in vitro* tools provide evidence for a functional membrane-bound ABC transporter which functions most probably as a homodimer.

Furthermore, we proceeded to *in silico* modeling of *An. coluzzii* ABCH2. The amino acid sequence of ABCH2 (Uniprot:A0A6E8VHH0) was submitted to the SWISS-MODEL in the automated protein modelling server provided by the GlaxoSmithKline center, using its standard settings [28]. The human homodimeric ABCG1 transporter involved in cholesterol trafficking [29] was identified as the closest homologue. The ABCH2 sequence was modelled after the dimeric ABCG1 structure, allowing to identify contacts stabilizing the inter-protomer interfaces using the Protein Interaction Calculator (PIC) web-server [30]. The number and nature of interactions stabilizing the dimeric ABCG1 interface is equivalent to those occurring in the modelled ABCH2 one (Figure 2.5A and 2.5B), suggesting that ABCH2 is likely to adopt a physiologically relevant homodimeric state. Since the modelled ABCH2 most probably acts as homodimer we next performed its *in vitro* expression. Using the baculovirus-mediated expression system in Sf9 cells we managed to functionally express ABCH2 *in vitro*. After validation of specific expression in ABCH2-infected cells, as opposed to cells infected with an empty-bacmid (Figure 2.5C, whole cells), we proceeded to sub-cellular fractionation. As illustrated in Figure 2.5C, the transporter, which is a multi-membrane spanning protein is only present in membrane fractions as opposed to the cytosolic ones and exclusively expressed in ABCH2-infected and not membranes of empty bacmid-infected cells. Additionally, to validate the functional expression of the transporter we reproduced an ATPase assay protocol. This takes advantage of the intrinsic ability of ABC transporters to hydrolyze ATP, producing inorganic Pi [31]. After using a membrane isolation protocol which favors inverted-oriented vesicle formation to make cytosolic ATP domains accessible to the provided ATP [31], we measured the liberated Pi. Interestingly, ABCH2 Sf9 membranes exhibit significantly higher activity expressed in pmoles of Pi/μg of membrane protein/min, when compared to control membranes (Figure 2.5E). This observation was validated in six different membrane preparations. As this comparison is based on total protein content estimation, whole membrane protein extracts were tested on SDS-Page and the separated polypeptides were visualized with Coomassie Blue (Figure 2.5D). According to that ABCH2 was slightly expressed in Sf9 membranes since an induced band was not apparent when expressing and control membranes were compared. At the end, deltamethrin exposed membranes were tested with the ATPase assay, but no further stimulation of the ABCH2 membrane vesicles was recorded.

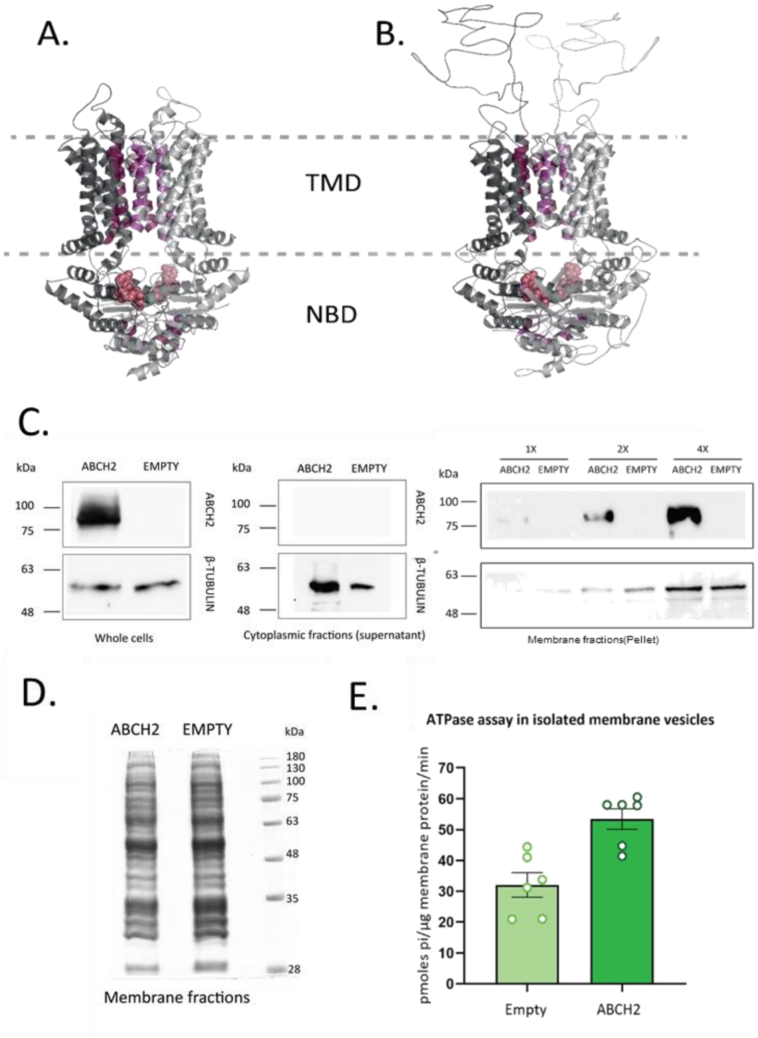

Figure 2.5. ABCH2 is functionally expressed, probably acting as homodimer. A and B. Interface residues participating in interactions stabilizing the homo-dimeric interface are presented with purple surface colors. Bound ATPs in the Nucleotide Binding Domains (NBDs) are presented with red spheres. The two protomers in the ABCG1 structure (A) or in the modelled ABCH2 (B) are distinguished by two grey scales, C. Western blot analysis using ABCH2 antibody in whole cell extracts of ABCH2- and Empty Bacmid-infected *Sf9* cells in whole cell lysates, cytosolic and membrane fractions. For membrane fractions different concentrations (1x, 2x, 3x) of membrane preparations were tested and in all cases

B-TUBULIN was used as loading control, D. Coomassie blue staining in ABCH2 and Empty membrane fractions. E. ATPase activity in empty and ABCH2-expressing isolated membrane vesicles. Mean + SEM of 6 biological replicates (six membrane preparations) and the average of 2-3 technical replicates for each biological is presented in bars. Mean + SEM; $\text{Mean}_{(\text{EMPTY})}$=32.03 + 4 and $\text{Mean}_{(\text{ABCH2})}$=53.4 + 3.32 for n=6 biological replicates; *P*-value=0.0021 (**).

2.4.6 Protein-ligand docking experiments indicate that deltamethrin is a putative substrate of ABCH2.

Based on huge limitations in large protein transport machineries reconstitution using *in vitro* systems, we searched for alternatives. Having built a structural model, we performed protein-ligand docking analysis to ask whether deltamethrin is a candidate ABCH2 ligand. ABCG1, the closest ABCH2 homologue with an available crystal structure, has been crystallized in many distinct liganded states [29], so cholesterol was tested both on the ABCG1 available structure and in the ABCH2 model structure constructed based on the former. In the nucleotide-free inward facing conformation (PDB:7R8D), cholesterol molecules have been allocated to the transmembrane part of the transporter. Two of them at the channel interior and three additional ones at its exterior. In the ATP bound state (PDB:7R8E), the cholesterol molecules were observed uniquely in the channel exterior. We assessed the cholesterol binding pockets via the Protein-Ligand Interaction Profiler Web-server and focused our subsequent analysis on the most well defined interior pockets present in the translocation path [29]. Initial protein-ligand docking experiments were carried out using AutoDock Smina [32] to retrieve the binding energies of Cholesterol (CHL) and Deltamethrin (DLM). From the top scores, we present (Figure 2.6A) the ones having binding modes resembling closely the crystal structure [29]. The results indicate that both ligands docked to the pocket with similar energies (Figure 2.6A). Moreover, the number and nature of interaction stabilizing the two ligands into the pocket is equivalent (Figure 2.6A). These observations suggest that DLM could act as a potential substrate of ABCG1. Next, to assess whether ABCH2 also could potentially transport DLM, we performed protein-ligand docking experiments on the modeled ABCH2 without a bias related to the substrate pocket. Thus, we widened our search grid to include the entire translocator (i.e. transmembrane region). The top scores emerged indicate a substrate pocket in the translocator interior, just above the one defined by the crystal structure (compare 2.6A *vs* B, left panels). In such pocket, both CHL and DLM dock with equivalent orientation, energies and interactions (Figure 2.6B). Taking all together, we anticipate DLM to act as a substrate of these homologous transporters.

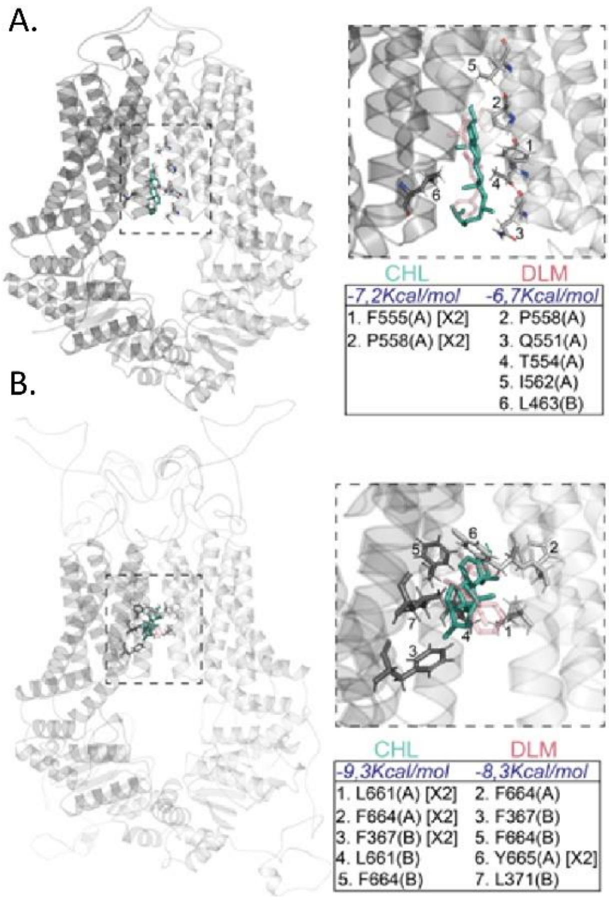
A.
5
2
1
4
6
3
CHL
DLM
-7,2Kcal/mol
-6,7Kcal/mol
1. F555(A) [X2]
2. P558(A) [X2]
2. P558(A)
3. Q551(A)
4. T554(A)
5. I562(A)
6. L463(B)
B.
6
5
2
7
4
1
3
CHL
DLM
-9,3Kcal/mol
-8,3Kcal/mol
1. L661(A) [X2]
2. F664(A) [X2]
3. F367(B) [X2]
4. L661(B)
5. F664(B)
2. F664(A)
3. F367(B)
5. F664(B)
6. Y665(A) [X2]
7. L371(B)

Figure 2.6. ABCG1 and ABCH2 protein docking analysis with deltamethrin (DLM) and cholesterol (CHL) ligands. A. ABCG1 having docked CHL and DLM. CHL is presented with green sticks, whereas DHL with transparent red sticks. Zoom-in of the indicated dotted area is presented (right top panel) together with the calculated energies and substrate-stabilizing interactions (right bottom panel). The residues participating in the hydrophobic interactions with the substrates are given in the table for each protomer (A) or B), and the number of hydrophobic bonds for each residue is indicated in brackets (when more than one), B. As in A with the modelled ABCH2 structure.

2.4.7 C^{14}-Deltamethrin experiments indicate that ABCH2-silenced mosquitoes exhibit increased insecticide penetration.

Finally, to test whether the devoid of the transporter mosquitoes internalize less deltamethrin we used C^{14}-deltamethrin cotact toxicity assays on silenced and control *An. coluzzii*. Following their exposure for 4 minutes on C^{14}-impregnated papers, mosquitoes were subjected to hexane washes and finally to homogenization. Internalized radiolabeled insecticide corresponding to the homogenized fraction versus external deltamethrin wahsed out with hexane were used to assess the penetration at this time point. dsABCH2 mosquitoes exhibit increased C^{14}-deltamethrin penetration compared to their dsGFP counterparts (Figure 2.7).

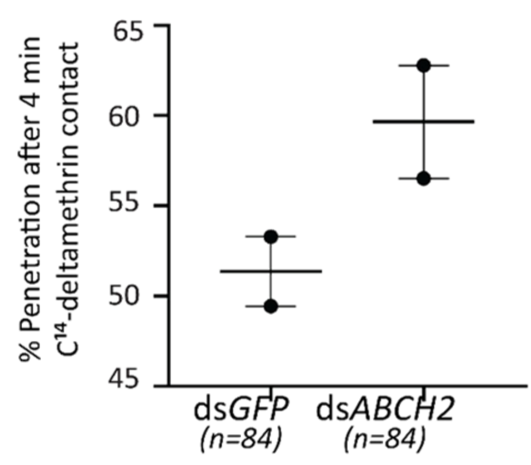

Figure 2.7. % Penetration of C^{14}-deltamethrin after 4 minutes of contact in dsGFP and dsABCH2 mosquitoes. Penetration corresponds to the ratio of the internal to the total counts per minute. Mean of two biological replicates (n=84 mosquitoes/condition).

2.5 Discussion

Based on how vector control is implemented, legs/appendages comprise the first line of defense against insecticides when mosquitoes come in contact with impregnated bednets and wall surfaces [33, 34]. Presence of transport systems in appendages apart from serving key physiological functions, could be relevant to tolerance against chemicals, such as insecticides [35]. A wealth of studies, support the up-regulation of ABC transporters after exposure to insecticides, dictating a role during the initial response [2-4, 36, 37]. According to mosquito leg transcriptome analysis, detoxification likely occurs in mosquito legs, with evident presence of ABCs after deltamethrin exposure [2]. *ABCH2* is one of them exhibiting a two-fold increase in legs of pyrethroid induced mosquitoes [2]. Despite the growing evidence, the way insect ABC transporters are implicated in drug toxicity remains largely elusive. To address this, we focused on ABCH2. RNAi-mediated silencing of *ABCH2* followed by pyrethroid exposure in adults enabled us to reveal the contribution of this transporter in pyrethroid toxicity, mediated probably via the legs/appendages. Remarkably, after one hour of contact (through the appendages), there was a dramatic increase in the number of knocked-down mosquitoes (Figure 2.1). The impressive knock-down in the *ABCH2*-silenced mosquitoes, is indicative of a fast-acting mechanism that makes the devoid of the transporter mosquitoes by far more vulnerable to the insecticide provided through the legs. Eventually mosquitoes lacking ABCH2 exhibited also much higher mortality 24 hours post exposure.

We next wanted to shed light to this transporter with essential role in deltamethrin toxicity on contact bioassays. Interestingly, it was identified in leg proteome and transcriptome [1, 2]. ABC transporters of B, G and H family have previously been identified in mosquito legs [2, 35]. In this work we tested transcript and protein levels of this gene in four tissues and demonstrated that it predominates in legs (Figure 2.2). Afterwards, we looked for sub-cellular tissue specific localization of ABCH2. Immunofluorescence pinpointed expression in leg epidermal cells (Figure 2.3), with a presumable apical polarity, oriented towards the cuticle [26]. It is common for transporters to compartmentalize on the membranes towards the site they exhibit their function [38]. A polarity towards the outermost part i.e the exoskeleton could suggest the ability of the transporter to facilitate transport of cuticular components and/or other substrates, such as insecticides, out of the organism. Suggested physiological roles for ABC transporters in appendages are to facilitate the cuticular lipid and steroid transport or protection of neuronal cells [35, 39, 40]. ABCH2 orthologue in *D. melanogaster* is also localized in epidermal cells, indicated by the high mortality observed upon the RNAi-mediated silencing with an epidermal-GAL4 and by localization experiments with fused GFP, showing its topology on the apical surface of larval epidermal cells [41]. Furthermore, *ABCH* expression in head sensory tissues (maxillary palps and antennae) [42] has been reported. Based on our phylogenetic analysis (Figure S2.3), *An. coluzzii* ABHC2 is orthologue to other insect ABCH transporters, all of them implicated in transport of cuticular components in early developmental stages. In *T.* castaneum TcABCH-9C and *P. xylostella* PxABCH1 RNAi-mediated knock-down resulted in 100% larval mortality and hatching failure of eggs from injected adults [17, 43], while less lipids and crumbled cuticles were observed in the silenced *Locusta migratoria* LmABCH-9C nymphs [14]. Moreover, *D. melanogaster Snu*, is an essential factor involved in construction of the barrier against dehydration and penetration of water and xenobiotics [41] and *Snu*-orthologue in *N. viridula* was the only gene among the *ABCH* expanded group that resulted in substantial mortality upon RNAi silencing [16] highlighting the essentiality of this gene across *Insecta*, probably associated with lipid transport. In all above studies RNAi in nymphal stages resulted in high mortality been attributed to desiccation. Cuticular abnormality observation and lipid stains of silenced individuals indicate the cuticular component transport, albeit to our knowledge, the exact molecules transported by this essential protein have not yet been identified. Zuber et al., observed a dotted signal after excitation with 405nm light source (405-dots) on the envelope, which was lost from envelopes of *Snu* mutants, as well as ablation of lipophilic components after permeability assays with lipid dye [41]. Additionally, a recent work on another ABCH transporter oksyddad (orthologue to ABCH1, Figure S2.2) indicates that it is required for CHC deposition at the surface of the wing cuticle either directly or indirectly, while it is not needed for envelope formation as *Snu* [44]. In our work, dsRNA injections were carried out in newly-emerged adults and mortality was not observed at this adult stage at least. This is not surprising, as transport of lipid or other components towards the cuticular structure is more enhanced and essential during molting events, hence essentiality of *An. coluzzii* ABCH2 could not be addressed in this system. However, adult *An. coluzzii* exhibiting high ABCH2 expression in the legs, heartened us exploit RNAi in newly-emerged adults to explore potential for transport of specific lipid species. The exact transport mechanism of lipids from the epidermis to the epicuticle in insects is still unknown [45]. Although, pore canals partially explain lipid transport no satisfactory explanation has been put forth for lipid deposition to the outermost cuticle [46]. In plants, which reminiscent arthropods in term of having multi-layered exoskeletons [47] trafficking of wax and cutin precursors depends on ABC transporters localized on the underlying epidermis [48]. Recent studies revealed that both leg procuticles and epicuticles of resistant *An. coluzzii* mosquitoes are thicker due to enhanced chitin, proteins and hydrocarbons [1]. More specifically, CHCs are considered to be the major lipid species in leg epicuticles and hence we analyzed *ABCH2*KD legs versus controls. However, the total hydrocarbon content in both cases were similar (Figure 2.4) and the relative abundances of each CHC species identified also showed non-significant differences (Figure S2.3). According to our data the dramatic increase in deltamethrin toxicity demonstrated in the *ABCH2*-silenced mosquitoes is not attributed to the reduction of CHCs. However, we cannot exclude the potential transport of CHC species either earlier in development or at different time points during adult life. Alternatively, it is possible that ABCH2 facilitates export of other lipid species present in leg epicuticles, such as fatty acids, esters, alcohols, sterols, phenols or other components of the envelope such as wax and cement of unknown composition [49].

To gain further insight into its functional characteristics we performed *in silico* analysis and also expressed the transporter *in vitro*. *In silico* analysis revealed that ABCH2, is a close homologue with ABCG1 cholesterol transporter, whose structure has recently been determined via crystallography [29]. ABCG1 is a half transporter, acting as homodimer [29] and according to our analysis we identified similar number of conserved interactions stabilizing the dimeric ABCH2 form (Figure 2.5A, B). This alludes to a functional transporter of homodimeric (or homo-oligomeric) nature, as ABCHs are half-transporters meaning they need to form either homo- or hetero-dimers in order to be functional [50]. Membrane preparations from recombinant Baculovirus infected Sf9 cells have been widely used to detect interactions of compounds with ABC transporters of several families, however to our knowledge this is the first *in vitro* functional expression of an ABC transporter of the H sub-family. Successful expression indicated the high abundance of the transporter in membrane fractions rather than cytoplasmic ones, indicating that our multi-spanning protein is correctly targeted (Figure 2.5C). Furthermore, taking advantage of ABC transporters' ability to hydrolyze ATP *in vivo*, we used an ATPase assay and calculated the released inorganic Pi, in ABCH2-expressed compared to control membranes, showing that ABCH2-mebranes result in higher Pi production and hence exhibit enhanced ATPase activity (Figure 2.5D), providing additional evidence to the *in* *silico* data that the transporter most probably adopts a homodimeric state. Moreover, evidence of insect ABCH2 orthologues also supports this scenario, as in RNAi screens (*D. melanogaster* [41], *N. viridula* [16], *T. castaneum* [13]) mortality was observed only in ABCH2-orthologues and no other partners exhibiting similar phenotypes (mortality) were recorded, hence overshadowing the heterodimer possibility.

Additionally, protein-ligand docking analysis was performed to ask whether deltamethrin is a substrate, due to the high deltamethrin toxicity observed upon silencing of the transporter. Indeed, according to docking analysis, deltamethrin could act as a substrate against ABCH2. This is based on the available crystal structure of ABCG1 homologue, whose known substrate is cholesterol. Interestingly, both cholesterol and deltamethrin dock in the same pocket of ABCG1 with similar orientations, energies and interactions (Figure 2.6A). Subsequently, docking analysis performed without bias in the whole transmembrane domain of ABCH2 modelled structure resulted in identification of a pocket just above that of ABCG1, where both substrates docked (Figure 2.6B). Interestingly, deltamethrin docks with higher energy in the ABCH2 model structure providing further support that it is a putative substrate.

Finally, C^{14}-Deltamethrin penetration experiments were carried out in RNAi-mediated silenced mosquitoes. *An. coluzzii* lacking the transporter showed increased penetration of radiolabeled insecticide after short contact (4 minutes). It seems that shortly after deltamethrin exposure a difference in the internalized insecticide is observed (Figure 2.7). One plausible scenario is that the transporter participates in phase 0 and/or III detoxification , as previously reported for ABC transporters [51], directly facilitating export of deltamethrin or its metabolic byproduct export. In that case the difference in penetration could be attributed to direct export from epidermal cells and sequestration of the insecticide into the cuticular structure. Alternatively, we cannot exclude mechanisms of sensing deltamethrin and triggering signaling pathways resulting eventually in slower insecticide entrance. Such a mechanism has been described in *B. subtilis*, where BceAB participates in bacitracin resistance as cosensor for signal transduction [52, 53].

Although, several works implicate ABC transporters in insecticide resistance and toxicity, understanding their implication in these phenomena in insects remains largely unknown. In this work we provide evidence for an ABC transporter-based, fast-acting mechanism present at the appendages, the first defense barrier during insecticide exposure in impregnated surfaces. Our results show high deltamethrin toxicity after silencing of this transporter. Due to the druggable characteristics of this molecule, which is an insect-specific, plasma membrane-bound transporter present in the epidermis of mosquito appendages, a highly epidemiologically relevant tissue in mosquito vector control, we consider this transporter could be a potential inseciticide target. In the future, both *in vitro* screening for identification of substrates/inhibitors of this transporter and dissecting its physiological role and potential essentiality using transgenic mosquito technology could further provide molecular underpinnings and shed light to its potential for applications.

2.6 Literature

1. Balabanidou, V., et al., *Mosquitoes cloak their legs to resist insecticides.* Proc Biol Sci, 2019. **286**(1907): p. 20191091.
2. Kefi, M., et al., *Transcriptomic analysis of resistance and short-term induction response to pyrethroids, in Anopheles coluzzii legs.* BMC Genomics, 2021. **22**(1): p. 891.
3. Ingham, V.A., F. Brown, and H. Ranson, *Transcriptomic analysis reveals pronounced changes in gene expression due to sub-lethal pyrethroid exposure and ageing in insecticide resistance Anopheles coluzzii.* BMC Genomics, 2021. **22**(1): p. 337.
4. Mastrantonio, V., et al., *Insecticide Exposure Triggers a Modulated Expression of ABC Transporter Genes in Larvae of Anopheles gambiae s.s.* Insects, 2019. **10**(3): p. 66.
5. Epis, S., et al., *ABC transporters are involved in defense against permethrin insecticide in the malaria vector Anopheles stephensi.* Parasit Vectors, 2014. **7**: p. 349.
6. Kennedy, C.J. and K.B. Tierney, *Xenobiotic Protection/Resistance Mechanisms in Organisms*, in *Environmental Toxicology: Selected Entries from the Encyclopedia of Sustainability Science and Technology*, E.A. Laws, Editor. 2013, Springer New York: New York, NY. p. 689-721.
7. Thomas, C. and R. Tampé, *Structural and Mechanistic Principles of ABC Transporters.* Annual Review of Biochemistry, 2020. **89**(1): p. 605-636.
8. Choi, C.C. and R.C. Ford, *ATP binding cassette importers in eukaryotic organisms.* Biological Reviews, 2021. **96**(4): p. 1318-1330.
9. Merzendorfer, H., *Chapter One - ABC Transporters and Their Role in Protecting Insects from Pesticides and Their Metabolites*, in *Advances in Insect Physiology*, E. Cohen, Editor. 2014, Academic Press. p. 1-72.
10. Dermauw, W., et al., *A burst of ABC genes in the genome of the polyphagous spider mite Tetranychus urticae.* BMC Genomics, 2013. **14**(1): p. 317.
11. Dean, M. and T. Annilo, *Evolution of the ATP-binding cassette (ABC) transporter superfamily in vertebrates.* Annu Rev Genomics Hum Genet, 2005. **6**: p. 123-42.
12. Dermauw, W. and T. Van Leeuwen, *The ABC gene family in arthropods: Comparative genomics and role in insecticide transport and resistance.* Insect Biochemistry and Molecular Biology, 2014. **45**: p. 89-110.
13. Broehan, G., et al., *Functional analysis of the ATP-binding cassette (ABC) transporter gene family of Tribolium castaneum.* BMC Genomics, 2013. **14**(1): p. 6.
14. Yu, Z., et al., *The ABC transporter ABCH-9C is needed for cuticle barrier construction in Locusta migratoria.* Insect Biochem Mol Biol, 2017. **87**: p. 90-99.
15. Zuber, R., et al., *The ABC transporter Snu and the extracellular protein Snsl cooperate in the formation of the lipid-based inward and outward barrier in the skin of Drosophila.* European journal of cell biology, 2018. **97**(2): p. 90-101.
16. Denecke, S., et al., *Comparative and functional genomics of the ABC transporter superfamily across arthropods.* BMC Genomics, 2021. **22**(1): p. 553.
17. Guo, Z., et al., *The novel ABC transporter ABCH1 is a potential target for RNAi-based insect pest control and resistance management.* Sci Rep, 2015. **5**: p. 13728.
18. Kefi, M., et al., *Two functionally distinct CYP4G genes of Anopheles gambiae contribute to cuticular hydrocarbon biosynthesis.* Insect Biochem Mol Biol, 2019. **110**: p. 52-59.
19. Sarkadi, B., et al., *Expression of the human multidrug resistance cDNA in insect cells generates a high activity drug-stimulated membrane ATPase.* J Biol Chem, 1992. **267**(7): p. 4854-8.
20. Karamanou, S., et al., *Preprotein-controlled catalysis in the helicase motor of SecA.* Embo j, 2007. **26**(12): p. 2904-14.

21. Lanzetta, P.A., et al., *An improved assay for nanomole amounts of inorganic phosphate.* Analytical Biochemistry, 1979. **100**(1): p. 95-97.
22. Balabanidou, V., et al., *Cytochrome P450 associated with insecticide resistance catalyzes cuticular hydrocarbon production in Anopheles gambiae.* Proceedings of the National Academy of Sciences, 2016. **113**(33): p. 9268-9273.
23. Tunggal, J.A., et al., *E-cadherin is essential for in vivo epidermal barrier function by regulating tight junctions.* The EMBO Journal, 2005. **24**(6): p. 1146-1156.
24. Knust, E. and M. Leptin, *Adherens junctions in the Drosophila embryo: the role of E-cadherin in their establishment and morphogenetic function.* Bioessays, 1996. **18**(8): p. 609-12.
25. Andersen, S., *Integument.* Encyclopedia of Insects, 2009: p. 528-529.
26. Nation, J.L., *Integument: Structure and Function*, in *Encyclopedia of Entomology*. 2005, Springer Netherlands: Dordrecht. p. 1200-1203.
27. Almagro Armenteros, J.J., et al., *DeepLoc: prediction of protein subcellular localization using deep learning.* Bioinformatics, 2017. **33**(21): p. 3387-3395.
28. Arnold, K., et al., *The SWISS-MODEL workspace: a web-based environment for protein structure homology modelling.* Bioinformatics, 2006. **22**(2): p. 195-201.
29. Sun, Y., et al., *Molecular basis of cholesterol efflux via ABCG subfamily transporters.* Proceedings of the National Academy of Sciences, 2021. **118**(34): p. e2110483118.
30. Tina, K.G., R. Bhadra, and N. Srinivasan, *PIC: Protein Interactions Calculator.* Nucleic Acids Research, 2007. **35**(suppl_2): p. W473-W476.
31. Glavinas, H., et al., *Utilization of membrane vesicle preparations to study drug–ABC transporter interactions.* Expert Opinion on Drug Metabolism & Toxicology, 2008. **4**: p. 721 - 732.
32. Koes, D.R., M.P. Baumgartner, and C.J. Camacho, *Lessons Learned in Empirical Scoring with smina from the CSAR 2011 Benchmarking Exercise.* Journal of Chemical Information and Modeling, 2013. **53**(8): p. 1893-1904.
33. Balabanidou, V., L. Grigoraki, and J. Vontas, *Insect cuticle: a critical determinant of insecticide resistance.* Curr Opin Insect Sci, 2018. **27**: p. 68-74.
34. Andriessen, R., et al., *Electrostatic coating enhances bioavailability of insecticides and breaks pyrethroid resistance in mosquitoes.* Proc Natl Acad Sci U S A, 2015. **112**(39): p. 12081-6.
35. Pignatelli, P., et al., *The Anopheles gambiae ATP-binding cassette transporter family: phylogenetic analysis and tissue localization provide clues on function and role in insecticide resistance.* Insect Mol Biol, 2018. **27**(1): p. 110-122.
36. Epis, S., et al., *Temporal dynamics of the ABC transporter response to insecticide treatment: insights from the malaria vector Anopheles stephensi.* Sci Rep, 2014. **4**: p. 7435.
37. De Marco, L., et al., *The choreography of the chemical defensome response to insecticide stress: insights into the Anopheles stephensi transcriptome using RNA-Seq.* Scientific reports, 2017. **7**: p. 41312-41312.
38. Panikashvili, D. and A. Aharoni, *ABC-type transporters and cuticle assembly: Linking function to polarity in epidermis cells.* Plant Signal Behav, 2008. **3**(10): p. 806-9.
39. Mayer, F., et al., *Evolutionary conservation of vertebrate blood-brain barrier chemoprotective mechanisms in Drosophila.* The Journal of neuroscience : the official journal of the Society for Neuroscience, 2009. **29**(11): p. 3538-3550.
40. Epis, S., et al., *ABC transporters are involved in defense against permethrin insecticide in the malaria vector Anopheles stephensi.* Parasites & Vectors, 2014. **7**(1): p. 349.

41. Zuber, R., et al., *The ABC transporter Snu and the extracellular protein Snsl cooperate in the formation of the lipid-based inward and outward barrier in the skin of Drosophila.* Eur J Cell Biol, 2018. **97**(2): p. 90-101.
42. Pitts, R.J., et al., *Transcriptome profiling of chemosensory appendages in the malaria vector Anopheles gambiae reveals tissue- and sex-specific signatures of odor coding.* BMC Genomics, 2011. **12**: p. 271.
43. Broehan, G., et al., *Functional analysis of the ATP-binding cassette (ABC) transporter gene family of Tribolium castaneum.* BMC Genomics, 2013. **14**(6): p. 1471-2164.
44. Wang, Y., et al., *Dysfunction of Oskyddad causes Harlequin-type ichthyosis-like defects in Drosophila melanogaster.* PLoS Genet, 2020. **16**(1): p. e1008363.
45. Blomquist, G.J. and A.-G. Bagnères, *Insect Hydrocarbons: Biology, Biochemistry and Chemical Ecology.* Cambridge Univ., 2010.
46. Blomquist, G.J., *Biosynthesis of cuticular hydrocarbons.* Insect Hydrocarbons: Biology, Biochemistry, and Chemical Ecology, 2010: p. 35-52.
47. Hadley, N.F., *Cuticular lipids of terrestrial plants and arthropods: A comparison of their structure, composition, and waterproofing function.* Biological Reviews, 2008. **56**: p. 23-47.
48. Yeats, T.H. and J.K. Rose, *The formation and function of plant cuticles.* Plant Physiol, 2013. **163**(1): p. 5-20.
49. Lockey, K.H., *Lipids of the insect cuticle: origin, composition and function.* Comparative Biochemistry and Physiology Part B: Comparative Biochemistry, 1988. **89**(4): p. 595-645.
50. Dermauw, W. and T. Van Leeuwen, *The ABC gene family in arthropods: comparative genomics and role in insecticide transport and resistance.* Insect Biochem Mol Biol, 2014. **45**: p. 89-110.
51. Kennedy, C.J. and K.B. Tierney, *Xenobiotic protection/resistance mechanisms in organisms*, in *Environmental Toxicology*. 2013, Springer. p. 689-721.
52. Ohki, R., et al., *The BceRS two-component regulatory system induces expression of the bacitracin transporter, BceAB, in Bacillus subtilis.* Mol Microbiol, 2003. **49**(4): p. 1135-44.
53. Bernard, R., et al., *Resistance to bacitracin in Bacillus subtilis: unexpected requirement of the BceAB ABC transporter in the control of expression of its own structural genes.* J Bacteriol, 2007. **189**(23): p. 8636-42.

Chapter 3

Characterization of the CYP4G enzymes implicated in cuticular alterations of resistant mosquitoes via hydrocarbon biosynthesis

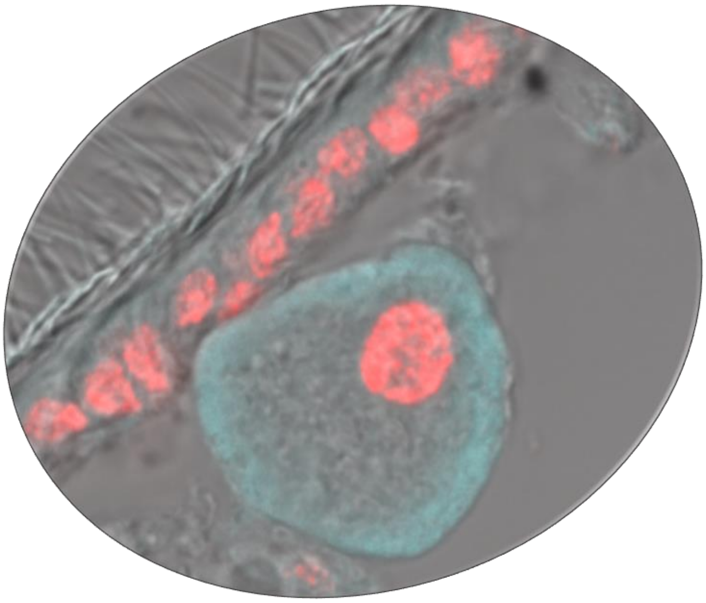

Publication

Kefi,M., Balabanidou,V., Douris,V., Lycett,G., Feyereisen,R., & Vontas,J. (2019). Two functionally distinct Anopheles gambiae CYP4Gs contribute to cuticular hydrocarbon biosynthesis. *Insect Biochem Mol Biology*, 110 (52-59). doi:10.1016/j.ibmb.2019.04.018

3.1 Abstract

Cuticular hydrocarbon (CHC) biosynthesis is a major pathway of insect physiology. In *Drosophila melanogaster* the cytochrome P450 CYP4G1 catalyzes the insect-specific P450 oxidative decarbonylase step, while in the malaria vector *An. coluzzii*, two CYP4Gs paralogues, CYP4G16 and CYP4G17 are present. The *An. coluzzii* CYP4G16 is bound on the plasma membrane (PM) in adult mosquito oenocytes, an unusual subcellular localization pattern, and has been shown to exhibit decarbonylase activity *in vitro*, whereas CYP4G17 is localized in oenocyte cytoplasm in adults, but its catalytic activity and function remains unknown.

Analysis of the subcellular localization of CYP4G17 and CYP4G16 in earlier developmental stages revealed that they are both on the cytoplasmic side of the PM of larval oenocytes. CYP4G16 preserves its PM localization across developmental stages analyzed; however, CYPG17 is differentially localized in pupae in two distinct types of pupal oenocytes, presumably oenocytes of larval and adult developmental specificity. Western blot analysis showed the presence of two CYP4G17 forms, potentially associated with each oenocyte type.

GAL4/UAS expression in *Drosophila melanogaster* oenocytes was used to express the *An. coluzzii* CYP4Gs in a *Cyp4g1* silenced background. CYP4G16 (one or two gene copies), CYP4G17 (only two gene copies) or their combination (one gene copy each) rescue the adult lethal phenotype of *Cyp4g1*-KD flies, which demonstrates that CYP4G17 is also a functional decarbonylase, albeit of somewhat lower efficiency than CYP4G16 in *Drosophila*.

Flies expressing mosquito CYP4G16 and/or CYP4G17 produced similar CHC profiles to ‘wild-type’ flies expressing the endogenous CYP4G1, but they also produce very long-chain dimethyl-branched CHCs not detectable in wild type flies, with higher abundance in CYP4G17 and CYP4G16/CYP4G17 flies than in CYP4G16 flies. Furthermore, flies with similar backgrounds and total cuticular hydrocarbon contents, differentiated in *CYP4G* alleles (*CYP4G16* or *CYP4G17*) were subjected to desiccation assay and toxicity assays, showing that CYP4G17-expressing flies compensate better these stresses, possibly due to the longer CHCs they produce.

Finally, we achieved the successful expression of CYP4G16 and CYP4G17 together with their obligatory electron donor, cytochrome P450 reductase (CPR), in Sf9 insect cells using baculovirus system of expression. This is the first time the *in vitro* expression of CYP4Gs is successfully performed using this system and will be further used for model and endogenous substrate screenings.

3.2. Introduction

Insect cuticular hydrocarbons (CHCs) are a complex blend of long-chain alkanes or alkenes and methyl-branched alkanes that act as essential waterproofing components of the insect epicuticular layer to prevent desiccation, and/or serve as species- and sex-specific semiochemicals [1-5]. Although CHC profiles differ among insect species, the main biosynthetic pathway is conserved [2]. Their synthesis from fatty acids requires a suite of elongases, desaturases and acyl-CoA reductases that function in concert in large, ectodermally derived cells, called oenocytes [6]. An additional enzyme required for the final step of CHC synthesis, a cytochrome P450 of the CYP4G subfamily was recently identified as oxidative decarbonylase [7]. *Drosophila* CYP4G1 is highly expressed in oenocytes together with NADPH cytochrome P450 reductase (CPR) and catalyzes the oxidative decarbonylation of long-chain aldehydes [7]. Oenocyte-specific RNAi-mediated knock down of CYP4G1 results in severe susceptibility to desiccation, conferring high mortality at emergence [7]. The CYP4G P450 subfamily is evolutionarily conserved across insects [8] but is absent in other orders, such as crustaceans and chelicerates. This may indicate an essential function of *CYP4G* genes specific to insects, suggested to be a key to success in terrestrial adaptation. Insect genomes sequenced so far possess at least one CYP4G (one in honey bee and aphid, two in *Drosophila* and several mosquito species) [7].

Several earlier studies indicate distinct lipid/CHC signatures across development. Firstly, the necessary renewal of the cuticular lipids at each molt [9] implies distinct lipids and presumably differences in their CHC derivatives at different developmental stages. Secondly, aquatic insects should prevent liquid entry into the tracheal system while apart from this terrestrial insects must be protected from desiccation which means they should prevent water loss. Adult *An. coluzzii* and *D. melanogaster* with their early developmental stages being aquatic or semi-aquatic respectively [10] presumably reflect the distinct needs in lipids/hydrocarbons through development. Larval oenocytes synthesize very-long-chain fatty acids (VLCFA) which are accumulated into spiracles, the organs controlling the entry of air into the trachea, protecting respiratory system from liquid entry [10]. Oenocyte-specific RNAi-based knock down of *Cyp4g1* or *Cpr* in larvae and adults results in severe depletion in epicuticular HC in the few adult survivors. The majority die at eclosion, presumably of extreme sensitivity to desiccation at the time of adult emergence [7]. Furthermore, pheromone-driven courtship was altered in *Cyp4g1*-KD CHC depleted females [7]. Similar phenotypes are produced when oenocytes are specifically ablated in adult *Drosophila* females.

Underlying this phenotype is the presence of two different oenocyte cells in larvae and adults that have separate developmental origins [11-13] and have been described in mosquitoes [14] and other Diptera [12]. Overall, these latter studies suggest that presumably larval oenocytes have a primary role in CHC production during molting and water-loss prevention in the tracheal system, while CHCs produced from adult oenocytes are mostly implicated in sex- and species-specificity, pheromonal communication and desiccation resistance [10, 12].

The fact that *An. coluzzii* oenocytes express two CYP4Gs (CYP4G16 and CYP4G17) as opposed to the single CYP4G expressed in *D. melanogaster* oenocytes is possibly indicative of a functional diversity. A recent study has shown that CYP4G16 is bound on the periphery of adult oenocytes, while CYP4G17 is dispersed among the cytoplasm [15]. In addition, *in vitro* experiments indicate the ability of CYP4G16 to catalyze the conversion of long-chain aldehydes to hydrocarbons, hence completing the final biosynthetic step, whereas the role of CYP4G17 remains unknown. While CYP4G16 was able to convert C18 aldehyde to HC, no such activity could be demonstrated for CYP4G17, although longer aldehydes could not be tested *in vitro* because of solubility issues [15]. A recent study in *Dendroctonus ponderosae* showed that shorter-chain alcohols can also be substrates of CYP4Gs [16], which can thus serve in the biosynthesis of the pine beetle pheromone exo-brevicomin as well as in CHC biosynthesis.

The variation in insect CHC blend has been associated with physiological adaption to ecological and reproductive parameters [5]. Indeed, methyl-branched CHCs have been shown to affect both waterproofing and mating in *Drosophila serrata* [17]. It is likely that longer carbon chains in CHCs increase the melting temperature of the insect epicuticular wax layer and probably influence desiccation resistance, and methyl branching increases the chemical information of the cuticle [5]. Some studies have indicated that *An. coluzzii* is rich in methyl-branched very long chain CHCs (mono- or dimethyl) [15, 18], which could potentially serve both biological functions.

Moreover, cuticular analysis of an insecticide resistant *An. coluzzii* population compared to a susceptible one, revealed a thicker epicuticle, the major deposition site of CHCs, in the femur leg segment, thus creating a thicker hydrophobic barrier to insecticide molecules, as shown by reduced penetration rate of radiolabeled insecticide [15]. The higher CHC amount is in line with the overexpression of CYP4Gs in the resistant mosquitoes, implicating an additional role of CHCs in insecticide penetration resistance [19].

In this study, the subcellular localization of *An. coluzzii* CYP4Gs was analyzed in oenocytes from earlier developmental stages, i.e. 4th instar larvae and pupae. Furthermore, functional analysis of the *An. coluzzii* CYP4Gs was performed *in vivo* using GAL4/UAS heterologous expression coupled with RNAi knock-down of the endogenous *Cyp4g1* gene in *Drosophila melanogaster* and the ability of CYP4G16 and/or CYP4G17 in different doses and in combination to rescue the lethal (*Cyp4g1* Knock-down) phenotype. CHC analysis of the rescued flies then gave insights into the catalytic efficiency and specificity of the two anopheline Cyp4Gs in a *Drosophila* background, also reflected in different response of the flies in desiccation and contact toxicity assays.

3.3. Materials and methods

3.3.1 Mosquito strains

The *An. coluzzii* N'Gousso strain was reared under standard insectary conditions at 27°C and 70-80% humidity under a 12:12 hour photoperiod. The strain is originally from Cameroon and it is susceptible to all classes of insecticide [20].

3.3.2 Antibodies

Rabbit polyclonal antibodies targeting CYP4G16 have previously been developed [15]. The specific antibodies that were used for the detection of CYP4G17 (AGAP000877) have previously been described [21]. The epitopes recognize residues 231-312 and 233-315 of CYP4G16 and CYP4G17 respectively.

3.3.3 Preparation of cryosections for immunohistochemistry, immunofluorescence and microscopy

4th instar *An. coluzzii* larvae and dissected pupal abdomens were fixed in cold solution of 4% PFA (methanol free, Thermo scientific) in phosphate-buffered saline (PBS) for 4 h, cryo-protected in 30% sucrose/PBS at 4° C for 12 h, immobilized in Optimal Cutting Temperature O.C.T. (Tissue-Tek, SAKURA) and stored at -80°C until use. Immunofluorescence analysis, followed by confocal microscopy, was performed on longitudinal sections of the frozen larval and pupal specimens as described previously [21]. Briefly, 7 μm sections, obtained in cryostat with UVC disinfection (Leica CM1850UV) were washed (3 x 5 min) with 0,05% Tween in PBS and blocked for 3 h in blocking solution (1% Fetal Bovine Serum, biosera, in 0,05% Triton/PBS). Then, the sections were stained with rabbit primary antibodies in 1/500 dilution, followed by goat anti-rabbit (Alexa Fluor 405, Molecular Probes) (1/1000) that gave the cyan color. Also, To-PRO 3-Iodide (Molecular Probes) which specifically stains DNA (red color), was used after RNAse A treatment. Finally, images were obtained on a Leica SP8 laser-scanning microscope, using the 40-objective.

3.3.4 Topology experiments: predictions and whole mounts (preparation of abdominal walls for immunohistochemistry and immunofluorescence)

The predicted membrane topology of both *An. coluzii* CYP4Gs was analyzed using Phobius, a transmembrane topology and signal peptide predictor program [22]. For whole-mount larval abdomen immunostaining, abdominal walls from 4thinstar larvae were dissected and fixed for 30 min at room temperature in 4% methanol-free formaldehyde (Thermo Scientific) in PBS supplemented with 2 mM $MgSO_4$ and 1 mM EGTA, washed for 5 min with PBS, and then washed with methanol for precisely 2 min. After methanol wash, the tissues were washed again with PBS and then blocked for 1 h in blocking solution (bl sol: 1% BSA, 0.1% Triton X-100 in PBS). Then the tissues were stained with rabbit primary antibodies in 1/500 dilution in the blocking solution, followed by goat anti-rabbit antibody (Alexa-Fluor 488; Molecular Probes; 1:1,000) that gave the green color. Up to this point the same protocol omitting the addition of Triton was used to create the non-permeabilized conditions. Finally, DNA was stained red with ToPRO 3-Iodide (Molecular Probes). Pictures were obtained on Leica M205 FA Fluorescent Stereomicroscope.

3.3.5 Fly strains

In order to drive oenocyte –specific expression, the RE-Gal4 driver line ([23]; kindly provided by Jean-François Ferveur, Université de Bourgogne, Dijon, France) was employed. This line contains the RE fragment of the *desat1* gene promoter, whose expression is mostly confined to oenocytes in *Drosophila* adults, (though some expression is also observed in accessory glands in males [23]). The responder strain UAS-Cyp4g1-KD (#102864 KK from Vienna Drosophila Resource Center) was used for RNAi mediated knock-down of CYP4G1.

3.3.6 Generation of UAS responder flies

Since both the RE-Gal4 driver and UAS-Cyp4g1-KD responder transgenes are located on *Drosophila* chromosome 2, the two ‘mosquito CYP4G’ responder fly strains were generated by ϕC31 integrase mediated attB insertion [24] using landing site VK13 in chromosome 3 to facilitate downstream manipulations. Two *ad hoc* integration vectors were generated by modifying the vector dPelican.attB.UAS_CYP6A51 [25]. This plasmid is a modification of pPelican [26] which contains *gypsy* insulator sequences flanking the expression cassette [27], and contains 5xUAS sequences upstream of a basal hsp70 promoter, and a SV40 polyA signal downstream of the cloned ORF. Kapa Taq DNA Polymerase (Kapa Biosystems) was used for the amplification of a 1713 bp fragment containing *CYP4G16* ORF using primer pair CYP4G16F/CYP4G16R (Table S3.1) that introduce a 5’ BssHII site and a 3’ XhoI site, while primer pair CYP4G17F/CYP4G17R (Table S3.1) was used to amplify a 1711 bp fragment containing the*CYP4G17* ORF and introducing a 5’ AscI and a 3’ SalI, respectively. The templates for the amplification of CYP4G16 and CYP4G17 ORFs were cDNAs of adult mosquito RNAs. PCR conditions were 95°C for 3 min, followed by 35 cycles of 95°C for 30 sec, 50°C for 30 sec, 72 for 2 min. The amplicons were purified, digested with the relevant enzyme combinations (BssHII/XhoI for *CYP4G16* fragment and AscI/SalI for *CYP4G17* fragment) and sub-cloned into the unique MluI/XhoI sites of dPelican.attB.UAS_CYP6A51 so that the existing ORF is removed and replaced by the *CYP4G16* or *CYP4G17* ORFs downstream of the 5xUAS-promoter sequence and just upstream of the SV40 polyadenylation sequence. Each *de novo* UAS recombinant plasmid (dPelican.attB.UAS_CYP4G16 and dPelican.attB.UAS_CYP4G17) contained also a mini-*white* marker for *Drosophila*. These plasmids were sequence verified using primers pPel_uas F/pPel_sv40 R (Table S 3.1) and used to inject preblastoderm embryos of the *D. melanogaster* strain *y[1] M{vas-int.Dm}ZH-2A w[*]; PBac{y[+]-attP-9A}VK00013* (referred hereafter as VK13 strain, #24864 in Bloomington *Drosophila* Stock Center, kindly provided by M. Monastirioti and C. Delidakis, IMBB) which enables ϕC31 integrase expression under *vasa* promoter in chromosome X and bears an attP landing site in the 3rd chromosome. G_0 injected VK13 flies were crossed with *yw* flies and G_1 progeny was screened for w^+ phenotypes (red eyes) indicating integration of the recombinant plasmid. Independent transformed lines were crossed with a balancer strain for the 3rd chromosome (*yw*; TM3 *Sb* / TM6B *Tb Hu*) and G_2 flies with red eyes and relevant marker phenotype were selected and crossed among themselves to generate the homozygous flies used to establish the transgenic responder lines (Figure S3.1).

3.3.7 Generation of flies used for rescue experiment

In order to generate flies where both oenocyte-specific *Drosophila* Cyp4g1 RNAi knock-down and *Anopheles CYP4G16* and/or *CYP4G17* expression by one or two transgene copies would take place, a series of standard genetic crosses (see Figure S3.1 for detailed strategy) was performed in order to generate homozygous lines bearing either both RE-Gal4 (2nd chromosome) and UAS-*CYP4G16* or UAS-*CYP4G17* (3rd chromosome), or both UAS-*Cyp4g1*-KD (2nd chromosome) and UAS-*CYP4G16* or UAS-*CYP4G17* (3rd chromosome). Then, several different combinations of crosses provided all the genotypes used for rescue experiments as shown in Table S3.2.

3.3.8 Quantification of eclosion (adult survival and adult mortality)

For quantification experiments appropriate fly crosses were set up by crossing 5 virgin females with 5 males of the appropriate genotypes as shown in Table S3.2. 2nd instar larvae were collected and transferred into fly food in batches of 20 (approximately 130 larvae per biological replicate were transferred). Pupae were then counted to determine pupation efficiency and successfully eclosed adults were measured. To address eclosion we measured the alive adults (males and females), while newly emerged adults that died immediately after eclosion were counted separately in order to address the adult mortality, in three biological replicates.

3.3.9 Extraction of cuticular lipids, Cuticular hydrocarbons (CHCs) Fractionation, Identification and Quantitation.

Crosses B x 2, B x 3, C x 3 and G x 1 (Table S3.2) were set up and the progeny (B2, B3, C3 and G1, Table S3.2) was separated by sex at emergence. One-day old male flies from each condition were dried in Room Temperature for at least 48 h. Approximately 150 flies of each condition were separated in 3 replicates, the dry weight of each replicate was measured and they were send for CHC analysis in VITAS-Analytical Services (Oslo, Norway). Briefly, cuticular lipids from all samples were extracted by 1-min immersion in hexane (x3) with gentle agitation; extracts were pooled and evaporated under a N_2 stream. CHCs were separated from other components and finally concentrated prior to chromatography by Solid Phase Extraction (SPE). CHC identification by gas chromatography-mass spectrometry (GC-MS) and CHC quantitation by GC-flame ionization detector (FID) were performed as described previously [15, 28]. Quantitative amounts were estimated by co-injection of nC24 as an internal standard (2890ng/ml in hexane). CHC quantification was calculated as the sum of area of 32 peaks in total (peaks 3 and 4 were excluded due to background noise) and the relative amount (mean value ± SD) of each component was calculated by dividing the corresponding peak area by the total CHC peak area, using the internal standard. Shorthand nomenclature of CHCs used in the text and tables is as follows: CXX indicates the total number of carbons in the straight chain; linear alkanes are denoted as n-CXX; the location of methyl branches is described as x-Me for monomethyl-alkanes and as x,x-DiMe for dimethyl-alkanes. Alkenes are shown as x-CXX:1. Statistics were analyzed using GraphPad Prism software, version 6.01. Differences in the total CHC values were analyzed with Student's *t*-test.

3.3.10 Western blot analysis

Abdominal walls from 4th instar larvae, 1-5 hour old pupae, 20-24 hour old pupae and 1-12 hour-old adults were homogenized into a Homogenization Buffer, containing 8 M Urea, 50 mM Tris-HCl, pH 8.0 and 0.5% SDS. Polypeptides resolved by SDS-PAGE (10% acrylamide) were electro-transferred on nitrocellulose membrane (GE Healthcare, Whatman) and probed with anti-CYP4G16, anti-CYP4G17 at a dilution of 1:250 in TBS-Tween. Antibody binding was detected using goat anti-rabbit IgG coupled to horseradish peroxidase (Cell Signaling) (diluted 1:10,000 in 1% skimmed milk in TBS-Tween buffer), visualized using a horseradish peroxidase sensitive ECL Western blotting detection kit (GE Healthcare, Little Chalfont, Buckinghamshire, UK) and the result was recorded using Fujifilm LAS3000 CCD camera imaging station.

3.3.11 Desiccation assay

The same number (20) of female REGal4;CYP4G16 and REGal4;CYP4G17 were crossed with the same number (20) of Cyp4g1KD;CYP4G16 males in large food vials. At emergence progeny were separated by sex. Males were placed in fresh food vials, including 20 individuals each for 2-3 days. After that they were transferred into empty glass vials covered by cotton and they were placed into a tray at 25°C containing silica gel (Honeyell Fluka^{TM}, Fisher Scientific), reducing relative humidity to 20%. Each condition included 3 glass vials containing 20 individuals per biological experiment. Every 30 minutes until all flies die, mortality was recorded. The whole procedure was repeated two times. The two biological experiments were statistically analyzed separately, using Kaplan-Meier survival analysis performed in Graphpad Prism. P-value and median survival from each condition were calculated with Log-rank (Mantel-Cox) test. To ensure the mortality observed was not due to the lack of food, but because of desiccation we also included a starvation control experiment. 20 male flies per conditions were placed into glass vials containing water-agar and kept at 25°C in proximity with the vials of desiccation assay, but without silica gel. Mortality was recorded every hour and the same statistical analysis as in desiccation assay was performed.

3.3.12 Permethrin toxicity assay

The same number (20) of female REGal4;CYP4G16 and REGal4;CYP4G17 were crossed with the same number (20) of Cyp4g1KD;CYP4G16 males in large food vials. At emergence progeny were separated by sex. Males were placed in fresh food vials, including 20 individuals each for 2-3 days. After that they were transferred into food vials and transferred in glass vials impregnated with permethrin in different concentrations (0 ppm, 25ppm, 50 ppm, 100 ppm, 200 ppm) and covered by cottons containing sugar-water. Permethrin was diluted in acetone and 0 ppm condition contained only acetone to measure toxicity because of that. In 0 ppm mortality was zero in all conditions and in 200ppm it was 100% and hence they are not depicted in Figure 3.9. The vials were placed into a tray at 25°C and mortality was recorded 24 hours later. Each condition included two glass vials containing 10 individuals per biological experiment and the whole experiment was repeated five times. Statistical analysis was performed for each permethrin concentration using un-paired t-test in GraphPad Prism.

3.3.13 CYP4G/CPR -Overexpressing Sf9 insect cells and membrane preparations.

CYP4G16 (17) along with CPR were expressed in *Spodoptera frugiperda* Sf9 insect cells using the Pfastbac1 vector, which was synthesized *de novo* (GenScript) and their ORF was subcloned in between NdeI and EcoRI restriction enzyme sites. *Musca domestica* CPR was also synthesized. At the C-termini both CYP4Gs and MdCPR were tagged with TEV-6xHis epitopes followed by a stop codon. Both sequences were codon optimized for *S. frugiperda* using GenSmart codon optimization tool (GenScript). Recombinant baculoviruses encoding *Cyp4g16 (17)* and *CPR* cDNAs were generated with BAC-TO-BAC Baculovirus Expression Systems (Invitrogen), following manufacturer's instructions. 2μg of Bacmid DNA, mixed with Escort IV Transfection Reagent (Merck) were used to transfect 5x10^5 Sf9 cells in 1ml of SF900 II SFM growth medium (ThermoFisher scientific). The complex was incubated for 45 min/RT and the lipid complexes were added dropwise to the appropriate well and were incubated at 27°C for 6 hours. After that, another 1ml of medium, supplemented with antibiotics (2x penicillin and streptomycin) and 20% FBS (ThermoFisher scientific) were added. After 24 hours DNA:lipid complexes were removed and 2ml of supplemented growth medium were added to the cells which were subsequently incubated at 27°C for 72 hours. Medium, containing the viruses stock were removed and stored, while cells were also collected by pipetting in ice-cold 1 X PBS. Cell pellets (after 3000g/5min/4°C centrifugation) were resuspended in RIPA supplemented with protease inhibitors followed by a 10000g/10 min /4°C centrifugation step. The supernatant was prepared for western blot analysis with the addition of 5x Sample Buffer (SB) and a 5min-boiling step (more details for western blot in section 2.5). After validation of recombinant protein expression of expected size in *Sf9* cells and determination of Viral Stock titers using baculoQUANT ALL-IN-ONE (GenWay), according to manufacturer's instructions, infection was performed. For infection 10^6 cells/ml were seeded in T75 Flasks in a final volume of 15 ml antibiotic and FBS supplemented growth medium. After 4-5 hour incubation at 27°C, viruses were added at the desired MOI, which after optimization was 8:1 (CYP4G:CPR). 6 hours post infection ferric citrate (0.2mM) and 5-aminolevulinic acid (0.3mM) were added and infected cells were incubated for extra 84 hours. Along with the CYP4G16(17):CPR infections, cells infected with an empty Bacmid together with CPR served as negative control. Then the cells were harvested and proceeded to microsomal preparations. Following a centrifugation step at 2000g/3min/4°C, cell pellets were resuspended in a buffer containing 0.1M sodium phosphate pH=7.4, 1mM EDTA, 0.2M sucrose, 1mM DTT, 1mM PMSF, 1ugr/ml aprotinin and 1ugr/ml leupeptin. Crude homogenate was centrifuged at 8.000g/10min/4°C and the supernatant was ultracentrifuged at 95,000g/1hour/4°C (Beckman AirFuge CLS Ultracentrifuge). Pellets were resuspended in the same buffer and used for downstream experiments or stored at -80°C. Membrane preparations were subjected to western blot analysis using anti-His antibody, CO-spectrum analysis and CPR activity analysis. CPR activity was measured by monitoring cytochrome C reduction.

3.4. Results

3.4.1 Both CYP4G17 and CYP4G16 are anchored on the plasma membrane of 4th instar larval oenocytes with the globular part facing cytoplasmically.

To determine the specific localization of CYP4G16 and CYP4G17 in 4th instar larvae, an immunohistochemistry approach was employed. Longitudinal sections from frozen pre-fixed mosquito specimens were immune-stained with anti-CYP4G17 and anti-CYP4G16 specific antibodies, respectively. CYP4G16 and CYP4G17 antibodies gave intense signals localizing in oenocytes. We were unable to detect specific signals in other tissues by immune-staining. Surprisingly, higher magnification confocal microscopy focusing on oenocytes revealed that both CYP4G17 and CYP4G16 are found at the periphery of the larval oenocytes, presumably associated with the plasma membrane (PM) (Figure 3.1). According to topology prediction tools both proteins were predicted to have one transmembrane domain each. CYP4G16 and CYP4G17 transmembrane domains are predicted to span the residues seventeen to thirty nine and twenty to forty one respectively. Hence, in order to investigate the hypothesis that they span the membrane with one helix with the N-terminus located in the extracellular space of oenocyte cells, separated from the remainder globular part of the protein that is located intracellularly we performed immunohistochemical experiments in abdominal larval walls in permeabilized and non-permeabilized conditions (Figure 3.2). The fact that specific antibodies used recognize epitopes closer to the C-termini of the proteins together with the absence of oenocyte-specific staining in non-permeabilized conditions for both CYP4G16 and CYP4G17 as well as *in silico* prediction strongly indicate that both are anchored on the plasma membrane, facing the cytoplasm, with their N-termini residing outside of the cell.

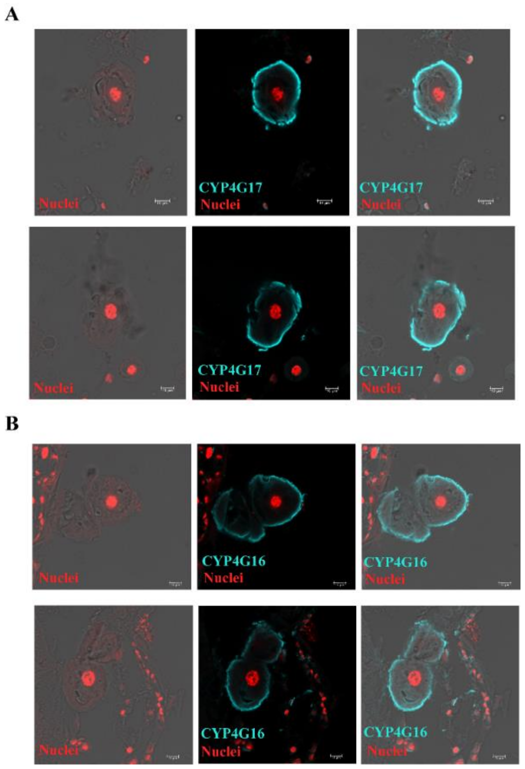

Figure 3.1. Immunohistochemical localization of CYP4Gs in larvae. Merged immunohistochemical images from longitudinal sections of 4th instar mosquito larvae focusing on oenocytes. A. CYP4G17

peripheral localization in *An. coluzzii* larval oenocytes, B. CYP4G16 peripheral localization in *An. coluzzii* larval oenocytes. Cell nuclei are stained red with TO-PRO-3; scale bar 10 μm. Left: bright-field with stained nuclei, middle: antibody, right: merge of bright-field, antibody and nuclei staining.

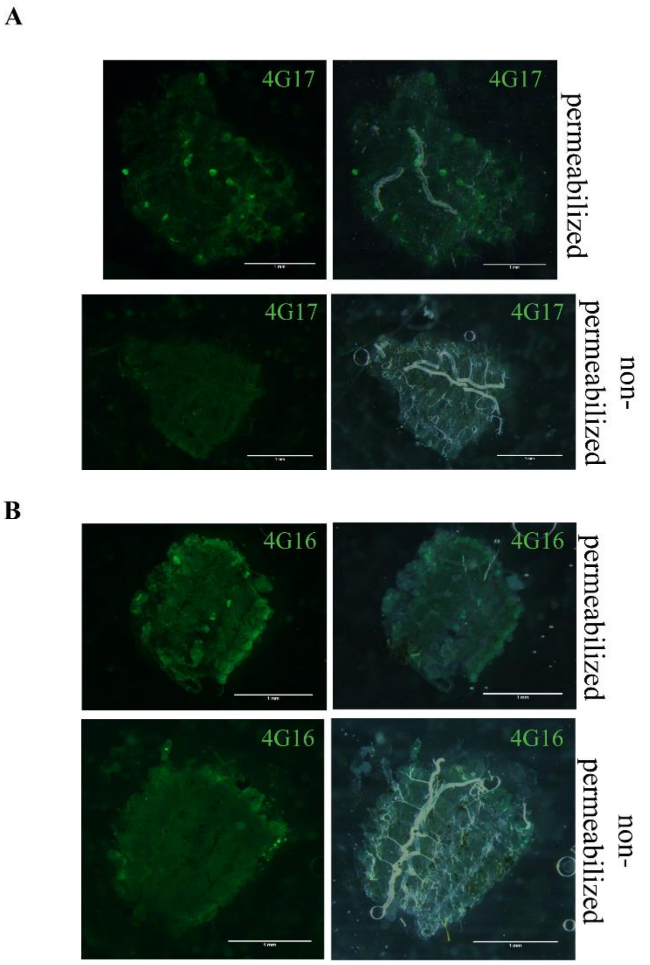

Figure 3.2 Membrane topology of CYP4Gs. Immunohistochemical images from abdominal walls (whole mounts) of 4th instar mosquito larvae focusing on oenocytes. A. CYP4G17 and B. CYP4G16 in permeabilized and non-permeabilized conditions.

3.4.2 Two differentially localized CYP4G17 forms in pupal oenocytes, of larval and adult origin.

To immunolocalize CYP4G17 and CYP4G16 in pupae, the same immunohistochemical approach in longitudinal cryosections in pupal abdominal walls was performed as above. In pupa, both CYP4G16 and CYP4G17 antibodies gave intense signals in two cell types. We detected both close to the lateral pupal cuticular walls. The larger cells, full of round-shaped vesicular structures and lipid droplets are the remaining larval oenocytes, while the smaller in size rounded-shaped cells that are also found singly and in clusters are the newly-developing adult oenocytes (Figure 3.3). CYP4G16 maintained a peripheral localization in both oenocyte types (Figure 3.3A and B), whereas CYP4G17 antibody gave localized signals of two distinct patterns. Peripheral staining (Figure 3.3C) was maintained in cells of larval origin, while the developing adult cells were stained with anti-CYP4G17 throughout their cytoplasm (Figure 3.3D).

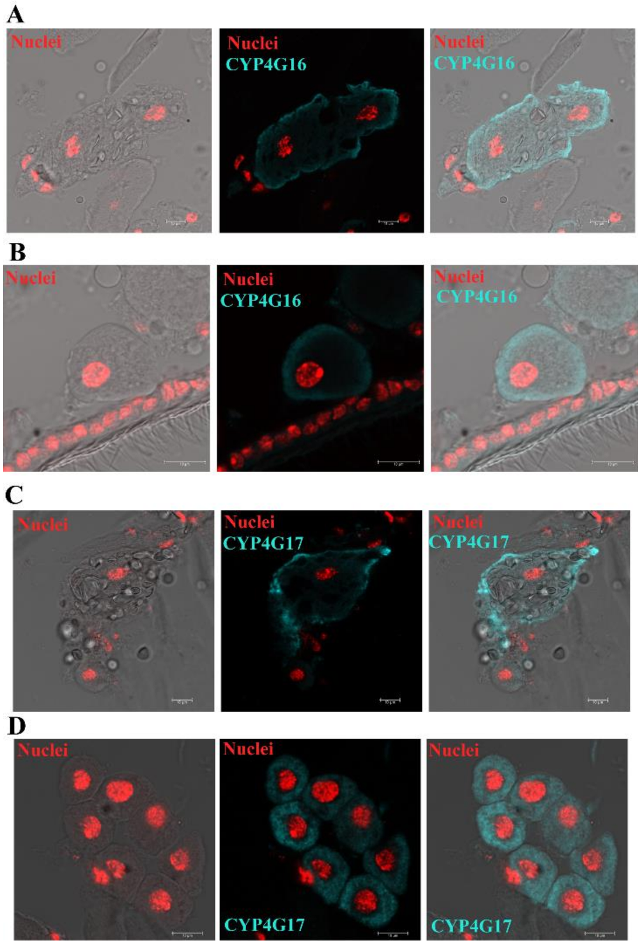

Figure 3.3. Immunohistochemical localization of CYP4Gs in pupae. Merged immunohistochemical images from longitudinal sections of pupal abdominal walls. A. CYP4G16 localization in larval-origin pupal oenocytes mainly on the periphery of oenocytes, B. CYP4G16 localization in adult-origin pupal oenocytes mainly on the periphery, C. CYP4G17 localization in larval-origin, pupal oenocytes mainly on the periphery of oenocytes, D. CYP4G17 localization in adult-origin, newly-developed oenocytes of pupae, forming a cluster, showing the protein dispersed throughout the cytoplasm. Cell nuclei are stained red with TO-PRO-3; scale bars= 10 µm. Left: bright-field with stained nuclei, middle: antibody and nuclei staining, right: merge of bright-field, antibody and nuclei staining.

To further examine the different sub-cellular localization observed in the two types of oenocytes found in pupae, we performed western blot analysis with anti-CYP4G17 using abdominal walls of 4th instar larvae, newly-formed pupae (1-5 hour-old), pupae prior to emergence (20-24 hour-old) and newly emerged adults (1-12 hour-old). Interestingly, we observed two bands in different molecular sizes in all developmental stages with a difference in the intensity in each condition tested (Figure 3.4). The lower band around the 65 KDa MW protein marker, is close to the estimated MW of the protein (calculated MW = 64 KDa), whereas the upper band migrates approximately at 70 KDa.

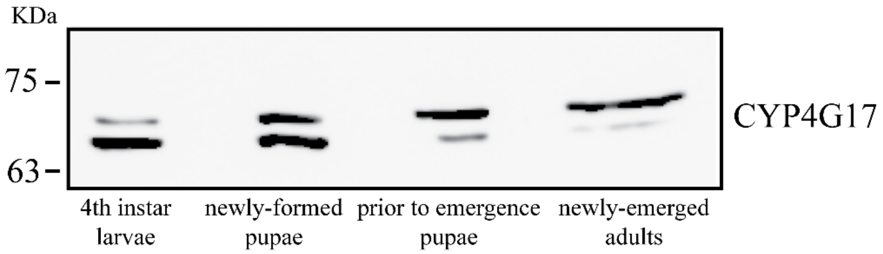

Figure 3.4. Expression pattern of CYP4G17 among different *An. coluzzii* developmental stages. Whole protein extracts from dissected abdominal walls of 4th instar larvae (lane 1), newly-formed pupae (lane 2), pupae prior to emergence (lane 3) and newly emerged adults (lane 4), were analyzed by Western blot using anti-CYP4G17.

3.4.3 Oenocyte-specific expression of *CYP4G16* and *CYP4G17* (two copies) in CYP4G1 knock-down *Drosophila* can restore viability.

Using a series of genetic manipulations we were able to induce the expression of either or both mosquito CYP4Gs while simultaneously silencing the endogenous *Cyp4g1* gene specifically in oenocytes (Figure S3.1 and Table S3.2). Phenotypic analysis showed that all *Cyp4g1*-KD flies die at emergence, not being able to eclose from the pupal case. However, viability was almost completely restored in the presence of two copies of *CYP4G16* and of *CYP4G16* in combination with *CYP4G17* (Figure S3.2). Quantitative analysis of all the different CYP4G conditions tested revealed that CYP4G16 and CYP4G17 exhibit differential ability to rescue the lethal phenotype in an oenocyte-specific *Cyp4g1*knock-down genetic background (Figures 3.5). As shown in Figure 3.5, 86% of the larvae expressing *CYP4G16* in two copies successfully emerged into adults, while *CYP4G17* in two copies is able to rescue approximately 33% of the flies, revealing its ability to partially complement *Cyp4g1* silencing. This demonstrates that CYP4G17 is also a functional oxidative decarbonylase. The ability of each transgene to rescue the lethal phenotype is dose-dependent since *CYP4G16* in one copy only partially restores viability (15% survivors), while overexpression of one copy of *CYP4G17* seems to generate flies arrested during eclosion. However, the combination of *CYP4G16* and *CYP4G17* gives a high percentage of survivors (83%), similar to a double dose of *CYP4G16*. Interestingly, in cases of partial rescue (1x *CYP4G16* or 2x *CYP4G17*), as well as in the case of 1x *CYP4G17*, where no long time survivors are observed, a remarkable number of newly-emerged adults, mostly females, survive the eclosion burden but die almost immediately and are found lying dead on the food. This is in contrast to *Cyp4g1*-KD flies where only dead adults unable to fully exit the puparium were observed (Figures 3.5 and S3.2). Moreover, in partially rescued CYP4G backgrounds (1x *CYP4G16* and 2x *CYP4G17*) the vast majority of successfully eclosed survivors (almost 80%) are males.

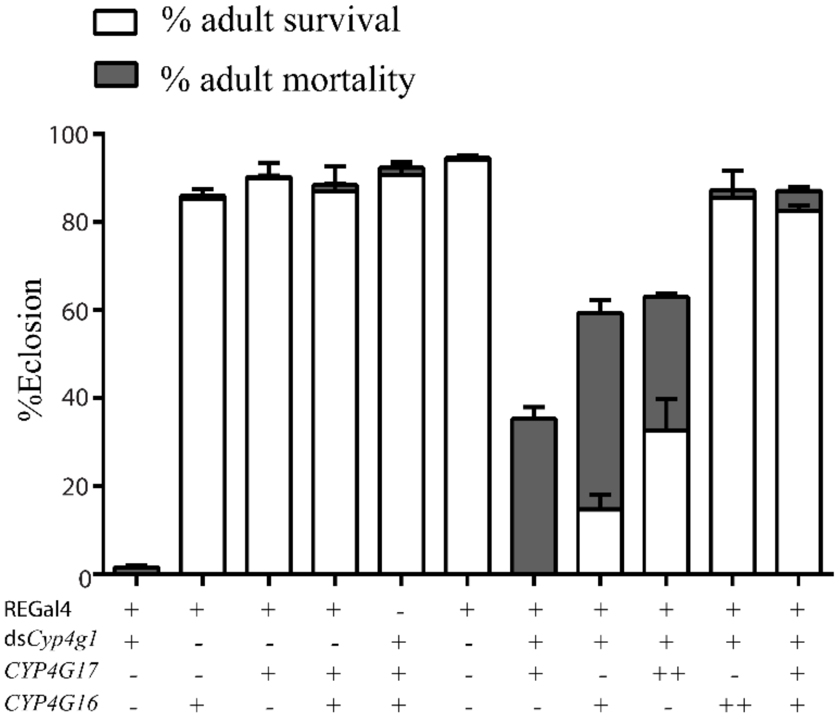

Figure 3.5. Percent eclosion of *D. melanogaster* flies in different CYP4G backgrounds. Quantification of adult flies that successfully eclosed corresponding to a known number of pupae. White bars represent successfully eclosed adults that survived (%), while flies that died as newly-emerged adults lying on the food were calculated to address mortality post successful eclosion (%) and are depicted with grey bars. Diffferent CYP4G background are described at the bottom of the graph with "+", representing the presence and "-" the absence of a P450 gene (*Cyp4g1*, *CYP4G17* and *CYP4G16*) or the oenocyte-specific GAL4 driver (REGal4). Mean of 3 biological experiments +SEM.

3.4.4. Three very long-chain dimethyl-branched CHCs are present in CYP4G16, CYP4G17 and CYP4G16/CYP4G17 flies, but not 'wild-type' CYP4G1 flies

After extraction of cuticular lipids and quantification, different total hydrocarbon amounts were identified per mg of dry weight in each condition tested (Figure 3.6), with the control flies (no knock-down of *Cyp4g1*) having the highest total CHC content and the flies bearing the *CYP4G17* transgene in the absence of *Cyp4g1* the lowest (p-value<0.001). CYP4G16/CYP4G17 and CYP4G16/CYP4G16 appeared to have approximately the same total CHC amount (non-significant difference) (Figure 3.6). Moreover, 18 CHCs species were identified in the control flies (no mosquito transgene) and 21 species (18 similar and 3 extra) in the *D. melanogaster* flies expressing mosquito transgenes. Interestingly, the three extra CHCs present in all *Drosophila* strains expressing mosquito CYP4Gs but not in the control (CYP4G1) flies, corresponded to the three longer CHCs (dimethyl-C45, dimethyl-C46 and dimethyl-C47) identified (Figure 3.7) often found in *Anopheles*. Additionally, the relative abundance of each CHC identified was calculated in % area and it was showed that CYP4G17 and CYP4G16/CYP4G17 produce significantly more of these three very-long chain methyl-branched compounds (Figure 3.7) than CYP4G16. Other statistically significant differences indicate that C31 is more enriched in the presence of CYP4G17 rather than CYP4G16 (p-value<0.001) and that C25 (p-value<0.0001), C27 (p-value<0.0001), methyl-C29 (p-value<0.0001) and C31:1 (p-value<0.001) are more abundant in CYP4G16 mosquitoes.

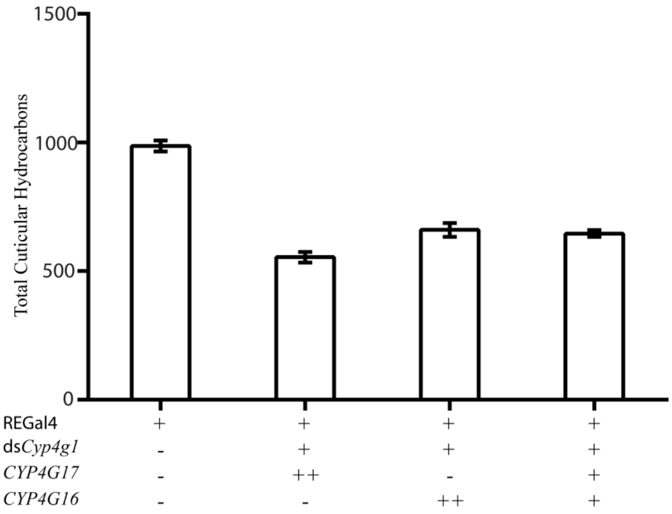

Figure 3.6. Total Cuticular Hydrocarbon content among different CYP4G background flies analyzed. Average total CHC content of the three replicates analyzed for each different CYP4G background (~50 male flies per replicate) corresponding to total nanograms of CHC per microgram of *D. melanogaster* dry weight. Different CYP4G backgrounds are described as in Figure 3.5 and correspond to G x 1, C x 3, B x 2 and B x 3 fly crosses of Table S3.2. Mean of 3 biological experiments ± SEM.

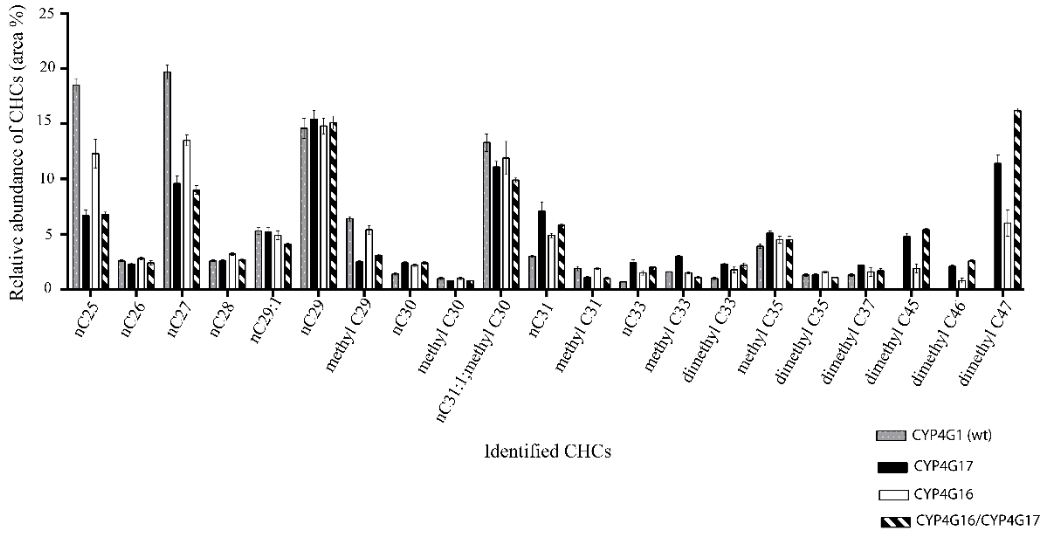

Figure 3.7. Relative abundance of Cuticular Hydrocarbons (CHCs) identified in different CYP4G backgrounds. Relative CHCs abundances in % area are depicted or each one of the 21 out of 32 CHCs identified in total. Differentially colored bars correspond to the different CYP4G background present in each Drosophila strain analyzed (grey: G x 1, black: C x 3, white: B x 2 and black/white: B x 3 fly crosses as described in S3.2). Mean of 3 biological experiments ± SEM.

3.4.5 CYP4G17/CYP4G16 flies compensate better desiccation stress and permethrin toxicity than CYP4G16 flies.

*Cyp4g1*KD *D. melanogaste*r which simultaneously express CYP4G16/16 or CYP4G16/17 in their oenocytes have identical genetic backgrounds and non-significant differences in cuticular hydrocarbons quantities and are therefore comparable in functional assays (Figure 3.6). The observed differences can be attributed to the *An. coluzzii* CYP4Gs that are present in each case. The flies were subjected to desiccation assay and the survival was recorded in time-points until all flies die (Figure 3.8A). At the same time a starvation control was used to ensure that mortality upon desiccation is estimated and not starvation (Figure 3.8B). CYP4G17/16 flies were able to survive longer in all time points comparing to CYP4G16/16 counterparts (Figure 3.8A, 3.8C). Additionally, flies of the same genetic background were analyzed in terms of penetration resistance with a permethrin contact bioassay where permethrin was used in different concentrations and survival was recorded. Again, CYP4G17/16 flies could compensate better than CYP4G16/16 flies (Figure 3.9).

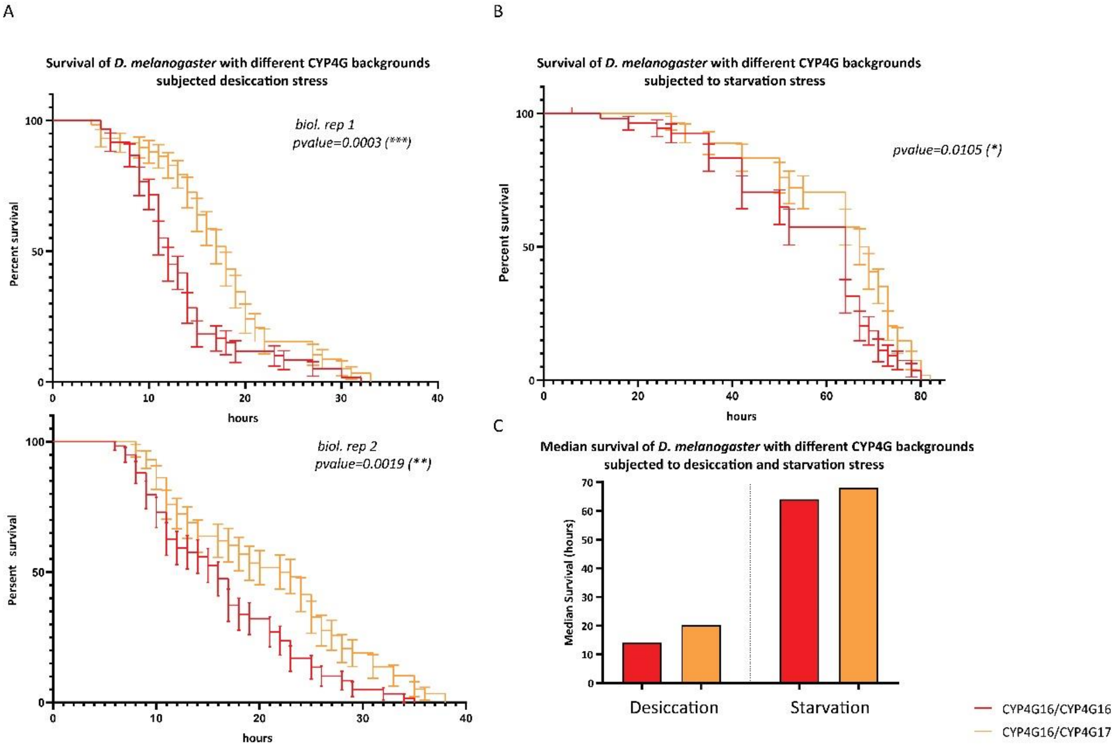

Figure 3.8. % Survival of male *D. melanogaster* with different CYP4G backgrounds subjected to desiccation stress. A. Time course of adult males fly survival in dry conditions. Two biological replicates are depicted, statistically analyzed separately, N=120 for each conditions including 3 technical replicates of 20 flies per condion (x 2 biological experiments), B. Time course of adult males fly survival in starvation conditions, N=40 for each condition including, including one technical replicate of 20 flies per condition (x 2 biologicial experiments), C. Median survival of flies in desiccation and starvation conditions. Red curve: CYP4G1 oenocyte-specific knock-down flies, which simultaneously express CYP4G16 (2X) in oenocytes, Orange curve: CYP4G1 oenocyte-specific knock-down flies, which simultaneously express CYP4G16 and CYP4G17 in oenocytes. Two biological experiments were statistically analyzed separately (A) N=60 for each condition including 3 technical replicates of 20 flies per condition. Mean of 3 biological replicate +SEM.

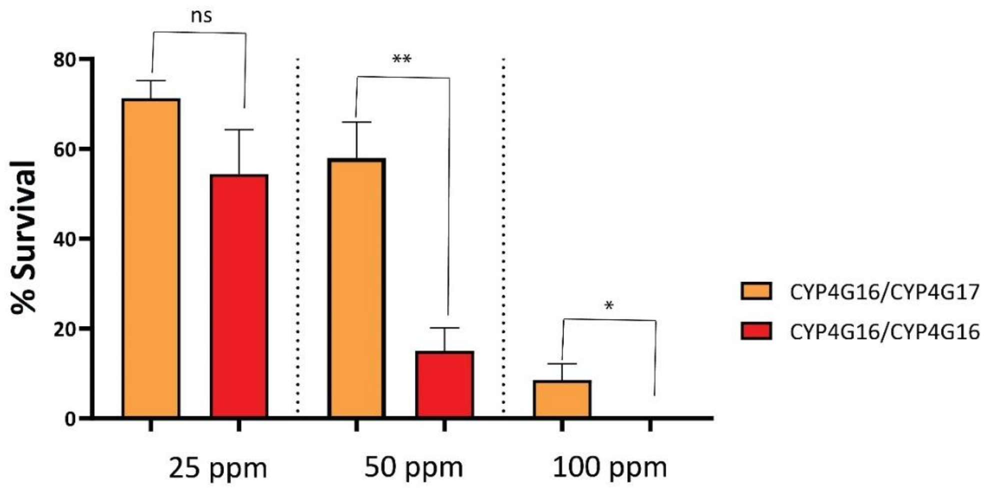

Figure 3.9. % Survival of male *D. melanogaster* with different CYP4G backgrounds subjected to permethrin stress. Red curve: CYP4G1 oenocyte-specific knock-down flies, which simultaneously express CYP4G16 (2X) in oenocytes. Orange curve: CYP4G1 oenocyte-specific knock-down flies, which simultaneously express CYP4G16 and CYP4G17 in oenocytes. Mean of 5 biological replicate +SEM. N=100 for each condition including 2 technical replicates of 10 flies per condition (x5 replicates).

3.4.6 CYP4G17 and CYP4G16 were successfully expressed *in vitro* together with CPR in Sf9 insect cells using *Baculovirus* expression system.

Successful *in vitro* expression of CYP4G16 and CYP4G17 along with CPR was achieved in insect cells. The co-expression of CPR with the CY4PGs was validated using anti-His antibody in Western blot analysis (Figure 3.10A), as both CYP4Gs and CPR and His-tagged at their C-termini. CPR activity assay (Figure 3.10B), indicates that the CPR is successfully expressed and able of reducing cytochrome C substrate provided. Furthermore, membrane isolations from co-infected cells were subjected in CO-spectrum differential analysis. When P450 heme iron (Fe^{+3}) is reduced (Fe^{+2}) and complexed with carbon monoxide (CO), P450 give a characteristic absorbance peak near 450 nm [29]. This is a common feature of all corrected folded P450 enzymes [29], hence we used this biochemical analysis to demonstrated correctly-folded proteins (Figure 3.10C).

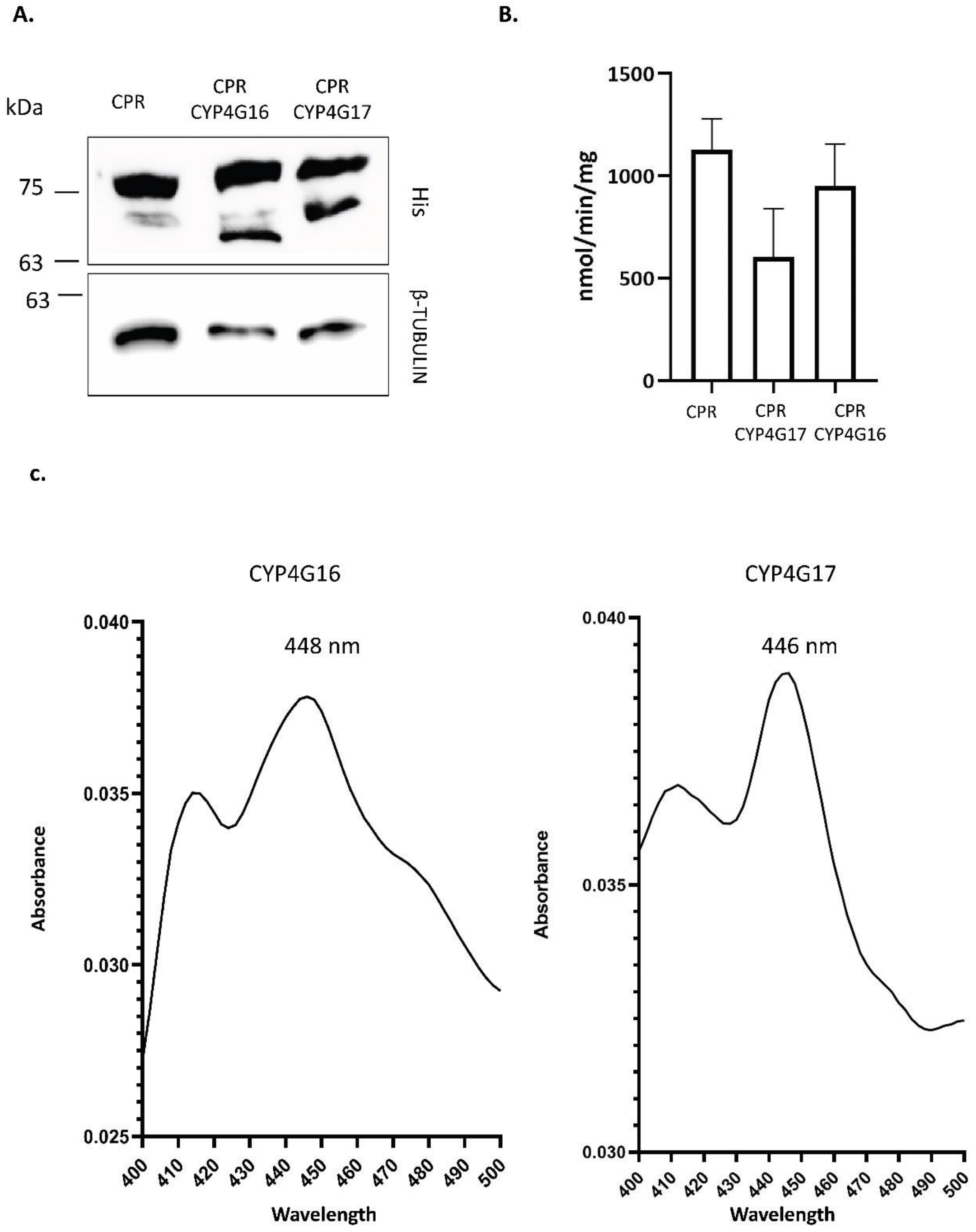

Figure 3.10. Successful functional expression of CYP4G/CPR in Sf9 insect cells. A. Western blot analysis for CPR-CYP4G expression in membranes preparations of CPR-CYP4G16 and CPR-CYP4G17 using anti-His B-tubulin was used as loading control, B. Activity of CPR was checked with its ability to reduce cytochrome C in the bacterial membranes. Means of three biological replicates + SEM, C. Representative CO spectra of from CYP4G16-CPR, CYP4G17-CPR and CPR-control membranes, indicating correct folding of each via CO-differential spectrum analysis.

3.5. Discussion

The CYP4G are highly conserved P450 enzymes in insects and the discovery that they serve as oxidative decarbonylases in the last step of hydrocarbon biosynthesis [7] was the first explanation provided for this high degree of conservation. However, much remains to be learned about these enzymes. In *Drosophila*, CYP4G1 is a major protein of oenocytes, whereas its paralog CYP4G15 is found in the brain [30] where its function is unknown. In the major malaria vector *An. coluzzii* the situation is different, because both the CYP4G1 and CYP4G15 paralogues, named CYP4G17 and CYP4G16 are highly expressed in oenocytes [15] . This study further showed that while a CPR-CYP4G16 fusion, was able to catalyze the oxidative decarbonylation of a C18 aldehyde, this activity was not detectable for CYP4G17 [31]. The two enzymes also differed in their subcellular localization in adult *An. coluzzii* oenocytes [15]. The results presented here address both differences between CYP4G16 and CYP4G17.

In contrast to what is expected for microsomal P450s, CYP4G16 was previously shown to be present on the internal side of the PM in adult oenocytes [15] and here we show that it has the same subcellular localization and topology in oenocytes from an earlier developmental stage and origin (Figures 3.1.B, 3.3A, 3.3B). In larval oenocytes, CYP4G17 also appears anchored to the PM (Figure 3.1A. and 3.3C). The N-terminus of each protein is predicted to be facing extracellularly with a transmembrane helix connecting to the catalytic part of the enzyme, shown to be on the cytoplasmic side (Figure 3.2). In pupae, CYP4G17 is found to be dispersed throughout the cytoplasm in developing adult-type oenocytes (Figures 3.3D) as we have observed previously in fully developed adults [15]. This difference in CYP4G17 localization is also accompanied by a difference in molecular weight, as indicated by western blot analysis of different developmental stages (Figure 3.4). One plausible scenario is that the two bands identified in Figure 3.4 represent developmentally specific isoforms; under this scenario adult CYP4G17 (*ad*CYP4G17) may be modified by a yet unidentified pre- or post-translational mechanism, sufficient for the protein to be rendered to the ER as a typical ER-resident P450, while larval CYP4G17 (*lar*CYP4G17) escapes the ER-rendering mechanism and is transported to the PM. Under this hypothesis *lar* or *ad*CYP4G17 may be also functionally distinct.

This hypothesis is in line with the observation that the two different types of oenocytes co-exist in the mosquito pupa. It is known that in *D. melanogaster*, larval and adult generations of oenocytes are morphologically distinct ectodermal derivatives with separate developmental origins [12]. In *An. coluzzii* two distinct types of oenocytes have previously been found in larvae and adults stained for Cytochrome p450 reductase [14]. Oenocyte functions seem to be close-related with molting, as a new generation of such cells is developed at each molt in some holometabolous species and the size and number of these cells can vary dramatically during *Drosophil*a larval development [12]. Under our immunostaining approach in pupal abdomens, CYP4G17 and CYP4G16 oenocyte-specific intense staining revealed the morphological difference of oenocytes forms at this stage. Two distinct cell types that had similar morphologies to those described previously in larvae [14] and adults[14, 15] were found in pupae probably owing to the existence of two different origins of oenocytes in the pupal developmental stage. Big cells in size, carrying numerous bundles of lipid droplets are considered to be oenocytes of larval origin persisting in the pupal stage as they are very similar to those obtained in larvae longitudinal sections (Figure 3.3A and 3.3C). Apart from these intense specific staining was obtained in smaller in size cells also found in clusters that are considered to be newly-developing oenocytes of adult-specificity (Figure 3.3B and 3.3D).

Our previous biochemical analysis could not detect decarbonylase activity of CYP4G17 on short chain aldehydes, and so we have examined the comparative functions of the CYP4Gs by a genetic, *in vivo* approach. In this study, we performed the conditional expression of *An. coluzzii* CYP4Gs in oenocytes of *Cyp4g1* knock-down *D. melanogaster* flies, in order to investigate if this expression could rescue the knock-down phenotype. Our results revealed that two copies of *CY4G16* or a *CYP4G16/CYP4G17* combination can almost completely restore the viability of *Cyp4g1*-KD flies, while one copy of CYP4G16 and two copies of *CYP4G17* only lead to a partial rescue, indicating that both mosquito CYP4Gs can functionally substitute the fly decarbonylase, albeit to a different extent. Interestingly 1x *CYP4G17* showed almost zero levels of adult survival although a remarkable number of dead, early-emerged adults were found lying on the food in contrast to control *Cyp4g1*-KD flies (Figure 3.5 and S3.2), which could not fully exit the puparium implying that even one copy of CYP4G17 can produce a phenotypic difference. The results show that gene copy number (i.e. dose) affects survival ability. This is consistent with the very high expression level of native oenocyte CYP4Gs [32], the sluggish enzyme activity observed *in vitro* until now [7, 33, 34] and the potentially lower level of activation provided by the RE driver. Interestingly, in cases of partial rescue (2x *CYP4G17* and 1x *CYP4G16*), males preferentially survive. Several studies on *Drosophila* species from temperate and tropical regions have shown a higher desiccation resistance of females than males [35]. Perhaps, if females require more CHC for desiccation resistance, a deficit is more difficult to compensate. Alternatively, this may be the result of subtle differences in expression levels or spatiotemporal profile of the RE-Gal4 driver [23] between males and females that may affect CYP4G1 knock-down efficiency or specificity.

Since both *Anopheles* CYP4Gs can function as decarbonylases, we investigated the cuticular hydrocarbon profile of ‘rescued’ flies where CYP4G1 native expression in oenocytes has been knocked down and functionally substituted with one or both of the mosquito genes. In *Drosophila* oenocytes, CYP4G1 is the only oxidative decarbonylase, so the blend of CHC produced reflects the catalytic activity of a single enzyme on a large number of substrates that differ in length, saturation, and methyl branching. Its substrate specificity must therefore be quite broad. In the rescued flies, the total amount of hydrocarbons produced was somewhat lower than wild type. However, the pattern of hydrocarbons produced in flies rescued with alternative *Anopheles* CYP4Gs was different, indicating that the CYP4G enzymes may have a different substrate specificity to each other, and to the CYP4G1 (Figure 3.7). In particular, three extra CHCs (dimethyl alkanes of very high MW) were detected in all cases where mosquito CYP4Gs (but not *Drosophila* CYP4G1) were present (Figure 3.7). These higher MW compounds are typically found on the *An. gambiae* cuticle [15]. The substrates for CYP4G enzymes are produced by a complex pathway of enzymes (ACCase, elongases, desaturases, acyl-CoA reductases), encoded by a large number of genes[36]. It is the flux through those enzymes that determines the substrate pool for the CYP4G enzymes. Transport in the hemolymph (on lipophorins) and then through the epidermis and differential loss from the epicuticle then determines the blend of CHC that is measured. It is intriguing how these processes contribute to the apparition of higher MW CHCs not detected in wild type *Drosophila*. It is entirely plausible that the dimethyl-C45, -46 and -47 substrates are produced in wild type *Drosophila* oenocytes at a level below detection in our assay (32) but are more efficiently converted by CYP4G16 and especially CYP4G17 than CYP4G1. By drawing on the pool of high MW substrates, CYP4G17 (and CYP4G16) would favor their synthesis by relieving product inhibition of the Elovl elongases. On the other hand, greater retention of the high MW CHC has been noted before[7] so that both processes may contribute to the presence of dimethyl-C45, -46 and -47 alkanes in transgenic flies. Our study therefore suggests that it is not only the activities of upstream enzymes in oenocytes that determines the blend of insect CHC [7], but that substrate specificity of the last enzymes, the CYP4Gs, also contributes to it.

The probable roles of CHC of various chain lengths, methyl-branching patterns, and degrees of saturation have been deduced from their relative abundance in arthropods from various habitats [37]. In general, desiccation stress leads to an adaptive shift towards increased levels of longer chain CHCs, a higher proportion of saturated CHCs, and/or greater proportions of straight- versus branched-chain CHCs [38]. Methyl-branched CHCs, have been shown to act as dual traits affecting both desiccation and mating [39]. Initially, we subjected the flies to desiccation stress, by reducing humidity to 10-20% until 100% mortality was achieved. Indeed, in our desiccation analysis flies with more abundant (di)methyl-branched long alkanes compensate better desiccation (Figure 3.8). Moreover, mean survival of CYP4G16/17 flies is enhanced in contact permethrin toxicity bioassay (Figure 3.9). In a recent study penetration rate of deltamethrin (another insecticide belonging to pyrethroid class) was reduced in multi-resistant mosquito population with increased CHCs when compared to a susceptible one [31] . In our case, where total CHC contents are comparable (Figure 3.6) this difference could be allocated to their qualitative differences alluding to the very-long chain dimethyl-branched which significantly differ among the two comparisons. Although the flies compared have similar genetic backgrounds and differ only in the presence/absence of one CYP4G17 allele, we cannot exclude that toxicity to permethrin differs due to other pathways/mechanisms modulated in presence of a different CYP4G allele.

To elucidate the substrate specificities observed among the different CYP4Gs, we also expressed recombinant CYP4Gs together with their obligatory electron donor CPR in Sf9 cells. Previous works have expressed CYP4Gs as fusions with CPR in insect cells. To our knowledge this is the first time that functional CYP4G expression is achieved where CYP4G and CPR are provided separately, albeit in 1:1 protein ratio, dictated by immuno-staining with anti-His which enables direct comparison of protein levels in microsomal preparations. The CO-spectrum analysis and the CPR activities reveal that we have successfully isolated membranes expressing correctly-folded P450s in the presence of CPR (Figure 3.10), which will be valuable tools for future substrate screenings.

Furthermore, the differential subcellular localization of CYP4G17 during development and its apparent ability to act as a more efficient decarbonylase of very long-chain dimethyl-branched compounds in *Drosophila* reveal an intriguing functional diversification of the *An. coluzzii* CYP4Gs. Further studies are needed to elucidate the molecular mechanisms of differential localization of CYP4G17 in larval and adult oenocytes, and to precisely delineate the substrate specificity of each CYP4G enzyme.

3.6. Literature

1. Cocchiararo-Bastias, L.M., et al., *epicuticle lipids mediate mate recognition in Triatoma infestans.* J Chem Ecol, 2011. **37**(3): p. 246-52.
2. Howard, R.W. and G.J. Blomquist, *Ecological, behavioral, and biochemical aspects of insect hydrocarbons.* Annu Rev Entomol, 2005. **50**: p. 371-93.
3. Gibbs, A.G., *Thermodynamics of cuticular transpiration.* Journal of Insect Physiology, 2011. **57**(8): p. 1066-1069.
4. Arcaz, A.C., et al., *Desiccation tolerance in Anopheles coluzzii: the effects of spiracle size and cuticular hydrocarbons.* J Exp Biol, 2016. **219**(Pt 11): p. 1675-88.
5. Chung, H. and S.B. Carroll, *Wax, sex and the origin of species: Dual roles of insect cuticular hydrocarbons in adaptation and mating.* Bioessays, 2015. **37**(7): p. 822-30.
6. Fan, Y., et al., *Hydrocarbon synthesis by enzymatically dissociated oenocytes of the abdominal integument of the German Cockroach, Blattella germanica.* Naturwissenschaften, 2003. **90**(3): p. 121-6.
7. Qiu, Y., et al., *An insect-specific P450 oxidative decarbonylase for cuticular hydrocarbon biosynthesis.* Proc Natl Acad Sci U S A, 2012. **109**(37): p. 14858-63.
8. Feyereisen, R., *Evolution of insect P450.* Biochem Soc Trans, 2006. **34**(Pt 6): p. 1252-5.
9. Wigglesworth, V.B., *The source of lipids and polyphenols for the insect cuticle: The role of fat body, oenocytes and oenocytoids.* Tissue Cell, 1988. **20**(6): p. 919-32.
10. Parvy, J.P., et al., *Drosophila melanogaster Acetyl-CoA-carboxylase sustains a fatty acid-dependent remote signal to waterproof the respiratory system.* PLoS Genet, 2012. **8**(8): p. 30.
11. Gutierrez, E., et al., *Specialized hepatocyte-like cells regulate Drosophila lipid metabolism.* Nature, 2007. **445**(7125): p. 275-80.
12. Makki, R., E. Cinnamon, and A.P. Gould, *The development and functions of oenocytes.* Annu Rev Entomol, 2014. **59**: p. 405-25.
13. Billeter, J.C., et al., *Specialized cells tag sexual and species identity in Drosophila melanogaster.* Nature, 2009. **461**(7266): p. 987-91.
14. Lycett, G.J., et al., *Anopheles gambiae P450 reductase is highly expressed in oenocytes and in vivo knockdown increases permethrin susceptibility.* Insect Mol Biol, 2006. **15**(3): p. 321-7.
15. Balabanidou, V., et al., *Cytochrome P450 associated with insecticide resistance catalyzes cuticular hydrocarbon production in Anopheles gambiae.* Proc Natl Acad Sci U S A, 2016. **113**(33): p. 9268-73.
16. MacLean, M., et al., *Mountain pine beetle (Dendroctonus ponderosae) CYP4Gs convert long and short chain alcohols and aldehydes to hydrocarbons.* Insect Biochem Mol Biol, 2018. **102**: p. 11-20.
17. Chung, H., et al., *A single gene affects both ecological divergence and mate choice in Drosophila.* Science, 2014. **343**(6175): p. 1148-51.
18. Caputo, B., et al., *Identification and composition of cuticular hydrocarbons of the major Afrotropical malaria vector Anopheles gambiae s.s. (Diptera: Culicidae): analysis of sexual dimorphism and age-related changes.* J Mass Spectrom, 2005. **40**(12): p. 1595-604.
19. Balabanidou, V., L. Grigoraki, and J. Vontas, *Insect cuticle: a critical determinant of insecticide resistance.* Curr Opin Insect Sci, 2018. **27**: p. 68-74.
20. Edi, C.V.A., et al., *Multiple-Insecticide Resistance in Anopheles gambiae Mosquitoes, Southern Cote d'Ivoire.* Emerg Infect Dis, 2012. **18**(9): p. 1508-1511.
21. Ingham, V.A., et al., *Dissecting the organ specificity of insecticide resistance candidate genes in Anopheles gambiae: known and novel candidate genes.* BMC Genomics, 2014. **15**(1): p. 1018.

22. Kall, L., A. Krogh, and E.L. Sonnhammer, *Advantages of combined transmembrane topology and signal peptide prediction--the Phobius web server.* Nucleic Acids Res, 2007. **35**(Web Server issue): p. 5.
23. Bousquet, F., et al., *Expression of a desaturase gene, desat1, in neural and nonneural tissues separately affects perception and emission of sex pheromones in Drosophila.* Proc Natl Acad Sci U S A, 2012. **109**(1): p. 249-54.
24. Groth, A.C., et al., *Construction of transgenic Drosophila by using the site-specific integrase from phage phiC31.* Genetics, 2004. **166**(4): p. 1775-82.
25. Tsakireli, D., et al., *Functional characterization of CYP6A51, a cytochrome P450 associated with pyrethroid resistance in the Mediterranean fruit fly Ceratitis capitata.* Pestic Biochem Physiol, 2019. **157**: p. 196-203.
26. Barolo, S., L.A. Carver, and J.W. Posakony, *GFP and beta-galactosidase transformation vectors for promoter/enhancer analysis in Drosophila.* Biotechniques, 2000. **29**(4).
27. Piwko, P., et al., *The Role of Insulators in Transgene Transvection in Drosophila.* Genetics, 2019. **212**(2): p. 489-508.
28. Girotti, J.R., S.J. Mijailovsky, and M.P. Juarez, *Epicuticular hydrocarbons of the sugarcane borer Diatraea saccharalis (Lepidoptera: Crambidae).* Physiological Entomology, 2012. **37**(3): p. 266-277.
29. Feyereisen, R., *8 - Insect CYP Genes and P450 Enzymes*, in *Insect Molecular Biology and Biochemistry*, L.I. Gilbert, Editor. 2012, Academic Press: San Diego. p. 236-316.
30. Maibeche-Coisne, M., et al., *A new cytochrome P450 from Drosophila melanogaster, CYP4G15, expressed in the nervous system.* Biochem Biophys Res Commun, 2000. **273**(3): p. 1132-7.
31. Balabanidou, V., et al., *Cytochrome P450 associated with insecticide resistance catalyzes cuticular hydrocarbon production in &lt;em&gt;Anopheles gambiae&lt;/em&gt;.* Proceedings of the National Academy of Sciences, 2016. **113**(33): p. 9268.
32. Chung, H., et al., *Characterization of Drosophila melanogaster cytochrome P450 genes.* Proc Natl Acad Sci U S A, 2009. **106**(14): p. 5731-6.
33. Debose-Boyd, R.A., *A helping hand for cytochrome p450 enzymes.* Cell Metab, 2007. **5**(2): p. 81-3.
34. Eser, B.E., et al., *Oxygen-independent alkane formation by non-heme iron-dependent cyanobacterial aldehyde decarbonylase: investigation of kinetics and requirement for an external electron donor.* Biochemistry, 2011. **50**(49): p. 10743-50.
35. Parkash, R. and P. Ranga, *Sex-specific divergence for adaptations to dehydration stress in Drosophila kikkawai.* J Exp Biol, 2013. **216**(Pt 17): p. 3301-13.
36. Wicker-Thomas, C., et al., *Flexible origin of hydrocarbon/pheromone precursors in Drosophila melanogaster.* J Lipid Res, 2015. **56**(11): p. 2094-101.
37. Young, H.P., et al., *Relationship Between Tissue-specific Hydrocarbon Profiles and Lipid Melting Temperatures in the Cockroach Blattella germanica.* Journal of Chemical Ecology, 2000. **26**(5): p. 1245-1263.
38. Otte, T., M. Hilker, and S. Geiselhardt, *Phenotypic Plasticity of Cuticular Hydrocarbon Profiles in Insects.* Journal of Chemical Ecology, 2018. **44**(3): p. 235-247.
39. Chung, H. and S.B. Carroll, *Wax, sex and the origin of species: Dual roles of insect cuticular hydrocarbons in adaptation and mating.* BioEssays, 2015. **37**(7): p. 822-830.

Chapter 4

Characterization of the brain specific CYP4G15 in *Drosophila melanogaster* and analysis of the CYP4G-specific insertion

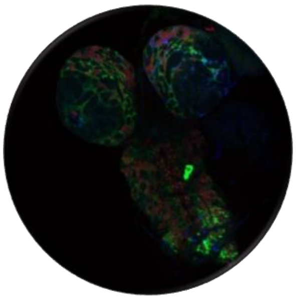

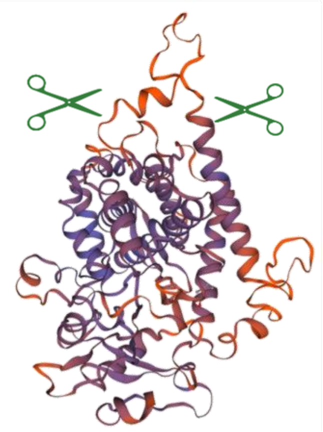

4.1 Abstract

CYP4Gs are enzymes of great interest as they serve multiple functions in insects. Some of these functions are well-studied, such as the decarbonylase activity of oenocyte CYP4Gs, catalyzing the last step in CHCs biosynthetic pathway. This role renders oenocyte CYP4Gs essential for life (desiccation resistance) and also, together with the up-steam enzymes in the CHC biosynthetic pathway, endows CYP4Gs with all other CHC-related functions (mating, reproductive isolation, species determination, pheromonal communication). However, they have received less attention in non-oenocyte tissues. One such unexplored case is the *D. melanogaster* CYP4G15, absent from oenocytes but present in head/brain as *in situ* hybridization experiments indicate, though no functional characterization of this enzyme has been elaborated so far.

Additionally, all CYP4Gs are characterized by the presence of a specific insertion, rich in acidic residues and most probably protruding from the globular part. The role of this insertion in CYP4G function has not been elucidated, however the presence of acidic residues and its exposed nature allude for interactions and/or stabilization of CYP4G structure.

Here, we ectopically expressed CYP4G15 in oenocytes, revealing its function as a decarbonylase there, showing it is able to produce a different CHC blend, rich in methyl- and dimethyl-branched species. Furthermore, according to immune-localization experiments in larval brains we concluded CYP4G15 is found in cortex glia. Concerning the CYP4G1-specific insertion, we used reverse genetics to create different deletions, a short (26aa) and a long (32 aa). The former resulted in no obvious defect (survival), while the latter resulted in mortality at eclosion, pinpointing perhaps a protein region functionally linked to CYP4G1 essentiality.

4.2. Introduction

CYP4G essentiality is tightly linked to the crucial for life exoskeleton, due to their participation in the last step of cuticular hydrocarbon biosynthesis in oenocytes [1-8]. As opposed to *Drosophila* oenocytes where one CYP4G (CYP4G1) has been found [1], two CYP4Gs have been localized to *Anopheles coluzzii* oenocytes (CYP4G16 and CYP4G17) [2], exhibiting differences on their contributions in cuticular hydrocarbon biosynthesis (Chapter 3, [3]). Two oenocyte CYP4Gs are capable of acting as oxidative decarbonylases in *Locusta migratoria* and also show different subcellular patterns and no full redundancy [9]. *Triatominae* are another example of hematophagous insects with two CYP4Gs implicated in CHC biosynthesis. According to a recent study *Rhodnius prolixus* CYP4G106 and CYP4G107 are present in oenocytes with different preferences towards straight-chain(CYP4G106) or methyl-branched substrates (CYP4G107) [4]. CYP4G76 and CYP4G105 of the economically important pest *Nilaparvata lugens*, have also been linked to CHC biosynthesis through RNAi-mediated silencing followed by desiccation and insecticide penetration assays [10].

Apart from the well-characterized function of CYP4Gs in the biosynthesis of CHCs in the oenocytes, expression in integument-independent tissues has also been reported. CYP4G15 of *Drosophila melanogaster* is detected in the larval central nervous system [11, 12], pea aphid CYP4G51 apart from abdomen is also detected in head and thorax, honey bee CYP4G11 is found in the forager antennae and legs with potential involvement in chemoreception [13], CYP4G20 in the antennae of *Mamestra brassicae* [14], while CYP4G24 of *Bombyx mori* and *D. melanogaster* CYP4G1 show high prothoracic gland expression with implication in steroid hormone regulation [15].

CYP4G15 was firstly identified and characterized as a Cytochrome P450 of the 4G family in 2000 [11]. *In situ* hybridization and qPCR experiments performed in this study revealed that CYP4G15 is expressed mainly in the larval central nervous system and in adult brains and thoracic ganglion[11] . Presence of CYP4G15 in both embryonic and larval nervous system was also confirmed by Chung et al , who also revealed that RNAi-mediated loss of function of CYP4G15 is viable [12]. Furthermore, CYP4G15 was identified in a *D. melanogaster* blood brain barrier (BBB) transcriptome dataset, specifically in surface glia [16]. Although there is a wealth of studies in different insects in respect to oenocyte CYP4G enzymes and their essential role in cuticular hydrocarbon production and hence desiccation resistance, the role of CYP4Gs in other tissues such as the central nervous system remains elusive.

Brain P450s have been implicated in neurosteroid biosynthesis as well as in neurotransmission [17]. In mammals several exogenous (clinical drugs and neurotoxins) and endogenous (fatty acids, steroids, neurotransmitters) have been identified as acting substrates of brain P450s[17]. Regarding drug metabolism, they are presumed to have impact on brain drug effect, playing roles in local drug metabolism. Brain heterogeneity though and local characteristics, such as heme availability add extra layers of complexity to brain P450 investigation[17]. The *Drosophila* nervous system is histologically complex, sharing similarities to the mammalian brain systems, in terms of neuronal electrophysiological properties and morphologically similar glia cells associating to the neurons [18]. Histologically *Drosophila* CNS can be subdivided into the neuronal cells which includes the cell bodies and the neuropil, the region where axons and dendrite projections reside [18]. According to their association with the basic CNS regions (surface, cortex and neuropile), glia are classified into groups [19]. The glia of the outermost layer on the CNS surface are called perineurial glia (PG), while below this subperineurial glial cells (SPG) reside [18]. PG form a discontinuous layer with gaps and SPG form a flattened monolayer, while both are sheet-like and result in a contiguous surface by septate junction formation, generating the blood brain barrier (BBB) which covers the nervous system [20, 21]. Specialized glia, associated with neurons reside deeper into the CNS and are classified into cortex, ensheathing and astrocyte glial subtypes [18]. The former are also called cell-body associated glia and form a scaffold, encapsulating neuronal somata, while the two latter are neuropile glia, either sheathing around or infiltrating the neuropile [19]. It is noteworthy, that the brain has high lipid demands and specifically cortex glia which insulate neuronal somata, have been associated to lipid processes [22]. Lipids of different classes exhibit critical roles in the CNS, throughout the development, acting as structural components, serving as bioactive molecules and used as energy substrates [23].

Another interesting unexplored question about CYP4Gs, concerns the amino-acid sequence which differentiates CYP4Gs, from their close-related CYP4C family and all other cytochrome P450s [24]. This is a specific insertion between G and H helices, comprised of ~44 residues in *D. melanogaster* CYP4G1, is characterized by increased representation of acidic amino acids (glutamate and aspartic acid residues) [1, 24], which are present in about double their usual abundance in this CYP4G-insertion [24]. Furthermore, CYP4G16 structural model based on the rabbit CYP4B1 available crystal structure, localize this loop on the cytoplasmic side, protruding from the rest of the protein globular part [24]. The exact structure of it cannot be elucidated, however it does not seem to interact with cytochrome P450 reductase (CPR) site, which is close to the I and B helices [1]. Whether the presence of this specific insertion provides characteristics to CYP4Gs, such as the essentiality of oenocyte-CYP4Gs and/ or other functions via mediating interactions with other proteins or lipids has not been elucidated.

In this chapter, we study one non-oenocyte CYP4G and for that we selected *D. melanogaster* CYP4G15, which is absent from oenocytes and is reported to be present in D. melanogaster heads/centra nervous system. We ectopically expressed CYP4G15 in oenocytes, using a UAS/oenocyte-Gal4 system to elucidate whether it has a decarbonylase activity, which characterizes the CHC-biosynthetic CYP4Gs. We also created tools including a specific antibody and *in vitro* expression system to reveal its specific cellular localization in heads and also perform substrate screening to provide novel insights into its function. Furthermore, in order to shed light into CYP4Gs, we used reverse genetics in *D. melanogaster* to remove the CYP4G-specific loop. The essentiality of the insertion was indicated with a long deletion we generated, however a shorter deletion of the insertion restored the survival, thus revealing an important region for CYP4G1 oenocyte function.

4.3 Materials and methods

4.3.1 Plasmid design and preparation for *Cyp4g1* deletions for UAS/GAL4 system

For the generation of the short deletion (CYP4G1Δ), used in UAS/Gal4 system an endogenous ClaI site close to the targeted sequence was exploited. GoTaq® DNA Polymerase (Promega) was used for the amplification of two fragments, 875 bp and 1027 bp respectively. The 875 bp fragment contains the anterior *CYP4G1* ORF, with the primers bearing such overhangs to introduce a BssHII restriction site at 5′ and a ClaI site at 3′. A primer pair for the 1027 bp fragment was designed such that the forward primer contains the endogenous ClaI and the reverse a ClaI followed by an XhoI restriction site. The template for the amplification of *CYP4G1Δ* was cDNA of adult *Drosophila* RNAs. PCR conditions were 95°C for 2 min, followed by 39 cycles of 95°C for 30 s, 58.5°C for 30 s, 72°C for 2 min and a final extension step of 72°C for 10 min. After PCR amplification the two fragments were sub-cloned into pGem-T easy vector (Promega). ClaI digestion in both plasmids resulted in fragments that were then cloned using the generated ClaI sites resulting to a pGem-T easy vector bearing the whole *Cyp4g1* sequence, but devoid of 26 aa (short deletion), which does not affect the ORF, as indicated by sequencing analysis. We note that for ClaI digestion Dam-/Dcm- competent *E. coli* cells were used, as ClaI digestion is blocked by methylation. Using BssHII-XhoI sites this fragment was cloned into pPelikan recipient plasmid (Paragraph 3.3.6). All PCR products described above were purified by using the PCR clean-up gel-extraction kit (Macherey Nagel), according to the manufacturer's protocol.

For the generation of the long 32aa-deletion (CYP4G1Δ′) pPelikan plasmid we exploited two restriction sites close to the region of interest (PciI and XbaI). A forward primer containing the endogenous PciI together with a reverse primer containing the endogenous XbaI site were used for PCR amplification from the plasmid containing the CYP4G1Δ′ (donor plasmid), resulting in a 202 bp fragment. This fragment replaced the PciI-XbaI digested 298 bp fragment from the Ppelikan:CYP4G1Δ - containing plasmid without disturbing the frame, as validated by sequencing analysis.

4.3.2 Generation of UAS responder lines

For the generation of the transgenic lines, exactly the same lines, vectors and series of crosses were used as in (Chapter 3, [3]). Briefly, oenocyte-specific RE-Gal4 driver and UAS-Cyp4g1-KD responder transgenes were used (located on 2nd chromosome), the *D. melanogaster* strain VK13 (y[1] M{vas-int.Dm}bZH-2A w[*]; PBac{y[+]-attP-9A}VK00013, #24864 in Bloomington Drosophila Stock Center), containing an attP landing site on 3rd chromosome and the integrase ORF on X chromosome to enable ϕC31 integrase-mediated insertion and the modified vector dPelican.attB.UAS_CYP6A51, previously generated by pPelican [25]. GoTaq® DNA Polymerase (Promega) was used for the amplification of a 1740 bp fragment containing the CYP4G15 ORF using primer pair BssHII 4g15 F/XhoI 4g15 R (Table S4.1) that introduce a 5′ BssHII site and a 3′ XhoI site. The template for the amplification of CYP4G15 was cDNA of adult *Drosophila* RNAs. PCR conditions were 95°C for 2 min, followed by 39 cycles of 95°C for 30 s, 62°C for 30 s, 72°C for 2 min and a final extension step of 72°C for 10 min. The *CYP4G15* PCR product was purified using the PCR clean-up gel-extraction kit (Mancherey Nagel), according to the manufacturer's protocol and subsequently cloned into pGEM-T easy vector. Positive clones that were validated after sequencing analysis were digested with the BssHII/XhoI and cloned into the unique MluI/XhoI sites of *dPelican.attB.UAS_CYP6A51.* The pPelican.attB.UAS-CYP4G15 recombinant plasmids generated were injected into preblastoderm embryos. The G_1

offspring was screened for red eyes, since the w^+ phenotype is proof of the recombinant plasmid integration (mini-white). Crosses for the establishment of the homozygous transgenic responder lines are described in Figure S4.1.

4.3.3 Quantification of eclosion (adult survival and adult mortality)

The appropriate fly crosses for eclosion estimation were Ax1, Ax3, Bx1, Bx2, Bx3 and Cx2 (Table S4.2) and were set up by crossing 5 virgin females with 5 males of the appropriate genotypes. Five days later approximately 100 2nd instar larvae per genotype were transferred into fly food. Pupae and adult survivors were calculated per condition to address % eclosion to evaluate pupation efficiency. After approximately 5 days, 20 to 25, 3rd instar larvae were transferred into fly-food (approximately 100 larvae per biological replicate). Pupae were then measured to evaluate the pupation efficiency and successfully eclosed adults were counted. Newly emerged adults that were deceased right after eclosion were measured separately so as to address the adult mortality. The whole experiment was performed in three biological replicates and statistics were analyzed using GraphPad Prism software version 8.

4.3.4 CRISPR-Cas9 genome editing strategy and generation of fly lines.

The CRISPR-Cas9 strategy was incorporated with the purpose of generating a deleted form (long deletion, CYP4G1Δ') of the insertion of *Drosophila Cyp4g1*. Optimal Target Finder software (http://targetfinder.flycrispr.neuro.brown.edu) [26] identified two targets located upstream and downstream of the insertion, with no predicted off-target effects. Based on those targets, single-stranded DNA oligos were designed (Table S4.1). Each ssDNA pair was heated at 100°C for 5 min and left to cool slowly until the mix reached RT in order for them to anneal and create a double-stranded DNA oligo. The dsDNA oligos have 5' and 3' single stranded overhangs, facilitating the ligation into digested with BbsI and dephosphorylated gRNA vector pU6-BbsIchiRNA; an RNA expressing plasmid [26]. After the ligation, the standard protocol of transformation into DH5a competent cells and plasmid purification took place. Five different colonies from each plasmid were checked accordingly by sequencing analysis. For the generation of a deleted form of the insertion of *Cyp4g1*, a donor plasmid was designed and ordered by Genscript (pUC57). It comprised of two ~1000 bp homology arms (to facilitate HDR) at both sides of the deleted region (96 bp) and had various synonymous mutations in the gRNAs and PAM sequences so as to avoid possible DSBs in the donor plasmid and/or the HDR-modified flies by the endogenous CRISPR mechanism (Figure S4.4) . The endogenous CRISPR mechanism is present due to the expression of the endonuclease Cas9 under the control of the promoting element *nanos* of the lab strain y1 M{nos-Cas9.P}ZH-2A w* (Bloomington Drosophila stock center), referred hereafter as nos.Cas9 [27].

All the plasmids described in the previous section (2x pU6-BbsI chiRNA and the donor plasmid) were injected (final concentration of 100 ng/ul for pCU57 and 400 ng/ul for the two pU6-BbsIchiRNA) to approximately 500 *Drosophila* eggs of the nos.Cas9 strain. The surviving instar larvae 24 hours after the injection procedure were collected and transferred into standard fly-food. The emerged adults however, each one considered as a different line, are not modified, because *nanos* is an embryonic marker, which is expressed in the posterior pole of the egg during oogenesis, and thus HDR occurs only in the pole cells of the egg [28]. The progeny (G_1) of these flies backcrossed with nos.Cas9 flies was pooled in batches of 30 pupae and genomic DNA was extracted using DNazol reagent (ThermoFisher Scientific), according to manufacturers' instructions, in order to perform PCR screening. PCR was performed with Kapa Taq polymerase (Kapa Biosystems) for the amplification of the possible modified *Cyp4g1* sequence, using a set of primer pairs resulting in a fragment of 843 bp for the wild-type and 742 bp for the CYP4G1Δ' form (Table S4.1) . The templates for the amplification of *Cyp4g1* were pupae pools, single flies and cDNA of adult *Drosophila* RNAs. PCR conditions were 94°C for 2 min, followed by 34 cycles of 94°C for 45 s, 57°C for 30 s, 72°C for 1 or 2 min and a final extension step of 72°C for 10 min. All molecular screening experiments of the modified flies were conducted along with two positive controls, pGEM:CYP4G1Δ' plasmid already available containing the short-deleted form (paragraph 4.3.1) for monitoring the size difference between the deleted and the wild type *Cyp4g1* and positive G_1 gDNA from pupae pools, negative control from nos.Cas9 gDNA and blank (no template). G_1 flies originated from positive G_0 lines were again backcrossed with nos.Cas9 flies and then screened for the identification of positive heterozygotes. According to mendelian inheritance, the 50% of the G_2 generation is expected to be positive for the modification. G_2 females originated from positive G1 lines, thus potential heterozygotes, were crossed with male flies from strain w^{+oc}/FM7yBHw that contain an X chromosome balancer and can maintain the mutation at a heterozygous state. Similarly, the 50% of the G_3 generation is expected to be modified. Subsequently, these G_2 females were screened and the progeny females (G_3) from positive G_2 flies were crossed again with balancer male flies. Now, non-Bar G_4 males (selection against the balancer) are hemizygous, meaning that they have solely the modified allele to survive. If the CRISPR event is not lethal, G_4 individuals are crossed among themselves so as to produce homozygous flies (selection against the balancer) and establish the transgenic responder lines.

4.3.5 Reverse transcriptase (RT) PCR for validation of UAS/oenocyte-Gal4 expression of *Cyp4g1Δ* and *Cyp4g15* ectopical expression

After dissection of abdominal walls (containing oenocytes) of flies from crosses B x 2 , Dx1 , E x 5, B x 3 (Table S4.2) corresponding to the presence or absence of *UAS.Cyp4g1KD*, *ReGal4* and *UAS.Cyp4g15*, they were subjected to RNA extraction and cDNA synthesis as described. For *Cyp4g1* deletion validation abdominal walls of the progeny of *ReGal4*;*Cyp4g1Δ* with the *Cyp4g1* null mutant strain (Δ4) (Figure S4.2) [29] was subjected to dissection, RNA extraction and cDNA synthesis. Reverse transcriptase (RT) PCR was performed with GoTaq® Flexi DNA Polymerase (Promega) following manufacturers' instructions. The conditions were 95°C for 2 min, followed by 25 cycles of 95°C for 30 s, 57°C (*Cyp4g1*) or 58°C (*Cyp4g15*) for 30 s, 72°C for 50 sec and a final extension step of 72°C for 5 min. Amplification resulted in a 497 bp *Cyp4g15* product and for *Cyp4g1Δ* in 742bp, as opposed to 843bp resulted size of the wild type allele, enabling their discrimination. For both cases the *rpl11 D. melanogaster gene* was used for normalization control. All molecular screening experiments of the modified flies were conducted along with two negative controls, no-RT and no-template.

4.3.6 Extraction of cuticular lipids, cuticular hydrocarbons (CHCs) fractionation, identification and quantitation

Crosses A x 4 and B x 3 (Table S4.2) were set up and the progeny was separated by sex at emergence. 1-3-day old male flies were dried at room temperature for at least 48h. 150 flies in total (3 replicates / 50 flies) were separated, their dry weight was measured and the CHC analysis was carried out in VITAS-Analytical Services (Oslo, Norway) as described in detail in (Chapter 3, [3]). Statistics were analyzed using GraphPad Prism software, version 8 and difference in total CHC content and relative abundance values were analyzed with Student's t-test.

4.3.7 Antibodies

Rabbit polyclonal antibodies targeting CYP4G15 and CYP4G1 peptides were synthesized and affinity purified by Davids Biotechnologie. The sequences of the peptides are: AGLSYGQSAGLKDDLDVEDNDIGEKKR for CYP4G15 and SDIELILSGHQHLTKAEEYR for CYP4G1. The epitopes recognize residues (321-347) and (111-130) of CYP4G15 and CYP4G1 respectively. Mouse anti-His (penta-His) antibody was purchased from QIAGEN.

4.3.8 Western Blot Analysis

Cells, or dissected tissues were homogenized into a Homogenization RIPA Buffer (50Mm Tris pH=8, 150mM NaCl, 1% SDS, 1% NP-40, 1mM EDTA, 1mM EGTA and 1mM PMSF), centrifuged for 10min at 10.000g, at 4C and boiled for 5 min after addition of 5x Sample Buffer. Polypeptides resolved by SDS-PAGE (10% acrylamide), were electro-transferred on nitrocellulose membrane (GE Healthcare Whatman) and probed with the corresponding antibody (anti-His or anti-CYP4G15) at a dilution of 1:1000 in 1% skimmed milk in TBS-Tween. Antibody binding was detected using goat anti-rabbit or anti-mouse IgG coupled to horseradish peroxidase (Cell Signaling) (dilution: 1:5000 in 1% skimmed milk in TBS-Tween). Visualization was performed using a horseradish peroxidase sensitive ECL western blotting detection kit (SuperSignal West Pico PLUS Chemiluminescent Substrate, ThermoScientific) and the result was recorded using Chemidoc Imaging System (Bio-Rad Laboratories)

4.3.9 CYP4G15/CPR-overexpressing Sf9 insect cells and membrane preparations.

CYP4G15 along with CPR were expressed in *Spodoptera frugiperda* Sf9 insect cells using the Pfastbac1 vector, which was synthesized *de novo* (GenScript) and Cyp4g15 ORF was subcloned in between NdeI and EcoRI restriction enzyme sites as described in detail in paragraph 3.3.13.

4.3.10 CYP4G15 and CYP4G1 immunofluorescence and microscopy on dissected CNS.

3rd instar *D. melanogaster* larval CNS were dissected and fixed in cold solution of 4% PFA (methanol free, Thermo scientific) in phosphate-buffered saline (PBS) for 45 minutes, followed by three 15-minute-PBS washes. The dissected CNS were then incubated into blocking solution (1% BSA, 0.1% Triton X-100 in PBS) for 2 hours with concomitant overnight incubation with the primary antibodies (1:500 rabbit anti-CYP4G15 , 1:500 rabbit CYP4G1, 1:50 mouse anti-REPO and 1:300 rat anti-ELAV). Then the tissues were PBS-washed and stained with the respective secondary antibodies (Alexa-Fluor 488, Alexa-Fluor 647, Cy3). After that 3 15-minute washes in 0.1% Triton X-100 /PBS buffer were carried out. For nuclei staining 30 minute DAPI incubation was performed. The tissues were placed on slides with cover slips and vectashield antifade mounting media (Vector Laboratories) and images were obtained on a Leica SP8 laser-scanning microscope, using the 40-objective.

4.4. Results

4.4.1 Oenocyte-specific expression of CYP4G15 in *Cyp4g1 knock-down Drosophila* can restore viability, suggesting CYP4G15 acts as decarbonylase.

After a series of crosses in *D. melanogaster* we generated flies that overexpress *Cyp4g15* in oenocytes while simultaneously silencing *Cyp4g1* gene in this tissue (Figure S4.1). *Cyp4g1* knock-down flies arrest at eclosion or die at emergence as previously shown with this oenocyte REGal4 driver [3]. Interestingly, this lethal phenotype could partially be rescued, since transgenic survivors were detected. Eclosion efficiency of flies with the highest dosage of transgenic alleles we could achieve in this system (two transgenic copies) was ~17% (Figure 4.1A), meaning that CYP4G15 can complement the function of CYP4G1 at a low degree, showing its ability to act as a functional decarbonylase in oenocytes, albeit not so effectively. Noteworthy, ~84% of the eclosed survivors are males. Concerning flies bearing only one transgenic allele (one transgenic copy) a significant amount of newly-emerged individuals endure the eclosion barrier but decease instantaneously and are spotted lying dead on the food (Figure 4.1A). This indicates that the transgene rescues the lethal phenotype in a dose-dependent manner. Representative flies arrested during eclosion and survivors are shown in Figure S4.1. Moreover, verification of *Cyp4g15* overexpression in oenocytes was performed with reverse-transcriptase (RT) PCR in dissected abdominal walls of flies with the different *Cyp4g* backgrounds (Figure 4.1B).

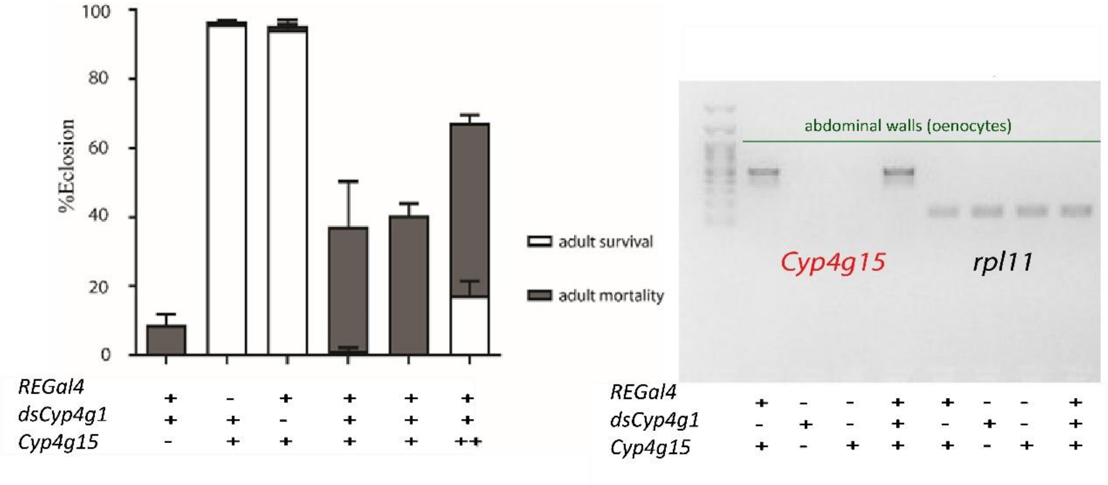

Figure 4.1. **Percent eclosion of *D. melanogaster* flies in different *Cyp4G* backgrounds.** A. Quantification of adult flies that successfully eclosed corresponding to a known number of pupae. White bars represent successfully eclosed adults that survived (%), while flies that died as newly-emerged adults lying on the food were calculated to address mortality post successful eclosion (%) and are depicted with grey bars. Mean of 3 biological experiments +SEM, B. Reverse transcriptase PCR in abdominal walls (oenocytes) of flies with different *Cyp4g* backgrounds. *Cyp4g15* and *Rpl11* (used as quantity control) genes are targeted 1.5% agarose gel with equal quantities of PCR products. Different CYP4G backgrounds are described at the bottom of the graph with "+" representing the presence and "–" the absence of a P450 gene (*Cyp4g1* and *Cyp4g15*) or the oenocyte-specific GAL4 driver (REGal4).

4.4.2 CYP4G15 can produce a blend of 27 cuticular hydrocarbons in *D. melanogaster* oenocytes favoring the production of methyl and dimethyl-branched species.

Extraction, quantification and identification of cuticular lipid species were performed in wild type flies (CHCs attributed to CYP4G1 function in oenocytes) and survivor CYP4G1KD flies that simultaneously express CYP4G15 in oenocytes (CHCs attributed to CYP4G15 function in oenocytes). In each condition CHCs were identified per mg of dry weight. Quantification revealed that CYP4G15 flies have almost half the CHCs of wild type flies (pvalue<0.0001) (Figure 4.2A), not surprisingly, based on the low survival of CYP4G15 expressing flies. Interestingly, identification of the CHCs species revealed that CYP4G15 can produce a greater blend of CHCs in oenocytes comparing to CYP4G1 wild-type background, as 9 extra CHCs were detected in the former (Figure 4.2B). More specifically, 27 CHCs are identified in CYP4G15 and 18 in wild type flies. Remarkably, the 9 extra CHCs present in CYP4G15-oenocyte-expressing flies and absent from the wild type control are very long, methyl- and dimethyl-branched species, with only one exception of a straight-chain CHC (nC24). Interestingly, CYP4G15 shows an impressive production of dimethyl C35, with each relative abundance reaching 18%, while CYP4G1 can produce less than 1.5% of that (Figure 4.2B). As shown in Figure 4.2C, where the sum of % CHC relative abundances is depicted in respect to methyl-branching, the CYP4G1 by far favors straight-chain CHC production (81.6%) and shows a very poor activity against dimethyl-branched substrates (3.6%), while CYP4G15 impressively favors dimethyl-branching (30.5%). This by nine times higher percentage of dimethyl-branched species in CYP4G15 flies is attributed to the five more dimethyl-branched CHCs produced by CYP4G15 (dimethyl C39, C41, C43, C45, C47) and to the very high abundance of dimethyl C35 in those flies. In terms of quantity methyl-branching does not show such dramatic differences in the two situations, but is higher in CYP4G15 flies (14.8% in CYP4G1 and 21.5% in CYP4G15 flies). CYP4G15 can produce 5 extra, very long, methyl-branched species (methyl C32, C39, methyl C41, methyl C43, methyl C45). On the contrary, methyl C31 is only present in CYP4G1 flies and methyl C29 is produced in significantly higher quantity in CYP4G1 flies. Straight-chain CHC relative abundances in CYP4G15 flies reach 48% and CYP4G15 can produce all straight chain CHCs CYP4G1 produces, plus one extra (nC24), however CYP4G1 catalysis against these short-straight chain substrates contribute to this dramatic differences observed both in the straight-chain CHC enrichment (Figure 4.2B, C) and in the total higher CHC content of the flies (Figure 4.2A).

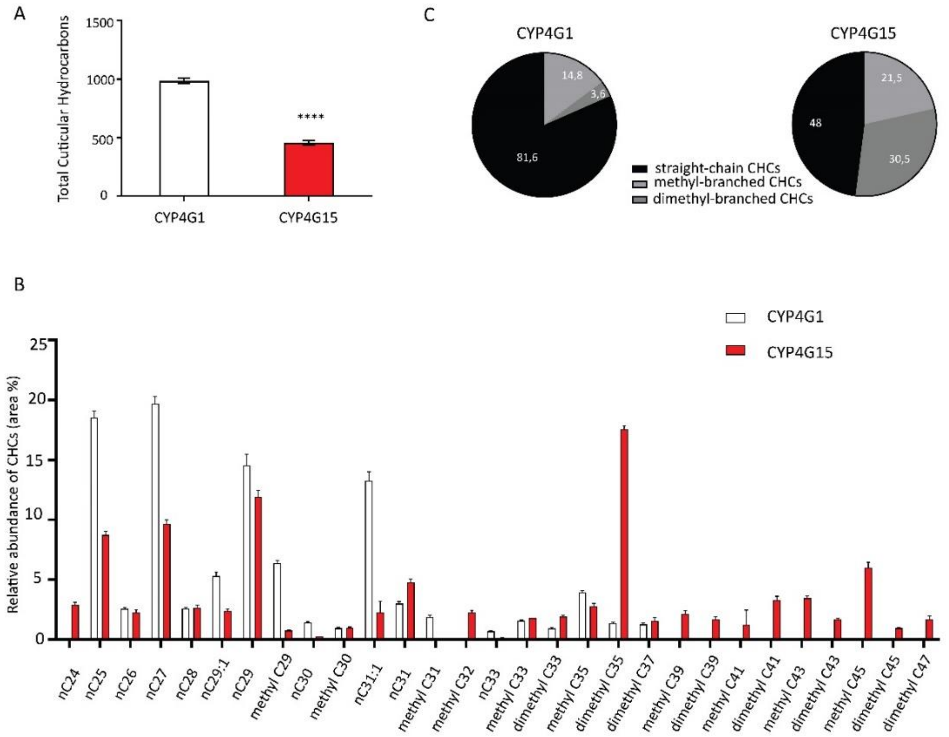

Figure 4.2. CHC analysis in different CYP4G backgrounds. A. Total CHC content between *Cyp4g1* (wt) and *Cyp4g15*-oenocyte overexpression flies. Total Cuticular Hydrocarbon content among different CYP4G background flies analyzed. Average total CHC content of the three replicates analyzed for each different CYP4G background (~50 male flies per replicate) corresponding to total nanograms of CHC per microgram of *D. melanogaster* dry weight, B. Relative CHCs abundances in % area are depicted for each one of the 29 identified in total. Differentially colored bars correspond to the different CYP4G background present in each *Drosophila* strain analyzed (white: A x 4 and red B x 3 fly crosses as described in S4.2). Mean of 3 biological experiments ± SEM, C. Pie charts representing the % relative abundance of three CHC groups (straight-chain , methyl-branched and dimethyl branched CHCs).

4.4.3. CYP4G15 is localized in the cortex glia of larval central nervous system while CYP4G1 is found in the CNS surface glia.

The specific antibodies designed against CYP4G15 and CYP4G1 where used in immunohistochemistry experiments on whole CNS tissues to reveal the cellular localization of these P450s. Whole larval CNS where dissected and subjected to fixation and staining protocol together with antibodies specific against REPO and ELAV. *D. melanogaster repo* (*reversed polarity*) is a marker gene for glial cells [30], while *elav* (*embryonic lethal, abnormal vision*) is a pan-neural marker gene [31]. After staining with anti-CYP4G15, we repeatedly observed a characteristic signal forming a close-meshed scaffold [32] on membranes surrounding the REPO-positive nuclei (glial) (Figure 4.3A, B, C, D) both in optical lobes (Figure 4.3E and F) and in ventral nerve cords (Figure 4.3G and H). CYP4G1 was also found to be localized on larval CNS but on different glia subtype than CYP4G15. CYP4G1 was found to be localized in the outermost CNS as indicated by its absence from inner regions found deeper into the CNS and its presence only in frontal confocal sections shaping the CNS periphery (Figure 4.4A and B). Further the signal co-localizes with repo-positive nuclei found on CNS surface (Figure 4.4C, D, E, F), most probably associated with the perineuarial and subperineurial glia which form the BBB.

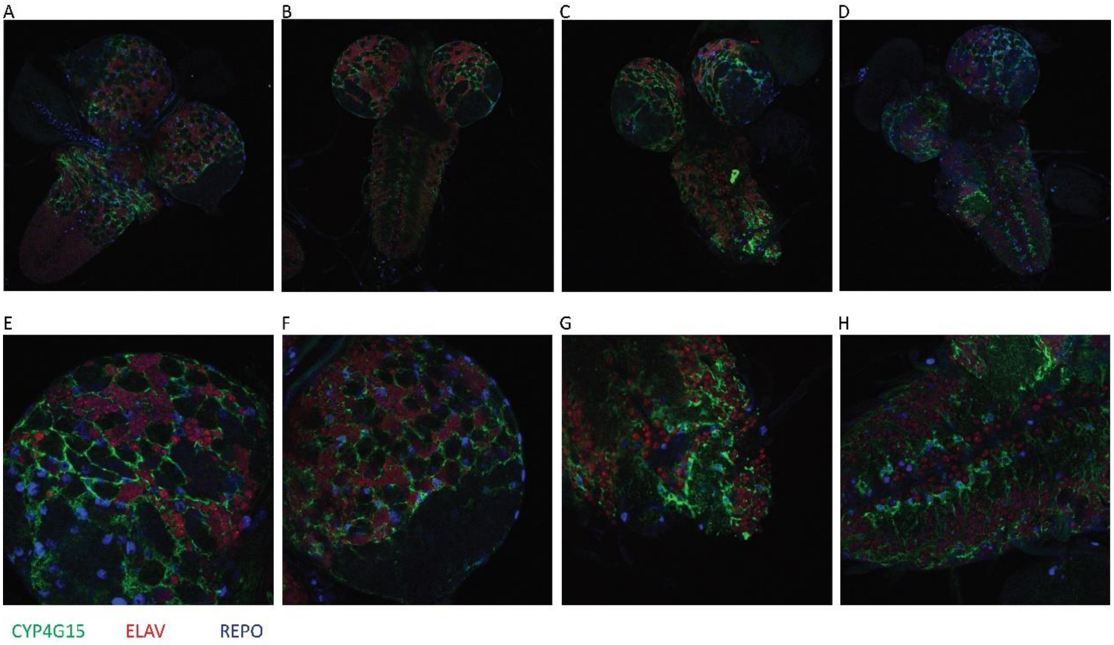

Figure 4.3. Immunohistochemistry on whole 3rd instar *D. melanogaster* larval central nervous systems with anti-CYP4G15. Representative confocal sections of a 3rd instar larval CNS (A, B, C, D), optic lobes (E, F) and ventral nerve cord (G, H), triple labeled with anti-Repo (blue), anti-Elav (red) and anti-CYP4G15 (green).

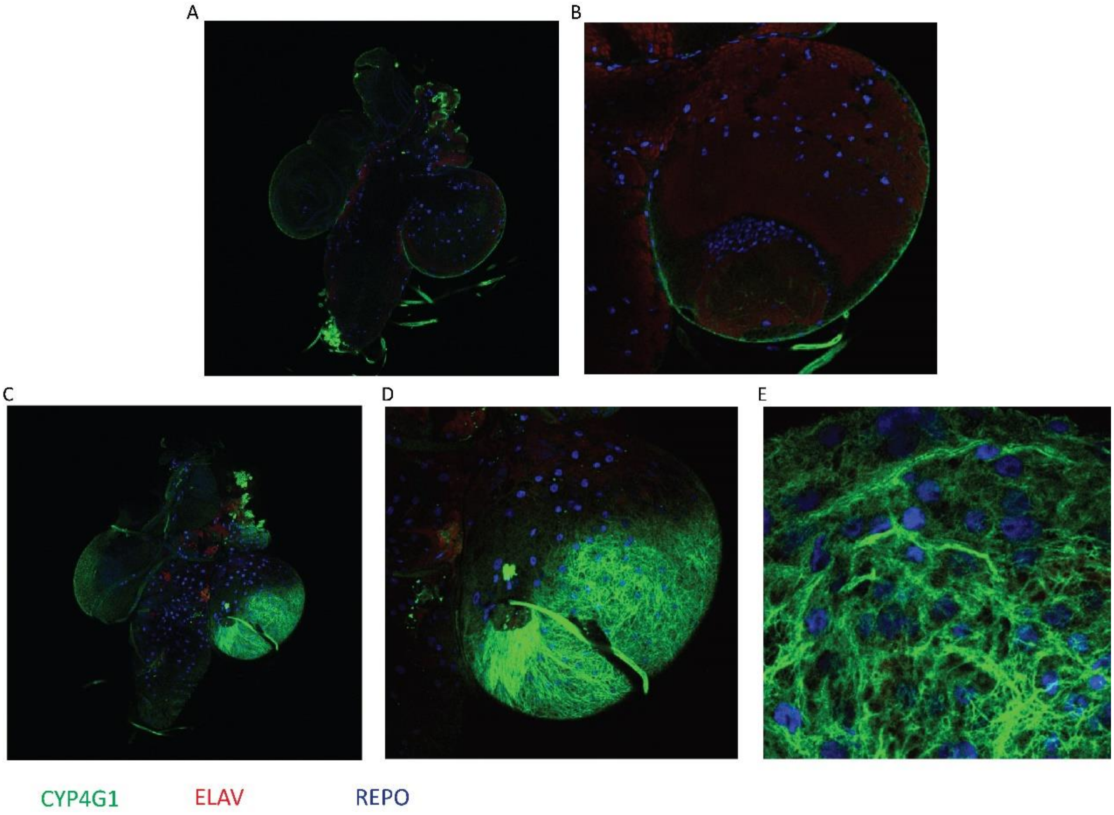

Figure 4.4. Immunohistochemistry on whole 3rd instar *D. melanogaster* larval central nervous systems with anti-CYP4G1. Representative confocal sections of 3rd instar larva CNS (A, C) and optic lobes (B, D,

E), triple-labeled with anti-Repo (blue), anti-Elav (red) and anti-CYP4G1 (green). Panels A and B show confocal sections of the inner CNS part, while panels C and D show frontal confocal sections of the outermost CNS part, E. Zoom into the optic lobe (outermost confocal section).

4.4.4 *In vitro* expression of CYP4G15 together with CPR in Sf9 insect cells using *Baculovirus* expression system.

Successful *in vitro* expression of CYP4G15 along with CPR was achieved in insect cells. CPR and CYP415 were detected in western blot analysis both in whole cell extracts and in membrane preparations (Figure 4.5A and B). Additionally, the P450 characteristic peak was obtained in a CO-spectrum analysis of membrane expression of both CYP4G15 and CPR, implying a correctly-folded protein (Figure 4.5C). Further, CPR activity assay indicates that the CPR is successfully expressed and able of reducing the cytochrome C substrate provided.

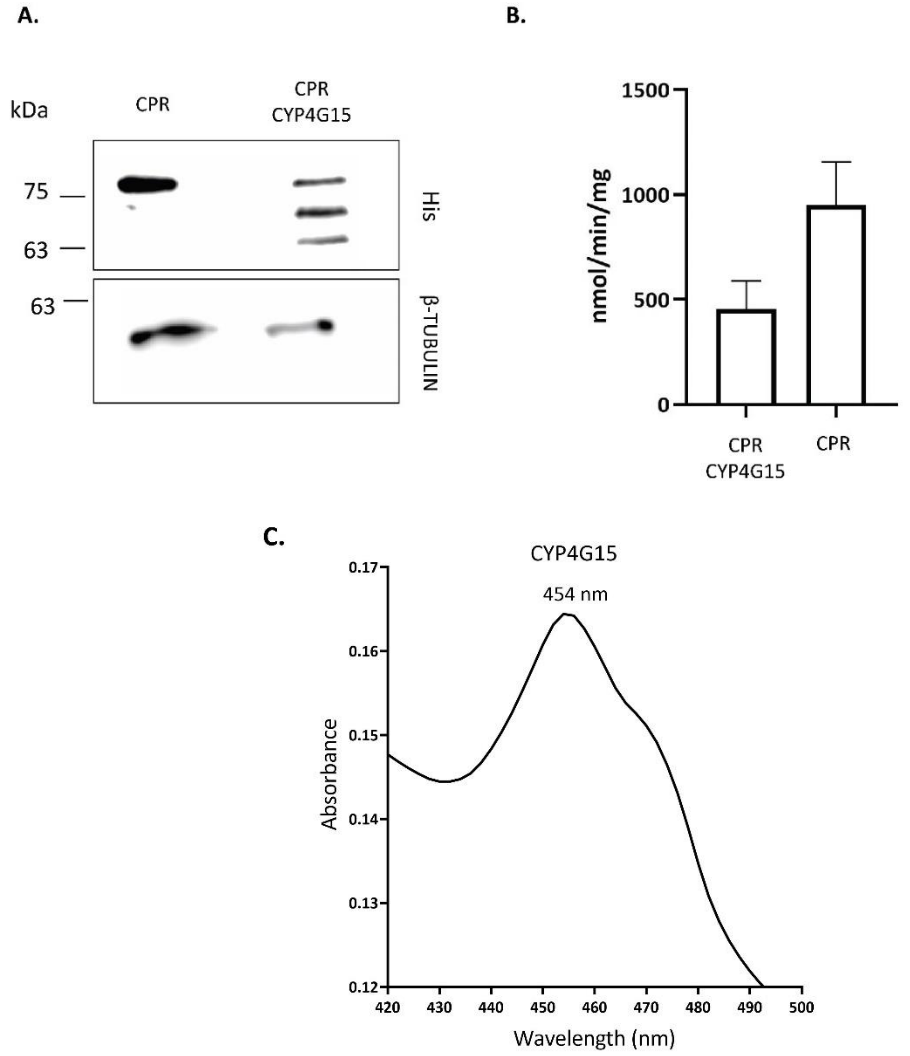

Figure 4.5. Successful functional expression of CYP4G15/CPR in Sf9 insect cells. A. Western blot analysis for CYP4G15 expression in Sf9 infected cells; Expression of CYP4G15 in Sf9 infected cells, A. Western blot analysis from membrane preparations of CYP4G15/CPR- and CPR-infected Sf9 cells, analyzed using anti-His and beta-tubulin as loading control, B. Activity of CPR was checked with its ability to reduce cytochrome C in the membranes. Means of three biological replicates + SEM, C. Representative CO spectra of from CYP4G15-CPR membranes, indicating correct folding of each via CO-differential spectrum analysis.

4.4.5 Generation of *Cyp4g1* deletions in *D. melanogaster*

In order to address the essentiality of CYP4G-specific loop, we created *Cyp4g1* deletions, using different systems, exploiting the *D. melanogaster* genetic toolbox. CRISPR-Cas9 was used to create flies bearing CYP4G1Δ′ (32aa-deletion), so as we can monitor the effect of the deleted insertion among all developmental stages. The second system is a UAS.CY4PG1Δ/oenocyte-Gal4 expression, generating the deletion only in oenocytes. After incorporation of Cyp4g1Δ (26aa-deletion) under UAS promoter in pPelikan expression vector, embryo injections and subsequent crosses (Figure S4.1) we ended up with flies expressing the deleted gene version under the UAS promoter together with the oenocyte-specific REGal4 driver. These flies were crossed with null mutants flies [29] and rescue was recorded. The alignments of the two deletions generated are depicted below (Figure 4.6).

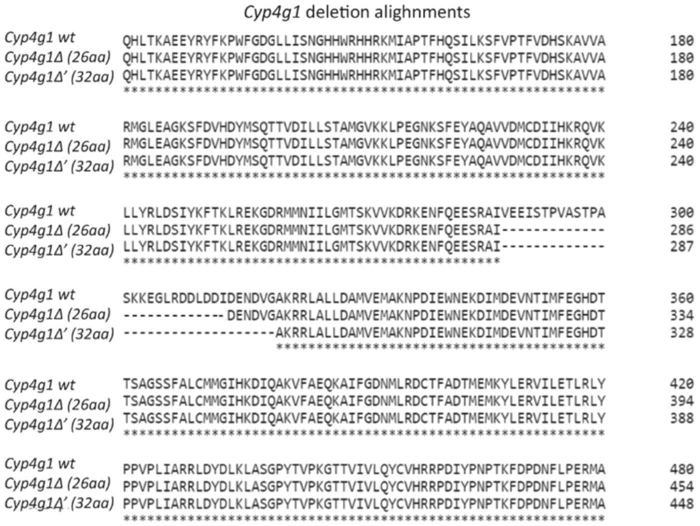

Cyp4g1 deletion alighnments

```
Cyp4g1 wt          QHLTKAEEYRYFKPWFGDGLLISNGHHWRHHRKMIAPTFHQSILKSFVPTFVDHSKAVVA    180
Cyp4g1Δ (26aa)     QHLTKAEEYRYFKPWFGDGLLISNGHHWRHHRKMIAPTFHQSILKSFVPTFVDHSKAVVA    180
Cyp4g1Δ' (32aa)    QHLTKAEEYRYFKPWFGDGLLISNGHHWRHHRKMIAPTFHQSILKSFVPTFVDHSKAVVA    180
                   ************************************************************

Cyp4g1 wt          RMGLEAGKSFDVHDYMSQTTVDILLSTAMGVKKLPEGNKSFEYAQAVVDMCDIIHKRQVK    240
Cyp4g1Δ (26aa)     RMGLEAGKSFDVHDYMSQTTVDILLSTAMGVKKLPEGNKSFEYAQAVVDMCDIIHKRQVK    240
Cyp4g1Δ' (32aa)    RMGLEAGKSFDVHDYMSQTTVDILLSTAMGVKKLPEGNKSFEYAQAVVDMCDIIHKRQVK    240
                   ************************************************************

Cyp4g1 wt          LLYRLDSIYKFTKLREKGDRMMNIILGMTSKVVKDRKENFQEESRAIVEEISTPVASTPA    300
Cyp4g1Δ (26aa)     LLYRLDSIYKFTKLREKGDRMMNIILGMTSKVVKDRKENFQEESRAI-------------    286
Cyp4g1Δ' (32aa)    LLYRLDSIYKFTKLREKGDRMMNIILGMTSKVVKDRKENFQEESRAI-------------    287
                   ***********************************************

Cyp4g1 wt          SKKEGLRDDLDDIDENDVGAKRRLALLDAMVEMAKNPDIEWNEKDIMDEVNTIMFEGHDT    360
Cyp4g1Δ (26aa)     -------------DENDVGAKRRLALLDAMVEMAKNPDIEWNEKDIMDEVNTIMFEGHDT    334
Cyp4g1Δ' (32aa)    -------------------AKRRLALLDAMVEMAKNPDIEWNEKDIMDEVNTIMFEGHDT    328
                                      *****************************************

Cyp4g1 wt          TSAGSSFALCMMGIHKDIQAKVFAEQKAIFGDNMLRDCTFADTMEMKYLERVILETLRLY    420
Cyp4g1Δ (26aa)     TSAGSSFALCMMGIHKDIQAKVFAEQKAIFGDNMLRDCTFADTMEMKYLERVILETLRLY    394
Cyp4g1Δ' (32aa)    TSAGSSFALCMMGIHKDIQAKVFAEQKAIFGDNMLRDCTFADTMEMKYLERVILETLRLY    388
                   ************************************************************

Cyp4g1 wt          PPVPLIARRLDYDLKLASGPYTVPKGTTVIVLQYCVHRRPDIYPNPTKFDPDNFLPERMA    480
Cyp4g1Δ (26aa)     PPVPLIARRLDYDLKLASGPYTVPKGTTVIVLQYCVHRRPDIYPNPTKFDPDNFLPERMA    454
Cyp4g1Δ' (32aa)    PPVPLIARRLDYDLKLASGPYTVPKGTTVIVLQYCVHRRPDIYPNPTKFDPDNFLPERMA    448
                   ************************************************************
```

Figure 4.6. Deletions the CYP4G1-specific insertion. Alignment of the expected protein sequences of *Cyp4g1* deletions. *Cyp4g1Δ* represents the short 26aa-deletion, while the *Cyp4g1Δ′* the longer 32aa-deletion.

4.4.5.1 Generation of *D. melanogaster* bearing the 32aa-deletion results in arrest upon eclosion.

4.4.5.1.1 Generation of 32aa-deletion using CRiSPR-Cas9 genome editing technique

The CRISPR-Cas9 system was used to generate flies containing a deletion of the specific CYP4G-insertion of *Cyp4g1* gene. *Cyp4g1* is located on the X chromosome and the crosses used are shown in Figure 4.7A. PCR was used as screening method, detecting the differences in MW generated by the 96bp deletion. Representative PCRs are depicted, starting from a genomic DNA of pooled larvae and subsequent single-fly crosses (Figure 4.7B). In G_3 generation after crossing with the appropriate balancer we end up with heterozygous females bearing the deletion. Eye-marker enabled us to discriminate between the different genotypes. However, in the next generation (G_4) no hemizigous males bearing the deletion (males with red, non-bar eyes) were obtained. The heterozygous females were present (red, heart-shaped eyes) (Figure 4.7C). As many pupae showed arrest upon eclosion, we dissected many of them and observed that the majority were males with red, normal-shaped eyes (Figure 4.7C), meaning that the CRISPR-Cas9-mediated deletion is lethal upon eclosion.

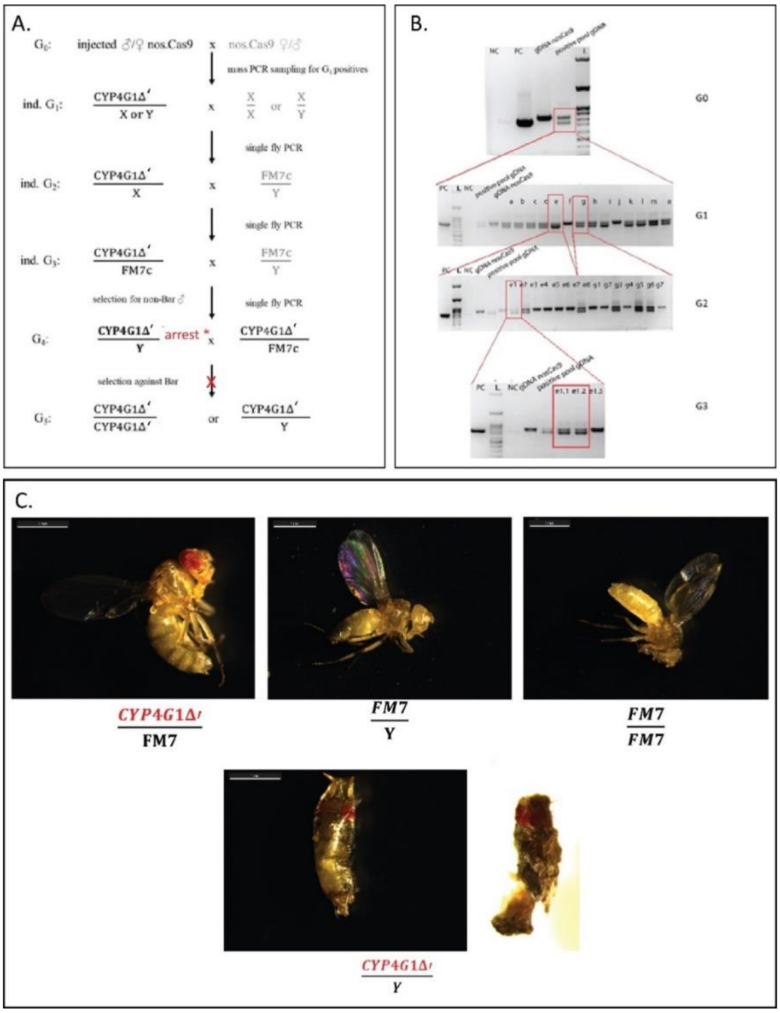
A.
G0:
injected ♂/♀ nos.Cas9
x
nos.Cas9 ♀/♂
mass PCR sampling for G1 positives
ind. G1:
CYP4G1Δ′ / X or Y
X/X or X/Y
single fly PCR
ind. G2:
CYP4G1Δ′ / X
FM7c / Y
single fly PCR
ind. G3:
CYP4G1Δ′ / FM7c
FM7c / Y
selection for non-Bar ♂
single fly PCR
G4:
CYP4G1Δ′ / Y
arrest *
CYP4G1Δ′ / FM7c
selection against Bar
G5:
CYP4G1Δ′ / CYP4G1Δ′
or
CYP4G1Δ′ / Y
B.
NC
PC
L
G0
G1
G2
G3
C.
CYP4G1Δ′ / FM7
FM7 / Y
FM7 / FM7
CYP4G1Δ′ / Y

Figure 4.7. Generation of 32aa-deletion using CRiSPR-Cas9 genome editing technique. nos.Cas9 embryos are injected and surviving adults (G_0) are back-crossed to nos.Cas9. The G_1 progeny is sampled (n≈ 30) and if positive, individual G_1 flies are crossed to nos.Cas9 and then screened with single fly PCR for homologous directed repair (HDR), i.e. CYP4G1Δ′. Individual G2 females are crossed to males of a strain bearing X chromosome balancer FM7c marked with Bar and then screened for CYP4G1Δ′. Individual G_3 females with heterozygous Bar phenotype are crossed to the balancer strain males and then screened for CYP4G1Δ′. G_4 females with Bar phenotype (bearing the desired deletion opposite to FM7c) would be crossed with male siblings selected against Bar (i.e. hemizygous for the genome modified chromosome bearing the HDR-derived allele) to create a homozygous line. However, arrest upon eclosion in G_3 males (red star) does not allow that (red x symbol in subsequent cross), hence the deletion is maintained against the FM7 balancer.

4.4.5.1.2 Complementation of *Cyp4g1 D. melanogaster* null mutants with *Cyp4g1Δ* 32aa-deletion in oenocytes using UAS/ReGal4 system

The 32aa-deletion was also tested in a rescue experiment of Cyp4g1 null mutants. Crossing Cyp4g1 null mutants with lines bearing the 32aa-deletion under the oenocyte-specific REGal4 driver enabled us to estimate a potential rescue of the lethal phenotype. These flies, due to a transposable element at position do not produce any CYP4G1 and die at eclosion [29]. In order to create flies bearing the deletion in oenocytes we used the ReGal4, which drives the expression of UAS transgenes specifically in the oenocytes. Our goal was to test the rescue of Cyp4g1 null mutants. Crossing of the ReGal4/UAS.Cyp4g1Δ with these flies resulted in a progeny including the FM7 males and females which have the wild-type *Cyp4g1* in their oenocytes and the heterozygous females which bear one allele of wild-type Cyp4g1 and one null mutant. The hemizygous males bearing the null-mutant allele and the ReGal4/UAS.Cyp4g1Δ' transgene were not able to eclose meaning that the 32aa-deleted CYP4G1 was not able to rescue the null-mutant males (Figure 4.8). This observation is in agreement with the previous result of these deletion generated by the CRISPR/Cas9 system.

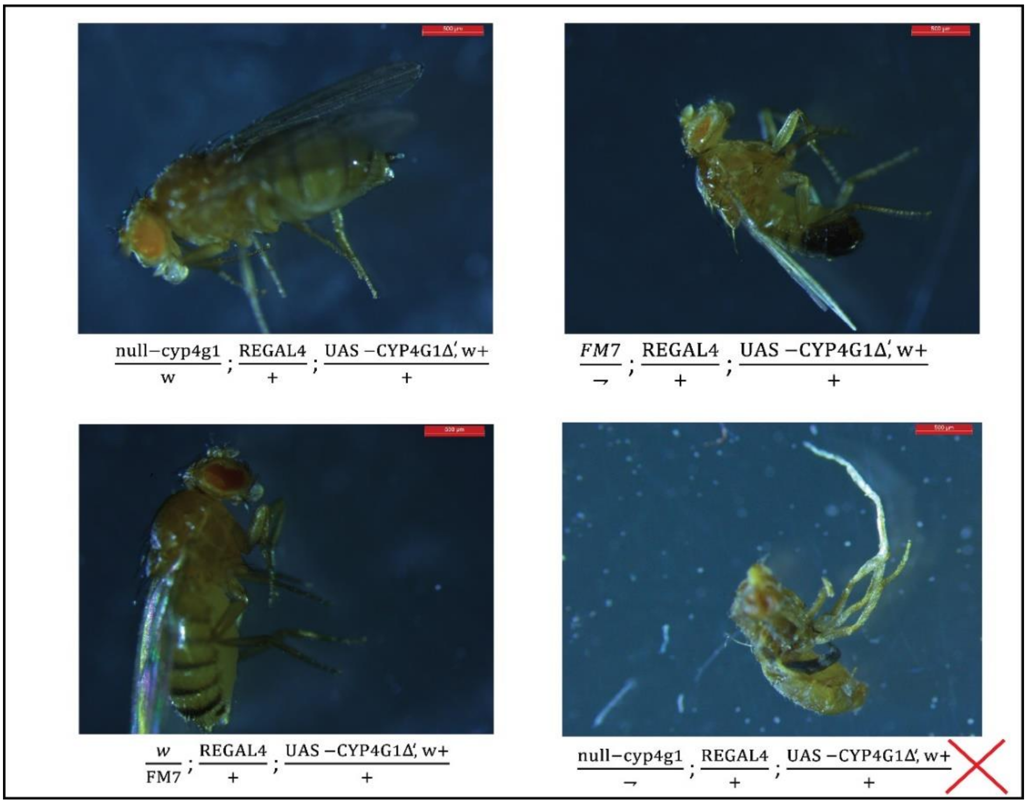
500 µm
null−cyp4g1/w ; REGAL4/+ ; UAS −CYP4G1Δ', w+/+
FM7/→ ; REGAL4/+ ; UAS −CYP4G1Δ', w+/+
w/FM7 ; REGAL4/+ ; UAS −CYP4G1Δ', w+/+
null−cyp4g1/→ ; REGAL4/+ ; UAS −CYP4G1Δ', w+/+

Figure 4.8. Survivors from rescue experiment with the CYP4G1Δ' (32aa deletion). A. Representative flies of the progeny resulted from cross (phenotype and genotype). They are discriminated owing to the Bar-eye. The red "X" indicates the hemizygous males that died at eclosion and were not rescued by the 32aa-deleted *Cyp4g1* allele.

4.4.5.2 Complementation of *Cyp4g1 D. melanogaster* null mutants with *Cyp4g1Δ* 26aa-deletion in oenocytes using UAS/ReGal4 system, rescues the lethality of null-mutant flies.

We next used the same system to incorporate a smaller deletion and test the rescue of the *Cyp4g1* null-mutant flies [29]. Crossing of the ReGal4/UAS.Cyp4g1Δ with these flies resulted in a progeny representing all expected genotypes in mendelian ratio. These include the FM7 males and females which have the wild-type *Cyp4g1* in their oenocytes, the heterozygous females which bear one allele of wild-type *Cyp4g1* and one null mutant and finally the hemizygous males, bearing only the null-mutant allele (Figure 4.9A). All flies bear the deletion at the 3rd chromosome, hence the male survivors cope only with the deleted allele incorporated in 3rd chromosome, in the absence of their wt *Cyp4g1*, located on X. This was also validated with reverse transcriptase PCR (Figure 4.9B).

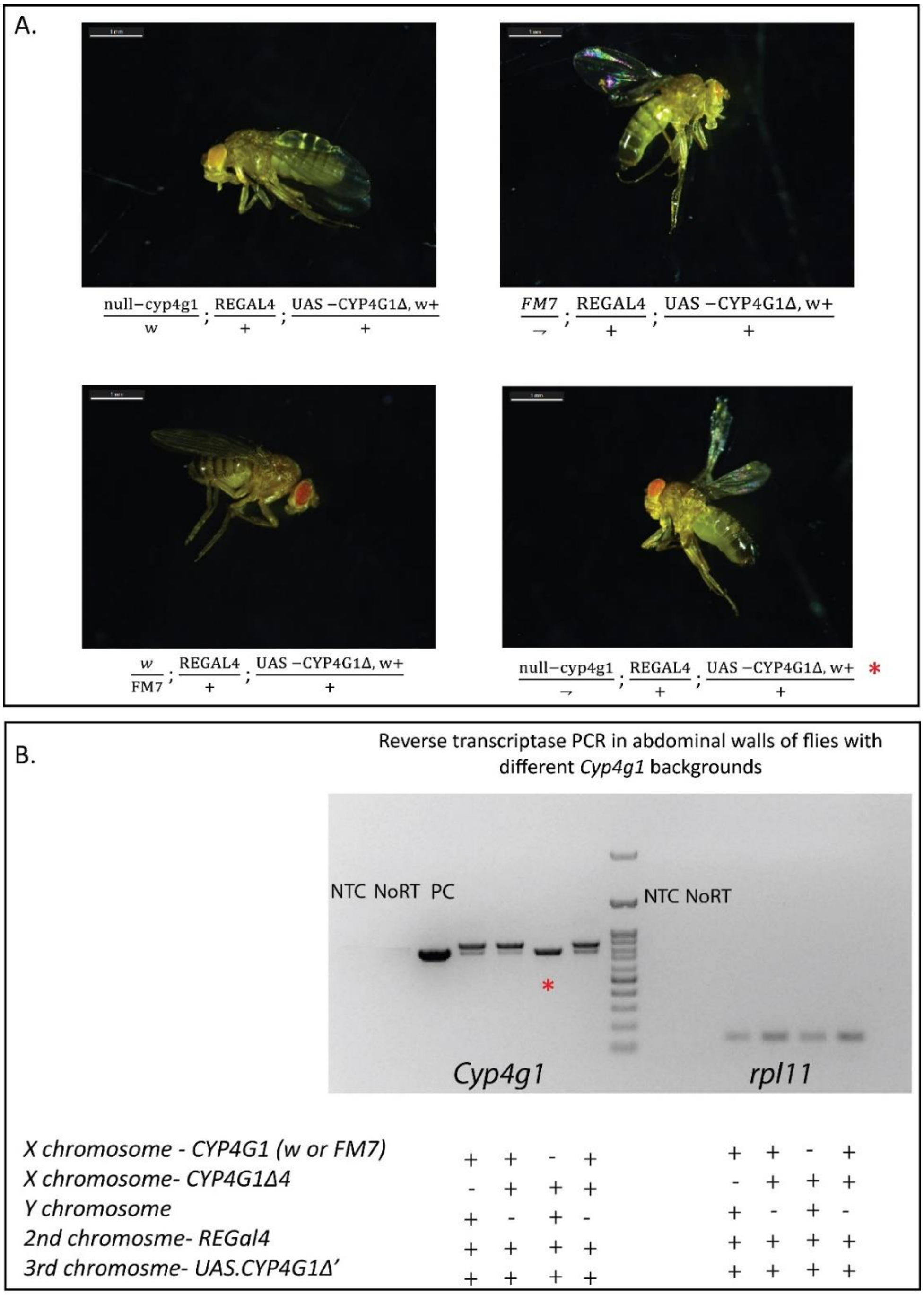
A.
1 mm
null−cyp4g1 / w ; REGAL4 / + ; UAS −CYP4G1Δ, w+ / +
FM7 / → ; REGAL4 / + ; UAS −CYP4G1Δ, w+ / +
w / FM7 ; REGAL4 / + ; UAS −CYP4G1Δ, w+ / +
null−cyp4g1 / → ; REGAL4 / + ; UAS −CYP4G1Δ, w+ / + *
B.
Reverse transcriptase PCR in abdominal walls of flies with different Cyp4g1 backgrounds
NTC NoRT PC
NTC NoRT
*
Cyp4g1
rpl11

	Cyp4g1				*rpl11*			
X chromosome - CYP4G1 (w or FM7)	+	+	-	+	+	+	-	+
X chromosome- CYP4G1Δ4	-	+	+	+	-	+	+	+
Y chromosome	+	-	+	-	+	-	+	-
2nd chromosme- REGal4	+	+	+	+	+	+	+	+
3rd chromosme- UAS.CYP4G1Δ’	+	+	+	+	+	+	+	+

Figure 9. Survivors from rescue experiment with the CYP4G1Δ (26aa deletion). A. Representative flies of the progeny resulted from crossing ReGal4/UAS.Cyp4g1Δ with Cyp4g1 null-mutants (phenotype and genotype). They are discriminated owing to the Bar-eye. B. Reverse-transcriptase (RT) PCR on the progeny, to test *Cyp4g1* forms (wt or deleted). *Rpl11* was used as quantity control. The products of no-RT control, no-template control, positive control (plasmid with the Cyp4g1Δ). “+” and “-” indicate presence or absence respectively of the allele from a chromosome (X, Y, 2nd, 3rd). The red asterisk marks the hemizygous male survivors.

Discussion

Although CYP4Gs have received much attention concerning their role in the last decarbonylation step in CHC biosynthesis taking place in oenocytes, CYP4Gs in other tissues are poorly characterized. The most characteristic example of such an unexplored protein stands for the *D. melanogaster* CYP4G15, previously reported to be localized in larval brains [11, 12]. Our ectopic expression system of CYP4G15 in oenocytes proved for first time its ability to produce CHCs, acting as a functional decarbonylase; albeit less effectively than the endogenous gene (Figure 4.1). Overall, the CHC amount produced by CYP4G15, was almost half of the amount CYP4G1 produces. This can be attributed both to the better catalytic activity of CYP4G1 against the substrates present in oenocytes (alcohols and/or aldehydes) but also to the potential lower enzyme amount achieved by the UAS/Gal4 system. The endogenous CYP4G1 is the most highly expressed gene in *Drosophila* oenocytes, hence enzyme amount could be an important parameter of the function of these generally sluggish enzymes [24]. Additional information derived from the CHC analysis indicates that flies expressing CYP4G15 ectopically in oenocytes and simultaneously silencing *Cyp4g1*, favor production of long methyl- and dimethyl-branched CHCs, not present in wild type counterparts (Figure 4.2). CYP4Gs endogenously expressed in oenocytes have been associated with methyl-branching or straight chain patterns in previous studies as well. In *Rhodnius prolixus,* there are two oenocyte CYP4Gs with CYP4G107 showing preference towards methyl-branched and CYP4G106 towards straight-chain substrates. [4]. In the same study, however, CYP4G106 was the one with a significant expression in the brain. Silencing each oenocyte CYP4G of *L. migratoria* revealed different CHC profiles of the survivors, with CYP4G102 being responsible for long-chain, methylated alkanes (methyl C29 and methyl C31) and CYP4G62 silencing having an effect only in shorter straight chain CHCs [5], yet with no other dramatic differences in CHC blend. Noteworthy, CYP4G102, which favors methyl-branching is the CYP4G15-type CYP4G of *L. migratoria* according to the phylogenetic analysis of all CYP4Gs [24]. In chapter 3, we introduced *An. gambiae* CYP4Gs in *D. melanogaster Cyp4g1*KD oenocytes and revealed substrate specificities of the two enzymes with CYP4G16 being more efficient towards straight-chain alkanes and CYP4G17 producing higher amounts of very long dimethyl branched ones (dimethyl C45, dimethyl C46, dimethyl C47) [3]. CYP4G15 CHC bouquet is reminiscent of CHC blend produced by mosquito CYP4Gs in the same system of expression (Chapter 3, [3]) with evident presence of methyl- and dimethyl-branched alkanes, albeit with many of them identified only in CYP4G15-oenocyte flies. Whether CYP4G15 ability to partially restore at least CYP4G1 function is an evolutionary residue or has to do with its function in the site of its endogenous expression is unknown. A possible scenario could be that CYP4Gs could produce CHC in non-oenocyte tissues, such as the head to shield internal organs, or alternatively they could have completely CHC-irrelevant functions.

To gain insight into its endogenous function we performed localization experiments in larval CNS, the tissue where CYP4G15 has been reported to be mainly expressed and simultaneously tested CYP4G1 expression there. CYP4G15 was found to have a characteristic meshwork-pattern surrounding the REPO-positive nuclei (Figure 4.3), hence we concluded that it is located in glia and specifically in the cortex-glia subtype, which have this characteristic pattern [32]. On the contrary, performing CNS immunohistochemistry experiments using also CYP4G1 we showed that this enzyme is also found in larval CNS, but it has a different localization than CYP4G15. It is found in the outermost layers, surrounding the surface REPO-positive nuclei, hence we conclude that it is found on the perineurial and perhaps subperineural glia (Figure 4.4). Both *D. melanogaster* CYP4Gs are present in glia, but their different subtype localization could reflect the divergent functions they perform in the CNS. The BBB glia do not allow penetration of substances from the periphery into the brain and are required for proper action of potential propagation [18]. Cortex glia support many CNS functions: they are known to provide metabolic support to neurons across development, trophic support and gas exchange, stabilizing the position of neurons, perform phagocytosis to clear cell bodies and also affect behavioral traits such as sleep and motor control [18]. Continuous lipid supply demands are high in brain and CNS lipid homeostasis relies on glia-neuron cross talk [23, 33]. Accumulation of lipid droplets have been reported in glial cells and are specifically more enriched in cortex glia, rendering them main storage depositories of LDs in larval brain [22, 34]. Additionally lipids are transferred into glia for detoxification and storage, providing protection of neurons which encounter oxidative stress and enhanced activity [33]. A possible scenario could be that CYP4G15 presence in cortex glia could be linked to lipid processing. Whether, CHCs are produced there to shield internal organs, or whether it catalyzes a completely different reaction than aldehyde decarbonylation in the CNS, having completely CHC-irrelevant functions remains elusive.

Finally, in an attempt to further elucidate the hidden aspects of this CYP4G15 we also generated an *in vitro* tool. We managed to successfully express this P450 using *Baculovirus* system of expression in insect cells, probably in a functional form based on the characteristic P450 peak indicating an appropriate protein folding (Figure 4.5). This may be a useful tool for future substrates screening with potential endogenous substrates, to determine substrate specificity and function.

Our next objective in this chapter was to shed light to the role of the CYP4G-specific insertion, which differentiates them from other P450s. This, acidic-rich loop, exposed in the cytoplasmic region is of unknown function and contribution to the CYP4G role. For this, we created two deletions using two different systems: a CRISPR-Cas9 KO and a UAS/oenocyte-Gal4 rescue of null mutants. The first system, where a 32aa-deletion (long deletion) was introduced in *D. melanogaster* genome, resulted in arrest of males in eclosion and due to that we never ended up with a homozygous line for the deletion (Figure 4.6). Arrest in pharate adult stage and inability of adults to exert the puparium is the characteristic phenotype for CY4G1KD and null mutants [1, 29]. We also introduced the same deletion (32aa) in Cyp4g1 null mutant flies, expressing the transgene specifically in oenocytes under the control of REGal4 in order to test their rescue (Figure 4.7). In agreement with the CRISPR/Cas9 result these flies were not able to eclose. To further explore the role of the loop we also generated a smaller deletion with the UAS/Gal4 system. More specifically, we introduced a transgene bearing a 26aa deletion (short) in oenocytes of Cyp4g1 null mutant flies. This by 6 aa (DENDVG) shorter deletion is able to completely restore the viability of hemizygous males which bear only the deleted transgene, as we observed them in the progeny in an expected mendelian ratio (i.e 25%) (Figure 4.8). Flies lacking *Cyp4g1* gene are adult lethal due to the lack of CHCs, essential for eclosion, which do not let them bypass this burden [1, 29]. Similarly flies devoid of the CYP4G1 acidic loop, show the same phenotype when we introduce the long deletion while they successfully eclose and survive when they bear the short deletion. Taken together these results allude either for a key role of this small protein region, deleted in the long version, useful for the essential CHC production or for a misfolding of the protein. There are some speculations about the role of this specific insertion, such as its implication in the stabilization of CYP4G-CPR complex or in interactions with other proteins [24]. Previous studies have demonstrated that acidic residues are involved in protein interactions and protein conformation changes. In toll-like receptors (TLRs) for example, mutations in specific acidic residues in their juxtamembrane region prevented their interaction with the polytopic membrane protein UNC93B1 [35], while acidic amino acids in extracellular loops are essential for ligand binding on neuropeptide Y receptor [36]. Furthermore, acidic amino acids affect the structure and function of yeast hexokinase A, by regulating domain movements [36] and have also been implicated in cation-dependent protein interactions in multiple studies [37-39]. Interestingly, such blocking of interactions has also been demonstrated for CPR with cytochrome P450 enzymes and cytochrome C [40]. In our case however, CPR-P450 interactions are expected to occur between different residues near I and B helices [24]. Hence, other molecules could be bound to CYP4Gs through these charged amino acids, such as the fatty acyl reductases (FARs) which are upstream of CYP4Gs in CHC biosynthetic pathway [24]. Another scenario could be that this region attracts the aldehyde and/or alcohol substrates that will be decarbonylated into hydrocarbons, and hence its absence in the 32aa deletion results in eclosion arrest due to inability to perform this essential function.

Overall, in this chapter we used *D. melanogaster* to unveil hidden aspects to CYP4Gs. On the one hand we studied the non-integument CYP4G15 of unknown function and on the other the CYP4G-specific insertions by using reverse genetics to create deletions. We show that CYP4G15 is a functional P450 and it can act as a decarbonylase when ectopically expressed in oenocytes, favoring the catalysis of methyl-branched substrates. Furthermore, we revealed it is placed in CNS glia and specifically, the cortex ones, as opposed to the other *D. melanogaster* CYP4G (CYP4G1) which is located on BBB glia. As far as the unique, acidic CYP4G insertion is concerned, it seems that removing it results in the characteristic CYP4G1KO lethality, implying its essential role for the function of this protein. Finally, we consider the *in vitro* tools and genetic tools generated in this chapter will address more questions in the future, further elucidating CYP4G functions.

5. Literature

1. Qiu, Y., et al., *An insect-specific P450 oxidative decarbonylase for cuticular hydrocarbon biosynthesis.* Proc Natl Acad Sci U S A, 2012. **109**(37): p. 14858-63.
2. Balabanidou, V., et al., *Cytochrome P450 associated with insecticide resistance catalyzes cuticular hydrocarbon production in Anopheles gambiae.* Proc Natl Acad Sci U S A, 2016. **113**(33): p. 9268-73.
3. Kefi, M., et al., *Two functionally distinct CYP4G genes of Anopheles gambiae contribute to cuticular hydrocarbon biosynthesis.* Insect Biochem Mol Biol, 2019. **110**: p. 52-59.
4. Dulbecco, A.B., et al., *Deciphering the role of Rhodnius prolixus CYP4G genes in straight and methyl-branched hydrocarbon formation and in desiccation tolerance.* Insect Molecular Biology, 2020. **29**(5): p. 431-443.
5. Wu, L., et al., *Both LmCYP4G genes function in decreasing cuticular penetration of insecticides in Locusta migratoria.* Pest Manag Sci, 2020. **76**(11): p. 3541-3550.
6. MacLean, M., et al., *Mountain pine beetle (Dendroctonus ponderosae) CYP4Gs convert long and short chain alcohols and aldehydes to hydrocarbons.* Insect Biochemistry and Molecular Biology, 2018. **102**: p. 11-20.
7. Guo, G.-z., et al., *Level of CYP4G19 Expression Is Associated with Pyrethroid Resistance in <i>Blattella germanica</i>.* Journal of Parasitology Research, 2010. **2010**: p. 517534.
8. Holze, H., L. Schrader, and J. Buellesbach, *Advances in deciphering the genetic basis of insect cuticular hydrocarbon biosynthesis and variation.* Heredity, 2020.
9. Wu, L., et al., *Both LmCYP4G genes function in decreasing cuticular penetration of insecticides in Locusta migratoria.* Pest Management Science, 2020. **76**(11): p. 3541-3550.
10. Wang, S., B. Li, and D. Zhang, *NlCYP4G76 and NlCYP4G115 Modulate Susceptibility to Desiccation and Insecticide Penetration Through Affecting Cuticular Hydrocarbon Biosynthesis in Nilaparvata lugens (Hemiptera: Delphacidae).* Frontiers in Physiology, 2019. **10**: p. 913.
11. Maïbèche-Coisne, M., et al., *A New Cytochrome P450 from Drosophila melanogaster, CYP4G15, Expressed in the Nervous System.* Biochemical and biophysical research communications, 2000. **273**: p. 1132-7.
12. Chung, H., et al., *Characterization of Drosophila melanogaster cytochrome P450 genes.* Proceedings of the National Academy of Sciences, 2009. **106**(14): p. 5731-5736.
13. Mao, W., M.A. Schuler, and M.R. Berenbaum, *Task-related differential expression of four cytochrome P450 genes in honeybee appendages.* Insect Mol Biol, 2015. **24**(5): p. 582-8.
14. Maïbèche-Coisne, M., et al., *P450 and P450 reductase cDNAs from the moth Mamestra brassicae: cloning and expression patterns in male antennae.* Gene, 2005. **346**: p. 195-203.
15. Niwa, R., et al., *Expressions of the cytochrome P450 monooxygenase gene Cyp4g1 and its homolog in the prothoracic glands of the fruit fly Drosophila melanogaster (Diptera: Drosophilidae) and the silkworm Bombyx mori (Lepidoptera: Bombycidae).* Applied Entomology and Zoology, 2011. **46**(4): p. 533.
16. DeSalvo, M.K., et al., *The Drosophila surface glia transcriptome: evolutionary conserved blood-brain barrier processes.* Front Neurosci, 2014. **8**: p. 346.
17. Ferguson, C.S. and R.F. Tyndale, *Cytochrome P450 enzymes in the brain: emerging evidence of biological significance.* Trends Pharmacol Sci, 2011. **32**(12): p. 708-14.
18. Freeman, M.R., *Drosophila Central Nervous System Glia.* Cold Spring Harb Perspect Biol, 2015. **7**(11).

19. Zwarts, L., F. Van Eijs, and P. Callaerts, *Glia in Drosophila behavior.* J Comp Physiol A Neuroethol Sens Neural Behav Physiol, 2015. **201**(9): p. 879-93.
20. Kim, T., B. Song, and I.S. Lee, *Drosophila Glia: Models for Human Neurodevelopmental and Neurodegenerative Disorders.* Int J Mol Sci, 2020. **21**(14).
21. Kremer, M.C., et al., *The glia of the adult Drosophila nervous system.* Glia, 2017. **65**(4): p. 606-638.
22. Kis, V., et al., *Specialized Cortex Glial Cells Accumulate Lipid Droplets in Drosophila melanogaster.* PLoS One, 2015. **10**(7): p. e0131250.
23. Tracey, T.J., et al., *Neuronal Lipid Metabolism: Multiple Pathways Driving Functional Outcomes in Health and Disease.* Front Mol Neurosci, 2018. **11**: p. 10.
24. Feyereisen, R., *Origin and evolution of the CYP4G subfamily in insects, cytochrome P450 enzymes involved in cuticular hydrocarbon synthesis.* Molecular Phylogenetics and Evolution, 2020. **143**: p. 106695.
25. Barolo, S., L.A. Carver, and J.W. Posakony, *GFP and beta-galactosidase transformation vectors for promoter/enhancer analysis in Drosophila.* Biotechniques, 2000. **29**(4): p. 726, 728, 730, 732.
26. Gratz, S.J., et al., *Genome engineering of Drosophila with the CRISPR RNA-guided Cas9 nuclease.* Genetics, 2013. **194**(4): p. 1029-35.
27. Port, F., et al., *Optimized CRISPR/Cas tools for efficient germline and somatic genome engineering in Drosophila.* Proc Natl Acad Sci U S A, 2014. **111**(29): p. E2967-76.
28. Dahanukar, A., J.A. Walker, and R.P. Wharton, *Smaug, a novel RNA-binding protein that operates a translational switch in Drosophila.* Mol Cell, 1999. **4**(2): p. 209-18.
29. Gutierrez, E., et al., *Specialized hepatocyte-like cells regulate Drosophila lipid metabolism.* Nature, 2007. **445**(7125): p. 275-80.
30. Xiong, W.C., et al., *repo encodes a glial-specific homeo domain protein required in the Drosophila nervous system.* Genes Dev, 1994. **8**(8): p. 981-94.
31. Robinow, S. and K. White, *The locus elav of Drosophila melanogaster is expressed in neurons at all developmental stages.* Developmental Biology, 1988. **126**(2): p. 294-303.
32. Pereanu, W., D. Shy, and V. Hartenstein, *Morphogenesis and proliferation of the larval brain glia in Drosophila.* Developmental Biology, 2005. **283**(1): p. 191-203.
33. Yin, J., et al., *Brain-specific lipoprotein receptors interact with astrocyte derived apolipoprotein and mediate neuron-glia lipid shuttling.* Nature Communications, 2021. **12**(1): p. 2408.
34. Dong, Q., et al., *Glial Hedgehog signalling and lipid metabolism regulate neural stem cell proliferation in Drosophila.* EMBO reports, 2021. **22**(5): p. e52130.
35. Kim, J., et al., *Acidic amino acid residues in the juxtamembrane region of the nucleotide-sensing TLRs are important for UNC93B1 binding and signaling.* J Immunol, 2013. **190**(10): p. 5287-95.
36. Walker, P., et al., *Acidic residues in extracellular loops of the human Y1 neuropeptide Y receptor are essential for ligand binding.* J Biol Chem, 1994. **269**(4): p. 2863-9.
37. Hu, J., et al., *Identification of Acidic Residues in the Extracellular Loops of the Seven-transmembrane Domain of the Human Ca2+ Receptor Critical for Response to Ca2+ and a Positive Allosteric Modulator*.* Journal of Biological Chemistry, 2002. **277**(48): p. 46622-46631.
38. Xiao, Q. and Y. Cui, *Acidic amino acids in the first intracellular loop contribute to voltage- and calcium- dependent gating of anoctamin1/TMEM16A.* PLoS One, 2014. **9**(6): p. e99376.
39. Li, X., et al., *Acidic residues of extracellular loop 3 of the Na+/H+ exchanger type 1 are important in cation transport.* Molecular and Cellular Biochemistry, 2020. **468**.

40. Shen, A.L. and C.B. Kasper, *Role of Acidic Residues in the Interaction of NADPH-Cytochrome P450 Oxidoreductase with Cytochrome P450 and Cytochrome c(*).* Journal of Biological Chemistry, 1995. **270**(46): p. 27475-27480.

Supplementary Information

Chapter 1

Name	Sequence 5'→3'
CPR125aF	TAATACGACTCACTATAGGGTGAGTGTGTAAAGGCTCCGT
CPR125aR	TAATACGACTCACTATAGGGGTACTGGTTCTGGCTGAAGT
CPR125bF	TAATACGACTCACTATAGGGCTGTGCTTTTCAGTGAACCCAA
CPR125bR	TAATACGACTCACTATAGGGAGTTGTGCTGGTTGTACTGG
CPR59aF	TAATACGACTCACTATAGGGACCAGATCGTGTGCCTGTAT
CPR59aR	TAATACGACTCACTATAGGGTGCCGCCCACTAACAAAGAA
CPR59bF	TAATACGACTCACTATAGGGCTCGCTTCGCTCGATGAAAAT
CPR59bR	TAATACGACTCACTATAGGGTGCTATGGTTGAGGTGAGGT
CPR62aF	TAATACGACTCACTATAGGGGCTCGTTCGTTCGCATAGTT
CPR62aR	TAATACGACTCACTATAGGGTCATTTGTGTTGGTTGGCTGT
CPR62bF	TAATACGACTCACTATAGGGTCATTTGTGTTGGTTGGCTGT
CPR62bR	TAATACGACTCACTATAGGGTTTGTGTTGGTTGGCTGTGCT
CPLCG5aF	TAATACGACTCACTATAGGGACAACACCAACCTACCAACCA
CPLCG5aR	TAATACGACTCACTATAGGGTCCTCACACTTCCGCTTTACA
CPLCG5bF	TAATACGACTCACTATAGGGAACACCAACCTACCAACCAC
CPLCG5bR	TAATACGACTCACTATAGGGTTCCTCGGGTCTATCACACA
dsCpr126F	TAATACGACTCACTATAGGGCCCTGGTTAGTGTTCGGTTGT
dsCpr126r	TAATACGACTCACTATAGGGCGTACCCGTACTTGCCCTTC
dsCPRmultF	TAATACGACTCACTATAGGGTTCAAATTCGCCGTCTTCGC
dsCPRmultR	TAATACGACTCACTATAGGGGCTGGGTATCCGTAAGGAGC

Table S1. 1. Primers for dsRNA generation against cuticular proteins genes.

Name	Sequence 5’ → 3’
CPR125qF	GATCGCTTCCACCCACTACG
CPR125qR	GGACGGAGCCTTTACACACT
CPR59qF	CACCTCACCTCAACCATAGC
CPR59qR	TGCCGCCCACTAACAAAG
CPR62qF	CTAAGCCAACGGAGCACAGC
CPR62qR	TCAGCGGACACCATTTCAACA
CPLCG5qF	TGATGTGTGATAGACCCGAGG
CPLCG5qR	AGCCAGCTATCCTGCCTTTC

CPR126qF	CGAGCCGAAGATCCGCTACT
CPR126qR	CACGGGGTTGGCAGATTTGG

Table S1.2. RT-qPCR primers for cuticular proteins gene relative expression estimation.

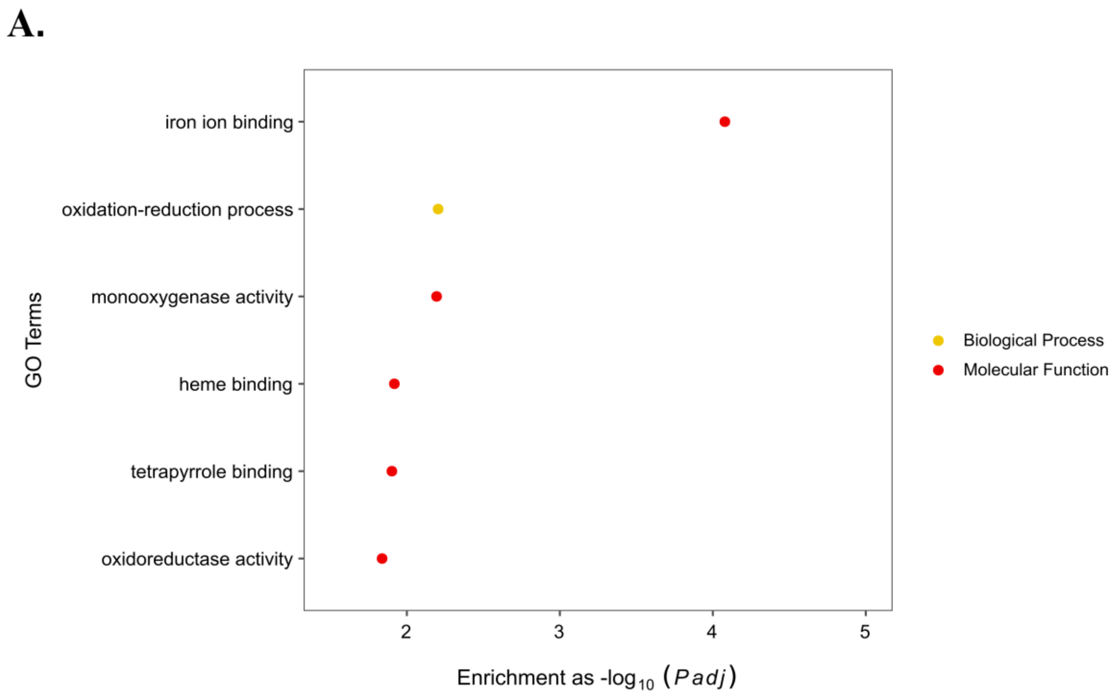

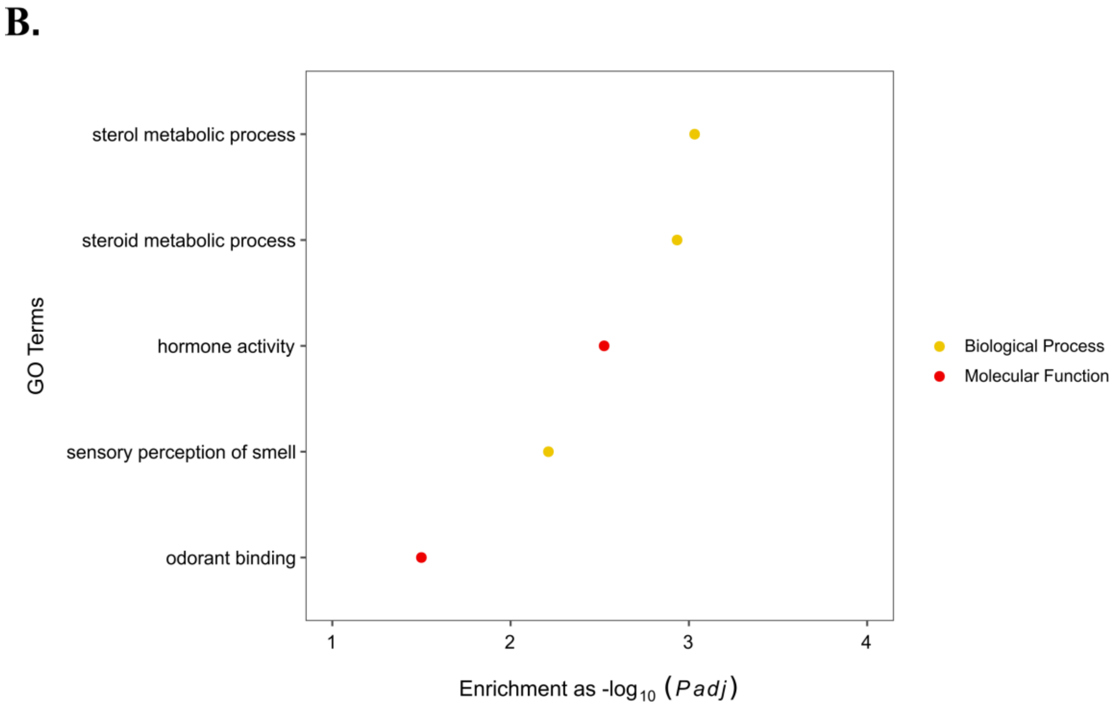

Figure S1.1. Over-represented GO terms (A) in the 73 commonly up-regulated, and (B) in the 159 commonly down-regulated genes in the two comparisons related to constitutive resistance (VK7-HR vs VK7-LR and VK7-HR vs N'Gousso).

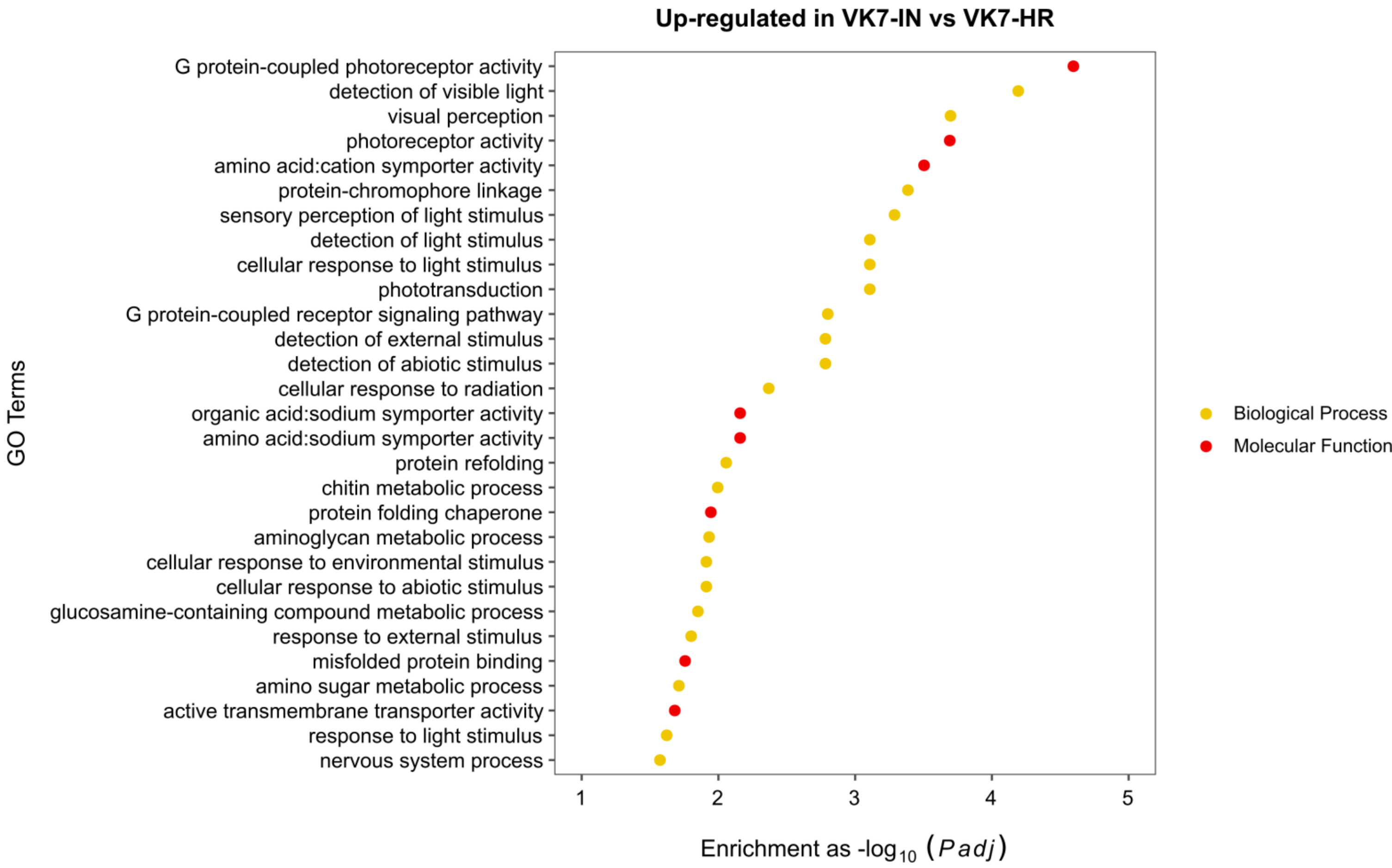

Figure S1.2. Enriched functions in the 348 up-regulated genes, after induction with deltamethrin (VK7-IN versus VK7-HR).

Chapter 2

Name	Sequence 5'→3'
ABCH2 dsF	TAATACGACTCACTATAGGGGATCCTGTTCTGTCTGGCGA-
ABCH2 dsR	TAATACGACTCACTATAGGGACTCCTGGTGCGACGAAATC
ABCH2 qF	GCAAGGAGGTGCTCATCAGT
ABCH2 qR	TCCCTTCGACGTAAAGTTGGA

Table S2.1 ABCH2 primers for dsRNA construction and RT-qPCR

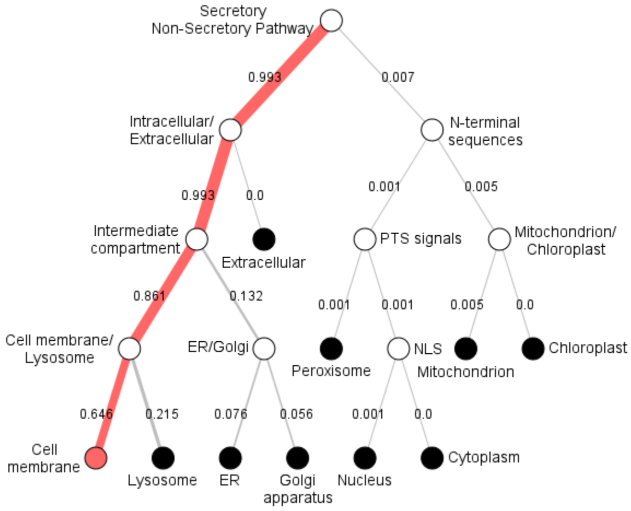
Secretory
Non-Secretory Pathway
0.993
0.007
Intracellular/
Extracellular
N-terminal
sequences
0.993
0.0
0.001
0.005
Intermediate
compartment
Extracellular
PTS signals
Mitochondrion/
Chloroplast
0.861
0.132
0.001
0.001
0.005
0.0
Cell membrane/
Lysosome
ER/Golgi
Peroxisome
NLS
Mitochondrion
Chloroplast
0.646
0.215
0.076
0.056
0.001
0.0
Cell
membrane
Lysosome
ER
Golgi
apparatus
Nucleus
Cytoplasm

Figure S2.1 ABCH2 subcellular localization is predicted to be on the plasma membrane using DeepLoc-1.0: Eukaryotic protein subcellular localization predictor

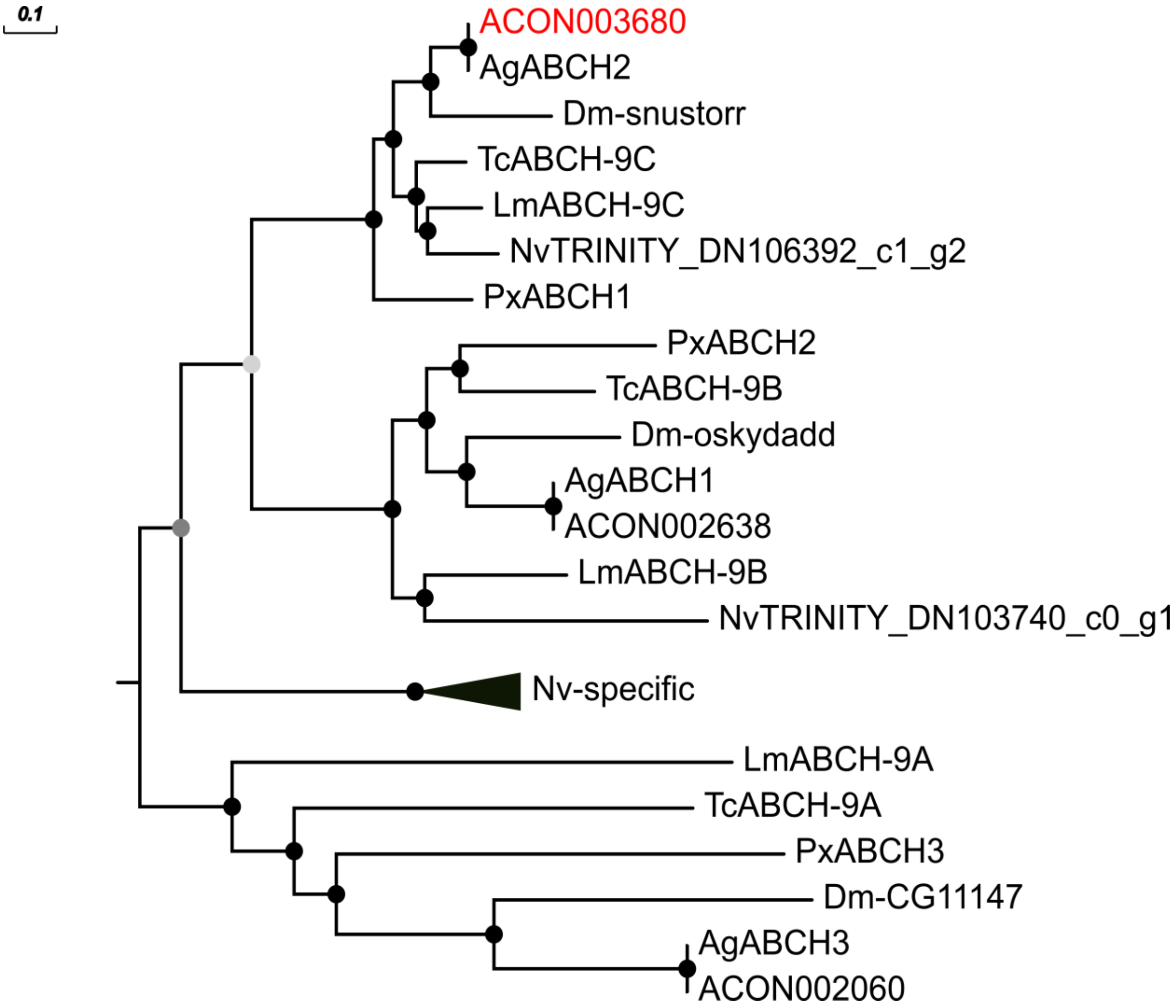
0.1
ACON003680
AgABCH2
Dm-snustorr
TcABCH-9C
LmABCH-9C
NvTRINITY_DN106392_c1_g2
PxABCH1
PxABCH2
TcABCH-9B
Dm-oskydadd
AgABCH1
ACON002638
LmABCH-9B
NvTRINITY_DN103740_c0_g1
Nv-specific
LmABCH-9A
TcABCH-9A
PxABCH3
Dm-CG11147
AgABCH3
ACON002060

Figure S2.2. ACON003680 is one-to-one ortholog of *snustorr*. Phylogenetic analysis of ABCH transporters from *Anopheles coluzzii* (ACON), *Anopheles gambiae* (Ag), *Drosophila melanogaster* (Dm), *Plutella xylostella* (Px), *Nezara viridula* (Nv), *Tribolium castaneum* (Tc) and *Locusta migratoria* (Lm). Tree was created under the LG+R5 substitution model with 5,000 bootstraps and was rooted using the *Danio rerio* ABCH gene as an outgroup. Nodes with bootstrap support < 50% and between 50% and 75% are

indicated with light grey and grey circles respectively. Nodes with bootstrap support greater than 75% are indicated with black circles. The phylogenetic tree was constructed by Jason Charamis.

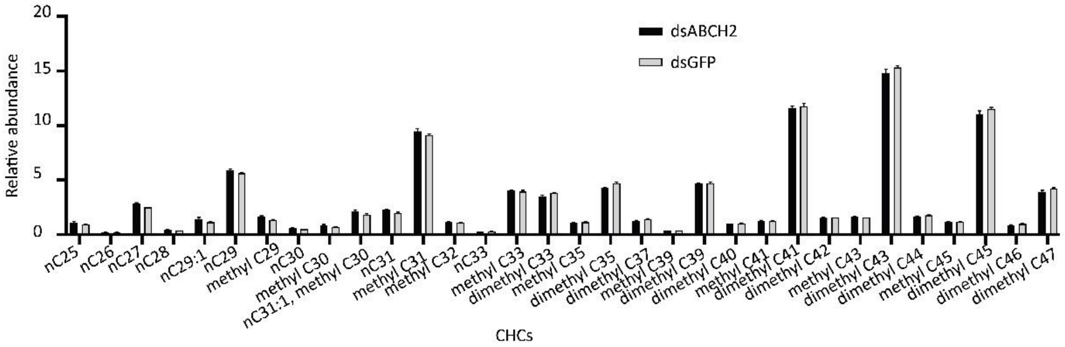

Figure S2.3. Relative abundance of cuticular hydrocarbons (CHCs) identified in legs of dsRNA injected mosquitoes (dsABCH2 and dsGFP-control). Relative abundances in % area are depicted for each one of the identified CHCs. Mean of 3 biological replicates +SEM.

Chapter 3

Gene	ID	Name	PrimerSequence (5’→3’)
CYP4G16	AGAP001076-PA	*CYP4G16*F (c)	GCGCGCACCATGTCAGCAACAATTGCGCATACAG
		*CYP4G16*R (c)	CTCGAGTCATAATGTCTTCGATTTGCGTTGA
CYP4G17	AGAP000877	*CYP4G17*F (c)	GGCGCGCCCACCATGGGCATTGAAACGATCCC
		*CYP4G17*R (c)	GTCGACTCATGCCCTCGGCTCCAGCT
		pPel_uas F (s)	GAAGAGAACTCTGAATAGGGAATTG
		pPel_sv40 R (s)	CAAATGTGGTATGGCTGATTATG

Table S3.1. Primer list: Names, IDs and sequences (5’-3’) of all primer pairs used for cloning (c) and sequencing (s) of *An. coluzzii* CYP4G ORFs.

♀ ♂	$\frac{\mathbf{REGal4}}{\mathbf{REGal4}};\frac{+}{+}$ **1**	$\frac{\mathbf{REGal4}}{\mathbf{REGal4}};\frac{\boldsymbol{UAS-CYP4G16}}{\boldsymbol{UAS-CYP4G16}}$ **2**	$\frac{\mathbf{REGal4}}{\mathbf{REGal4}};\frac{\boldsymbol{UAS-CYP4G17}}{\boldsymbol{UAS-CYP4G17}}$ **3**	$\frac{\boldsymbol{UAS-dsCyp4g1}}{\mathbf{UAS-ds}\boldsymbol{Cyp4g1}};\frac{\boldsymbol{UAS-CYP4G17}}{\boldsymbol{UAS-CYP4G17}}$ **4**
$\frac{\mathbf{UAS-ds}\boldsymbol{Cyp4g1}}{\mathbf{UAS-ds}\boldsymbol{Cyp4g1}};\frac{+}{+}$ **A**	$\frac{\mathrm{REGal4}}{\mathrm{UAS-ds}Cyp4g1};\frac{+}{+}$	-	-	-
$\frac{\mathbf{UAS-ds}\boldsymbol{Cyp4g1}}{\mathbf{UAS-ds}\boldsymbol{Cyp4g1}};\frac{\boldsymbol{UAS-CYP4G16}}{\boldsymbol{UAS-CYP4G16}}$ **B**	$\frac{\mathrm{REGal4}}{\mathrm{UAS-ds}Cyp4g1};\frac{UAS-CYP4G16}{+}$	$\frac{\mathrm{REGal4}}{\mathrm{UAS-ds}cyp4g1};\frac{UAS-CYP4G16}{UAS-CYP4G16}$	$\frac{\mathrm{REGal4}}{\mathrm{UAS-ds}Cyp4g1};\frac{UAS-CYP4G17}{UAS-CYP4G16}$	$\frac{\mathrm{UAS-ds}Cyp4g1}{\mathrm{UAS-ds}Cyp4g1};\frac{UAS-CYP4G17}{UAS-CYP4G16}$
$\frac{\mathbf{UAS-ds}\boldsymbol{Cyp4g1}}{\mathbf{UAS-ds}\boldsymbol{Cyp4g1}};\frac{\boldsymbol{UAS-CYP4G17}}{\boldsymbol{UAS-CYP4G17}}$ **C**	$\frac{\mathrm{REGal4}}{\mathrm{UAS-ds}Cyp4g1};\frac{attB.UAS-CYP4G17}{+}$	$\frac{\mathrm{REGal4}}{\mathrm{UAS-ds}Cyp4g1};\frac{UAS-CYP4G17}{attB.UAS-CYP4G16}$	$\frac{\mathrm{REGal4}}{\mathrm{UAS-ds}Cyp4g1};\frac{UAS-CYP4G17}{UAS-CYP4G17}$	-
$\frac{\mathbf{REGal4}}{\mathbf{REGal4}};\frac{\boldsymbol{UAS-CYP4G17}}{\boldsymbol{UAS-CYP4G17}}$ **D**	-	$\frac{\mathrm{REGal4}}{\mathrm{REGal4}};\frac{UAS-CYP4G16}{UAS-CYP4G17}$	-	-
$\frac{+}{+};\frac{\boldsymbol{UAS-CYP4G16}}{\boldsymbol{UAS-CYP4G16}}$ **E**	-	$\frac{\mathrm{REGal4}}{+};\frac{UAS-CYP4G16}{UAS-CYP4G16}$	-	-

$\frac{+}{+};\frac{\boldsymbol{UAS-CYP4G17}}{\boldsymbol{UAS-CYP4G17}}$ **F**	-		$\frac{\mathrm{REGal4}}{+};\frac{UAS-CYP4G17}{UAS-CYP4G17}$	-
$\frac{+}{+};\frac{\boldsymbol{VK13}}{\boldsymbol{VK13}}$ **G**	$\frac{\mathrm{REGal4}}{+};\frac{VK13}{+}$	-	-	-

Table S3.2. Combinations of crosses for the construction of all genotypes used for downstream experiments (eclosion estimation and phenotypic observation of flies and cuticular hydrocarbon analysis).

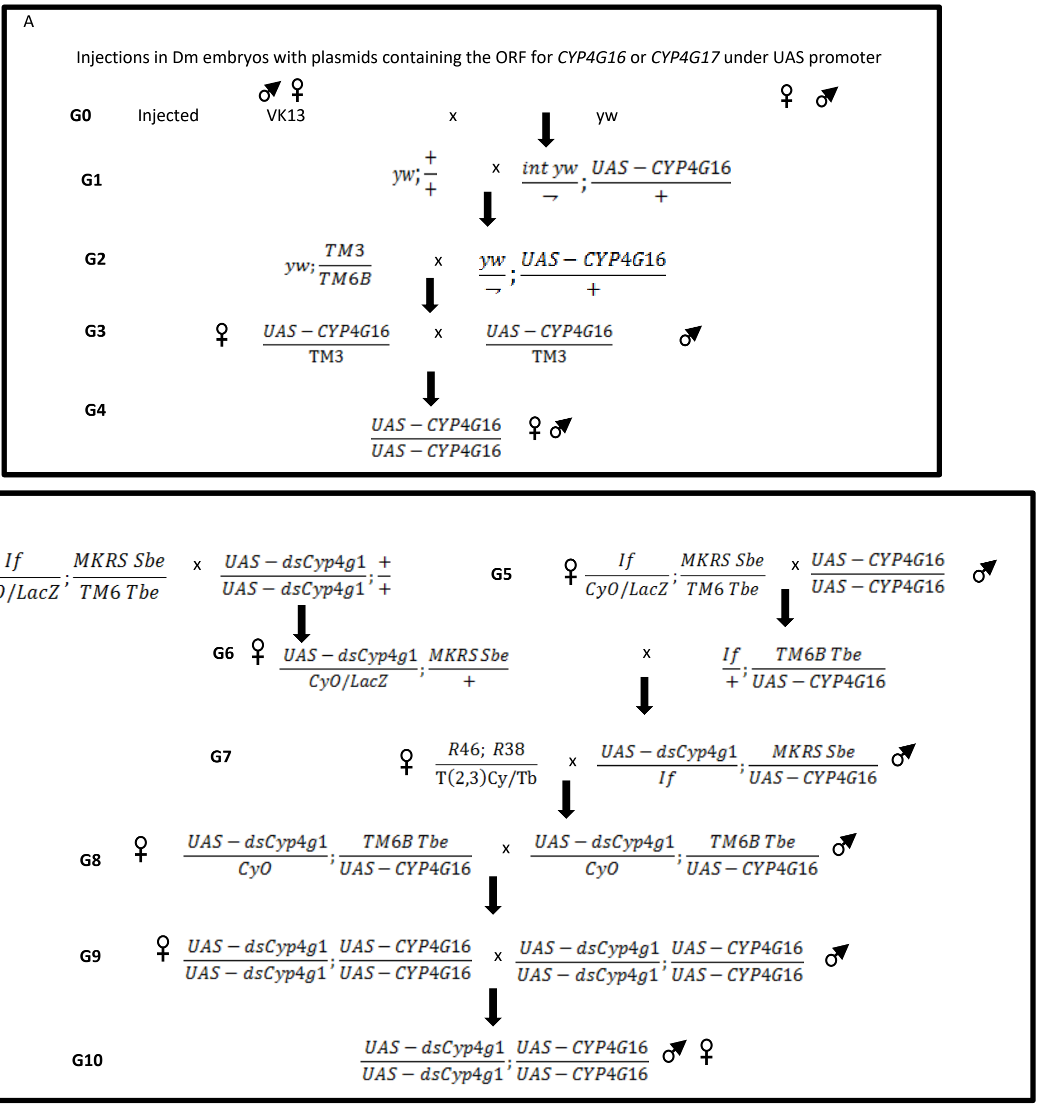
A
Injections in Dm embryos with plasmids containing the ORF for *CYP4G16* or *CYP4G17* under UAS promoter
G0 Injected ♂♀ VK13 x yw ♀♂
G1 $yw;\frac{+}{+}$ x $\frac{int\ yw}{\rightharpoondown};\frac{UAS-CYP4G16}{+}$
G2 $yw;\frac{TM3}{TM6B}$ x $\frac{yw}{\rightharpoondown};\frac{UAS-CYP4G16}{+}$
G3 ♀ $\frac{UAS-CYP4G16}{TM3}$ x $\frac{UAS-CYP4G16}{TM3}$ ♂
G4 $\frac{UAS-CYP4G16}{UAS-CYP4G16}$ ♀♂
B
$\frac{If}{CyO/LacZ};\frac{MKRS\ Sbe}{TM6\ Tbe}$ x $\frac{UAS-dsCyp4g1}{UAS-dsCyp4g1};\frac{+}{+}$
G5 ♀ $\frac{If}{CyO/LacZ};\frac{MKRS\ Sbe}{TM6\ Tbe}$ x $\frac{UAS-CYP4G16}{UAS-CYP4G16}$ ♂
G6 ♀ $\frac{UAS-dsCyp4g1}{CyO/LacZ};\frac{MKRS\ Sbe}{+}$ x $\frac{If}{+};\frac{TM6B\ Tbe}{UAS-CYP4G16}$
G7 ♀ $\frac{R46;\ R38}{T(2,3)Cy/Tb}$ x $\frac{UAS-dsCyp4g1}{If};\frac{MKRS\ Sbe}{UAS-CYP4G16}$ ♂
G8 ♀ $\frac{UAS-dsCyp4g1}{CyO};\frac{TM6B\ Tbe}{UAS-CYP4G16}$ x $\frac{UAS-dsCyp4g1}{CyO};\frac{TM6B\ Tbe}{UAS-CYP4G16}$ ♂
G9 ♀ $\frac{UAS-dsCyp4g1}{UAS-dsCyp4g1};\frac{UAS-CYP4G16}{UAS-CYP4G16}$ x $\frac{UAS-dsCyp4g1}{UAS-dsCyp4g1};\frac{UAS-CYP4G16}{UAS-CYP4G16}$ ♂
G10 $\frac{UAS-dsCyp4g1}{UAS-dsCyp4g1};\frac{UAS-CYP4G16}{UAS-CYP4G16}$ ♂♀

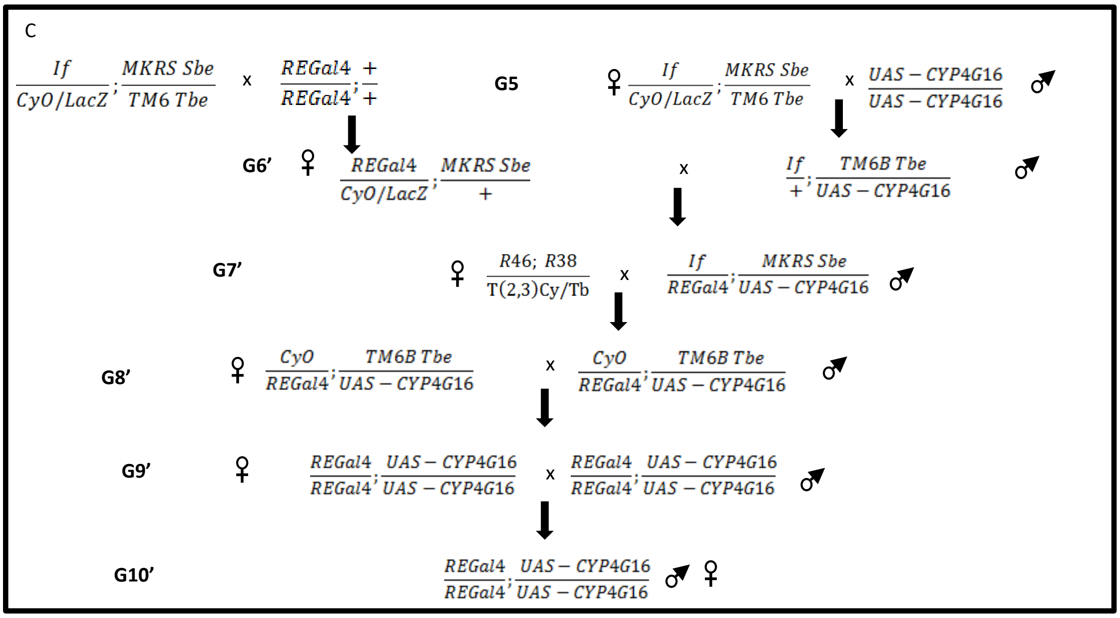
C
If/CyO/LacZ ; MKRS Sbe/TM6 Tbe x REGal4/REGal4 ; +/+
G5 ♀ If/CyO/LacZ ; MKRS Sbe/TM6 Tbe x UAS – CYP4G16/UAS – CYP4G16 ♂
G6' ♀ REGal4/CyO/LacZ ; MKRS Sbe/+ x If/+ ; TM6B Tbe/UAS – CYP4G16 ♂
G7' ♀ R46; R38/T(2,3)Cy/Tb x If/REGal4 ; MKRS Sbe/UAS – CYP4G16 ♂
G8' ♀ CyO/REGal4 ; TM6B Tbe/UAS – CYP4G16 x CyO/REGal4 ; TM6B Tbe/UAS – CYP4G16 ♂
G9' ♀ REGal4/REGal4 ; UAS – CYP4G16/UAS – CYP4G16 x REGal4/REGal4 ; UAS – CYP4G16/UAS – CYP4G16 ♂
G10' REGal4/REGal4 ; UAS – CYP4G16/UAS – CYP4G16 ♂ ♀

Figure S3.1. Series of genetic crosses for the generation of flies with both oenocyte-specific *Drosophila cyp4g1* RNAi knock-down and *Anopheles CYP4G16* and/or *CYP4G17* expression. A) Injections in *Dm* embryos with plasmids containing *CYP4G16* were followed by a series of standard genetic crosses to end up with 3rd chromosome homozygotes for *CYP4G16* (*CYP4G16* example is depicted here; exactly the same strategy was carried out for *CYP4G17*-injected embryos), B) Series of crosses for construction of double homozygote flies containing *CYP4G16* (3rd chromosome) with ds*Cyp4g1* (2nd chromosome), C) Series of crosses for construction of double homozygote flies containing *CYP4G16* (3rd chromosome) with REGal4 (2nd chromosome). The same genetic strategy was used for the generation of *CYP4G17* double homozygotes.

***D. melanogaster* phenotypes in different CYP4G backgrounds**

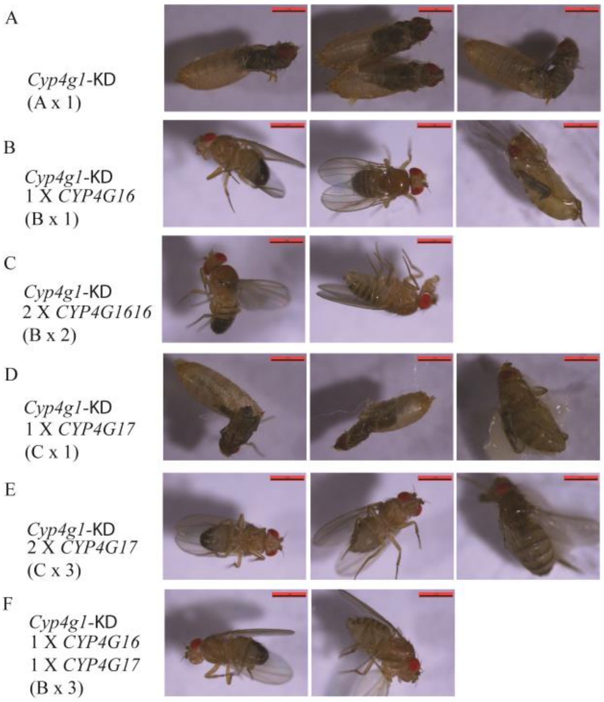
A
Cyp4g1-KD
(A x 1)
B
Cyp4g1-KD
1 X CYP4G16
(B x 1)
C
Cyp4g1-KD
2 X CYP4G1616
(B x 2)
D
Cyp4g1-KD
1 X CYP4G17
(C x 1)
E
Cyp4g1-KD
2 X CYP4G17
(C x 3)
F
Cyp4g1-KD
1 X CYP4G16
1 X CYP4G17
(B x 3)

Figure S3.2. Phenotypes of *D. melanogaster* flies with different CYP4G backgrounds. A) *Cyp4g1*-KD flies unable to eclose, B) *Cyp4g1*-KD flies with one copy of *CYP4G16*: Male and female survivors and one dead desiccated fly are shown, C)*Cyp4g1*-KD flies with two copies of *CYP4G16*: A male and a female survivor are shown, D)*Cyp4g1*-KD flies with one copy of *CYP4G1*: No survivors in this case, males and females either do not eclose or are lying dead on the food, E) *cyp4g1*-KD flies with two copies of *CYP4G17*: Male and female survivors, as well as dead flies which are found in a quite high ratio, F) *Cyp4g1*-KD flies with one copy of *CYP4G16* and one copy of *CYP4G17*: A male and a female survivor are represented. Different CYP4G backgrounds correspond to offspring of A x 1, B x 1, B x 2, C x 1, C x 3, B x 3 fly crosses of Table S2.

Chapter 4.

.

Gene	ID	Primer name	Primer Sequence (5’-3’)
Cyp4g15	CG11715	BssHII 4g15 F	GCGCGCACCATGGAGGTGCTGAAGAAGGAC
		Xhoi 4g15 R	CTCGAGTCAACTGGTCCGCGGCTG
		CYP4G15F	GAGTTCGTGTTCACCCTGACG
		CYP4G15R	GAGTTCTCGTTGAACAACTCGA
Ribosomal protein L11	CG7726	RPL11F	CGATCCCTCCATCGGTATCT
		RPL11R	AACCACTTCATGGCATCCTC
Cyp4g1		CYP4G1 BssHII F	GCGCGCACCATGGCAGTGGAAGTAGTTCAGGA
		CYP4G1 ClaI R	ATCGATCGCACGTGACTCCTCTTG
		CYP4G1 CLAI F	ATCGATGAAAATGATGTGGGCG
		CYP4G1 XhoIR	ATCGATCTCGAG CTAGGCCACCGTGGCGTA
		CYP4G1 PciI F	ACATGTGTGATATCATACATAAGAGGCAGG
		CYP4G1 Xba R	TCTAGAAAGAGCCAATCGCCTCT
		CYP4G1 scrF	AGCAAGGTGGTCAAGGATCG
		CYP4G1 scrR	ACGCTTCTCCAACGAGACAT
		Sense oligo	P- CTTCGGTTAAATTACTGTACCGCC
		Antisense oligo	P-AAACGCCGAGGTGGTATCGTGGCC

Table S4.1 Primer list: Names, IDs and sequences (5’-3’) of all primer pairs used for cloning and screening

♀ \ ♂	$\frac{UAS-dsCyp4g1}{UAS-dsCyp4g1};\frac{+}{+}$ 1	$\frac{REGAL4}{REGAL4};\frac{UAS-CYP4G15}{UAS-CYP4G15}$ 2	$\frac{UAS-dsCyp4g1}{UAS-dsCyp4g1};\frac{UAS-CYP4G15}{UAS-CYP4G15}$ 3	$\frac{+}{+};\frac{VK13}{VK13}$ 4	$\frac{+}{+};\frac{UAS-CYP4G15}{UAS-CYP4G15}$ 5
$\frac{REGal4}{REGal4};\frac{+}{+}$ A	$\frac{REGal4}{UAS-dsCyp4g1};\frac{+}{+}$	-	$\frac{REGAL4}{UAS-dsCyp4g1};\frac{UAS-CYP4G15}{+}$	$\frac{REGAL4}{+};\frac{VK13}{+}$	
$\frac{REGAL4}{REGAL4};\frac{UAS-CYP4G15}{UAS-CYP4G15}$ B	$\frac{REGal4}{UAS-dsCyp4g1};\frac{UAS-CYP4G15}{+}$	$\frac{REGAL4}{REGAL4};\frac{UAS-CYP4G15}{UAS-CYP4G15}$	$\frac{REGAL4}{UAS-dsCyp4g1};\frac{UAS-CYP4G15}{UAS-CYP4G15}$		
$\frac{UAS-dsCyp4g1}{UAS-dsCyp4g1};\frac{UAS-CYP4G15}{UAS-CYP4G15}$ C	-	-	$\frac{UAS-dsCyp4g1}{UAS-dsCyp4g1};\frac{UAS-CYP4G15}{UAS-CYP4G15}$	-	
$\frac{UAS-dsCyp4g1}{UAS-dsCyp4g1};\frac{+}{+}$ D	$\frac{UAS-dsCyp4g1}{UAS-dsCyp4g1};\frac{+}{+}$				
$\frac{+}{+};\frac{UAS-CYP4G15}{UAS-CYP4G15}$ E					$\frac{+}{+};\frac{UAS-CYP4G15}{UAS-CYP4G15}$

Table S4.2. Combinations of crosses for the construction of all genotypes used for downstream experiments (eclosion estimation and phenotypic observation of flies and cuticular hydrocarbon analysis).

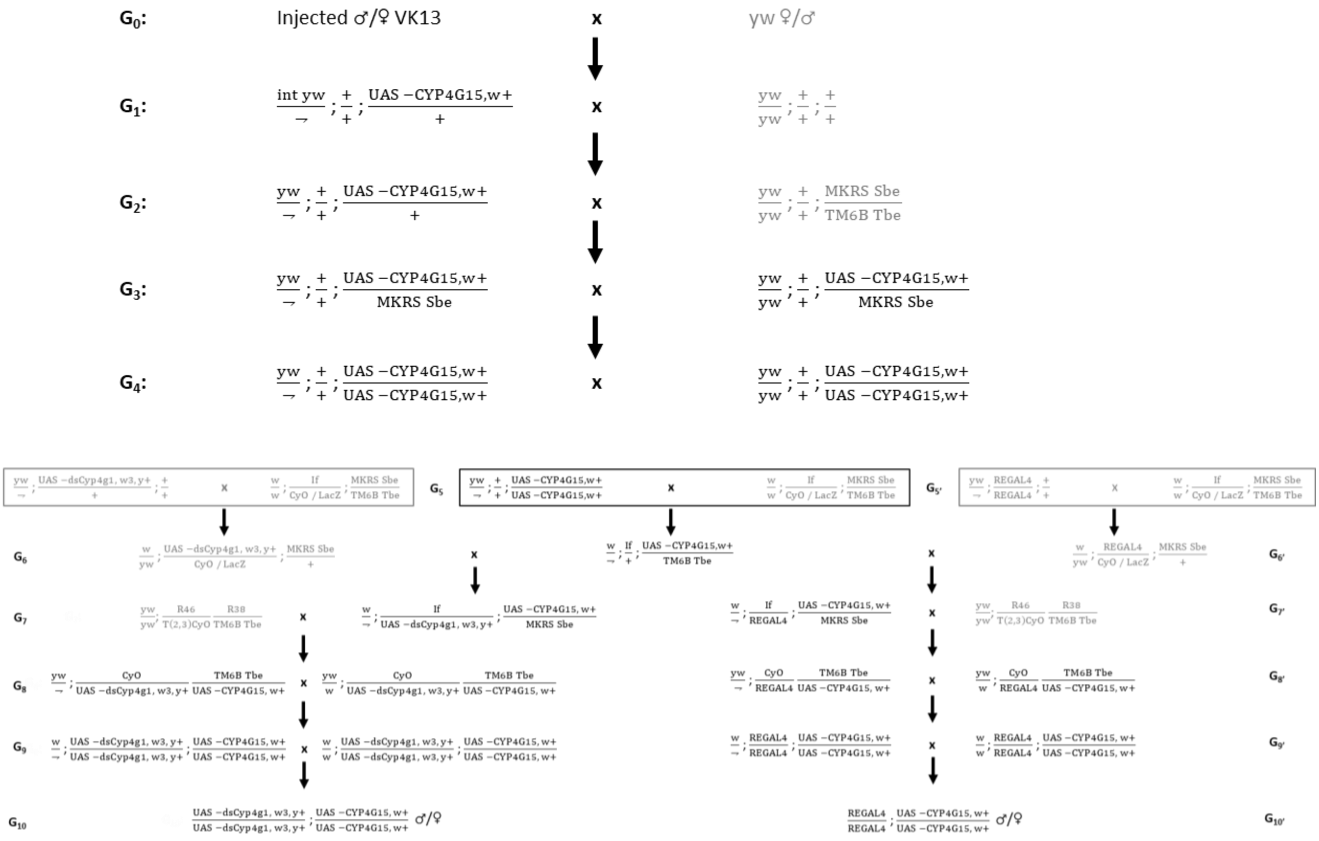
G0:
Injected ♂/♀ VK13
x
yw ♀/♂
G1:
int yw/→ ; +/+ ; UAS −CYP4G15,w+/+
yw/yw ; +/+ ; +/+
G2:
yw/→ ; +/+ ; UAS −CYP4G15,w+/+
yw/yw ; +/+ ; MKRS Sbe/TM6B Tbe
G3:
yw/→ ; +/+ ; UAS −CYP4G15,w+/MKRS Sbe
yw/yw ; +/+ ; UAS −CYP4G15,w+/MKRS Sbe
G4:
yw/→ ; +/+ ; UAS −CYP4G15,w+/UAS −CYP4G15,w+
yw/yw ; +/+ ; UAS −CYP4G15,w+/UAS −CYP4G15,w+
yw/→ ; UAS −dsCyp4g1, w3, y+/+ ; +/+
w/w ; If/CyO / LacZ ; MKRS Sbe/TM6B Tbe
G5
yw/→ ; +/+ ; UAS −CYP4G15,w+/UAS −CYP4G15,w+
w/w ; If/CyO / LacZ ; MKRS Sbe/TM6B Tbe
G5'
yw/→ ; REGAL4/REGAL4 ; +/+
w/w ; If/CyO / LacZ ; MKRS Sbe/TM6B Tbe
G6
w/yw ; UAS −dsCyp4g1, w3, y+/CyO / LacZ ; MKRS Sbe/+
w/→ ; If/+ ; UAS −CYP4G15,w+/TM6B Tbe
w/yw ; REGAL4/CyO / LacZ ; MKRS Sbe/+
G6'
G7
yw/yw ; R46/T(2,3)CyO R38/TM6B Tbe
w/→ ; If/UAS −dsCyp4g1, w3, y+ ; UAS −CYP4G15, w+/MKRS Sbe
w/→ ; If/REGAL4 ; UAS −CYP4G15, w+/MKRS Sbe
yw/yw ; R46/T(2,3)CyO R38/TM6B Tbe
G7'
G8
yw/→ ; CyO/UAS −dsCyp4g1, w3, y+ TM6B Tbe/UAS −CYP4G15, w+
yw/w ; CyO/UAS −dsCyp4g1, w3, y+ TM6B Tbe/UAS −CYP4G15, w+
yw/→ ; CyO/REGAL4 TM6B Tbe/UAS −CYP4G15, w+
yw/w ; CyO/REGAL4 TM6B Tbe/UAS −CYP4G15, w+
G8'
G9
w/→ ; UAS −dsCyp4g1, w3, y+/UAS −dsCyp4g1, w3, y+ ; UAS −CYP4G15, w+/UAS −CYP4G15, w+
w/w ; UAS −dsCyp4g1, w3, y+/UAS −dsCyp4g1, w3, y+ ; UAS −CYP4G15, w+/UAS −CYP4G15, w+
w/→ ; REGAL4/REGAL4 ; UAS −CYP4G15, w+/UAS −CYP4G15, w+
w/w ; REGAL4/REGAL4 ; UAS −CYP4G15, w+/UAS −CYP4G15, w+
G9'
G10
UAS −dsCyp4g1, w3, y+/UAS −dsCyp4g1, w3, y+ ; UAS −CYP4G15, w+/UAS −CYP4G15, w+ ♂/♀
REGAL4/REGAL4 ; UAS −CYP4G15, w+/UAS −CYP4G15, w+ ♂/♀
G10'

Figure S4.1. Series of genetic crosses for the generation of flies with both oenocyte-specific *Drosophila Cyp4g1* RNAi knock-down and CYP4G15 expression. (A) Injections in *Drosophila* embryos with plasmids containing CYP4G15 were followed by a series of standard genetic crosses to end up with 3rd chromosome homozygotes for CYP4G15. (B) Series of crosses for construction of double homozygote flies containing CYP4G15 (3rd chromosome) with *dsCyp4g1* (2nd chromosome) (left). Series of crosses for construction of double homozygote flies containing CYP4G15 (3rd chromosome) with REGal4 (2nd chromosome) (right).

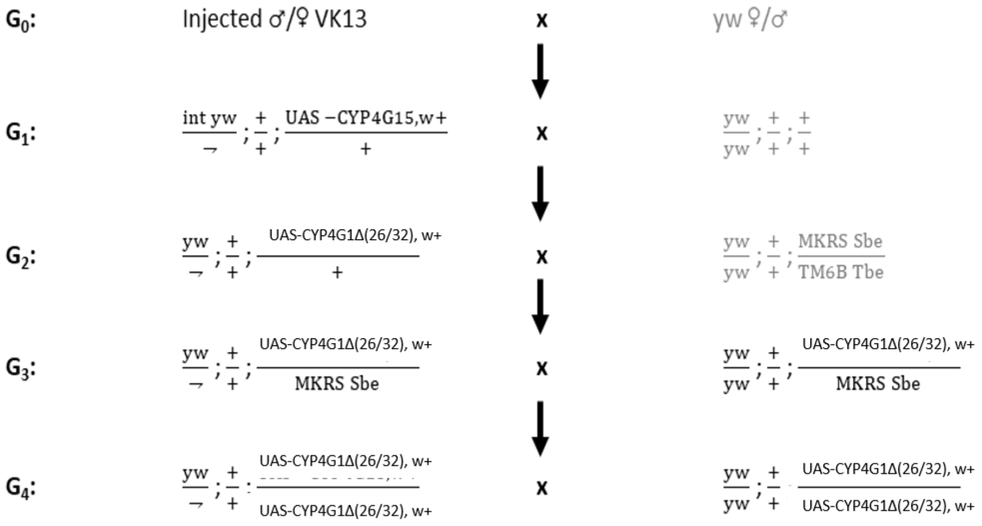
G0: Injected ♂/♀ VK13 x yw ♀/♂
G1: int yw/→ ; +/+ ; UAS −CYP4G15,w+/+ x yw/yw ; +/+ ; +/+
G2: yw/→ ; +/+ ; UAS-CYP4G1Δ(26/32), w+/+ x yw/yw ; +/+ ; MKRS Sbe/TM6B Tbe
G3: yw/→ ; +/+ ; UAS-CYP4G1Δ(26/32), w+/MKRS Sbe x yw/yw ; +/+ ; UAS-CYP4G1Δ(26/32), w+/MKRS Sbe
G4: yw/→ ; +/+ ; UAS-CYP4G1Δ(26/32), w+/UAS-CYP4G1Δ(26/32), w+ x yw/yw ; +/+ ; UAS-CYP4G1Δ(26/32), w+/UAS-CYP4G1Δ(26/32), w+

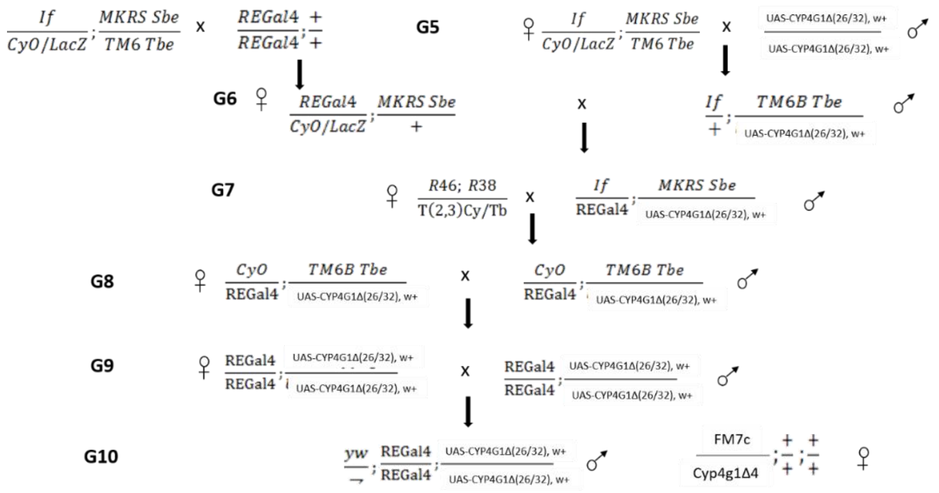
If/CyO/LacZ ; MKRS Sbe/TM6 Tbe x REGal4/REGal4 ; +/+
G5 ♀ If/CyO/LacZ ; MKRS Sbe/TM6 Tbe x UAS-CYP4G1Δ(26/32), w+/UAS-CYP4G1Δ(26/32), w+ ♂
G6 ♀ REGal4/CyO/LacZ ; MKRS Sbe/+ x If/+ ; TM6B Tbe/UAS-CYP4G1Δ(26/32), w+ ♂
G7 ♀ R46; R38/T(2,3)Cy/Tb x If/REGal4 ; MKRS Sbe/UAS-CYP4G1Δ(26/32), w+ ♂
G8 ♀ CyO/REGal4 ; TM6B Tbe/UAS-CYP4G1Δ(26/32), w+ x CyO/REGal4 ; TM6B Tbe/UAS-CYP4G1Δ(26/32), w+ ♂
G9 ♀ REGal4/REGal4 ; UAS-CYP4G1Δ(26/32), w+/UAS-CYP4G1Δ(26/32), w+ x REGal4/REGal4 ; UAS-CYP4G1Δ(26/32), w+/UAS-CYP4G1Δ(26/32), w+ ♂
G10 yw/→ ; REGal4/REGal4 ; UAS-CYP4G1Δ(26/32), w+/UAS-CYP4G1Δ(26/32), w+ ♂ FM7c/Cyp4g1Δ4 ; +/+ ; +/+ ♀

Figure S4.2. Series of crosses for construction of double homozygote flies containing CYP4G1 deletions (Δ26 or Δ32) (3rd chromosome) with REGal4 (2nd chromosome) (right). These flies (G10) are crossed with null mutant CYP4G1Δ4 (Gutierez et al., 2007) to test if the deletions we generate rescue the adult lethality of these CYP4G1-null flies.

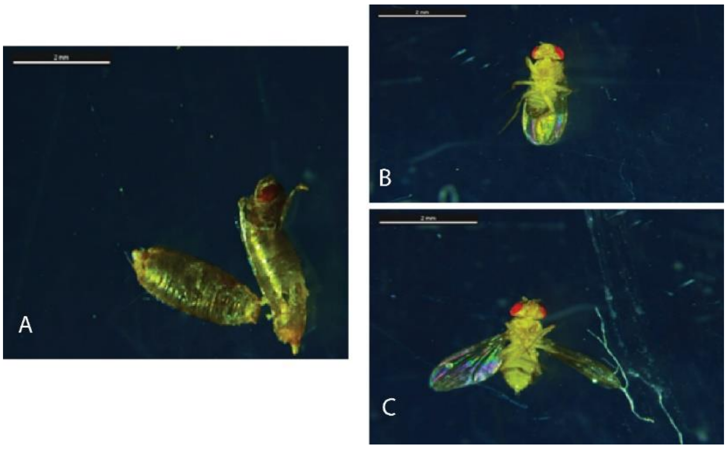

gure S4.3. Phenotypes of *D. melanogaster* expressing *Cyp4g15* and silencing *Cyp4g1***.** A) Flies unable to eclose, B) Male survivor, C) Female survivor. Depicted individuals correspond to offspring of B x 3 crosses of Table S2.

TCACTCAAAGGCGGTAGTTGCCAGGATGGGCTTAGAAGCGGGCAAATCCTTTGATGTTCATGACTATATGTCGCAGACCACGGTTGACATCC
TGTTGTCTACCGCCATGGGTGTGAAGAAGCTTCCGGAGGGTAACAAGAGTTTCGAATACGCCCAAGCCGTCGTCGACATGTGTGATATCATA
CATAAGAGGCAGGTTAAATTACTGTACCGCCTGGATTCCATCTACAAGTTTACTAAGCTTCGCGAGAAGGGCGATCGCATGATGAACATCAT
CTTGGGTATGACCAGCAAGGTGGTCAAGGATCGTAAGGAGAACTTCCAAGAGGAGTCACGTGCGATT~~GTTGAGGAGATTTCTACACCTGTT~~
~~GCCAGCACTCCCGCTTCCAAGAAGGAGGGTCTTCGCGATGATCTGGATGATATCGATGAAAATGATGTGGGC~~GCCAAGAGGCGATTGGCTC
TTCTAGATGCCATGGTGGAAATGGCTAAGAACCCCGATATCGAGTGGAACGAGAAGGACATCATGGATGAGGTGAATACAATTATGTTTGA
GGGCCACGATACCACCTCGGCGGGATCTAGTTTCGCCCTCTGCATGATGGGAATCCACAAGGACATCCAGGCTAAAGTCTTCGCCGAACAGA
AGGCCATCTTCGGGGATAATATGCTGAGGGATTGCACCTTTGCCGATACCATGGAGATGAAATATTTGGAGCGCGTAATTTTAGAGACTTTG
AGGTTGTACCCACCAGTACCACTTATCGCCAGGCGTCTGGACTACGACCTGAAGTTGGCCAGTGGTCCGTACACGGTTCCCAAGGGCACTAC

Figure S4.4. The donor plasmid appropriate for the CRISPR strategy. The synonymous mutations in the gRNAs (yellow) and PAM (grey) sequences are depicted in red. The start of the two homology arms is indicated with a dashed green line. The 96 bp deleted region is illustrated with the gray strikethrough line.

General discussion and future directions

During my PhD entitled "The Achilles heel of the malaria vector *Anopheles coluzzii"*: I) I analyzed the legs of insecticide resistant *An. coluzzii* compared to susceptible controls. II) I studied the role of an ATP-binding cassette (ABC) leg transporter in insecticide toxicity and III) I provided insights into enzymes implicated in CHC biosynthesis in *An. coluzzii* and *D. melanogaster*.

The transcriptomic dataset presented in Chapter 1, provides gene transcripts identified in legs and allows two comparisons: (1) the transcriptional differences of legs derived from constitutively resistant mosquito populations versus two susceptible populations and (2) the transcriptional differences between the legs of unexposed mosquitoes and those exposed with deltamethrin. These comparisons serve as a useful starting point for studying both resistance and induction mechanisms in mosquito legs, with the data analysis outlining divergent transcriptional patterns and revealing many candidates or whole gene families that deserve further attention. The leg transcriptomic analysis, together with the comparative proteomic and lipidomic analysis, recently performed in the same resistant population create an arsenal that can be harnessed to identify novel insecticide resistance mechanisms and key players. In this PhD I focused on cuticular proteins and on an ABC transporter, revealed by the leg datasets.

The former are structural cuticular components possibly contributing to insecticide resistance, with evident presence in the resistant leg proteome and transcriptome. Thus, I performed functional experiments for individual genes to evaluate their role in protection against insecticides. According to the results, silencing individually cuticular protein genes is not sufficient to restore mosquito susceptibility, which could be explained by the high redundancy of these structural components. The contribution of this protein family could be evaluated more precisely by targeting many cuticular proteins at the same time via multiple dsRNAs, or by targeting their regulators. Indeed, when we silenced multiple cuticular proteins simultaneously using a dsRNA targeting a conserved region among a small group of such genes, susceptibility was restored to a small degree. Based on recent data showing enhanced or remodeled cuticular structures in resistant mosquito legs [5, 6], we expect that effectively perturbing this structure would make mosquitoes more vulnerable to the insecticide.

As far as the ABC transporter is concerned, it was identified in leg transcriptome with its presence being significantly evident after insecticide exposure. Its silencing followed by contact insecticide application resulted in a significant knock-down and subsequent mortality. Additionally, it is mainly found in legs but also other appendages of the head and specifically it is located on the epidermis polarized towards the cuticle. Having evidence that the transporter is sub-cellularly localized on the plasma membrane is an important step towards the understanding of its function and the set-up of an appropriate *in vitro* assay.

The first step was to test the dimeric nature of this half-transporter. To study this we initially performed ABCH2 *in silico* modelling based on the available crystal structure of human ABCG1, a close homologue. The data supported that ABCH2 forms homodimers, stabilizing its protomers with similar nature and number of interactions as ABCG1 homodimeric transporter. To validate this we expressed ABCH2 in Sf9 insect cells (after appropriate codon optimization), isolated membranes with an extraction protocol favoring the formation of vesicles (both right-side and inside-out vesicles are formed) and reproduced an ATPase protocol using malachite green reagent. This colorimetric assay enabled as measure the released Pi after ATP hydrolysis, which was significantly increased in ABCH2-expressing membranes thus dictating a functional molecule in homodimeric state.

The next step was to test whether deltamethrin is an ABCH2 substrate. Initially we performed docking experiments on the modelled ABCH2 using deltamethrin. The results indicated that deltamethrin is a potential ABCH2 ligand, with the analysis identifying a deltamethrin pocket in the translocator region closed to that identified for ABCG1 substrate (cholesterol). I next tested whether deltamethrin is a substrate using the insect cell system of expression coupled with the ATPase assay, examining whether deltamethrin further stimulates the ABCH2-overexpressing membranes, resulting in the production of more Pi (higher ATP hydrolysis in the presence of the substrate). Although, I introduced deltamethrin in the ATPase assay, no further stimulation of the ABCH2-expressing membranes was recorded in the presence of the substrate and ATP, possibly due to the system limitations (see below).

In general, providing direct proof of the ability of a transporter to translocate a specific molecule is challenging. Decades of research in biological transport systems have highlightened the difficulty in assigning a substrate to an ABC transporter and the reproducibility issues which arise when using different systems. Among the general culprits of unsuccessful/incomplete trials lie the impaired insertion or misfolding into the host membranes (lack of chaperones), the aggregation bodies formed by accumulation of unfolded molecules, the improper localization, possible misregulation due to divergent post-translation modifications and cytotoxicity of the expressed protein [7]. In our case the basal activity observed in ABCH2-expressing membranes advocates for a functional transporter, at least to a certain degree. It should be noted that deltamethrin itself adds an extra layer of complexity to the setup of this reaction, due to its high hydrophobicity. This could be confronted either by solubilizing deltamethrin in another organic solvent or by using water soluble pyrethroid analogues. Alternatively, to achieve higher sensitivity, the development of membrane reconstitution systems, that is purified proteins incorporated into artificial lipid membranes (liposomes) [10] can be exploited. These *in vitro* systems exclude the interference with endogenous transporters, thus allowing the analysis only of the transporter of interest [7]. Variations of that systems have been used for ABC transporters to monitor transport and binding of candidate substrates [11].

Although, no direct *in vitro* evidence is provided here that deltamethrin efflux is facilitated by ABCH2, other lines of evidence presented, support deltamethrin could be at least an ABCH2 ligand. Firstly, *in silico* docking experiments on the modelled ABCH2, derived by the available crystal structure of ABCG1 homolog, indicate that deltamethrin is a potential ABCH2 substrate. Secondly, when we exposed mosquitoes to C^{14}-deltamethrin we observed a small increase in insecticide penetration in early time points in ABCH2-silenced *An. coluzzii*. Entrance of more insecticide in the absence of the transporter reflects the implication of the transporter in deltamethrin efflux, either directly or via stimulation of a different export/sequestration mechanism. Thirdly, the localization of the transporter on the apical membrane of the epidermal layer is in accordance with the hypothesis that this molecule is able to pump out compounds into the exoskeleton and perhaps out of the organism.

An approach to combat ABC transporter-mediated drug resistance is to use high-affinity inhibitors [8]. Given the association of this transporter in deltamethrin toxicity, described in this work, inhibitor screening could result in the identification of a compound that could be used synergistically with an existing chemical (insecticide) to enhance mosquito toxicity. The transporter of interest, which belongs to an insect-specific sub-family, is located on appendage epidermis plasma membrane and its silencing results in mortality in presence of deltamethrin, gathers important features required for a target to be druggable.

Concerning *in vivo* studies, we consider the dsRNA experiments of great importance, as in the lack of specific inhibitors to date, we can silence ABCH2 and test multiple phenotypes. In that fashion, I performed C^{14}-Deltamethrin penetration experiments in silenced mosquitoes to test whether in the absence of the transporter insecticide penetration is enhanced. Such *in vivo* approaches using ABC transporter inhibitors have been proposed with labeled-insecticide to evaluate the *in vivo* distribution in tissues of interest [12]. Although useful in such experimental settings, RNAi is not sufficient to address essentiality of this protein. It only provides a partial knock-down of a gene at the adult stage, while targeting nymphal or pronymphal stages is significantly tough in mosquitoes using nanoinjections. To encounter this limitation I propose the generation of transgenic mosquito lines. Generation of knock-out (KO) mosquitoes using CRISPR/Cas9 will address the essentiality of the gene in earlier developmental stages. If the essentiality is high this research can lead to the further evaluation of this candidate as novel drug target. In case the KO lines do not show high mortality they can be examined in downstream assays coupled with substrates (leg extracts/insecticides) to provide direct indication on the implication of these protein in leg component and/or insecticide transport.

In the next two chapters (Chapter 3 and 4) I worked on the characterization of cytochrome P450 enzymes of 4G subfamily (CYP4Gs), implicated in cuticular hydrocarbon (CHC) biosynthesis. As CHCs are enhanced in resistant mosquito legs, I studied these proteins participating in their biosynthesis. Two *An. coluzzii* CYP4Gs (CYP4G16 and CYP4G17) were possibly associated with the thicker-epicuticle phenotype observed previously in a multi-resistant population [6]. CYP4Gs catalyze the last decarbonylation step of CHC biosynthesis [13]. This takes place in oenocytes, large cells attached to the integument [14]. Apart from their evident presence in oenocytes, CYP4Gs have also been detected in other non-integument tissues, with unknown functions there. *D. melanogaster* CYP4G15 previously reported in larval heads/brains [15, 16], was also studied in an attempt to delineate extra roles of CYP4G enzymes.

Initially, I considered of great importance the sub-cellular localization analysis of these enzymes. For *An. coluzzii* CYP4Gs I provided the distinct developmental localization patterns, revealing that CYP4G17 is found in two different sub-cellular localizations among development (plasma membrane and/or microsomal), while CYP4G16 is present only in plasma membrane. This result is perhaps in accordance with the existence of two origins of oenocytes (larval and adult), as previously described for other insects [14]. It is plausible that shifting localization during development could reflect divergent functions. Proteomic analysis to identify differences between the two CYP4G17 isoforms (post-translation modification or cleavage) could unravel the nature of the modification. Additionally, cross-linking experiments in the two states coupled with mass-spectroscopy (MS) analysis are expected to reveal the protein interactions mediated by the two isoforms and hence provide information about their functional profile across development. Regarding *D. melanogaster* CYP4G15, its transcripts were previously identified in larval brains using *in situ* hybridization. Here, we generated a specific antibody against that and identified the protein in the larval central nervous system (CNS) and more specifically in cortex glia. CYP4G1 localization in the larval CNS was also tested and it was found to be in (sub)perineurial glia, known to participate in the blood brain barrier (BBB) formation [17]. The different localizations could reflect divergent roles. To delineate that future experiments should focus on RNAi silencing of the two CYP4Gs using specific glial Gal4 drivers (tools that are available in *D. melanogaster* [18]). Phenotypes upon cell-specific CYP4G ablation are expected to advance the understanding towards their function there.

Additionally, I used *D. melanogaster* as a tool to ectopically express mosquito CYP4Gs (CYP4G16 and CYP4G17) and *D. melanogaster* CYP4G15 in oenocytes while simultaneously silencing the endogenous oenocyte gene (CYP4G1). Thus, I revealed the decarbonylase activity of these enzymes. So far, that was shown only for CYP4G16 (*in vitro*)[6] and CYP4G1 (*in vitro* and *in vivo*) [13]. Here we showed that these enzymes exhibit different degrees of decarbonylase activities *in vivo* and we provide the CHC blends produced by their function in oenocytes. Although, other oenocyte enzyme families implicated in biosynthesis are considered to mainly contribute to CHC diversity, as intermediate enzymes of the pathway [19] [20], paradoxically the research described here reveals that the last enzymes of the pathway (CYP4Gs) exhibit an extra layer of specificity against the provided substrates. Although both *An. coluzzii* CYP4Gs can produce the same blend of CHCs, CYP4G17 showed increased specificity against very long-chain, dimethyl-branched substrates, while CYP4G16 could produce some shorter alkanes more effectively. Interestingly, the three very long, dimethyl-branched species were not identified in *D. melanogaster* of wild-type state (CYP4G1). Additionally, the CNS-CYP4G15 when ectopically expressed in oenocytes produced a different CHC blend favoring long, methyl species, not identified in the other CYP4G hydrocarbonomes. These results outline the generation of different CHCs profiles determined by altered CYP4G presence into the oenocytes. For CYP4G15 specifically, this could be interpreted as an evolutionary residue of some remaining decarbonylase activity, which was induced when expressed ectopically into the oenocyte environment. Alternatively, this ability could reflect functional aspects of CYP4G15 in its endogenous place; it could produce CHCs there to shield internal organs for example. Going a step further, the flies producing different CHCs, were subjected to desiccation and insecticide toxicity stresses to test their ability to cope with these conditions. Flies expressing CYP4G17(with characteristic abundance of very long, dimethyl-branched CHCs) encountered better these challenges in both cases, outlining advantages provided by divergent oenocyte CYP4G profiles, probably owing to the different CHC blends.

Furthermore, an additional tool to study different CYP4G properties was their *in vitro* expression. Using Baculovirus we expressed CYP4G15, CYP4G16 and CY4G17 together with CPR obligatory electron donor in Sf9 insect cells and evaluated their correct folding and adequate CPR activity. Membranes expressing these proteins are intended to be used in substrate model screening. Such experiments will advance our knowledge regarding substrate specificity preferences. Remarkably, this tool could bridge the gap between the *in vivo* indications (phenotypes observed upon tissue-specific CYP4G15 knock-down) and the concomitant hypotheses built regarding their role there, as specific endogenous substrates can also be provided to the CYP4G/CPR-expressing membranes for validation of their ability to be catalyzed. Last but not least, the functional expression tool can be utilized in future CHC assay experiments to directly study the catalytic activities against different substrates i.e. alcohols and aldehydes of various lengths, methylation and saturation degree.

Finally, to elicit more information about CYP4Gs we decided to remove the extra, unique insertion they possess and differentiates them from other CYPs [19]. This is a highly acidic, antigenic and exposed loop of unknown contribution in CYP4G function [13][19]. To study this we generated two different deletions in *D. melanogaster* CYP4G1 (32aa and 26aa deletion). The short one did not affect survival while the long 32aa resulted in arrest before eclosion, the characteristic phenotype observed upon oenocyte CYP4G1 knock-out[21] and knock-down[13]. Assuming the long deletion did not disturb the correct protein folding of the P450, we speculate that the loop is needed for the CYP4G1 essential function i.e. CHC decarbonylation. How this is mediated by the loop is yet to be discovered. It could participate in protein interactions with other enzymes of the pathway, such as fatty acid reductases (FARs), which are preceded in the biosynthetic pathway, or it could interact with the substrates (attraction/binding).

Current work of our group is focused on the *in vitro* expression of the different CYP4G1 forms (wild type and the two deletions), proving so far that all the enzyme forms can generate the characteristic for P450 spectral absorbance peak at 450 nm, meaning they are correctly folded [22, 23]. *In silico* modelling of the deletions coupled with docking analysis has been performed showing that the substrate tested could not dock to the long deletion. More substrates will be used in the future in the modelled proteins to evaluate this finding. Lastly, the direct evidence on the participation of the loop in protein or substrate interaction is expected to be provided by two experimental settings: (1) *in vitro* expressed CYP4G1 forms in CHC assay will reveal whether they still have their decarbonylase activity, (2) Cross-linking and comparative proteomics of wild-type flies and survivors bearing the short deletion is expected to provide evidence on the different interactions allowed into the oenocytes in the presence and absence of this mysterious loop.

The outcomes of these results are expected to provide valuable insight in the insect essential pathway of CHC biosynthesis. How CYP4Gs interact with other partners of the pathway and how they stabilize their interactions with CPR and other proteins is still elusive. An exposed, insect-specific loop that mediates an essential function, either by serving as the point of recognition/attraction to the lipid substrate or by providing the ability of protein-protein interaction and/or complexes stability could be evaluated as potential novel insecticide target. On the one hand, if the specific region interacting with the lipid substrate is identified it can be targeted with chemical compounds, antagonizing the natural substrates. Otherwise, delineating protein partners can result in designing novel compounds blocking the essential interactions.

Concluding Remarks

Mosquitoes are the worlds' biggest killers, due to their ability to transmit infectious diseases, with malaria being the deadliest among them. For decades, humans try to fight them, with chemical insecticides being the most efficient weapon in their arsenal. Selection pressure upon extensive insecticide exposure, however, resulted in well-trained mosquitoes in resisting human threats, eventually equipped with strong armors against them. Identifying the weak points of the opponent now requires deep understanding of the mechanisms underlying their defense. In this context, this research aimed to investigate insecticide resistance mechanisms. Given that legs are the first hurdle the insecticide confronts to enter mosquito body, my research focused on mosquito legs to identify insecticide resistant contributors there. At the same time, it was expanded in other mosquito tissues and the model organism *D. melanogaster* in an attempt to provide insight into other key-players, which govern the synthesis of leg components, participating to insecticide resistance. The findings provided in this PhD, are considered to contribute to the understanding of the 'Achilles heel' of malaria mosquitoes and to the potential future applications which will target it.

Literature

1. Andriessen, R., et al., *Electrostatic coating enhances bioavailability of insecticides and breaks pyrethroid resistance in mosquitoes.* Proc Natl Acad Sci U S A, 2015. **112**(39): p. 12081-6.
2. Ranson, H., *Current and Future Prospects for Preventing Malaria Transmission via the Use of Insecticides.* Cold Spring Harb Perspect Med, 2017. **7**(11).
3. Stica, C., et al., *Characterizing the molecular and metabolic mechanisms of insecticide resistance in Anopheles gambiae in Faranah, Guinea.* Malar J, 2019. **18**(1): p. 244.
4. Hemingway, J., *The molecular basis of two contrasting metabolic mechanisms of insecticide resistance.* Insect Biochem Mol Biol, 2000. **30**(11): p. 1009-15.
5. Balabanidou, V., L. Grigoraki, and J. Vontas, *Insect cuticle: a critical determinant of insecticide resistance.* Curr Opin Insect Sci, 2018. **27**: p. 68-74.
6. Balabanidou, V., et al., *Cytochrome P450 associated with insecticide resistance catalyzes cuticular hydrocarbon production in Anopheles gambiae.* Proc Natl Acad Sci U S A, 2016. **113**(33): p. 9268-73.
7. Lefèvre, F., A. Baijot, and M. Boutry, *Plant ABC transporters: Time for biochemistry?* Biochemical Society Transactions, 2015. **43**: p. 931-936.
8. Shukla, S., C.P. Wu, and S.V. Ambudkar, *Development of inhibitors of ATP-binding cassette drug transporters: present status and challenges.* Expert Opin Drug Metab Toxicol, 2008. **4**(2): p. 205-23.
9. Krumpochova, P., et al., *Transportomics: screening for substrates of ABC transporters in body fluids using vesicular transport assays.* Faseb j, 2012. **26**(2): p. 738-47.
10. Geertsma, E.R., et al., *Membrane reconstitution of ABC transporters and assays of translocator function.* Nature Protocols, 2008. **3**(2): p. 256-266.
11. Patzlaff, J.S., T. van der Heide, and B. Poolman, *The ATP/Substrate Stoichiometry of the ATP-binding Cassette (ABC) Transporter OpuA*.* Journal of Biological Chemistry, 2003. **278**(32): p. 29546-29551.
12. Gott, R.C., et al., *Implicating ABC Transporters in Insecticide Resistance: Research Strategies and a Decision Framework.* Journal of Economic Entomology, 2017. **110**(2): p. 667-677.
13. Qiu, Y., et al., *An insect-specific P450 oxidative decarbonylase for cuticular hydrocarbon biosynthesis.* Proceedings of the National Academy of Sciences of the United States of America, 2012. **109**(37): p. 14858-14863.
14. Makki, R., E. Cinnamon, and A.P. Gould, *The development and functions of oenocytes.* Annu Rev Entomol, 2014. **59**: p. 405-25.
15. Maïbèche-Coisne, M., et al., *A new cytochrome P450 from Drosophila melanogaster, CYP4G15, expressed in the nervous system.* Biochem Biophys Res Commun, 2000. **273**(3): p. 1132-7.
16. Chung, H., et al., *Characterization of &lt;em&gt;Drosophila melanogaster&lt;/em&gt; cytochrome P450 genes.* Proceedings of the National Academy of Sciences, 2009. **106**(14): p. 5731.
17. Hartenstein, V., *Morphological diversity and development of glia in Drosophila.* Glia, 2011. **59**(9): p. 1237-52.
18. Awasaki, T. and T. Lee, *New tools for the analysis of glial cell biology in Drosophila.* Glia, 2011. **59**(9): p. 1377-86.
19. Feyereisen, R., *Origin and evolution of the CYP4G subfamily in insects, cytochrome P450 enzymes involved in cuticular hydrocarbon synthesis.* Mol Phylogenet Evol, 2020. **143**: p. 106695.

20. Chung, H. and S.B. Carroll, *Wax, sex and the origin of species: Dual roles of insect cuticular hydrocarbons in adaptation and mating.* BioEssays : news and reviews in molecular, cellular and developmental biology, 2015. **37**(7): p. 822-830.
21. Gutierrez, E., et al., *Specialized hepatocyte-like cells regulate Drosophila lipid metabolism.* Nature, 2007. **445**(7125): p. 275-80.
22. Luthra, A., I.G. Denisov, and S.G. Sligar, *Spectroscopic features of cytochrome P450 reaction intermediates.* Arch Biochem Biophys, 2011. **507**(1): p. 26-35.
23. Danielson, P.B., *The cytochrome P450 superfamily: biochemistry, evolution and drug metabolism in humans.* Curr Drug Metab, 2002. **3**(6): p. 561-97.